THE UNIVERSITY OF QUEENSLAND

AUSTRALIA

Characterising candidate genes for roles in *Fusarium pseudograminearum*-host interactions in the model cereal *Brachypodium distachyon*

Mark Turner

Bachelor of Biotechnology (Hon I), Postgraduate diploma of Education

ORCID: 000-0001-9240-814x

A thesis to be submitted for the degree of Doctor of Philosophy at

The University of Queensland in January 2020

School of Chemistry and Molecular Biosciences

Abstract

Fusarium Crown Rot (FCR) is a crop disease of global concern, causing yield losses and grain quality reduction in wheat and barley. In Australia, FCR is predominantly caused by the fungal pathogen *Fusarium pseudograminearum* (*Fp*) and costs the Australian wheat industry approximately AU$88 million dollars annually. *Fp* has a biphasic lifestyle and hence is classified as a hemi-biotrophic pathogen. Generally, during initial infection and colonisation of the host *Fp* is thought to be biotrophic and sources nutrition from living host tissue, whereas at later stages of infection, *Fp* switches to a necrotrophic lifestyle and sources nutrition from dead host tissue. Additionally, *Fp* can live saprophytically on residual plant material in the soil and produce spores that can remain viable for up to 16 months. Current control measures are focussed on reducing inoculum load. However, due to environmental and socioeconomic factors these can be difficult to implement. While the use of a highly FCR resistant cultivar is seen as a viable control measure in the long term, no high yielding, highly FCR resistant cultivar is currently available. Classically, the plant phytohormones salicylic acid (SA) and jasmonic acid (JA) / ethylene (ET) are associated with promoting defence against biotrophic and necrotrophic pathogens, respectively. Contemporary understanding of defence against hemi-biotrophic pathogens is that both SA and JA/ET are required at different stages of infection to confer tolerance/resistance. To facilitate wheat breeding programs, it is necessary to develop a deeper understanding of the key genes and processes involved in regulating defence against and interactions with *Fp*. The inherent complexity of wheat's polyploid genome has hampered the progress of genetic studies, and consequently, the use of model plant organisms is required to rapidly test the utility of candidate genes for their efficacy against *Fp* and better understand how the host plant defends itself against *Fp*.

The current PhD project utilised the model grass species *Brachypodium distachyon*, hereafter referred to as *Brachypodium*, as a model organism for wheat to elucidate the role of candidate genes in host-*Fp* interactions. Firstly, I characterised the roles of *Brachypodium PHYTOCHROME AND FLOWERING TIME 1* (*BdPFT1*) as a candidate gene for involvement in interactions with *Fp*. *PFT1* encodes MEDIATOR 25, a subunit of the highly conserved mediator complex that fine tunes gene expression by interacting with the RNA polymerase II transcription complex. Characterisation of

BdPFT1 was undertaken by the identification and use of two transgenic *BdPFT1* overexpression (*BdPFT1*-OE) lines. Like its homolog in *Arabidopsis thaliana*, *BdPFT1* was found to promote flowering. Additionally, *BdPFT1* was found to promote susceptibility to *Fp*. Previous studies have reported that *AtPFT1* conferred susceptibility towards *Fusarium oxysporum* in a JA-dependent manner. Whether *BdPFT1* mediated *Fp* susceptibility is also JA-dependent remains undetermined. This is because no clear trend in the phytohormone marker genes surveyed with qRT-PCR were observed between *BdPFT1*-OE lines and the WT under basal growth and *Fp* inoculated conditions. Unexpectedly, overexpression of *BdPFT1* resulted in the development of a spontaneous lesion phenotype on photosynthetic tissue. The spontaneous lesion phenotype has been previously reported in *Arabidopsis* as consequence of wheat *PFT1* overexpression but not overexpression of *AtPFT1*. Together, this has provided initial evidence of a role for PFT1 in mediating cell death and potential differences in the regulation of PFT1-mediated cell death between monocots and dicots. Indeed, the characterisation of *BdPFT1* has uncovered apparent differences in the regulation of developmental and defence pathways between monocots and dicots, despite being part of highly conserved transcription machinery. Consequently, despite *PFT1* being well characterised in *Arabidopsis*, further research is required in monocot systems to elucidate its modes of action and viability as target for manipulation to reduce FCR.

Secondly, I investigated the role of SA in mediating host defence against *Fp* and disease outcomes in *Brachypodium*. This was achieved by characterising three independent *nahG* expressing *Brachypodium* lines. *nahG* is a bacterial enzyme that degrades SA and when expressed *in planta* results in a SA-deficient plant. The *nahG* transgenic lines of *Brachypodium* were found to be more susceptible to *Fp* compared to WT, indicating that SA promotes FCR resistance. Using RNA-sequencing and transcriptomic analysis performed on *nahG* and WT *Brachypodium* under basal growth and *Fp* inoculated conditions, candidate genes and pathways involved in defence and reliant on SA were identified. Based on transcriptomic changes, deposition of lignin and accumulation of defence-related proteins appear to be among the processes regulated by SA in mediating resistance. This investigation has highlighted the importance of SA in conferring resistance towards *Fp*, while providing avenues for

further research by identifying SA-responsive genes in the host that could affect the severity of FCR.

Lastly, I investigated how *Fp* adapts to SA-associated defences *in planta* by examining differentially expressed fungal genes during infection of SA-deficient *nahG Brachypodium*. The *Fp* gene F*PSE_08867* was down-regulated during infection of SA-deficient plants, and further characterized for a putative role in benzoic acid (BA) metabolism and virulence. Through phylogenetic and syntenic analysis, *FPSE_08867* was identified as a member of a partially conserved gene cluster in *Fp* and several other *Fusarium* species. An earlier automated annotation of *FPSE_08867* predicted it to encode a cytochrome P450 enzyme (CYP) with benzoate parahydroxylase (*bph*) activity. However, further phylogenetic analysis revealed that *FPSE_08867* did not cluster with other known *bph* enzymes, but rather clustered with CYPs involved with mycotoxin biosynthesis. This indicated that the original automated annotation of this gene was incorrect. To further investigate the function of FPSE_08867, I created three independent knockout lines (Δ*fpse_08867)*. Δ*fpse_08867* knockouts did not exhibit altered sensitivities towards exogenous SA or BA but mostly displayed enhanced FCR virulence on wheat and *Brachypodium* seedlings and appeared to lack the polyketide mycotoxin pigment aurofusarin. Whilst the exact function of FPSE_08867 remains to be further analysed, this investigation has provided new clues on how *Fp* adapts to SA-associated defences and identified a candidate gene that can be manipulated to affect *Fp* virulence.

To conclude, this PhD project has utilised a variety of transgenic lines and approaches to examine how candidate genes *BdPFT1* and *FPSE_08867*, and the phytohormone SA contribute towards the development of FCR. The project has generated knowledge on host and pathogen genes and pathways that contribute to FCR, and genetic resources to facilitate future research aimed at reducing the impact of FCR on wheat and barley yields in Australia.

Declaration by author

This thesis is composed of my original work, and contains *no material previously published or written by another person except where due reference has been made in the text. I have clearly stated the contribution by others to jointly-authored works* that I have included in my thesis.

I have clearly stated the contribution of others to my thesis as a whole, including statistical assistance, survey design, data analysis, significant technical procedures, professional editorial advice, financial support and any other original research work used or reported in my thesis. The content of my thesis is the result of work I have carried out since the commencement of my higher degree by research candidature and does not include a substantial part of work that has been submitted *to qualify for the award of any* other degree or diploma in any university or other tertiary institution. I have clearly stated which parts of my thesis, if any, have been submitted to qualify for another award.

I acknowledge that an electronic copy of my thesis must be lodged with the University Library and, subject to the policy and procedures of The University of Queensland, the thesis be made available for research and study in accordance with the Copyright Act 1968 unless a period of embargo has been approved by the Dean of the Graduate School.

I acknowledge that copyright of all material contained in my thesis resides with the copyright holder(s) of that material. Where appropriate I have obtained copyright permission from the copyright holder to reproduce material in this thesis and have sought permission from co-authors for any jointly authored works included in the thesis.

Publications included in this thesis

None

Submitted manuscripts included in this thesis

None

Other publications during candidature

Peer reviewed papers

None

Book chapters

None

Conference Abstracts

Turner M.H., Gursanscky N.R., Taochy C., Cao J. Coleman M., McKeough L., Fletcher S.J, Kazan K and Carroll B.J. PLEIOTROPIC REGULATORY LOCUS 1 is required for root to shoot transmission of RNA silencing in *Arabidopsis* embryos and seedlings, ComBio2016, Brisbane, Australia

Contributions by others to the thesis

Kemal Kazan, Bernard Carroll and Jonathan Powell contributed to experimental design in all research chapters as well as writing and editing of thesis. Jonathan Powell transformed initial T0 lines for the BdPFT1-OE and BdPFT1-RNAi lines for Chapter 2. Jonathan Powell generated initial lines and performed initial characterisation of the *nahG* lines (transgene expression, SA measurements and generated RNAseq data for *nahG* vs WT *Brachypodium* under basal growth and *Fp* innoculated for Chapter 3. Donald Gardiner supplied the vector construct used for transforming the fungal knockouts for Chapter 4.

Statements of parts of the thesis submitted to qualify for the award of another degree

No works submitted towards another degree have been included in this thesis

Research involving human or animal subjects

No animal or human subjects were involved in this research

Financial support

This research was supported by an Australian Government Research Training Program Scholarship'

Keywords

brachypodium, *fusarium*, wheat, *nahG*, PFT1, transgenic, salicylic acid

Australian and New Zealand Standard Research Classifications (ANZSRC)

ANZSRC code: 060405 Gene Expression

ANZSRC code: 060702 Plant Cell and Molecular Biology

ANZSRC code: 070308 Crop and Pasture Protection (Pests, Diseases and Weeds)

Fields of Research (FoR) Classification

FoR code: 0604, Genetics, 40%
FoR code: 0605, Microbiology, 20%
FoR code: 0607, Plant Science, 40%

Dedications

Wow, what a ride! I'd never thought I would have the opportunity to undertake and complete a PhD project. This achievement has only been made possible by the people around me, who have provided support, encouragement and understanding. It's difficult for me to put into words the impact they have had on me; hence, I would like to take this opportunity to provide a heartfelt genuine thank you.

Thank you to the Australian Federal Government for the provision of a scholarship, without which I would never have been able to undertake a PhD.

Thank you to my PhD supervisor team; Professor Bernard Carroll, Professor Kemal Kazan and Doctor Jonathan Powell. Thank you to my CSIRO line manager and associate supervisor Doctor Donald Gardiner. My supervisory team are outstanding with the amount of support, guidance and friendship they have provided throughout my project.

Thank you to my lab colleagues for answering my questions, looking out for me, and showing me how various scientific apparatus work.

Thank you to my fellow PhD student, lab mate, and friend Mohammed Khudair. I appreciated your humour and the 'Friday Parties' we shared.

Thank you to Brenton Lang and the team at Microelectronics Technology (M*e*T) at Brisbane Technology park for allowing me use of your office space, during the time I was writing my PhD thesis.

Thank you to my supportive family, parents, grandparents, and brother, who without their support, encouragement and belief I would never have achieved as much as I have.

Table of Contents

List of Figures

Figure 4.12: Δ*fpse08667* isolates do not show altered mycelial growth in Potato Dextrose Broth amended with 12.5mM Citrate Buffer System, buffered at 4.6pH, 0.06% DMSO (V:V) and supplemented with 0.58mM benzoic acid or 1.56mM salicylic acid.

List of Tables

List of Abbreviations

Abbreviation	Term
ACC	1-aminocyclopropane carboxylic acid
ACD	ACC-DEAMINASE
ACID	Activator Interactor Domain
ANOVA	Analysis of variance
AOS	ALLENE OXIDE SYNTHASE
BA	Benzoic acid
bp	Basepair
bph	Benzoate parahydroxylase
BRs	Brassinosteroids
CDK8	CYCLIN DEPENDENT KINASE 8
cDNA	complementary DNA
CKs	Cytokinins
CO	CONSTANS
CYP	CYTOCHROME P450
DAB	3,3'-Diamonbenzidine
DNA	Deoxyribonucleic acid
DON	Deoxynivalenol
dpi	days post inoculation
EDS1	ENHANCED DISEASE SUSCEPTIBILITY 1
EIL1	ETHYLENE INSENSTIVE3-LIKE1
ERF1	ETHYLENE RESPONSE FACTOR1
ET	Ethylene
FCKs	*Fusarium* cytokinins
FCR	Fusarium crown rot
Ff	*Fusarium fujikuroi*
Fg	*Fusarium graminearum*
FHB	Fusarium head blight
FLC	FLOWERING LOCUS C
Fo	*Fusarium oxysporum*
Fp	*Fusarium pseudograminearum*
FT	FLOWERING LOCUS T
FUL	FRUITFULL
Fv	*Fusarium verticilloides*
GST	Glutathione-S-transferase
HP	Hairpin
HR	Hypersensitive response
HY5	ELONGATED HYPOCOTYL 5
IAA	Auxin
JA	Jasmonic acid
JAZs	Jasmonate Zim Domain proteins
LC-MS	Liquid chromatography mass spectroscopy
LFY	LEAFY
LSD1	LEISION SIMULATING DISEASE 1
MANOVA	Multivariate analysis of variance

Mbp	Mega basepairs
MBR1	MED25-BINDING RING-H2
MED16	MEDIATIOR 16
MED25	MEDIATOR 25
MGCs	Metabolic gene clusters
min	minute
nahG	*Pseudomonas putida* salicylate hydroxylase G
NBT	nitroblue tetrazolium
OE	Overexpressor
OETC	Overexpressor transformant control
OPR	12-OXYPHYTODIENOATE REDUCTASE OCTADECANOID-RESPONSIVE
ORA59	ARABIDOPSIS AP2/ERF59
PAD4	PHYTOALEXIN DEFECIENT 4
PAL1	PHENYLALANINE AMMONIA LYASE 1
PCR	Polymerase chain reaction
PFT1	PHYTOCHROME and FLOWERING TIME 1
PHY	Phytochrome
pol II	RNA polymerase II
PRX	PEROXIDASE
qRT-PCR	quantitative Real Time PCR
QTL	Quantitative Trait Loci
RNA	Ribonucleic acid
RNAi	RNA interference
RNA-seq	RNA sequencing
ROS	Reactive oxygen species
SA	Salicylic acid
SAR	Systemic acquired resistance
sec	second
SPL10	SQUASMASA PROMOTER BINDING PROTIEN-LIKE10
TAE	Tris base acetic acid and EDTA
TCP	TEOSINTE BRANCHED/CYCLOIDEA/PCF
TF	Transcription factor
UBC18	UBIQUITIN CONJUGATING ENZYME 18
V	volts
vWF-A	von Willebrand Factor type A
WT	Wild type
Xt	*Xanthomonas translucens*

Chapter 1

Literature Review and Project Overview

1.1 Literature Review

1.1.1 Overview of Fusarium Crown Rot economics and causes in Australia

Fusarium Crown Rot (FCR) is a disease of economic concern that is impacting the wheat and barley cropping industries in Australia (Akinsanmi et al., 2004, Burgess et al., 1975), New Zealand (Cromey et al., 2006), China (Ji et al., 2016, Li et al., 2012, Xu et al., 2015, Zhang et al., 2015), the Middle East (Alkadri et al., 2013, Hameed et al., 2012, Pouzeshimiab et al., 2016, Saremi et al., 2007, Tunali et al., 2006, Tunali et al., 2008), North Africa (Gargouri et al., 2011, Kammoun et al., 2009), and regions of North (Cook, 1968, Cook, 1980, Fernandez and Zentner, 2005, Mishra et al., 2006, Smiley et al., 2005a, Smiley and Patterson, 1996) and South America (Castañares et al., 2012). The use of FCR resistant wheat cultivars is a potential economically and environmentally sustainable management technique for grain growers. Evidence for the existence of large-effect Quantitative Trait Loci (QTL), conferring FCR resistance in wheat (Bovill et al., 2010, Ma et al., 2010, Zheng et al., 2014) and barley (Chen et al., 2013) suggests it could be feasible to breed highly FCR resistant wheat and barley varieties. To date, however, no specific genes underlying these QTL have been identified and cloned (Liu and Ogbonnaya, 2015).

Despite the ability of multiple *Fusarium* species to cause FCR, the hemi-biotroph *Fusarium pseudograminearum* (*Fp*) is the most frequently isolated species from FCR affected crops in Australia, and it is considered to be the predominant causative agent (Akinsanmi et al., 2004, Backhouse et al., 2004, Backhouse and Burgess, 2002, Burgess et al., 1975, Khangura et al., 2013, McKnight and Hart, 1966). In the field, a common pathway for *Fp* infection is through the cereal's coleoptile tissue before progressing to the sub-crown internode, then the stem epidermal tissue, and later colonising the vascular tissue. The resulting symptomatic development of FCR includes browning of the stem and leaf sheaths (Knight and Sutherland, 2016, Knight and Sutherland, 2013a, Knight and Sutherland, 2013b) as well as the formation of white heads. White head formation represents the premature senescence of wheat heads, leading to shrivelled or absent grain development. Colonisation of the vascular tissue by *Fp* mycelia has been reported to block the transport of water and nutrients within the plant, which most likely interrupts seed fill and contributes to formation of

white heads (Burgess et al., 2001, Knight and Sutherland, 2016, Smiley, 2009). This is further supported by the incidence of white head formation increasing under drought stress (Smiley, 2009, Hollaway et al., 2013). Consequently, there is a positive correlation between incidence and severity of FCR and reduction of grain yield and quality in cereals (Smiley et al., 2005b). In Australia, the estimated average annual FCR related loss to the wheat industry is approximately 10% of yield, costing $88 million Australian dollars, with losses potentially increasing under favourable environmental conditions or lack of disease control (Murray and Brennan, 2009). Hence *Fp* is an economically important pathogen in Australia.

1.1.2 Infection process of *Fusarium pseudograminearum*

Fp is capable of aseuxally producing a thick-walled resting structure called a chlamydospore (Figure. 1.1). Chlamydospores enable *Fusarium* to become dormant and have been reported to persist in the the enivornment for up to 16 months for a variety of species (Couteaudier and Alabouvette, 1990, Sitton and Cook, 1981, Nyvall, 1970). Presently, the contribution of chlamydospores as a source of inoculum has not been reported (Kazan and Gardiner, 2018). The ability for *Fp* to remain dormant makes it a difficult pathogen to eradicate, once its inoculum is present within the soil. The principal source of FCR inoculum in field cropping environments is thought to be infected stubble left over from previous years' crops. *Fp* can remain viable on stubble for up to three years (Burgess, 2005). During infection of the wheat stem base, *Fp* has been demonstrated to produce mycotoxins such as trichothecene deoxynivalenol (DON) (Mudge et al., 2006). DON is a potent inhibitor of eukaryotic protein synthesis (Rotter, 1996). Consequently, DON contaminated grain is unfit for consumption by humans and livestock (Bennett and Klich, 2003). Jansen et al. (2005) reported that DON's functional role is surpressing the thickening of plant cell wall during fungal colonisation of the host. Mudge et al. (2006) demonstrated that *Fp* mutants defective in DON production have a reduced ability to colonise wheat stems, despite no difference in symptom development being observed when compared with wild-type (WT) *Fp*. This reflects previous reports where DON defective *Fg* strains cause Fusarium Head Blight (FHB) symptoms but cannot colonise the wheat heads (Bai et al., 2002, Okubara et al., 2002, Proctor et al., 1995). It is thought that the development of FCR sypmtoms, i.e. necrosis at the stem crown and base, interferes with water and

nutrient transport leading to unfilled grain and eventually plant death (Burgess et al., 2001).

1.1.3 FCR disease management techniques

A variety of different disease control measures exist for the management of FCR, with each varying in their efficacy and practicality for economic and implementation reasons (reviewed by Alahmad et al., 2018). Current fungicide seed coating treatments have been found to be ineffective as chemical control measures for FCR in the field. This is because whilst the fungicide treatment is effective at reducing seedling damping-off, no long-term protective benefit is gained beyond the seedling stage and FCR infection can occur throughout the season contributing to the inoculum load of the next season (Lamprecht et al. 1990 Balmas et al. 2006; Akgul and Erkilic 2016, Simpfendorfer 2016). Field application of the commercial chemical spray Prosaro, (active ingredients: tebuconazole + prothioconazole) produced by Bayer Crop Science was reported to increase wheat yield under FCR infection but still failed to achieve full yield potential in absence of FCR, indicating incomplete control of FCR (Simpfendorfer et al., 2014).

Cultural methods of disease control refer to agronomic decisions such as land management, crop rotation and use resistant or tolerant crop varieties to minimize inoculum load and disease incidence. Since the 1970s, increased adoption of minimum till soil management practices, to reduce erosion (Crofts et al. 1988) and increase retention of water content (Harte and Armstrong 1983), has appeared to facilitate increased inoculum load and FCR incidence (reviewed by Chakraborty et al., 2006; Paulitz, 2006; Paulitz et al., 2002). This is due to the ability of *Fp* to survive in wheat stubble, left over from harvesting, for up to three years and that the stubble creates damp microclimates after rain promoting infection (Burgess, 2014; Summerell and Burgess, 1988; Summerell et al., 1989, 1990). Minimising seedling contact with infected stubble through interrow can reduce FCR incidence in with presence of high inoculum loads (Burgess et al., 2001, Verrell et al., 2009; Bentley et al., 2009., Simpfendorfer et al 2012, Verrel et al., 2017). Furthermore, crop rotations from wheat to non-host crops such as chickpea, faba bean, canola, lupins and sorghum have been demonstrated to reduce inoculum load and hence incidence of FCR in the field

(Burgess et al., 1993, Burgess et al., 1996, Wildermuth et al., 1997, Evans et al., 2010). However, the choice and ability to implement a crop rotation sequence can be influenced by current economic market forces, governmental policy and social conditions (Maaz et al., 2018).

Currently there is no completely FCR resistant cultivar of wheat available, at least not with desirable agronomic traits such as high yield and grain quality. Older varieties of wheat such as Sunco, Kukri, Baxter, Lang, Gluyas Early, offer partial resistance to FCR but are relatively low yielding. Varietal differences in resistance towards disease in the same species can be due to difference in gene expression, particularly the level or timing of defence gene expression (Adhikari et al., 2007, Desmond et al., 2008). Consequently, the manipulation of gene expression or disease inducible signalling pathway components can improve pathogen resistance (Pasonen et al., 2004, Way et al., 2002, Kazan et al., 1998).

Resistance towards FCR in wheat is a quantitative trait, meaning that many genes most likely contribute to resistance (Bovill et al., 2006, reviewed by Liu and Ogbannaya, 2015). Multiple Quantitative Trait Loci (QTL) and their chromosomal regions have been identified that contribute to resistance (Bovill et al. 2006, Collard et al. 2005a, Liu et al. 2011); however, the gene/s underlying each QTL have not been cloned and identified. Pyramiding QTL through breeding practices and incorporating other traits such as high osmoregulation to limit water stress has been proposed for obtaining high levels of FCR resistance (Collard et al. 2005a; Wildermuth and Morgan 2004, Bovill et al., 2006). One of the key limitations of FCR resistance breeding is the lack of knowledge for the genetic basis of resistance and the development of additional markers for marker-assisted selection (Collard et al. 2005a. Liu and Ogbannaya, 2015). Hence, with a better understanding of the genetic basis of host responses toward *Fp* infection, breeders will be able to target key genes for introgression or exclusion in breeding programs to improve FCR resistance.

1.1.4 Wheat gene expression changes in response to *Fusarium pseudograminearum* infection

Currently there is a limited understanding of the signaling mechanisms that regulate wheat plant defense against FCR. *Fp* infection has been found to induce expression of genes in wheat seedlings and stem base tissue with mainly defensive functions, such as genes encoding anti-microbial proteins, oxidative stress-related proteins, signaling molecules and proteins involved in primary and secondary metabolism (Desmond et al., 2008, Powell et al., 2016). Powell et al. (2016) reported 30 transcription factors including 16 WRKYs, four MYBs, five NACs and three bHLHs, as being differentially expressed with *Fp* infection. Interestingly, the *Fp* inducible genes share a significant overlap with genes induced by the biotrophic rust pathogen *Puccinia triticina*, excluding the oxidative stress-related genes (Desmond et al., 2008). Furthermore, many of these *Fp* inducible genes were also responsive to application of the hormones jasmonic acid (JA) and salicylic acid (SA) hormone, and to DON treatment (Desmond et al., 2008, Desmond et al., 2006). Taken together, these results (Desmond et al., 2006, Desmond et al., 2008, Powell et al., 2016) suggest that JA- and SA-mediated gene expression plays a role in wheat's response to *Fp* infection.

1.1.5 Plant hormones co-ordinate defence

Plants have finite energy resources that must be appropriately apportioned towards growth, maintenance, reproduction and pathogen defence. To mount a successful defence response, the plant must correctly identify the attacking pathogen and respond accordingly with suitable timing and magnitude. To co-ordinate responses towards pathogen incursion, plants have evolved an intricate network of defence signaling pathways that can induce gene expression locally and systemically in non-inoculated tissues (Fu and Dong, 2013, Pieterse et al., 2014). Components of the plant defense signaling networks include but are not limited to hormones and transcription factors. Plant hormones, hereby referred to as phytohormones, are chemical messenger molecules capable of affecting specific adaptive physiological responses at a systemic (whole organism) level. Phytohormones mediate defense responses by inducing selective expression of transcription factors (TFs), which then in turn induce the selective expression of downstream defense pathways. In scientific literature, the

phytohormones SA, JA and ethylene (ET) have been described as playing a role in mediating plant defense responses locally and systemically (Fu and Dong, 2013, Pieterse et al., 2014).

During pathogen infection, the host plant's defence responses are underpinned by phytohormone signalling, leading to transcriptional reprogramming and defence gene expression (Pieterse et al., 2012, Pieterse et al., 2009). SA is considered to be the classic defence hormone mediating responses against biotrophic and hemi-biotrophic pathogens during their initial biotrophic phase (see review by Glazebrook (2005)). Whereas JA operates synergistically with ET, and has been classically described in *Arabidopsis* to mediate defence against necrotrophs (Glazebrook, 2005). Further, it has been well established that JA/ET and SA signalling pathways antagonistically regulate each other (Pieterse et al., 2009, Spoel et al., 2007, Kloek et al., 2001). SA potentiates the hypersensitive response (HR) pathway, whereby reactive oxygen species (ROS) production leads to cell death, denying the attacking pathogen living tissue as a source of nutrition (Greenberg et al., 1994, Lam et al., 2001, Chen et al., 1993). Additionally, SA responses lead to localised fortification of plant cell walls to contain the incurring pathogen (Halim et al., 2007), production of antimicrobials, and priming of defence gene expression in uninfected leaves in a phenomenon termed systemic acquired resistance (SAR) (Delaney et al., 1994, Gaffney et al., 1993). In addition to contributing to defence against necrotrophic pathogens, JA/ET-mediated gene expression is important for adaptive responses towards abiotic stress (see review Kazan (2015)) and insect pests (see review by Yan and Xie (2015).

1.1.6 Roles of SA and JA in Fusarium defence

SA accumulation-deficiency in wheat and its model species *Brachypodium*, has reportedly enhanced susceptibility towards FHB caused by *Fg* and FCR caused by *Fp* infection, respectively (Makandar et al., 2012, Powell et al., unpub). Interestingly, SA may also have an antifungal role because it has an inhibitory effect on *Fg* growth under acidic pH conditions (Qi et al., 2012). Through infection assays and gene expression studies, JA treatment has been shown to attenuate SA-related defence gene expression (Makandar et al., 2010, Makandar et al., 2012) but delay symptom development from *Fp* (Desmond et al., 2006) and *Fusarium culmorum* (*Fc*) (Motallebi

et al., 2015) infection. Hence, SA-signalling is likely to contribute towards resistance by limiting *Fusarium* infection during the initial biotrophic phase; whereas, JA signalling is proposed to have a dichotomous role by attenuating SA-signalling during initial infection but promoting resistance during the necrotrophic phase of *Fusarium* infection (Makandar et al., 2010, Makandar et al., 2012, Motallebi et al., 2015, Desmond et al., 2006).

1.1.7 Manipulation of phytohormone signalling by *Fusarium*

SA and other phytohormones such as JA, ET, auxin (IAA), cytokinins (CKs), brassinosteroids (BRs) and abscisic acid (ABA), have been described to interact with each other in a complex manner to fine tune defence and development (Pieterse et al., 2012, Pieterse et al., 2009). Given the underpinning importance of phytohormones in defence, it is not surprising that *Fusarium* and other microbes have evolved and/or acquired the ability to manipulate plant phytohormones (Han and Kahmann, 2019).

As mentioned previously, under acidic conditions, SA has an inhibitory effect on *Fg* spore germination and mycelial growth (Qi et al., 2012); however, under basic conditions *Fg* is able to metabolise SA as a carbon source. Recent investigations have characterised several SA-responsive *Fg* enzymes involved in SA metabolism, including but not limited to a salicylate hydroxylase (FgShy1) (Hao et al., 2018), a catechol 1,2-dioxygenase (FGSG_03667) and a 2,3-dihydroxybenzoic acid decarboxylase (FGSG_09061) (Rocheleau et al., 2019). Both FgShy1 and FGSG_03667 were identified as the first two enzymes for oxidative SA degradation via catechol leading into the β-ketoadipate pathway, while the activity of FGSG_09061 indicates the presence of a non-oxidative pathway for the conversion of SA to catechol (Rocheleau et al., 2019). The contribution of FpShy1 to SA degradation appears inconsistent with reports of complete abolishment (Rocheleau et al., 2019) and partial impairment (Hao et al., 2018) of SA degradation abilities in FpSHY1 knockout mutants. Analysis of independent knockout mutants of FGSG_03367 and FGSG_09061 revealed complete and partial impairment of SA degradation, respectively (Rocheleau et al., 2019). The role of SA degradation on *Fusarium* pathogenesis has been questioned as independent knockout lines of *FgShy1 (Hao et al., 2018)* and *FGSG_03367* (Rocheleau et al., 2019) did not alter virulence in wheat. Indeed, additional components of the SA pathway need to be characterized to understand the

role of SA degradation by *Fusarium*. If *Fg* is capable of degrading SA to the detriment of the host plant, then given the genetic relatedness of *Fg* to *Fp* (Figure 1.2), it is likely that *Fp* is also capable of degrading SA. JA is a classic defence hormone reported to mediate defence against necrotrophs and operate antagonistically towards SA signalling (Glazebrook, 2005). By secreting the SIX4 effector (Thatcher et al., 2012) and producing bioactive JA (Cole et al., 2014), *Fusarium oxysporum* (*Fo*) can induce JA-signalling in *Arabidopsis.* This leads to increased senescence-associated gene expression and disease susceptibility (Thatcher et al., 2009b). Relatedly, *Fg* can degrade 1-aminocyclopropane carboxylic acid (ACC), a precursor for production of ET (Svoboda et al., 2019), through an encoded ACC-Deaminase (ACD). As mentioned earlier, ET synergistically interacts with JA during defence signalling against necrotrophs (Li et al., 2019, Van der Ent and Pieterse, 2018, Broekaert et al., 2006). Svoboda et al. (2019) hypothesized that degradation of ACC may interfere with the JA/ET-mediated signalling during the necrotrophic phase of *Fg*'s lifecycle. However, no differences in virulence were observed in ACD knockouts.

Interestingly, *Fp* has recently been described to induce cytokinin signalling during initial infection (Blum et al., 2019, Sørensen et al., 2018) by production of cytokinin-like molecules, referred to as *Fusarium* cytokinins (FCKs) (Sørensen et al., 2018). Plant cytokinins are responsible for growth promotion, cell differentiation and delaying senescence in plants (Ferreira and Kieber, 2005). Remarkably, the FCK biosynthetic gene cluster is present in homologous clusters in *Fo*, *F. fujikuroi*, *F. verticilloides* but not in the closely related fungi *Fg* (Sørensen et al., 2018). Furthermore, despite evidence that the FCK cluster is upregulated during initial infection (Blum et al., 2019), no differences in virulence were reported in knockout strains of *Fo*, *Ff and Fv* (Sørensen et al., 2018).

Secondary metabolite production by metabolic gene clusters (MGCs) in fungal pathogens (Keller, 2015) are often associated with adaptive metabolic processes, such as phytohormone manipulation, and ecological phenotypes (Thynne et al., 2019, Gluck‐Thaler et al., 2018). MGCs are comprised of co-ordinately expressed neighbouring genes, with some individual gene components playing supportive functions like regulation, transport and self-protection from the encoded metabolite if

required (Kjærbølling et al., 2019). Evolution of secondary metabolism can occur from gene duplication or horizontal gene transfer events of gene modules or MGCs (reviewed by Wisecaver et al. (2014)). There is extensive evidence of horizontal gene transfer events affecting virulence in multiple *Fusarium* species (Ma et al., 2013) including: *Fo* (Czislowski et al., 2018, Laurence et al., 2015, van Dam and Rep, 2017, Vlaardingerbroek et al., 2016), *Fv* (Khaldi and Wolfe, 2011), *Fg* (Sieber et al., 2014) and *Fg* (Gardiner et al., 2012).

1.2 Project overview

As previously mentioned Fusarium Crown Rot (FCR) is a significant wheat and barley disease of economic concern globally and is predominantly caused by the fungal pathogen *Fusarium pseudograminearum* (*Fp*) in Australia (Kazan and Gardiner, 2018). Control measures for FCR often involve inoculum load management techniques but due to environmental or socioeconomic reasons can be unsuitable and difficult to implement (Maaz et al., 2018). Hence, development of a high-yielding, highly resistant wheat variety represents a feasible strategy for protection against FCR (Liu and Ogbonnaya, 2015). Resistance to FCR is conferred by quantitative trait loci (QTLs); however, presently no gene/s underlying a QTL have been cloned and identified (Liu and Ogbonnaya, 2015). Given the importance of phytohormones as underlying regulators of defence signaling, their genetic regulatory networks represent candidates for modification to improve FCR resistance. Further, to gain a comprehensive insight into the *Fp*:plant interaction it is important to understand how *Fp* adapts to host defence responses. Hence, with improved understanding of the genetic basis of *Fp* host interactions, breeders will be able to target key genes and defense pathways for modification/s through traditional or molecular approaches to improve FCR resistance

1.2.1 Candidate gene *PHYTOCHROME FLOWERING TIME1*

PHYTOCHROME FLOWERING TIME1 (*PFT1*) encodes MEDIATOR25, a subunit of the mediator complex (Bäckström et al., 2007). The mediator complex is highly conserved throughout Eukarya, and acts as an adaptor that fine-tunes regulatory

inputs from transcription factor activators and repressors of RNA polymerase II (Kim et al., 1994, Koleske and Young, 1994, Malik and Roeder, 2005). *PFT1* was first identified as a positive regulator of flowering time in *Arabidopsis* (Cerdán and Chory, 2003). Subsequently, PFT1 has been extensively characterised in *Arabidopsis* and found to be involved in multiple processes including growth (Seguela-Arnaud et al., 2015) and development (Raya-González et al., 2014, Sundaravelpandian et al., 2013), light signalling (Klose et al., 2012, Koprivova et al., 2014), modulation of reactive oxygen signalling (ROS) (Sundaravelpandian et al., 2013), abiotic stress responses (Yang et al., 2014, Elfving et al., 2011) and defence signalling (Kidd et al., 2009, Wang et al., 2015, Chen et al., 2012). PFT1 is a positive regulator of JA signalling in *Arabidopsis* and is required for uncompromised JA-dependent defense gene expression and resistance towards necrotrophic pathogens *A. brassicicola* and *B. cinerea* (Kidd et al., 2009). Further, PFT1 confers susceptibility towards the hemi-biotrophic *F. oxysporum* in a JA-dependent manner (Kidd et al., 2009, Thatcher et al., 2009a). Whilst there is evidence for a conserved role between *Arabidopsis* and wheat (Kidd et al., 2009), investigations into the role of *TaPFT1* in wheat defence are limited due to genetic complexities of wheat (Fitzgerald et al., 2015b, Liu et al., 2016). Hence, the use of a representative model organism is a valid approach to further research into genetic interactions between cereals and pathogenic *Fusarium* (Ankeny and Leonelli, 2011).

1.2.2 *Brachypodium* as a model to study *Fp*-host interactions

Previously, *Arabidopsis thaliana* has served as a model plant species and has offered insights into *Fusarium* plant interactions. However, due to differences in physiology of monocots, the dicot *Arabidopsis* may not be representative of the family Poaceae which includes wheat, corn and rice. However, *Brachypodium distachyon* is a member of the Poaceae family and is emerging as a tractable model for cereal crops (Fitzgerald et al., 2015a). *Brachypodium* offers several advantages as a model organism. *Brachypodium's* small physical stature, lack of quarantine or intellectual property restrictions, and relatively quick generation time of as short as 8 weeks facilitate laboratory-based research. Further *Brachypodium* is transformable and ideal for forward and reverse genetic screens, with a wide collection of mutant lines (both T-DNA insertions and chemically induced) available for research (Thole et al., 2010,

Bragg et al., 2012, Dalmais et al., 2013). Additionally, *Brachypodium* has a small diploid genome (272Mbp) that has been sequenced and a variety of RNA-seq datasets performed on plants grown under differing conditions are available (Vogel and Bragg, 2009, Garvin et al., 2008, Vain, 2011, Brkljacic et al., 2011. Importantly, *Brachypodium* has been demonstrated to be a host for a variety of economically relevant pathogens including *Fp*. Brachypodium has been reported as having high genetic synteny with wheat and rice (Huo et al., 2009, Molnár et al., 2013), and recently as possessing a similar global transcriptomic response as wheat under *Fp* inoculated conditions (Powell et al., 2017), further reinforcing *Brachypodium*'s position as a tractable model pathosystem to investigate *Poaceae* grass responses towards *Fp* infection.

1.2.3 Current study aims

Previously, Powell (2016) further developed *Brachypodium* as a model for studying FCR by generating transformed lines constitutively expressing a bacterial enzyme, *nahG* (Van Wees and Glazebrook, 2003), capable of degrading SA. Powell (2016) also produced transgenic overexpression and knockdown lines for *BdPFT1.* Consequently, the current study has selected the host model patho-system of *Brachypodium* and *Fp* to investigate the molecular mechanisms of SA and *BdPFT1* in pathogen virulence and host responses in cereal plants towards FCR. Further analysis of how *Fp* adapts to host environment, particularly a host deficient in SA, and characterisation of a fungal candidate pathogenicity gene has been conducted. The outcomes of this study are to generate increased knowledge of the mechanisms for *Fp* virulence and/or resistance in a model host *Brachypodium* with possible applications for the development of FCR resistant cereal varieties.

1.3 Figures

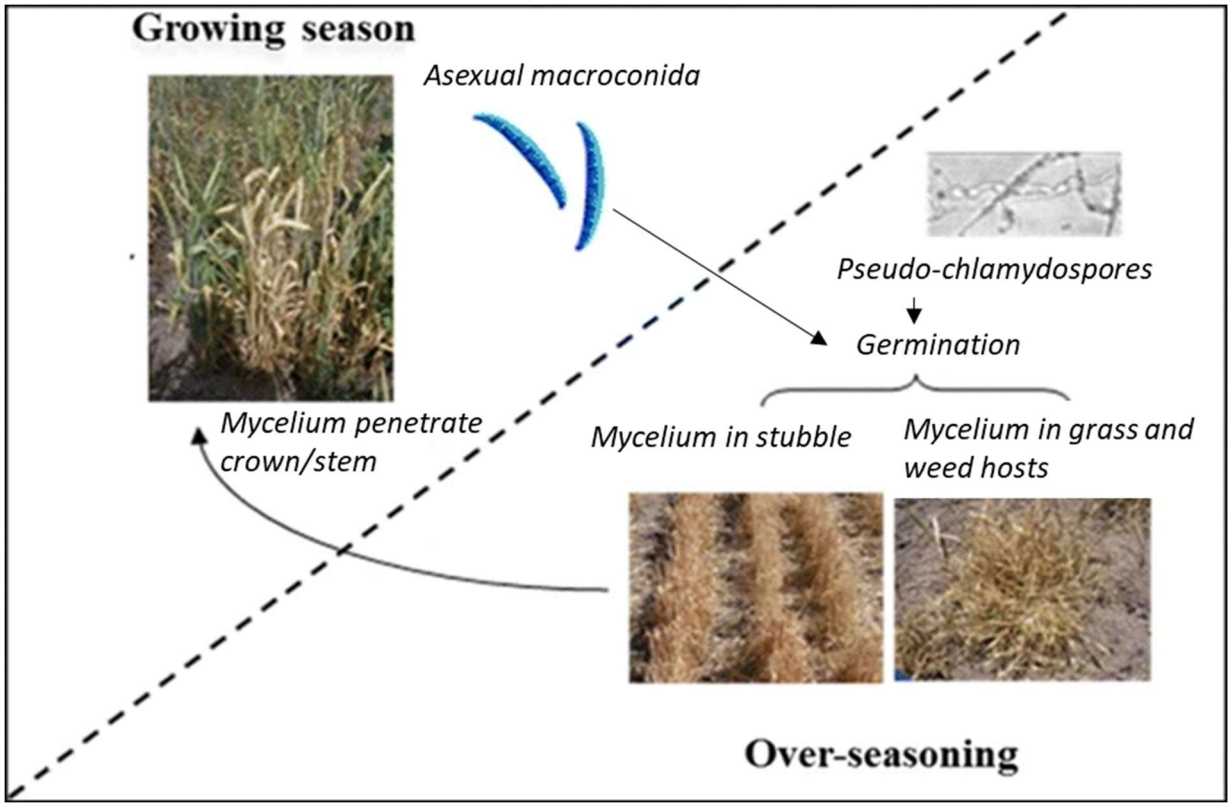

Figure 1.1: Diagram illustrating generalised life cycle of *Fusarium pseudograminearum* during wheat growing season and over-seasoning. Figure adapted from Alahmad et al. (2018)

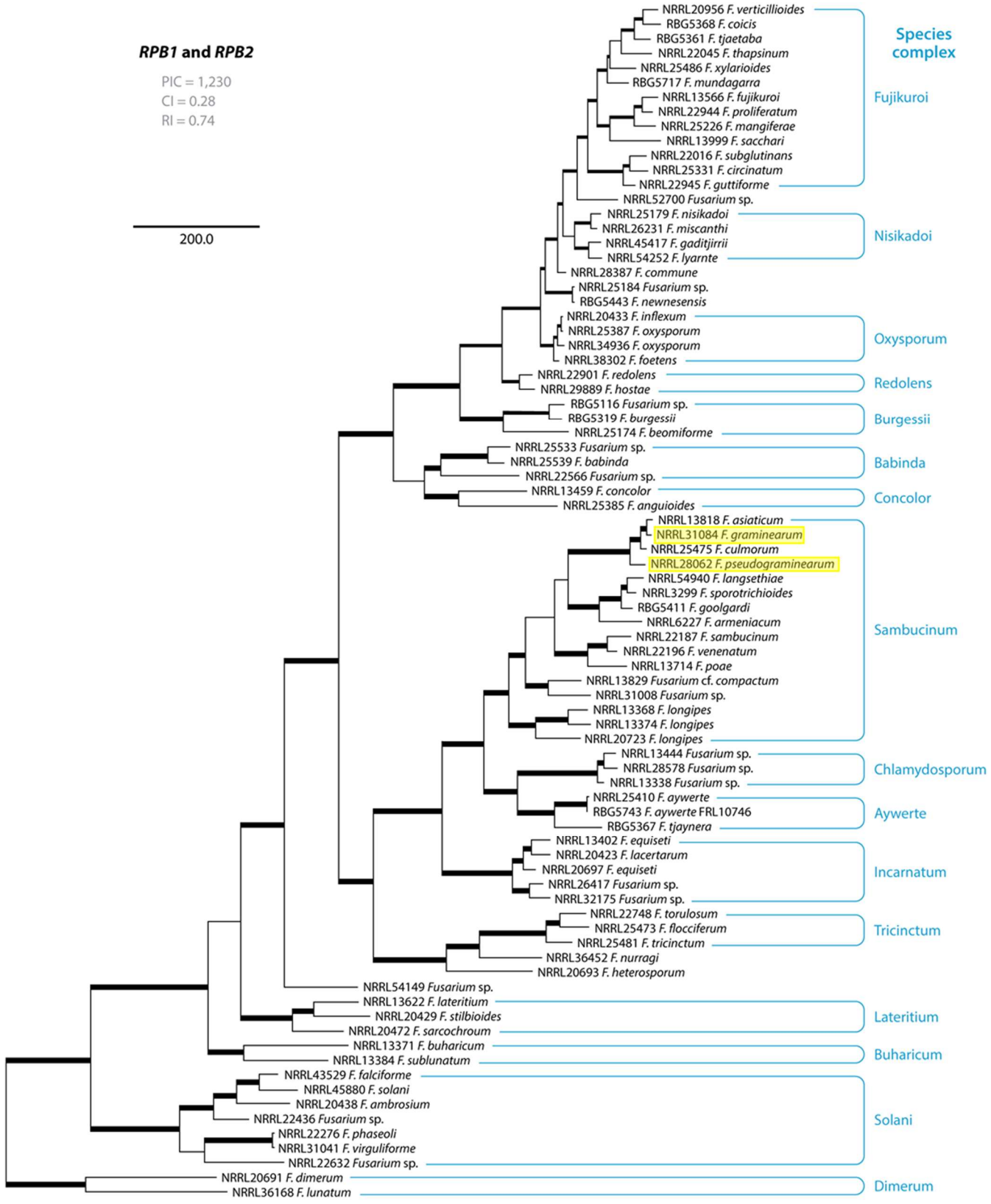
RPB1 and RPB2
PIC = 1,230
CI = 0.28
RI = 0.74
200.0
Species complex
NRRL20956 F. verticillioides
RBG5368 F. coicis
RBG5361 F. tjaetaba
NRRL22045 F. thapsinum
NRRL25486 F. xylarioides
RBG5717 F. mundagarra
NRRL13566 F. fujikuroi
NRRL22944 F. proliferatum
NRRL25226 F. mangiferae
NRRL13999 F. sacchari
NRRL22016 F. subglutinans
NRRL25331 F. circinatum
NRRL22945 F. guttiforme
Fujikuroi
NRRL52700 Fusarium sp.
NRRL25179 F. nisikadoi
NRRL26231 F. miscanthi
NRRL45417 F. gaditjirrii
NRRL54252 F. lyarnte
Nisikadoi
NRRL28387 F. commune
NRRL25184 Fusarium sp.
RBG5443 F. newnesensis
NRRL20433 F. inflexum
NRRL25387 F. oxysporum
NRRL34936 F. oxysporum
NRRL38302 F. foetens
Oxysporum
NRRL22901 F. redolens
NRRL29889 F. hostae
Redolens
RBG5116 Fusarium sp.
RBG5319 F. burgessii
NRRL25174 F. beomiforme
Burgessii
NRRL25533 Fusarium sp.
NRRL25539 F. babinda
NRRL22566 Fusarium sp.
Babinda
NRRL13459 F. concolor
NRRL25385 F. anguioides
Concolor
NRRL13818 F. asiaticum
NRRL31084 F. graminearum
NRRL25475 F. culmorum
NRRL28062 F. pseudograminearum
NRRL54940 F. langsethiae
NRRL3299 F. sporotrichioides
RBG5411 F. goolgardi
NRRL6227 F. armeniacum
NRRL22187 F. sambucinum
NRRL22196 F. venenatum
NRRL13714 F. poae
NRRL13829 Fusarium cf. compactum
NRRL31008 Fusarium sp.
NRRL13368 F. longipes
NRRL13374 F. longipes
NRRL20723 F. longipes
Sambucinum
NRRL13444 Fusarium sp.
NRRL28578 Fusarium sp.
NRRL13338 Fusarium sp.
Chlamydosporum
NRRL25410 F. aywerte
RBG5743 F. aywerte FRL10746
RBG5367 F. tjaynera
Aywerte
NRRL13402 F. equiseti
NRRL20423 F. lacertarum
NRRL20697 F. equiseti
NRRL26417 Fusarium sp.
NRRL32175 Fusarium sp.
Incarnatum
NRRL22748 F. torulosum
NRRL25473 F. flocciferum
NRRL25481 F. tricinctum
Tricinctum
NRRL36452 F. nurragi
NRRL20693 F. heterosporum
NRRL54149 Fusarium sp.
NRRL13622 F. lateritium
NRRL20429 F. stilbioides
NRRL20472 F. sarcochroum
Lateritium
NRRL13371 F. buharicum
NRRL13384 F. sublunatum
Buharicum
NRRL43529 F. falciforme
NRRL45880 F. solani
NRRL20438 F. ambrosium
NRRL22436 Fusarium sp.
NRRL22276 F. phaseoli
NRRL31041 F. virguliforme
NRRL22632 Fusarium sp.
Solani
NRRL20691 F. dimerum
NRRL36168 F. lunatum
Dimerum

Figure 1.2: Phylogenetic relationship of the major species complexes in *Fusarium* based on the combined data set of the second largest subunits of RNA polymerase II (RPB1 and RPB2) published from Laurence et al. (2016). *Fusarium graminearum* and *F. pseudograminearum* (highlighted in yellow) are closely related and are located in the Sambucinum species complex. PIC = preinitiation complex; CI= Confidence interval; RI = repeat interval. Figure adapted from Summerell (2019).

1.4 References

ADHIKARI, T. B., BALAJI, B., BREEDEN, J. & GOODWIN, S. B. 2007. Resistance of wheat to *Mycosphaerella graminicola* involves early and late peaks of gene expression. *Physiological and Molecular Plant Pathology,* 71**,** 55-68.

AKINSANMI, O. A., MITTER, V., SIMPFENDORFER, S., BACKHOUSE, D. & CHAKRABORTY, S. 2004. Identity and pathogenicity of *Fusarium* spp. isolated from wheat fields in Queensland and northern New South Wales. *Australian Journal of Agricultural Research,* 55**,** 97-107.

ALAHMAD, S., SIMPFENDORFER, S., BENTLEY, A. & HICKEY, L. 2018. Crown rot of wheat in Australia: *Fusarium pseudograminearum* taxonomy, population biology and disease management. *Australasian Plant Pathology,* 47**,** 285-299.

ALKADRI, D., NIPOTI, P., DÖLL, K., KARLOVSKY, P., PRODI, A. & PISI, A. 2013. Study of fungal colonization of wheat kernels in Syria with a focus on *Fusarium* species. *International journal of molecular sciences,* 14**,** 5938-5951.

ANKENY, R. A. & LEONELLI, S. 2011. What's so special about model organisms? *Studies in History and Philosophy of Science Part A,* 42**,** 313-323.

BACKHOUSE, D., ABUBAKAR, A., BURGESS, L., DENNISC, J., HOLLAWAY, G., WILDERMUTH, G., WALLWORK, H. & HENRY, F. 2004. Survey of *Fusarium* species associated with crown rot of wheat and barley in eastern Australia. *Australasian Plant Pathology,* 33**,** 255-261.

BACKHOUSE, D. & BURGESS, L. 2002. Climatic analysis of the distribution of *Fusarium graminearum*, *F. pseudograminearum* and *F. culmorum* on cereals in Australia. *Australasian Plant Pathology,* 31**,** 321-327.

BAI, G.-H., DESJARDINS, A. & PLATTNER, R. 2002. Deoxynivalenol-nonproducing *Fusarium graminearum* causes initial infection, but does not cause disease spread in wheat spikes. *Mycopathologia,* 153**,** 91-98.

BENNETT, J. W. & KLICH, M. 2003. Mycotoxins. *Clinical Microbiology Reviews,* 16**,** 497-+.

BLUM, A., BENFIELD, A. H., SØRENSEN, J. L., NIELSEN, M. R., BACHLEITNER, S., STUDT, L., BECCARI, G., COVARELLI, L., BATLEY, J. & GARDINER, D. M. 2019. Regulation of a novel Fusarium cytokinin in *Fusarium pseudograminearum*. *Fungal biology,* 123**,** 255-266.

BOVILL, W., HORNE, M., HERDE, D., DAVIS, M., WILDERMUTH, G. & SUTHERLAND, M. 2010. Pyramiding QTL increases seedling resistance to crown rot (*Fusarium pseudograminearum*) of wheat (*Triticum aestivum*). *Theoretical and Applied Genetics,* 121**,** 127-136.

BRAGG, J. N., WU, J., GORDON, S. P., GUTTMAN, M. E., THILMONY, R., LAZO, G. R., GU, Y. Q. & VOGEL, J. P. 2012. Generation and characterization of the Western Regional Research Center *Brachypodium* T-DNA insertional mutant collection. *PLoS One,* 7**,** e41916.

BROEKAERT, W. F., DELAURÉ, S. L., DE BOLLE, M. F. & CAMMUE, B. P. 2006. The role of ethylene in host-pathogen interactions. *Annu. Rev. Phytopathol.,* 44**,** 393-416.

BURGESS, L. 2005. Intermediate hosts and the management of crown rot and head blight. *Annual Report of GRDC strategic initiative on crown rot, common root rot and Fusarium head blight. Grains Research and Development Corporation, Kingston, Australia***,** 34-36.

BURGESS, L., WEARING, A. & TOUSSOUN, T. 1975. Surveys of *Fusaria* associated with crown rot of wheat in eastern Australia. *Australian Journal of Agricultural Research,* 26**,** 791-799.

BURGESS, L. W., BACKHOUSE, D., SUMMERELL, B. A. & SWAN, L. J. Crown rot of wheat. Fusarium: Paul E. Nelson Memorial Symposium. APS Press, St. Paul, Minnesota, 2001. 1-294.

CASTAÑARES, E., WEHRHAHNE, L. & STENGLEIN, S. 2012. *Fusarium pseudograminearum* associated with barley kernels in Argentina. *Plant disease,* 96**,** 763-763.

CERDÁN, P. D. & CHORY, J. 2003. Regulation of flowering time by light quality. *Nature,* 423**,** 881.

CHEN, G., LIU, Y., MA, J., ZHENG, Z., WEI, Y., MCINTYRE, C. L., ZHENG, Y.-L. & LIU, C. 2013. A novel and major quantitative trait locus for Fusarium crown rot resistance in a genotype of wild barley (*Hordeum spontaneum* L.). *PloS one,* 8**,** e58040.

CHEN, R., JIANG, H., LI, L., ZHAI, Q., QI, L., ZHOU, W., LIU, X., LI, H., ZHENG, W. & SUN, J. 2012. The Arabidopsis mediator subunit MED25 differentially regulates jasmonate and abscisic acid signaling through interacting with the MYC2 and ABI5 transcription factors. *The Plant Cell,* 24**,** 2898-2916.

CHEN, Z., SILVA, H. & KLESSIG, D. F. 1993. Active oxygen species in the induction of plant systemic acquired resistance by salicylic acid. *Science,* 262**,** 1883-1886.

COLE, S. J., YOON, A. J., FAULL, K. F. & DIENER, A. C. 2014. Host perception of jasmonates promotes infection by *Fusarium oxysporum* formae speciales that produce isoleucine‐and leucine‐conjugated jasmonates. *Molecular plant pathology,* 15**,** 589-600.

COOK, R. J. 1968. Fusarium root and foot rot of cereals in Pacific Northwest. *Phytopathology,* 58**,** 127-&.

COOK, R. J. 1980. Fusarium foot rot of wheat and its control in the Pacific Northwest. *Plant Dis,* 64**,** 1061-1066.

COUTEAUDIER, Y. & ALABOUVETTE, C. 1990. Survival and inoculum potential of conidia and chlamydospores of *Fusarium oxysporum* f. sp. lini in soil. *Canadian Journal of Microbiology,* 36**,** 551-556.

CROMEY, M., PARKES, R. & FRASER, P. 2006. Factors associated with stem base and root diseases of New Zealand wheat and barley crops. *Australasian Plant Pathology,* 35**,** 391-400.

CZISLOWSKI, E., FRASER‐SMITH, S., ZANDER, M., O'NEILL, W. T., MELDRUM, R. A., TRAN‐NGUYEN, L. T., BATLEY, J. & AITKEN, E. A. 2018. Investigation of the diversity of effector genes in the banana pathogen, *Fusarium oxysporum* f. sp. *cubense*, reveals evidence of horizontal gene transfer. *Molecular plant pathology,* 19**,** 1155-1171.

DALMAIS, M., ANTELME, S., HO-YUE-KUANG, S., WANG, Y., DARRACQ, O., D'YVOIRE, M. B., CEZARD, L., LÉGÉE, F., BLONDET, E. & ORIA, N. 2013. A TILLING platform for functional genomics in *Brachypodium distachyon*. *PLoS One,* 8**,** e65503.

DELANEY, T. P., UKNES, S., VERNOOIJ, B., FRIEDRICH, L., WEYMANN, K., NEGROTTO, D., GAFFNEY, T., GUT-RELLA, M., KESSMANN, H. & WARD, E. 1994. A central role of salicylic acid in plant disease resistance. *Science,* 266**,** 1247-1250.

DESMOND, O. J., EDGAR, C. I., MANNERS, J. M., MACLEAN, D. J., SCHENK, P. M. & KAZAN, K. 2006. Methyl jasmonate induced gene expression in wheat delays symptom development by the crown rot pathogen *Fusarium pseudograminearum*. *Physiological and Molecular Plant Pathology,* 67**,** 171-179.

DESMOND, O. J., MANNERS, J. M., SCHENK, P. M., MACLEAN, D. J. & KAZAN, K. 2008. Gene expression analysis of the wheat response to infection by *Fusarium pseudograminearum*. *Physiological and Molecular Plant Pathology,* 73**,** 40-47.

ELFVING, N., DAVOINE, C., BENLLOCH, R., BLOMBERG, J., BRÄNNSTRÖM, K., MÜLLER, D., NILSSON, A., ULFSTEDT, M., RONNE, H. & WINGSLE, G. 2011. The *Arabidopsis thaliana* Med25 mediator subunit integrates environmental cues to control plant development. *Proceedings of the National Academy of Sciences,* 108**,** 8245-8250.

FERNANDEZ, M. & ZENTNER, R. 2005. The impact of crop rotation and N fertilizer on common root rot of spring wheat in the Brown soil zone of western Canada. *Canadian journal of plant science,* 85**,** 569-575.

FERREIRA, F. J. & KIEBER, J. J. 2005. Cytokinin signaling. *Current opinion in plant biology,* 8**,** 518-525.

FITZGERALD, T. L., POWELL, J. J., SCHNEEBELI, K., HSIA, M. M., GARDINER, D. M., BRAGG, J. N., MCINTYRE, C. L., MANNERS, J. M., AYLIFFE, M. & WATT, M. 2015a. *Brachypodium* as an emerging model for cereal–pathogen interactions. *Annals of Botany,* 115**,** 717-731.

FITZGERALD, T. L., POWELL, J. J., STILLER, J., WEESE, T. L., ABE, T., ZHAO, G., JIA, J., MCINTYRE, C. L., LI, Z. & MANNERS, J. M. 2015b. An assessment of heavy ion irradiation mutagenesis for reverse genetics in wheat (*Triticum aestivum* L.). *PLoS One,* 10**,** e0117369.

FU, Z. Q. & DONG, X. 2013. Systemic acquired resistance: turning local infection into global defense. *Annual review of plant biology,* 64**,** 839-863.

GAFFNEY, T., FRIEDRICH, L., VERNOOIJ, B., NEGROTTO, D., NYE, G., UKNES, S., WARD, E., KESSMANN, H. & RYALS, J. 1993. Requirement of salicylic acid for the induction of systemic acquired resistance. *Science,* 261**,** 754-756.

GARDINER, D. M., MCDONALD, M. C., COVARELLI, L., SOLOMON, P. S., RUSU, A. G., MARSHALL, M., KAZAN, K., CHAKRABORTY, S., MCDONALD, B. A. & MANNERS, J. M. 2012. Comparative pathogenomics reveals horizontally acquired novel virulence genes in fungi infecting cereal hosts. *PLoS pathogens,* 8**,** e1002952.

GARGOURI, S., MTAT, I., KAMMOUN, L. G., ZID, M. & HAJLAOUI, M. R. 2011. Molecular genetic diversity in populations of *Fusarium pseudograminearum* from Tunisia. *Journal of phytopathology,* 159**,** 306-313.

GLAZEBROOK, J. 2005. Contrasting mechanisms of defense against biotrophic and necrotrophic pathogens. *Annu. Rev. Phytopathol.,* 43**,** 205-227.

GLUCK‐THALER, E., VIJAYAKUMAR, V. & SLOT, J. C. 2018. Fungal adaptation to plant defences through convergent assembly of metabolic modules. *Molecular ecology,* 27**,** 5120-5136.

GREENBERG, J. T., GUO, A., KLESSIG, D. F. & AUSUBEL, F. M. 1994. Programmed cell death in plants: a pathogen-triggered response activated coordinately with multiple defense functions. *Cell,* 77**,** 551-563.

HALIM, V. A., ESCHEN-LIPPOLD, L., ALTMANN, S., BIRSCHWILKS, M., SCHEEL, D. & ROSAHL, S. 2007. Salicylic acid is important for basal defense of *Solanum tuberosum* against *Phytophthora infestans*. *Molecular Plant-Microbe Interactions,* 20**,** 1346-1352.

HAMEED, M., RANA, R. & ALI, Z. 2012. Identification and characterization of a novel Iraqi isolate of *Fusarium pseudograminearum* causing crown rot in wheat. *Genetics and Molecular Research,* 11**,** 1341-1348.

HAN, X. & KAHMANN, R. 2019. Manipulation of phytohormone pathways by effectors of filamentous plant pathogens. *Frontiers in plant science,* 10.

HAO, G., NAUMANN, T. A., VAUGHAN, M. M., MCCORMICK, S., USGAARD, T., KELLY, A. & WARD, T. J. 2018. Characterization of a *Fusarium graminearum* salicylate hydroxylase. *Frontiers in microbiology,* 9**,** 3219.

HOLLAWAY, G., EVANS, M., WALLWORK, H., DYSON, C. & MCKAY, A. 2013. Yield loss in cereals, caused by *Fusarium culmorum* and *F. pseudograminearum*, is related to fungal DNA in soil prior to planting, rainfall, and cereal type. *Plant disease,* 97**,** 977-982.

HUO, N., VOGEL, J. P., LAZO, G. R., YOU, F. M., MA, Y., MCMAHON, S., DVORAK, J., ANDERSON, O. D., LUO, M.-C. & GU, Y. Q. 2009. Structural characterization of *Brachypodium* genome and its syntenic relationship with rice and wheat. *Plant molecular biology,* 70**,** 47-61.

JANSEN, C., VON WETTSTEIN, D., SCHÄFER, W., KOGEL, K.-H., FELK, A. & MAIER, F. J. 2005. Infection patterns in barley and wheat spikes inoculated with wild-type and trichodiene synthase gene disrupted *Fusarium graminearum*. *Proceedings of the National Academy of Sciences,* 102**,** 16892-16897.

JI, L., KONG, L., LI, Q., WANG, L., CHEN, D. & MA, P. 2016. First report of *Fusarium pseudograminearum* causing Fusarium head blight of wheat in Hebei Province, China. *Plant Disease,* 100**,** 220-220.

KAMMOUN, L. G., GARGOURI, S., HAJLAOUI, M. R. & MARRAKCHI, M. 2009. Occurrence and distribution of *Microdochium* and *Fusarium* species isolated from durum wheat in northern Tunisia and detection of mycotoxins in naturally infested grain. *Journal of phytopathology,* 157**,** 546-551.

KAZAN, K. 2015. Diverse roles of jasmonates and ethylene in abiotic stress tolerance. *Trends in plant science,* 20**,** 219-229.

KAZAN, K. & GARDINER, D. M. 2018. Fusarium crown rot caused by *Fusarium pseudograminearum* in cereal crops: recent progress and future prospects. *Molecular plant pathology,* 19**,** 1547-1562.

KAZAN, K., GOULTER, K. C., WAY, H. M. & MANNERS, J. M. 1998. Expression of a pathogenesis-related peroxidase of *Stylosanthes humilis* in transgenic tobacco and canola and its effect on disease development. *Plant Science,* 136**,** 207-217.

KELLER, N. P. 2015. Translating biosynthetic gene clusters into fungal armor and weaponry. *Nature chemical biology,* 11**,** 671.

KHALDI, N. & WOLFE, K. H. 2011. Evolutionary origins of the fumonisin secondary metabolite gene cluster in *Fusarium verticillioides* and *Aspergillus niger*. *International journal of evolutionary biology,* 2011.

KHANGURA, R. K., MACNISH, G. C., MACLEOD, W. J., VANSTONE, V. A., HANBURY, C. D., LOUGHMAN, R. & SPEIJERS, J. E. 2013. Current status of cereal root diseases in Western Australia under intensive cereal production and their comparison with the historical survey conducted during 1976–1982. *Journal of Phytopathology,* 161**,** 828-840.

KIDD, B. N., EDGAR, C. I., KUMAR, K. K., AITKEN, E. A., SCHENK, P. M., MANNERS, J. M. & KAZAN, K. 2009. The mediator complex subunit PFT1 is a key regulator of jasmonate-dependent defense in Arabidopsis. *The Plant Cell,* 21**,** 2237-2252.

KIM, Y.-J., BJÖRKLUND, S., LI, Y., SAYRE, M. H. & KORNBERG, R. D. 1994. A multiprotein mediator of transcriptional activation and its interaction with the C-terminal repeat domain of RNA polymerase II. *Cell,* 77**,** 599-608.

KJÆRBØLLING, I., VESTH, T. & ANDERSEN, M. R. 2019. Resistance Gene-Directed Genome Mining of 50 *Aspergillus* species. *MSystems,* 4**,** e00085-19.

KLOEK, A. P., VERBSKY, M. L., SHARMA, S. B., SCHOELZ, J. E., VOGEL, J., KLESSIG, D. F. & KUNKEL, B. N. 2001. Resistance to *Pseudomonas syringae* conferred by an *Arabidopsis thaliana* coronatine-insensitive (coi1) mutation occurs through two distinct mechanisms. *Plant Journal,* 26**,** 509-522.

KLOSE, C., BÜCHE, C., FERNANDEZ, A. P., SCHÄFER, E., ZWICK, E. & KRETSCH, T. 2012. The mediator complex subunit PFT1 interferes with COP1 and HY5 in the regulation of Arabidopsis light signaling. *Plant physiology,* 160**,** 289-307.

KNIGHT, N. & SUTHERLAND, M. 2013a. Histopathological assessment of wheat seedling tissues infected by *Fusarium pseudograminearum*. *Plant Pathology,* 62**,** 679-687.

KNIGHT, N. & SUTHERLAND, M. 2013b. Spread of *Fusarium pseudograminearum* in wheat seedling tissues from a single inoculation point. *Australasian Plant Pathology,* 42**,** 609-615.

KNIGHT, N. L. & SUTHERLAND, M. W. 2016. Histopathological assessment of *Fusarium pseudograminearum* colonization of cereal culms during crown rot infections. *Plant disease,* 100**,** 252-259.

KOLESKE, A. J. & YOUNG, R. A. 1994. An RNA polymerase II holoenzyme responsive. *Nature,* 368.

KOPRIVOVA, A., CALDERWOOD, A., LEE, B.-R. & KOPRIVA, S. 2014. Do PFT1 and HY5 interact in regulation of sulfate assimilation by light in *Arabidopsis*? *FEBS letters,* 588**,** 1116-1121.

LAM, E., KATO, N. & LAWTON, M. 2001. Programmed cell death, mitochondria and the plant hypersensitive response. *Nature,* 411**,** 848.

LAURENCE, M., SUMMERELL, B. & LIEW, E. 2015. *Fusarium oxysporum* f. sp. *canariensis*: evidence for horizontal gene transfer of putative pathogenicity genes. *Plant pathology,* 64**,** 1068-1075.

LAURENCE, M., WALSH, J., SHUTTLEWORTH, L., ROBINSON, D., JOHANSEN, R., PETROVIC, T., VU, T., BURGESS, L., SUMMERELL, B. & LIEW, E. 2016. Six novel species of *Fusarium* from natural ecosystems in Australia. *Fungal diversity,* 77**,** 349-366.

LI, H., YUAN, H., FU, B., XING, X., SUN, B. & TANG, W. 2012. First report of *Fusarium pseudograminearum* causing crown rot of wheat in Henan, China. *Plant disease,* 96**,** 1065-1065.

LI, N., HAN, X., FENG, D., YUAN, D. & HUANG, L.-J. 2019. Signaling crosstalk between salicylic acid and ethylene/jasmonate in plant defense: do we understand what they are whispering? *International journal of molecular sciences,* 20**,** 671.

LIU, C. & OGBONNAYA, F. C. 2015. Resistance to Fusarium crown rot in wheat and barley: a review. *Plant Breeding,* 134**,** 365-372.

LIU, J., ZHANG, T., JIA, J. & SUN, J. 2016. The Wheat Mediator Subunit TaMED25 Interacts with the Transcription Factor TaEIL1 to Negatively Regulate Disease Resistance against Powdery Mildew. *Plant Physiology,* 170**,** 1799-1816.

MA, J., LI, H., ZHANG, C., YANG, X., LIU, Y., YAN, G. & LIU, C. 2010. Identification and validation of a major QTL conferring crown rot resistance in hexaploid wheat. *Theoretical and applied genetics,* 120**,** 1119-1128.

MA, L.-J., GEISER, D. M., PROCTOR, R. H., ROONEY, A. P., O'DONNELL, K., TRAIL, F., GARDINER, D. M., MANNERS, J. M. & KAZAN, K. 2013. *Fusarium* pathogenomics. *Annual review of microbiology,* 67**,** 399-416.

MAAZ, T., WULFHORST, J., MCCRACKEN, V., KIRKEGAARD, J., HUGGINS, D. R., ROTH, I., KAUR, H. & PAN, W. 2018. Economic, policy, and social trends and challenges of introducing

oilseed and pulse crops into dryland wheat cropping systems. *Agriculture, Ecosystems & Environment,* 253**,** 177-194.

MAKANDAR, R., NALAM, V., CHATURVEDI, R., JEANNOTTE, R., SPARKS, A. A. & SHAH, J. 2010. Involvement of salicylate and jasmonate signaling pathways in *Arabidopsis* interaction with *Fusarium graminearum*. *Molecular plant-microbe interactions,* 23**,** 861-870.

MAKANDAR, R., NALAM, V. J., LEE, H., TRICK, H. N., DONG, Y. & SHAH, J. 2012. Salicylic acid regulates basal resistance to Fusarium head blight in wheat. *Molecular Plant-Microbe Interactions,* 25**,** 431-439.

MALIK, S. & ROEDER, R. G. 2005. Dynamic regulation of pol II transcription by the mammalian Mediator complex. *Trends in biochemical sciences,* 30**,** 256-263.

MCKNIGHT, T. & HART, J. 1966. Some field observations on crown rot disease of wheat caused by *Fusarium graminearum*. *Queensland Journal of Agricultural and Animal Sciences,* 23**,** 373-378.

MISHRA, P. K., TEWARI, J. P., CLEAR, R. M. & TURKINGTON, T. K. 2006. Genetic diversity and recombination within populations of *Fusarium pseudograminearum* from western Canada. *International Microbiology,* 9**,** 65-68.

MOLNÁR, I., ŠIMKOVÁ, H., LEVERINGTON-WAITE, M., GORAM, R., CSEH, A., VRÁNA, J., FARKAS, A., DOLEŽEL, J., MOLNÁR-LÁNG, M. & GRIFFITHS, S. 2013. Syntenic Relationships between the U and M Genomes of *Aegilops*, Wheat and the Model Species *Brachypodium* and Rice as Revealed by COS Markers. *PLOS ONE,* 8**,** e70844.

MOTALLEBI, P., NIKNAM, V., EBRAHIMZADEH, H., HASHEMI, M., PISI, A., PRODI, A., TONTI, S. & NIPOTI, P. 2015. Methyl jasmonate strengthens wheat plants against root and crown rot pathogen *Fusarium culmorum* infection. *Journal of plant growth regulation,* 34**,** 624-636.

MUDGE, A. M., DILL-MACKY, R., DONG, Y., GARDINER, D. M., WHITE, R. G. & MANNERS, J. M. 2006. A role for the mycotoxin deoxynivalenol in stem colonisation during crown rot disease of wheat caused by *Fusarium graminearum* and *Fusarium pseudograminearum*. *Physiological and Molecular Plant Pathology,* 69**,** 73-85.

MURRAY, G. M. & BRENNAN, J. P. 2009. Estimating disease losses to the Australian wheat industry. *Australasian Plant Pathology,* 38**,** 558-570.

NYVALL, R. F. 1970. Chlamydospores of *Fusarium roseum* 'Graminearum'as survival structures. *Phytopathology,* 60**,** 1175-1177.

OKUBARA, P., BLECHL, A., MCCORMICK, S., ALEXANDER, N., DILL-MACKY, R. & HOHN, T. 2002. Engineering deoxynivalenol metabolism in wheat through the expression of a fungal trichothecene acetyltransferase gene. *Theoretical and Applied Genetics,* 106**,** 74-83.

PASONEN, H.-L., SEPPÄNEN, S.-K., DEGEFU, Y., RYTKÖNEN, A., VON WEISSENBERG, K. & PAPPINEN, A. 2004. Field performance of chitinase transgenic silver birches (*Betula pendula*): resistance to fungal diseases. *Theoretical and Applied Genetics,* 109**,** 562-570.

PIETERSE, C. M., LEON-REYES, A., VAN DER ENT, S. & VAN WEES, S. C. 2009. Networking by small-molecule hormones in plant immunity. *Nature chemical biology,* 5**,** 308.

PIETERSE, C. M., VAN DER DOES, D., ZAMIOUDIS, C., LEON-REYES, A. & VAN WEES, S. C. 2012. Hormonal modulation of plant immunity. *Annual review of cell and developmental biology,* 28**,** 489-521.

PIETERSE, C. M., ZAMIOUDIS, C., BERENDSEN, R. L., WELLER, D. M., VAN WEES, S. C. & BAKKER, P. A. 2014. Induced systemic resistance by beneficial microbes. *Annual review of phytopathology,* 52**,** 347-375.

POUZESHIMIAB, B., RAZAVI, M., ZARE, R. & MOMENI, H. 2016. The genetic structure and aggressiveness of *Fusarium pseudograminearum* populations in Iran. *Journal of Plant Diseases and Protection,* 123**,** 257-266.

POWELL, J. J. 2016. *Identifying sources of resistance to Fusarium diseases using the model plant Brachypodium distachyon.* Doctor of Philosophy, University of Queensland.

POWELL, J. J., CARERE, J., FITZGERALD, T. L., STILLER, J., COVARELLI, L., XU, Q., GUBLER, F., COLGRAVE, M. L., GARDINER, D. M. & MANNERS, J. M. 2016. The Fusarium crown rot pathogen *Fusarium pseudograminearum* triggers a suite of transcriptional and metabolic changes in bread wheat (*Triticum aestivum* L.). *Annals of Botany***,** mcw207.

POWELL, J. J., CARERE, J., SABLOK, G., FITZGERALD, T. L., STILLER, J., COLGRAVE, M. L., GARDINER, D. M., MANNERS, J. M., VOGEL, J. P., HENRY, R. J. & KAZAN, K. 2017. Transcriptome analysis of *Brachypodium* during fungal pathogen infection reveals both shared and distinct defense responses with wheat. *Scientific Reports,* 7**,** 17212.

PROCTOR, R. H., HOHN, T. M. & MCCORMICK, S. P. 1995. Reduced virulence of Gibberella zeae caused by disruption of a trichthecine toxin biosynthetic gene. *MPMI-Molecular Plant Microbe Interactions,* 8**,** 593-601.

QI, P.-F., JOHNSTON, A., BALCERZAK, M., ROCHELEAU, H., HARRIS, L. J., LONG, X.-Y., WEI, Y.-M., ZHENG, Y.-L. & OUELLET, T. 2012. Effect of salicylic acid on *Fusarium graminearum*, the major causal agent of fusarium head blight in wheat. *Fungal Biology,* 116**,** 413-426.

RAYA-GONZÁLEZ, J., ORTIZ-CASTRO, R., RUÍZ-HERRERA, L. F., KAZAN, K. & LÓPEZ-BUCIO, J. 2014. PHYTOCHROME AND FLOWERING TIME1/MEDIATOR25 regulates lateral root formation via auxin signaling in *Arabidopsis*. *Plant physiology,* 165**,** 880-894.

ROCHELEAU, H., AL-HARTHI, R. & OUELLET, T. 2019. Degradation of salicylic acid by *Fusarium graminearum*. *Fungal biology,* 123**,** 77-86.

ROTTER, B. A. 1996. Invited Review: TOXICOLOGY OF DEOXYNIVALENOL (VOMITOXIN). *Journal of Toxicology and Environmental Health,* 48**,** 1-34.

SAREMI, H., AMMARELLOU, A. & JAFARY, H. 2007. Incidence of crown rot disease of wheat caused by *Fusarium pseudograminearum* as a new soil born fungal species in North West Iran. *Pakistan Journal of Biological Sciences,* 10**,** 3606-3612.

SEGUELA-ARNAUD, M., SMITH, C., URIBE, M. C., MAY, S., FISCHL, H., MCKENZIE, N. & BEVAN, M. W. 2015. The Mediator complex subunits MED25/PFT1 and MED8 are required for transcriptional responses to changes in cell wall arabinose composition and glucose treatment in *Arabidopsis thaliana*. *BMC plant biology,* 15**,** 215.

SIEBER, C. M., LEE, W., WONG, P., MÜNSTERKÖTTER, M., MEWES, H.-W., SCHMEITZL, C., VARGA, E., BERTHILLER, F., ADAM, G. & GÜLDENER, U. 2014. The *Fusarium graminearum* genome reveals more secondary metabolite gene clusters and hints of horizontal gene transfer. *PLoS One,* 9**,** e110311.

SITTON, J. & COOK, R. J. 1981. Comparative Morphology and Survival of Chlamydospores of. *Fusarium roseum***,** 85-90.

SMILEY, R. W. 2009. Water and temperature parameters associated with winter wheat diseases caused by soilborne pathogens. *Plant disease,* 93**,** 73-80.

SMILEY, R. W., GOURLIE, J. A., EASLEY, S. A. & PATTERSON, L.-M. 2005a. Pathogenicity of fungi associated with the wheat crown rot complex in Oregon and Washington. *Plant disease,* 89**,** 949-957.

SMILEY, R. W., GOURLIE, J. A., EASLEY, S. A., PATTERSON, L.-M. & WHITTAKER, R. G. 2005b. Crop damage estimates for crown rot of wheat and barley in the Pacific Northwest. *Plant Disease,* 89**,** 595-604.

SMILEY, R. W. & PATTERSON, L.-M. 1996. Pathogenic fungi associated with Fusarium foot rot of winter wheat in the semiarid Pacific Northwest. *Plant Disease,* 80**,** 944-949.

SØRENSEN, J. L., BENFIELD, A. H., WOLLENBERG, R. D., WESTPHAL, K., WIMMER, R., NIELSEN, M. R., NIELSEN, K. F., CARERE, J., COVARELLI, L., BECCARI, G., POWELL, J., YAMASHINO, T., KOGLER, H., SONDERGAARD, T. E. & GARDINER, D. M. 2018. The cereal pathogen *Fusarium pseudograminearum* produces a new class of active cytokinins during infection. *Molecular Plant Pathology,* 19**,** 1140-1154.

SPOEL, S. H., JOHNSON, J. S. & DONG, X. 2007. Regulation of tradeoffs between plant defenses against pathogens with different lifestyles. *Proceedings of the National Academy of Sciences of the United States of America,* 104**,** 18842-18847.

SUMMERELL, B. A. 2019. Resolving *Fusarium*: Current Status of the Genus. *Annual review of phytopathology,* 57**,** 323-339.

SUNDARAVELPANDIAN, K., CHANDRIKA, N. N. P. & SCHMIDT, W. 2013. PFT1, a transcriptional Mediator complex subunit, controls root hair differentiation through reactive oxygen species (ROS) distribution in *Arabidopsis*. *New Phytologist,* 197**,** 151-161.

SVOBODA, T., PARICH, A., GÜLDENER, U., SCHÖFBECK, D., TWARUSCHEK, K., VÁCLAVÍKOVÁ, M., HELLINGER, R., WIESENBERGER, G., SCHUHMACHER, R. & ADAM, G. 2019. Biochemical Characterization of the *Fusarium graminearum* Candidate ACC-Deaminases and Virulence Testing of Knockout Mutant Strains. *Frontiers in Plant Science,* 10.

THATCHER, L. F., GARDINER, D. M., KAZAN, K. & MANNERS, J. M. 2012. A highly conserved effector in *Fusarium oxysporum* is required for full virulence on *Arabidopsis*. *Molecular plant-microbe interactions,* 25**,** 180-190.

THATCHER, L. F., MANNERS, J. M. & KAZAN, K. 2009a. *Fusarium oxysporum* hijacks COI1-mediated jasmonate signaling to promote disease development in *Arabidopsis*. *The Plant Journal,* 58**,** 927-939.

THATCHER, L. F., MANNERS, J. M. & KAZAN, K. 2009b. *Fusarium oxysporum* hijacks COI1‐mediated jasmonate signaling to promote disease development in *Arabidopsis*. *The Plant Journal,* 58**,** 927-939.

THOLE, V., WORLAND, B., WRIGHT, J., BEVAN, M. W. & VAIN, P. 2010. Distribution and characterization of more than 1000 T‐DNA tags in the genome of *Brachypodium distachyon* community standard line Bd21. *Plant biotechnology journal,* 8**,** 734-747.

THYNNE, E., MEAD, O. L., CHOOI, Y.-H., MCDONALD, M. C. & SOLOMON, P. S. 2019. Acquisition and loss of secondary metabolites shaped the evolutionary path of three emerging phytopathogens of wheat. *Genome biology and evolution,* 11**,** 890-905.

TUNALI, B., NICOL, J., EROL, F. Y. & ALTIPARMAK, G. 2006. Pathogenicity of Turkish crown and head scab isolates on stem bases on winter wheat under greenhouse conditions. *Plant Pathology Journal,* 5**,** 143-149.

TUNALI, B., NICOL, J. M., HODSON, D., UCKUN, Z., BÜYÜK, O., ERDURMUŞ, D., HEKIMHAN, H., AKTAŞ, H., AKBUDAK, M. A. & BAĞCI, S. A. 2008. Root and crown rot fungi associated with spring, facultative, and winter wheat in Turkey. *Plant Disease,* 92**,** 1299-1306.

VAN DAM, P. & REP, M. 2017. The distribution of Miniature Impala elements and SIX genes in the Fusarium genus is suggestive of horizontal gene transfer. *Journal of molecular evolution,* 85**,** 14-25.

VAN DER ENT, S. & PIETERSE, C. M. 2018. Ethylene: multi‐tasker in plant‐attacker interactions. *Annual Plant Reviews online*, 343-377.

VAN WEES, S. C. M. & GLAZEBROOK, J. 2003. Loss of non-host resistance of Arabidopsis NahG to *Pseudomonas syringae* pv. phaseolicola is due to degradation products of salicylic acid. *The Plant Journal,* 33, 733-742.

VLAARDINGERBROEK, I., BEERENS, B., ROSE, L., FOKKENS, L., CORNELISSEN, B. J. & REP, M. 2016. Exchange of core chromosomes and horizontal transfer of lineage‐specific chromosomes in *Fusarium oxysporum*. *Environmental microbiology,* 18, 3702-3713.

WANG, C., YAO, J., DU, X., ZHANG, Y., SUN, Y., ROLLINS, J. A. & MOU, Z. 2015. The *Arabidopsis* mediator complex subunit16 is a key component of basal resistance against the necrotrophic fungal pathogen *Sclerotinia sclerotiorum*. *Plant physiology,* 169, 856-872.

WAY, H. M., KAZAN, K., MITTER, N., GOULTER, K. C., BIRCH, R. G. & MANNERS, J. M. 2002. Constitutive expression of a phenylalanine ammonia-lyase gene from *Stylosanthes humilis* in transgenic tobacco leads to enhanced disease resistance but impaired plant growth. *Physiological and Molecular Plant Pathology,* 60, 275-282.

WISECAVER, J. H., SLOT, J. C. & ROKAS, A. 2014. The evolution of fungal metabolic pathways. *PLoS Genetics,* 10, e1004816.

XU, F., SONG, Y., YANG, G., WANG, J., LIU, L. & LI, Y. 2015. First report of *Fusarium pseudograminearum* from wheat heads with fusarium head blight in North China Plain. *Plant disease,* 99, 156-156.

YAN, C. & XIE, D. 2015. Jasmonate in plant defence: sentinel or double agent? *Plant biotechnology journal,* 13, 1233-1240.

YANG, Y., OU, B., ZHANG, J., SI, W., GU, H., QIN, G. & QU, L. J. 2014. The *Arabidopsis* Mediator subunit MED 16 regulates iron homeostasis by associating with EIN 3/EIL 1 through subunit MED 25. *The Plant Journal,* 77, 838-851.

ZHANG, X.-X., SUN, H.-Y., SHEN, C.-M., LI, W., YU, H.-S. & CHEN, H.-G. 2015. Survey of *Fusarium* spp. causing wheat crown rot in major winter wheat growing regions of China. *Plant disease,* 99, 1610-1615.

ZHENG, Z., KILIAN, A., YAN, G. & LIU, C. 2014. QTL conferring Fusarium crown rot resistance in the elite bread wheat variety EGA Wylie. *PloS one,* 9, e96011.

Chapter 2:

Characterisation of *Brachypodium distachyon* PHYTOCHROME FLOWERING TIME 1 (BdPFT1) for roles in defence and development

2.1 Abstract

Fusarium Crown Rot (FCR) is a significant global wheat crop disease, and is predominantly caused by *Fusarium pseudograminearum* (*Fp*) in Australia. Currently FCR management is centred on inoculum load management techniques; however, they are of limited efficacy and can be subject to constraints by social and economic factors. A long term solution is the development of a highly FCR resistant, high yielding wheat cultivar but to date no gene/s underlying the quantitative trait loci (QTL) conferring FCR resistance have been cloned. Consequently further genetic studies are required to identify candidate genes involved in host resistance to FCR in wheat. *PHYTCHOME FLOWERING TIME 1* (*PFT1*) encodes MEDIATOR25 (MED25), a subunit of the mediator complex. The mediator complex is highly conserved throughout eukaraya and fine-tunes regulatory input to mediate gene expression by interaction with the RNA polymerase II complex. Given its role in signal transduction, PFT1 has been implicated in a variety functions including but not limited to; ROS signalling, flowering, light quality responses, biotic and abiotic stress responses. *PFT1* was first identified in *Arabidopsis thaliana* (*At*) and was subsequently well characterised. *AtPFT1* was found to promote susceptibility to *Fusarium oxysporum* (*Fo*) through Jasmonic acid (JA)-dependent signalling. Due to underlying difference between dicots and monocots and PFT1's role in conferring susceptibility to *Fo*, *PFT1* is a desirable candidate gene to investigate in wheat. However, the complex nature of wheat's polyploid genome has been reported to hamper studies and the use of a suitable model organism recommended The current study used the model *Pooid* grass *Brachypodium distachyon* (*Bd*) to investigate the role of BdPFT1 in defence against *Fp*. Two independent transgenic *BdPFT1* overexpression lines and one transformant control were identified for further characterisation. *BdPFT1* overexpression similar to *AtPFT1* was found to promote early flowering. Further *BdPFT1* overexpression also promoted susceptibility to *Fp* and the wheat bacterial pathogen *Xanthomonas translucens*. The mechanism underlying *BdPFT1* promotion of *Fp* susceptibility and cell death is unclear but may be linked because qRT-PCR analysis of phytohormone markers gene under mock and infection conditions displayed no clear trend. Interestingly, BdPFT1 overexpressors developed a spontaneous lesion development on photosynthetic tissues. A previous study reported overexpression of wheat *PFT1*

but not *AtPFT1* in *Arabidopsis* resulted in a spontaneous lesion development phenotype. This provides tentative evidence for a conserved role for PFT1 in cell death but a difference in regulation of the pathway between monocots and dicots. Hence, whilst there are apparent similarities between AtPFT1 and BdPFT1 with relation to flowering time and disease phenotype there appear to be differences in regulatory mechanisms that warrant further investigation as outlined in this report.

2.2 Introduction

2.2.1 Fusarium Crown Rot (FCR) overview and economic impact

Fusarium Crown Rot (FCR) is a disease of economic concern that is impacting wheat and barley cropping industries in Australia (Akinsanmi et al., 2004, Burgess et al., 1975) and globally (see review by Kazan and Gardiner (2018)). Through multiple surveys, *Fusarium pseudograminearum* (*Fp*) has been identified as the most frequently associated *Fusarium* species with FCR and hence the common causative agent of FCR in Australia (Akinsanmi et al., 2004, Backhouse and Burgess, 2002, Backhouse et al., 2004, Burgess et al., 1975, Khangura et al., 2013, McKnight and Hart, 1966). Current FCR disease management techniques involve an integrated approach using chemical and cultural approaches to manage inoculum load and reduce the incidence of disease with variable efficacy. Further implementation of control measures is constrained by economic and technical factors (Alahmad et al. (2018). The development of a highly FCR resistant cultivar of wheat, with desirable agronomic traits such as high yield and grain quality, has been proposed as a long-term solution to FCR (Purss, 1969). Resistance towards FCR in wheat is a quantitative trait (Bovill et al. (2006) reviewed by Liu and Ogbonnaya (2015)). Multiple Quantitative Trait Loci (QTL) have been identified to confer resistance (Bovill et al., 2006, Collard et al., 2005, Liu et al., 2012); however, the gene underlying each QTL have not been cloned and identified. One of the key limitations of FCR resistance breeding is the lack of knowledge for the genetic basis of resistance (Collard et al., 2005, Liu and Ogbonnaya, 2015). Improving the understanding of the genetic basis for resistance will enable breeders to target key genes for introgression or exclusion in breeding programs.

2.2.2 Candidate gene PHYTOCHROME FLOWERING TIME 1

The outcome of plant diseases is reliant on the timely identification of, and appropriate response towards the incurring pathogen, which is underpinned by signalling, genetic reprogramming and gene expression. In an agriculture setting, losses associated with crop diseases may represent an inappropriate response pathway elicited during pathogen infection, resulting in plant susceptibility. One candidate gene that is likely to play a role in the wheat-*Fp* interaction is *PHYTOCHROME FLOWERING TIME 1* (*PFT1*), due to its involvement in signalling as a transcriptional regulator.

PFT1 has been extensively studied in the model plant *Arabidopsis* and has been found to encode a subunit of the mediator complex named MEDIATOR 25 (MED25) (Bäckström et al., 2007). The mediator complex is highly conserved and present in all eukaryotes. The mediator complex is comprised of multiple subunits organised into four modules; head, middle, and tail, representing the core, with the fourth module being a CYCLIN DEPENDENT KINASE (CDK8). The role of the mediator complex is to transduce environmental and endogenous signals from transcription factors (TFs) and modify RNA polymerase II (pol II) transcription by influencing formation of the pre-initiation complex, chromatin remodelling, transcript elongation, pausing and re-initiation (Allen and Taatjes, 2015). Hence, the mediator complex plays an integrative role in fine tuning gene expression in response to varied stimuli. The head of the complex interacts with RNA pol II complex; while the tail interacts with the TFs, and the middle undergoes functional conformational changes after RNA pol II interaction (Karijolich and Hampsey, 2012). The CDK8 module reversibly associates with the core mediator modules and is reported to affect transcription in Metazoan and yeast species by phosphorylating TFs and modifying interactions between the mediator and RNA pol II. Further, the CDK8 module can bind the Tail module repressing transcription and inhibiting RNA Pol II interactions with mediator (Conaway and Conaway, 2011). MED25 hereafter referred to as PFT1 is proposed to be located in the Tail module based on its ability to interact directly with a variety of TFs and a known Tail mediator subunit, MED16 (Yang et al., 2014).

PFT1 possesses multiple conserved protein domains including a von Willebrand Factor type A (vWF-A) domain located at the N-terminus, an Activator Interacting Domain (ACID) region, and a glutamine (Q) rich poly-track at the C-terminus. The vWF-A domain is required for PFT1's interaction with the mediator complex by binding to MED16 (Yang et al., 2016). The function of the ACID region is to interact with TFs that include but are not limited to AP2/ERF, MYCs (transcriptional activators) and JAZ (repressor) proteins (Çevik et al., 2012, Chen et al., 2012, Zhang et al., 2015). Lastly, the Q rich region can be alternatively spliced, to form one of two isoforms (Rival et al., 2014). The length, presence or absence of the Q rich has been reported to affect the flowering-associated functions of PFT1 and is predicted to contribute to its diverse functions (Rival et al., 2014). As a mediator subunit that functionally interacts with TFs, PFT1 is involved in regulating diverse pathways in growth and development and responses towards biotic and abiotic stressors (see review by Kazan (2017)). Notably, PFT1 is involved in biological processes such as transitioning to flowering (Cerdán and Chory, 2003), photomorphogenic changes (Klose et al., 2012), root hair development (Sundaravelpandian et al., 2013a, Sundaravelpandian et al., 2013b) and defence (Kidd et al., 2009).

Infection by *Fusarium oxysporum* (*Fo*) (Lyons et al., 2015) and the bacterial pathogen *Pseudomonas syringae* (Korves and Bergelson, 2003) alters flowering time in *Arabidopsis*. Early and late flowering ecotypes of *Arabidopsis*, exhibit enhanced susceptibility and resistance towards *Fo* infection, respectively (Lyons et al., 2015). Furthermore, QTL studies have reported significant associations between flowering time and disease resistance in various crop plants (Pinson et al., 2010, Van Inghelandt et al., 2012, Mizobuchi et al., 2013). Hence, there appears to be a link between flowering time and disease resistance (reviewed by Kazan and Lyons (2015)). *PFT1* was first identified in *Arabidopsis* (*AtPFT1*) as a positive regulator of flowering (Cerdán and Chory, 2003). The regulation of flowering by AtPFT1 is complex, involving multiple components and mechanisms (Wollenberg et al., 2008). AtPFT1 promotes flowering through both CONSTANS (CO)-dependent and -independent mechanisms (Iñigo et al., 2012a). Initially, AtPFT1 was placed downstream of PHYB signalling and reported to promote flowering under low red to far-red light conditions, as part of the 'shade-avoidance syndrome' response to light quality (Cerdán and Chory, 2003). AtPFT1 was

found to promote expression of *CO* (Cerdán and Chory, 2003), a key activator of flowering time under long photoperiods. Liu et al. (2017) reported a mechanism for AtPFT1 to promote *CO* expression by forming a complex with flowering activators FLOWERING BHLHs (FBHs) and microRNA319-regulated TEOSINTE BRANCHED/CYCLOIDEA/PCF (TCP) TFs. Other studies reported PFT1 operating downstream of PHYA signalling to promote expression of *FLOWERING LOCUS T* (*FT*), an activator of flowering, by suppressing the expression *FLOWERING LOCUS C* (*FLC)*, a negative regulator of flowering (Klose et al., 2012). Ubiquination of AtPFT1 by MED25-BINDING RING-H2 PROTEIN1 (MBR1) and MBR2 to facilitate proteasome-mediated turnover of AtPFT1 is another reported mechanism for promoting expression of *FT* (Iñigo et al., 2012b). Recently, AtPFT1 has been demonstrated to be recruited by SQUAMASA PROMOTER BINDING PROTEIN-LIKE10 (SPL10) to the promoters of TFs FRUITFULL (*FUL)* and LEAFY (*LFY),* promoting floral transition in the age pathway for flowering (Yao et al., 2019). Analyses of LFY genome wide binding sites have revealed targets involved in diverse processes, indicating involvement of LFY in processes other than flowering (Deng et al., 2011) such as plant defence (Winter et al., 2011). As mentioned previously, the Q rich region of AtPFT1 is involved in modulating flowering time, as mutants lacking this region exhibit delayed flowering (Rival et al., 2014).

Production and accumulation of reactive oxygen species (ROS) such as hydrogen peroxide (H_2O_2) and superoxide (O_2^-), act as signals during plant development and stress responses (reviewed by Noctor et al. (2018)). AtPFT1 has also been implicated in modulating ROS production in the roots to control root hair development by increasing expression of a subset of hydrogen peroxide (H_2O_2) producing class III peroxidases and decreasing expression of superoxide (O_2^-) producing NADPH enzymes (Sundaravelpandian et al., 2013a). One of the hallmarks of the hypersensitive response (HR) is accumulation of salicylic acid (SA) and ROS resulting in localised cell death (Overmyer et al., 2003). Interestingly, AtPFT1 promotes expression of the TF *ELONGATED HYPOCOTYL5* (*HY5*) (Klose et al., 2012, Koprivova et al., 2014), which is a positive regulator of light-dependent gene expression (Gangappa and Botto, 2016). Notably, HY5 mediates the accumulation of reactive oxygen species (ROS) and SA resulting in cell death during de-etiolation and excess light conditions (Chai et al., 2015). Additionally, HY5 directly binds to the

promoters of *ENHANCED DISEASE SUSCEPTIBILITY1* (*EDS1*) (Chai et al., 2015) and multiple WRKY TFs involved in defence responses (Lee et al., 2007, Rushton et al., 2010). This indicates a potential role for AtPFT1 in light-dependent defence signalling.

In *Arabidopsis*, AtPFT1 confers resistance to necrotrophic fungal pathogens *Sclerotinia sclerotiorum*, *Botrytis cinerea* and *Alternaria brassicicola,* and susceptibility to the hemi-biotrophic fungus *Fo* (Kidd et al., 2009, Wang et al., 2015). Jasmonic acid (JA) is a plant phytohormone that plays an important role in defence against necrotrophic pathogens but confers susceptibility towards biotrophic and hemi-biotrophic pathogens (Thatcher et al., 2009, Kidd et al., 2009). AtPFT1 has been described as a positive regulator of JA gene expression, explaining its associated defence phenotypes. *Atpft1* mutants were found to be insensitive to induction of JA-signalling by a potent agonist of the JA pathway called bestatin (Zheng et al., 2006) and exhibit reduced expression of JA-defence marker genes *PDF1.2, VSP2* and *MYC2* under basal growth and JA treated conditions (Kidd et al., 2009). Through direct interaction with key regulators of the JA signalling pathway, including ORA59 (OCTADECANOID-RESPONSIVE ARABIDOPSIS AP2/ERF59), ERF1 (ETHYLENE RESPONSE FACTOR1) and TF MYC2, AtPFT1 can induce MYC2-dependent activation of *VSP1* and ERF1-dependent activation of *PDF1.2* (Çevik et al., 2012). Further, AtPFT1 is also involved in MYC2-dependent repression of *PDF1.2* (Çevik et al., 2012). Interestingly, wheat *PFT1 (TaPFT1*) has been found to interact with EIL1 (ETHYLENE INSENSTIVE3-LIKE1) and synergistically activate *ERF1* to confer susceptibility towards the biotrophic pathogen *Blumeria graminis f.sp. tritici* by repressing pathogen-related gene expression and ROS accumulation (Liu et al., 2016).

The ability of wheat *PFT1* (*TaPFT1*) to complement *Arabidopsis pft1* developmental and defence phenotypes suggests that the role of PFT1 is conserved (Kidd et al., 2009) between monocots and dicots. However, to date limited functional characterization of *TaPFT1* has been reported. This is due to difficulties associated with functional characterisation of genes in wheat due to the polyploid nature of its genome (Fitzgerald et al., 2015b). Therefore, an approach to gain a better

understanding of the role of PFT1 in wheat-*Fp* interaction is the use of the model cereal organism *Brachypodium distachyon* (Kazan et al., 2012).

2.2.3 *Brachypodium* as a model to study *Fp*-host interactions

Whilst the functional role of PFT1 has been extensively studied in *Arabidopsis,* as a model plant species, and the *Fusarium-Arabidopsis* pathosystem has offered insights into disease pathogenesis and resistance mechanisms, it may not be representative of the role of TaPFT1 in the *Fp*-wheat interaction. This is due to the physiological differences between *Arabidopsis* as a dicot and wheat as a monocot. *B. distachyon,* hereafter referred to as *Brachypodium*, is a member of the grass subfamily *Pooideae* that includes important crop species such as wheat and barley (Soreng et al., 2015). *Brachypodium* is a uniquely positioned model organism for the study of pooid grasses. Recently, *Brachypodium* has been identified as a host for a variety of pathogens (reviewed by Fitzgerald et al. (2015a)) including *Fp* (Powell et al., 2017, Rana et al., 2018). Further, *Brachypodium* and wheat exhibit a similar global transcriptional response under *Fp* infection conditions (Powell et al., 2017). Hence, *Brachypodium* is uniquely positioned as a tractable model to investigate *Fp*-cereal crop interactions.

PFT1 is of interest because it confers susceptibility towards *Fo* in *Arabidopsis*. *TaPFT1* is a candidate gene for modification to improve wheat's resistance towards *Fp* infection, to reduce losses associated with FCR. In the current study, we generated and identified two independent transgenic *BdPFT1* overexpressor (*BdPFT1* OE) lines in the *Brachypodium distachyon* 21-3 (*Bd21-3*) genetic background. We report that overexpression of *BdPFT1* results in an early flowering phenotype and susceptibility towards *Fp* and *Xanthomonas translucens* infection. These phenotypes indicate that the role of PFT1 in flowering and defence is conserved between *Arabidopsis* and *Brachypodium*. However, further research is required to elucidate whether the mode of action is also conserved. Interestingly, qRT-PCR analysis revealed no significantly different induction of JA phytohormone marker genes under *Fp*-treated conditions in a *BdPFT1* OE line. This indicates that BdPFT1-mediated susceptibility to *Fp* may not be JA-dependent, contrasting reports in *Arabidopsis*. Further, a spontaneous lesion-forming phenotype was observed in both *BdPFT1* overexpressor lines. The

mechanism of the lesion phenotype is unknown but may be representative of a role for BdPFT1 in light-induced cell death.

2.3 Results

2.3.1 Identification and confirmation of stably transformed PFT1/MED25 overexpressors and RNAi lines (genotyping).

Previous work by Powell (2016) had generated multiple *BdPFT1* overexpressor (OE) and hairpin (HP) knockdown transformants through *Agrobacterium*-mediated transformation of embryogenic callus (Vogel and Hill, 2008, Vogel et al., 2006, Bragg et al., 2012). To reduce the risk of transgene expression silencing (Vaucheret et al., 1998), the current work screened T1 transformant progeny with a low copy number, using PCR amplification of the insert for a predicted segregation ratio of 3:1 for a single-copy T-DNA inheritance. Subsequently, the selected T2 generation was assessed for progeny with 100% inheritance of transgenes indicative of a homozygous line. Three *PFT1* OE lines (CO330, CO360 and CO364) and a single *PFT1* HP (CO578) line were identified as stably transformed (Supplementary. Figure 2.1 & 2.2). Due to the absence of additional single-copy PFT1 HP lines, no further characterisation of the CO578 line was conducted because there was no way to distinguish between the effects of the *BdPFT1* knock-down and the ectopic effects of T-DNA insertion in the absence of at least another independently transformed line that showed significantly reduced BdPFT1 levels.

To confirm transgenes are stably expressed in these lines, quantitative real time PCR (qRT-PCR) analyses were conducted using leaf tissue from 4-week-old plants. PFT1-OE lines CO360 and CO364 hereafter referred to as OE1 and OE2, had a significantly increased expression of *BdPFT1* (Two-way Student's t test, $P<0.001$). Interestingly, the *PFT1*-OE CO330 line, despite being stably transformed, did not have a significantly altered level of *PFT1* expression relative to the WT. Hence the CO330 line will be referred to as OETC, a negative control for the *PFT1* overexpressor lines OE1 and OE2 (Figure 2.1).

2.3.2 *BdPFT1-OE* lines have an early onset flowering phenotype

In *Arabidopsis*, *AtPFT1* overexpressors and knockout mutants have early and delayed onset of flowering phenotypes, respectively (Cerdán and Chory, 2003). To investigate

whether the *Brachypodium PFT1-OE* lines also exhibit an altered flowering time phenotype, a flowering time assay was conducted using long day (16h L: 8h D) conditions. OE1 and OE2 plants flowered significantly earlier than wild type (WT) (P<0.01, Wilcoxon rank test); whereas, OETC was not significantly different from WT (Figure 2). The altered flowering time phenotypes reflect the *BdPFT1* expression levels, as measured by qRT-PCR, providing evidence that *BdPFT1* transgenes are functional in OE1 and OE2 (Figures 2.1 and 2.2).

2.3.3 *BdPFT1* overexpression confers susceptibility towards *Fusarium pseudograminearum* (*Fp*) infection

To investigate the effect of *BdPFT1* expression on *Fp* (CS3096) infection outcomes, soilless infection assays were conducted and disease scores, a qualitative measurement, and leaf counts, a quantitative measurement, of disease progression were recorded. The OE lines at 9 days post inoculation (dpi) showed significantly increased disease score rankings (Wilcoxon rank test, P<0.001) relative to the WT (Figure 2.3). OE2 also showed a significant reduction in leaf number under infection (Wilcoxon rank test, P<0.001), while OE1 tended towards a lower leaf number relative to the WT. The OETC line was not significantly different to the WT in disease score or leaf number (Figure 2.3). When disease score and leaf number were analysed together using a one-way permutational MANOVA, both OE lines were reported as significantly different to the WT (P<0.05). The experiment was repeated twice with similar results for the OE and OETC lines. In summary, these results indicate that BdPFT1 may act as a susceptibility factor towards *Fp* infection.

2.3.4 *BdPFT1-OE* lines display a spontaneous lesion development and stunted growth phenotype

At approximately 21 days post emergence and continuing until seed set and death, OE1 and OE2 plants were observed to manifest a spontaneous lesion phenotype. The lesions initiate as a visible brown spot on mature leaves and soon expanded to cover the whole leaf, causing leaf death. Lesions were also observed in other photosynthetic organs of the plants such as the stem and seed coats (Figure 2.4) and plants grown under sterile conditions. The lesions were observed to be more severe, when plants

were grown under long day conditions (16h L; 8h D) compared to plants grown under neutral day conditions (12h L: 12h D). Additionally, *BdPFT1*-OE plants were also observed to exhibit a stunted growth phenotype, exemplified by reduced plant height (Figure 2.4) and leaf length (Figure 2.5-2.7), compared to WT *Brachypodium.*

2.3.5 *BdPFT1* overexpression-mediated lesion formation interferes with histo-chemical detection of ROS-mediated cell death

In *Arabidopsis*, PFT1 has been demonstrated to affect ROS distribution in the roots during root hair formation (Sundaravelpandian et al., 2013a). Accumulation of ROS can lead to cell death (Overmyer et al., 2003). To investigate if the OE plants had an altered accumulation / distribution of ROS, 3,3'-Diamonbenzidine (DAB) and nitroblue tetrazolium (NBT) stains were employed. DAB forms a brown precipitate in the presence of H_2O_2; whereas, a blue pigment is formed in the presence of NBT and O_2^-. The WT leaves showed a significant increase in the coloured areas of the DAB and NBT treatment respective to their mock controls (buffer without stain; Figure 2.5 & 2.6). This result confirmed that both the DAB and NBT stains worked. The observation of increased patches and foci of blue pigment present in the NBT stained OE2 leaves compared to WT, suggested an over accumulation of O_2^- in OE2 leaves (Figure 2.6A). However, the presence of the lesions in the OE2 leaves appeared to cause retention of a green pigment, despite repeated ethanol clearing treatments, in both mock, DAB and NBT staining treatments (Figure 2.5 & 2.6). Consequently, it is inconclusive as to whether PFT1-OE have a different accumulation / distribution of ROS compared to the WT.

2.3.6 Overexpression of *BdPFT1* confers susceptibility towards *Xanthomonas translucens* (*Xt*)

To investigate the effect of *BdPFT1* overexpression on a wheat bacterial pathogen that is known to be compatible with *Bd* (Fitzgerald et al., 2015a), *Xanthomonas translucens* (*Xt)* leaf infection assays were conducted. Due to workflows and given that the OE lines performed similarly in the *Fp* infection assays, the *Xt* infection assay was conducted using OE2 as a representative line. OE2 at 7 dpi had significantly larger lesion percentage coverage of the infiltrated area relative to the WT (Figure 2.7). The

size of the lesion can be used as an indicator of host plant susceptibility (Hayward, 1993). No spontaneous lesion formation or *Xt* induced lesions were observed in the mock control treatment on either OE2 or WT plants at 7 dpi (Figure 2.7A). Consequently, the lesions observed in the inoculation treatment were due to *Xt* infection and not the spontaneous lesion formation phenotype of OE2, which develops later in plant development (see above).

2.3.7 qRT-PCR marker gene analysis of *BdPFT1* transgenic lines under mock and inoculated conditions

To investigate the effect of *BdPFT1* overexpression on gene expression during *Fp* infection, a series of marker, validation and reference genes (Table 2.1) were assayed at 2- and 7-days post inoculation (dpi) under mock and inoculated conditions (Figure 2.8). Due to workflows and given that the OE lines performed similarly in the *Fp* infection assays, the marker gene analysis was conducted using OE1 as a representative line. To validate transgenic *BdPFT1* overexpression, the expression level of *BdPFT1* (*Bradi4g27747)* was quantified. As expected *BdPFT1* expression was significantly higher (Student's T test $P<0.01$) in the OE1 background compared to the WT (Figure 2.8D).

A *Brachypodium* homolog of *Oryza sativa allene oxide synthase (BdAOS Bradi1g699330)* (Kakei et al., 2015, Kouzai et al., 2016*), 12-oxyphytodienoate reductase* (*BdOPR*, *Bradi2g35907*) (Wang et al., 2017, Powell et al., 2017) and an *Arabidopsis thaliana phenylalanine ammonia lyase 1* homolog (*BdPAL1, Bradi3g48840)* (Kouzai et al., 2016, Cass et al., 2015) were selected as suitable JA markers based on the results of the cited literature. Relative gene expression of *BdAOS* was significantly reduced in OE1 compared to WT under mock conditions at 7 dpi (Student's T test $P<0.05$) (Figure 2.8A). Interestingly under *Fp* inoculated conditions at 7 dpi compared to the WT, OE1 trended towards increased expression of *BdAOS.* No significant differences were recorded for either *BdOPR* or *BdPAL1* between WT and OE1; however, a trend towards increased relative *BdPAL1* gene expression in OE1 compared to WT was observed across treatments and timepoints (Figure 2.8A).

Bradi1g57580 (Mandadi and Scholthof, 2012, Wang et al., 2017) and *Bradi1g12360 (Pasquet et al., 2014)*, which encode *pathogenesis related 1 like* proteins, were selected as SA markers based on the results in the literature. In the OE1 background, *Bradi1g57580* was trending towards increased expression with significant increases (Student's T test $P<0.05$) observed under 2 dpi *Fp* inoculated and 7 dpi mock treatments. *Bradi*1g12360 was significantly upregulated (Student's T test $P<0.05$) at 2 dpi in *Fp* inoculated OE1 plants (Figure 2.8B).

Bradi3g31880 encodes *a* glutathione-S-transferase (BdGST), a protein family involved in ROS metabolism (Gallé et al., 2019). GST enzymes scavenge reactive carbonyl species, which are formed from lipid peroxides, as a result of ROS accumulation (Mano et al., 2017, Mittler, 2002). *BdGST* was selected as a marker for ROS metabolism because it was significantly upregulated in *Brachypodium* infected by *Fp* (Powell et al., 2017). There was a trend towards increased expression of *BdGST* in OE1 recorded at each time point and treatment compared to the WT; however, a significant increase (Student's T test $P<0.05$) was only recorded for the 2 dpi mock treatment (Figure 2.8C).

BdPrx019 encodes a Class III peroxidase that is a member of subfamily 14, which shares high similarity with *Arabidopsis thaliana PEROXIDASE33* (*AtPrx33*) and *PEROXIDASE34* (*AtPrx34*) (Zhu et al., 2019). Previously, AtPrx33 and 34 have been shown to generate H_2O_2 in oxidative bursts during basal defence responses (Bindschedler et al., 2006, Rouet et al., 2006, Daudi et al., 2012, O'Brien et al., 2012). Further AtPrx33 and 34 have been shown to be differentially regulated by *AtPFT1* (Sundaravelpandian et al., 2013a). Hence *BdPrx019* was selected as a marker genes for ROS metabolism based on similarity to known genes regulated by AtPFT1 involved in ROS production and defence. *BdPrx019* appeared to be conversely expressed by OE1 compared to WT at each time point. At 2 dpi, *BdPrx019* trended towards increased expression and was significantly (Student's T test $P>0.05$) expressed by *Fp* inoculated OE1. At 7 dpi, *BdPrx019* trended towards decreased expression and was significantly (Student's T test $P<0.01$) repressed under mock treatment conditions in OE1 (Figure 2.8C).

2.4 Discussion

The long-term aim of this work was to investigate the role of *PFT1* defence responses against *Fp* in cereal plants. PFT1 has been extensively characterized in *Arabidopsis* and found to be involved in growth and development, and responses towards biotic and abiotic stressors (Kazan, 2017). Due to underlying differences between monocots and dicots (Lyons et al., 2013), and the genetic complexities associated with wheat (Fitzgerald et al., 2015b), a suitable model system is required. *Brachypodium distachyon*, a member of the Pooid cereals, was shown to share similar transcriptomic response (Powell et al., 2017) to *Fp* infection and possesses highly conserved gene synteny (Initiative, 2010) with wheat. Consequently, *Brachypodium* was selected as a suitable monocotyledonous plant model to study the role of PFT1 in *Fp* defence. The current work identified, validated and characterised two independent *BdPFT1* overexpressor lines, OE1 and OE2, and a transgenic overexpression negative control, OETC, in *Fp* interactions.

2.4.1 BdPFT1 promotes early flowering

PFT1 was first identified in *Arabidopsis* as a component of the flowering time signalling pathway. *Atpft1* mutants displayed a delayed onset of flowering under long (16h L: 8h D) photoperiods while *AtPFT1* overexpressor lines exhibited early onset of flowering under long day conditions (Cerdán and Chory, 2003). Similarly, in the current study, the OE1 and OE2 lines exhibited significantly early onset flowering under long photoperiods relative to the WT. The OETC control transgenic line did not significantly differ in flowering time relative to the WT, indicating the overexpression of *BdPFT1* to be responsible for the early flowering phenotype. In *Arabidopsis*, AtPFT1 is thought to function downstream of phytochrome B (PHYB) signalling to promote expression of *CONSTANS* (*CO*), which in turn increases expression of *FLOWERING LOCUS T* (*FT*) (Iñigo et al., 2012a), and it also has a proposed role in repressing the flowering repressor *FLOWERING LOCUS C* (*FLC*) (Klose et al., 2012). Higgins et al. (2010), through comparative genomics, has identified well conserved homologues of the *Arabidopsis* photoperiod pathway genes in *Brachypodium*. Interestingly, despite conservation of the genes involved between *Arabidopsis*, rice and *Brachypodium*, their mode of action may be somewhat different. An example is the *CO* homolog in rice

(*Hd1*) that promotes flowering under short days and represses it under long days, contrary to its mode of action in *Arabidopsis*, where it promotes flowering under long days (Yano et al., 2000). Consequently, the early flowering time phenotype of *BdPFT1 OE* lines indicates that role of BdPFT1 in the photoperiod induction pathway of flowering time may be conserved between *Arabidopsis* and *Brachypodium*. However, the mode of action for BdPFT1 has not been described in scientific literature and requires additional study.

2.4.2 BdPFT1 overexpression confers susceptibility towards *Fp* infection

AtPFT1 has been implicated as a susceptibility factor in *Arabidopsis* towards *F. oxysporum* infection. The mode of action of AtPFT1-mediated susceptibility is believed to be through its role in JA-mediated defence signalling (Kidd et al., 2009). *F. oxysporum* has been shown to hijack the JA signalling pathway to promote lesion development through plant senescence (Thatcher et al., 2009). *BdPFT1*-OE lines show significantly enhanced disease scores (Wilcoxon rank test, $P<0.001$) under *Fp* inoculation conditions relative to the WT and OETC controls, implicating BdPFT1 as a susceptibility factor. Kidd et al. (2009) proposed that AtPFT1 acts as a convergence point for both SA- and JA-mediated defence signalling, with JA signalling being its primary role. This was based on the observation that *Atpft1* T-DNA insertion mutants exhibited attenuated expression of SA and JA defence marker genes under their respective phytohormone treatment but only exhibited differential gene expression of JA marker genes under basal conditions. In the current study, none of the assayed JA marker genes were significantly differentially expressed in *Fp* inoculated OE1 compared to WT. However, the SA marker genes, encoding *pathogenesis related 1-like* (*PR1-like*) proteins, *Bradi1g57580* and *Bradi1g12360* were significantly upregulated (Student's T test, $P<0.05$) at 2 dpi in OE1. This appears to suggest that in *Brachypodium* PFT1's primary role may be SA signalling during *Fusarium* infection, which is contrary to the reported primary role of AtPFT1 in *Arabidopsis* (Kidd et al., 2009). Hence, the mode of BdPFT-mediated susceptibility towards *Fp* infection in cereals may not be due to a potential role in JA signalling.

To elucidate the mode of action for BdPFT1 conferred susceptibility towards *Fp* with respect to the phytohormones SA and JA, further experiments should be conducted.

Firstly, RNA-seq should be performed to understand any global transcriptional changes under uninfected versus *Fp*-infected plants in the *BdPFT1* OE background compared to the WT. Phytohormone treatments of *BdPFT1* OE lines and WT should also be conducted using SA and JA to determine if OE lines show enhanced SA/JA sensitive phenotypes and if the phytohormone marker genes (Kouzai et al., 2016) are differentially regulated or if the response is *BdPFT1* dose-dependent.

In addition, to determine if BdPFT1 conferred *Fp* susceptibility is mediated by JA, the OE lines should be crossed into a JA insensitive Bd21-3 background. Assuming JA-insensitivity confers *Fusarium* resistance in *Brachypodium* similar to *Arabidopsis* (Thatcher et al., 2009), then if the *BdPFT1*-OE increased susceptibility phenotype is suppressed the mode of action for BdPFT1 susceptibility is JA-dependent. To conduct this experiment, a JA-insensitive *Brachypodium* line must be created. A potential method to achieve this is RNA-mediated knockdown of three COI1-like genes (Bradi2g55210, Bradi2g23730, and Bradi1g67160) present in *Brachypodium* (Lyons et al., 2013). To further elucidate the role of BdPFT1-mediated SA signalling in *Brachypodium*, the *BdPFT1* OE lines can be crossed with the transgenic *nahG* expressing *Brachypodium*, which have lower levels of SA compared to WT (Powell et al, unpub.). If the resulting hybrid showed enhanced *Fp* susceptibility than this would be consistent with *BdPFT1* mediating SA-dependent resistance towards *Fp*.

Also, the creation/identification of additional *BdPFT1* hairpin knockdown lines will allow reliable characterization of the impact of the reduced expression of *BdPFT1* on *Fp* plant defence and phytohormone regulation.

2.4.3 Possible role for BdPFT1 in mediating cell death

A potential mode of action for BdPFT1 conferred susceptibility towards *Fp* is through inappropriate regulation of signalling leading to cell death. Senescence, a form of regulated cell death, is established to promote susceptibility towards *F. oxysporum* in *Arabidopsis* (Schenk et al., 2005, Thatcher et al., 2009). The development of foliar lesions at ~3 weeks post germination in *BdPFT1* OE plants under basal growth conditions appeared to be exacerbated under long photoperiods (16h L:8h D) compared to neutral day (12h L:12h D), which suggests inappropriate activation of a

light-induced cell death response. Furthermore, *BdPFT1* OE2 plants develop larger lesions under *Xt* inoculation compared to WT plants. Whether photoperiod exacerbates lesion formation in *BdPFT1*-OE under infection relative to WT remains to be tested.

A similar cell death phenotype has been reported in the *Arabidopsis* mutant *lsd1*. The *lsd1* cell death phenotype is initiated by growth under long photoperiods (≥16h Light) and inoculation with fungal and bacterial pathogens (Dietrich et al., 1994). The cell death phenotype of *lsd1* is due to mis-regulation of an integrative hub of signalling, EDS1 and interacting partner PAD4, involved in systemic acquired acclimation (SAA) to high light (Rustérucci et al., 2001, Mateo et al., 2004, Mühlenbock et al., 2008, Mühlenbock et al., 2007), the hypersensitive response (HR) (Mateo et al., 2004, Mühlenbock et al., 2008, Mühlenbock et al., 2007, Chang et al., 2009, Frenkel et al., 2009) and systemic acquired resistance (SAR) (Coll et al., 2011, Luna et al., 2012, Luna and Ton, 2012). EDS1 and PAD4 promote extracellular superoxide (O_2^-) production (Jabs et al., 1996) and subsequent SA and ET accumulation (Aviv et al., 2002, Rustérucci et al., 2001, Mühlenbock et al., 2008) resulting in cell death. LSD1 is shown to negatively regulate *EDS1* expression; whereas another transcription factor HY5 positively regulates *EDS1* (Chai et al., 2015). Klose et al. (2012) demonstrated that a mis-sense mutation located in the VP16 domain of AtPFT1 resulted in constitutive activation of multiple light signalling marker genes, including HY5. The mutation is believed to replicate an early event in light signalling photomorphogenic pathways. Relevantly the two assayed ROS metabolism marker genes *Bradi3g31880* and *Bradi1g27920,* encoding a GLUTATHIONE S-TRANSFERASE (BdGST) enzyme and PEROXIDASE 019 (BdPrx019) respectively, were differentially expressed in OE 1 compared to the WT under mock and *Fp* treatment conditions. The differential expression of *BdGST* and *BdPrx019* in the *BdPFT1*-OE backgrounds, suggests that *BdPFT1* may regulate ROS metabolism. The similarities between the *lsd1* and *BdPFT1*-OE cell death phenotype; the role of AtPFT1 as a positive regulator of *HY5* gene expression, and a potential role for BdPFT1 in regulating ROS metabolism, suggests the BdPFT1 may play a somewhat similar role to AtPFT1 in mediating light induced cell death.

Interestingly, the overexpression of wheat *PFT1* (*TaPFT1*) in *Atpft1* backgrounds; not only complemented the disease and flowering phenotypes of *pft1* but introduced a light sensitive cell death phenotype absent in native *AtPFT1 OE* backgrounds (Kidd et al., 2009). The cell death phenotypes present in BdPFT1 OE and *TaPFT1 OE*/ *Atpft1* but absent in *AtPFT1* OE genotypes suggest conservation of a light induced cell death pathway between monocotyledons and dicotyledons but divergence in the regulation of the pathway.

To determine if BdPFT1 indeed operates in a similar antagonistic pathway to LSD1 several experiments should be conducted. Initiation of the runaway cell death (RCD) observed in *lsd1* is dependent on ROS production, SA and ET accumulation (Jabs et al., 1996, Aviv et al., 2002, Rustérucci et al., 2001, Mühlenbock et al., 2008). Exogenous application of an anti-oxidant, such as ascorbate, to *BdPFT1* OE leaves should prevent ROS accumulation and hence stop the lesion formation if ROS production is involved. Further, by crossing *BdPFT1* OE and *nahG* expressing lines (Powell et al. unpub.) SA accumulation should be attenuated and suppress lesion formation. To elucidate whether BdPFT1 modulates the activity of an integrative hub of signalling involving homologs of EDS1 and interacting partner PAD4, epistasis studies should be conducted.

2.4.4 Concluding remarks

To conclude, the current study identified and characterised two independent *BdPFT1* overexpressor lines. The early flowering phenotype of the *BdPFT1*-OE lines suggests that the photoperiod induction pathway may be conserved between *Arabidopsis* and *Brachypodium*. While *BdPFT1* conferred increased susceptibility to *Fp* like *AtPFT1* and *Fo*, further experiments are required to determine if the mode of PFT1 conferred susceptibility is the same. The spontaneous lesion development phenotype, and differentially expressed SA and ROS marker genes are hallmarks of a mis-regulated light-induced cell death signalling as observed in *lsd1* mutants of *Arabidopsis* (Jabs et al., 1996, Aviv et al., 2002, Rustérucci et al., 2001, Mühlenbock et al., 2008). Further, the spontaneous lesion development phenotype is also present in *TaPFT1 OE*/ *Atpft1* but absent in *AtPFT1* OE (Kidd et al., 2009). Hence, *BdPFT1* may play a somewhat similar role in light-induced cell death signalling pathway as *AtPFT1*, but the pathway

may be differentially regulated between monocots and dicots. Overall this study has identified *BdPFT1* as conferring susceptibility towards *Fp*, highlighted similarities and potential differences between BdPFT1 and AtPFT1 in their respective species and presented avenues for further research.

2.5 Materials and methods

2.5.1 BdPFT1 genotyping assays

2.5.1.1 Extraction of *Brachypodium* genomic DNA

QuickExtract™ DNA extraction solution (Epicentre, Madison, WI) was used as per manufacturer's instruction to prepare DNA from leaf tissue samples for PCR-based genotyping assays.

2.5.1.2 Polymerase Chain Reaction (PCR)

To conduct the PCR, the Phire Plant Direct PCR kit (Thermo Fisher, Waltham, MA) was used as per manufacturer's instructions. Each reaction contained 10µL of PCR buffer 2x (includes $MgCl_2$ and dNTPs), 0.5µM of each oligonucleotide primer, 1.5ng of DNA, and 1 unit of Phire Hot Start II DNA polymerase in a final reaction volume of 20µL. A heated lid ABI 2720 Thermal Cycler (Applied Biosystems; Thermo Fisher Scientific, MA, USA) was used.

2.5.1.3 PCR based assay for detection of the *BdPFT1-OE* transgene

The PFT1-OE T-DNA constructs have a Maize ubiquitin promoter driving the expression of the native *BdPFT1* coding sequence. A forward primer targeting the maize ubiquitin promoter was used in conjunction with a reverse primer targeting the *PFT1* coding sequence. The OE product appeared as a 410bp. A set of specific primers targeting the endogenous gene *UBC18* were used as a positive control for amplification. The *UBC18* PCR product appeared as a 101bp product (Table 2.2).

Thermal cycle conditions comprised of a 5min denaturation step at 98˚C; followed by 40 cycles of 98˚C for 5sec, 59˚C for 5sec, 72˚C for 20sec; and a final elongation step at 72˚C for 5min. The PCR products were run on a 1% Agarose:TAE gel at 120V for 20min and subsequently visualised under ultraviolet light using a transilluminator

2.5.2 RNA isolation and complementary DNA (cDNA) synthesis

RNA extraction was performed using the RNeasy plant mini kit (Qiagen,Hilde, Germany) as per the manufacturer's instructions. The RNA extraction was subsequently treated with a DNAse I (amplification grade, Invitrogen) to remove any DNA contamination before cDNA synthesis. cDNA synthesis was conducted using the Superscript III First-Strand cDNA synthesis SuperMix (Thermo Fisher, Waltham, MA) as per the manufacturer's instructions.

2.5.3 RT-qPCR protocol

The real time PCR was conducted using a ViiA 7 Real-Time PCR system. Where possible, the 3' end junction of an intron-exon boundary were targeted to be spanned by the primer pairs during primer design (Table 2.3). The PCR was performed using a total reaction volume of 10µL containing; 5µL of SYBR Green, 3µM of each primer and 0.4µg of cDNA. The RT-PCR conditions consisted of an initial activation step of the polymerase for 10min at 95˚C; followed by 40 cycles of 95˚C for 15sec and 60˚C for 1min to facilitate denaturation, annealing and extension respectively. Immediately after the RT-PCR cycles, a melt curve analysis was performed to assess the specificity of the reaction. The melt curve analysis consisted of an initial denaturation step of 95˚C for 15sec, then an annealing step of 60˚C for 1min followed by a slow increase of temperature at a rate of 0.05˚C/sec to 95˚C to measure primer dissociation. Quantification of the target genes' expression was calculated using the comparative C_T method as described by Livak and Schmittgen (2001). The *UBIQUITIN CONJUGATING ENZYME 18* (*UBC18)* was used as a reference gene for the C_T calculations, as described by Hong et al. (2008) and subsequently endorsed by Chambers et al. (2012).

2.5.4 Flowering time assay

Seeds were imbibed and stratified at 4˚C for 3 days to promote even germination and growth. The seeds were subsequently sown, 6 per pot, into 100mm Super Space Saver pots (P100SS Garden City Plastics, Queensland, Logan) containing commercial potting mix, Searles Peat 80 plus. The seeds were germinated and grown under a mix of HID and incandescent lamps (400 µmol/m^2/s) set to long day conditions (16h L : 8h D) with temperatures of 22˚C and 18˚C during light and dark periods

respectively. Time to flowering was recorded as number of days since sowing for the spike to emerge. The data yielded from the flowering time assay was interval data and hence followed a non-parametric distribution. The Wilcox Rank test was selected as an appropriate non-parametric statistic and applied using the statistical computing language R (ver. 3.5.1) base{stats} function *pairwise.wilcox()* with Bonferroni's correction for multiple comparison (RCoreTeam, 2018).

2.5.5 Plant culture for infection assay

Brachypodium seeds were surface sterilised, using a 10% bleach and 0.5% Tween 20 w/v solution, for a period of 3 min, before being rinsed with sterile water. Subsequently the seeds were imbibed and stratified for three days at 4˚C, to promote even germination. The stratified seeds were plated onto 150×25mm petri dishes containing two layers of damp 12.5cm Whatman filter paper grade 3 disks. The plated seeds were germinated and grown under fluorescent lighting (42 µmol/m^2/s), set to a neutral day length (12h L : 12h D) with a diurnal temperature of 22˚C and 20˚C respectively.

2.5.6 Soilless laboratory-based paper towel infection assay

Sterilised 5-7 day old *Brachypodium* seedlings, with coleoptile emerged from the leaf sheath, were used in the soilless laboratory based infection assay. The *Fp* CS3096 isolate (deposited in the CSIRO collection) used to generate inoculum for the infection assays was derived from a highly aggressive strain isolated from infected wheat crowns in Northern New South Wales, Australia (Akinsanmi et al., 2004, Mitter et al., 2006) The seedlings were immersed in either mock (milliQ water amended with 5% Tween 20 w/v) or inoculum (1×10^6 spores/mL amended with 5% Tween 20 w/v) solutions for a period of three minutes. Afterwards the treated seedlings were rolled in a double layer of paper towel, six seeds per roll. For symptom development, the paper towel rolls containing seedlings, were placed into a growth chamber with fluorescent lighting (42 µmol/m^2/s), set to a neutral day length (12h L : 12h D) with a diurnal temperature of 22˚C and 20˚C respectively. At 12 days post inoculation the plants were assessed for their disease score ranking and number of visible leaves. The disease score ranking scale attributes a score from 0, no signs of visible symptom development to 5, completely necrotised, to each plant at an instance of time (Powell, 2016)

(Supplementary Figure 2.3). Disease score and leaf number counts respectively yield ordinal and interval datasets, which follow a non-normal distribution, requiring the use of non-parametric statistical tests for analysis.

The statistical analyses were conducted using the computing language R (ver. 3.5.1). Disease score and leaf counts were analysed as univariate data, using the *base{stats} pairwise.wilcox()* function to perform a Wilcox rank test with Bonferroni's correction for multiple comparisons (RCoreTeam, 2018). A two way permutational MANOVA was performed using the *adonis()* function from the *vegan* package (Oksanen et al., 2007), to assess the relative contribution of Genotype and Treatment grouping factors as sources of variation contributing to the response variable of disease score and leaf number. A post hoc one way permutational MANOVA was applied to determine which levels of the grouping factors contributed significantly to the group differences. As input for the permutational MANOVAs a Gower dissimilarity matrix was calculated by applying the *vegdist()* function from the *vegan* package to the disease score and leaf number datasets (Oksanen et al., 2007).

2.5.7 ROS staining protocol

In *Arabidopsis* PFT1 has been implicated in maintaining the homeostasis between ROS such as H_2O_2 and O^- in roots (Sundaravelpandian et al., 2013a). The OE lines under basal growth conditions develop a constitutive lesion forming phenotype (Figure 2.4) in older leaves, which could be related to ROS production. To test for altered ROS levels in OE2 relative to WT leaves, 3,3'-Diamonbenzidine (DAB) and nitroblue tetrazolium (NBT) leaf staining was performed. DAB detects H_2O_2 and forms a brown precipitate stain; whereas, NBT detects O_2^- and forms a blue precipitate stain. The DAB and NBT leaf staining protocol were performed as described by Jambunathan (2010) with minor modifications. Briefly, the most recently fully emerged leaf (termed as "new") and the third or fourth emerged levels (termed as "old") were excised from five-week-old OE2 and WT plants. For NBT staining leaves were immersed in either 50mM potassium phosphate buffer (pH 6.4) containing 0.1% (w/v) NBT (Thermo Fisher, Waltham, MA), as a treatment solution, or a mock solution containing no NBT. For DAB staining leaves were immersed into a DAB liquid substrate system, prepared as per the manufacturer's instructions (Sigma, St. Louis, MO), or a mock solution. The

immersed leaves were vacuum infiltrated for a period of 30 minutes. Subsequently the NBT leaves were incubated under cool fluorescent light for 20min; while the DAB infiltrated leaves were incubated under high humidity conditions for 5 hours to facilitate stain development. After incubation the leaves were boiled in 96% (v/v) Ethanol to clear the leaves, until no more chlorophyll was able to be removed. Cleared leaves were mounted and imaged by an Epson expression 1100XL flatbed scanner.

The images were subsequently analysed using the WinRHIZO Pro 2016 software (Regent, Quebec, Canada) colour detection tool, which returns the area of stained and cleared tissue per leaf. The percentage of stained tissue per leaf was calculated using the computing language R (ver. 3.5.1) (RCoreTeam, 2018) and the resulting data arcsin transformed to increase normality. According to the Shapiro-Wilks test for normality the transformed data was not normally distributed; consequently, the non-parametric Wilcox Rank test with Bonferroni's correction for multiple comparisons was applied to test for significance. The Wilcox Rank test was applied using the *base{stats} pairwise.wilcox()* function (RCoreTeam, 2018).

2.5.8 *Xanthomonas* leaf infiltration assay

To test for *BdPFT1* involvement in mediating diseases resistance to biotrophic pathogens, a *Xanthomonas translucens* (*Xt*) was conducted. OE2 and WT seeds were imbibed and stratified at 4˚C for 3 days to promote even growth and germination. Subsequently the seeds were sown into commercial potting mix, Searles peat 80 plus, six seeds per 100mm Super Space Saver pots (Garden City Plastics, P100SS). The seeds and inoculated plants were grown in a controlled environment under fluorescent lighting (200 µmol/m^2/s) set to a photoperiod of 14 h L: 10h D) with diurnal temperatures of 20˚C and 16˚C respectively. *Xt* strain DAR61454 (Gardiner et al., 2014) was incubated in LB broth (10g L^{-1} Tryptone, 10g L^{-1} NaCl, 5g L^{-1} of yeast extract) on an orbital mixer at an ambient temperature of 22˚C for 3-5 days. The broth was harvested and the Xt diluted to an OD_{600} of 0.05, in 10mM $MgCl_2$. 1ml of either OD_{600} 0.05 *Xt* suspended in 10mM $MgCl_2$ or mock solution was used to infiltrate the most recently fully emerged leaf per plant at 4 weeks post germination. The boundaries of the infiltrated area were marked using a black felt tip marker pen. At 7 dpi the infiltrated areas were excised, mounted and imaged using an Epson expression 1100XL flatbed scanner. The software ImageJ (Schneider et al., 2012) was

used to record the total infiltrated and lesion areas per leaf. Using the statistical computing language R (ver. 3.5.1) the proportion of lesion and coverage of the infiltrated area was calculated and an arcsin transformation applied to increase normality. According to the Shapiro Wilks test for normality the transformed data does not have a normal distribution; consequently, the non-parametric Wilcox rank test with Bonferroni correction for multiple comparisons was used to test for significance. The Wilcox Rank test was applied using the *base{stats} pairwise.wilcox()* function (RCoreTeam, 2018).

Chapter 2 Figures

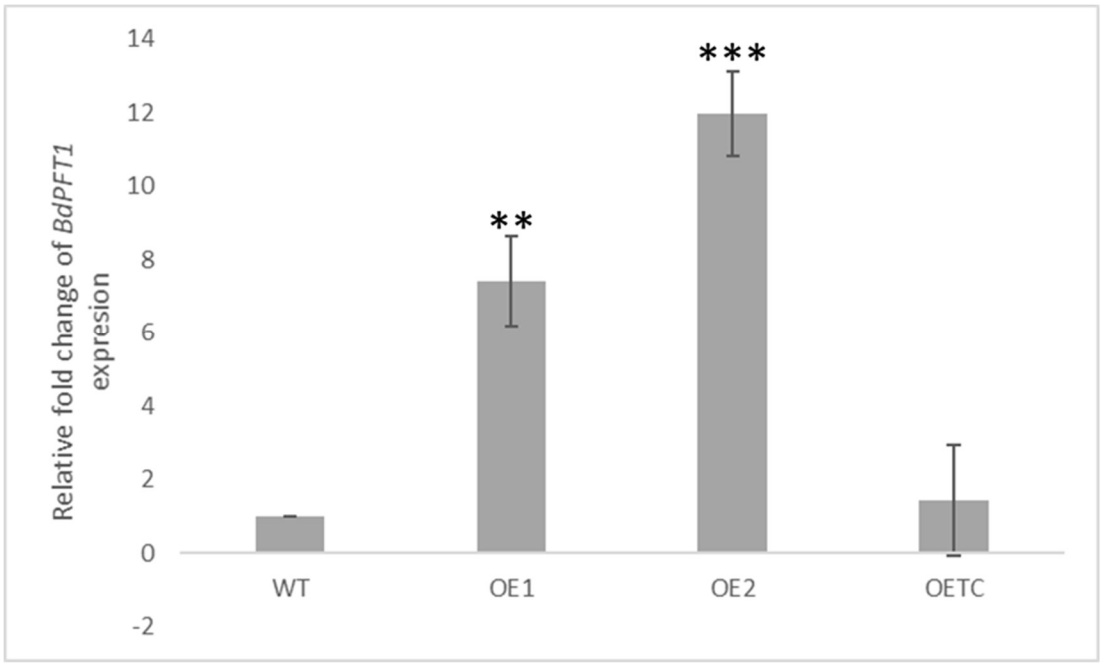

Figure 2.1: Stably transformed *Brachypodium PFT1* overexpressor (OE) transgenic lines have higher endogenous *PFT1* expression levels relative to WT. Mean fold change of *PFT1* expression levels in *PFT1* OE and OETC lines relative to endogenous *PFT1* expression in WT. *** and ** denote statistical significance of P<0.001 and P<0.01 (*Student's two-way T-test*), respectively compared to the WT. Values represent the mean ± SE of three biological replicates each containing a leaf tissue sample from three individual plants.

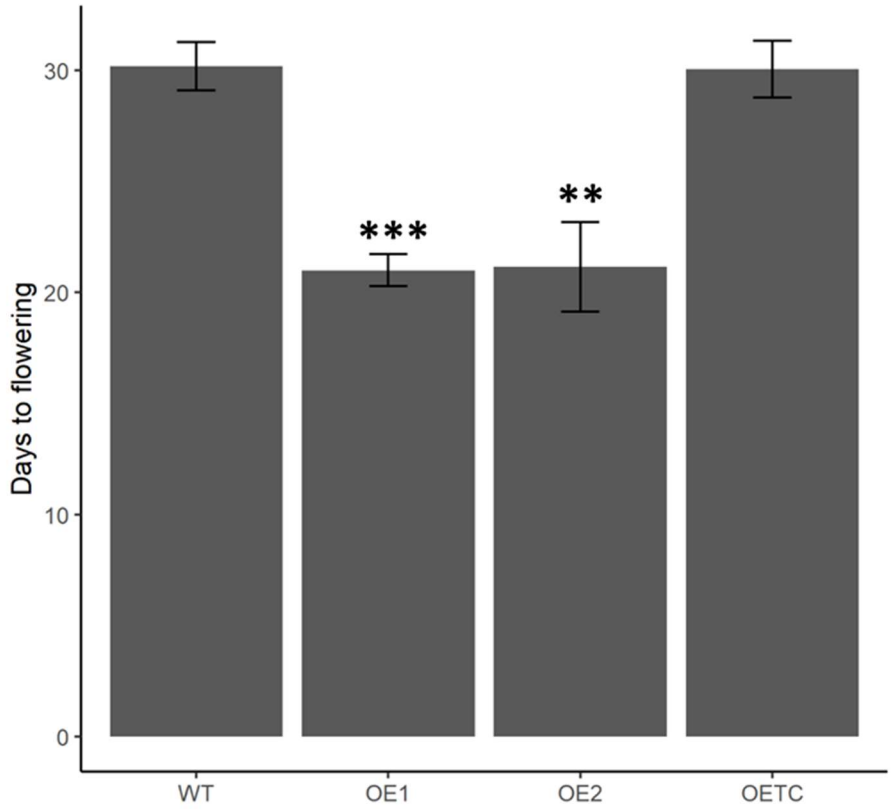

Figure 2.2: Transgenic *Brachypodium PFT1* overexpressor (OE) lines have an early flowering time phenotype. Mean (n=20) number of days to flowering for WT, *PFT1* OE and OETC plants ± SE. *** and ** denote statistical significance of P<0.001 and P<0.01 (*Wilcoxon rank test*), respectively when compared to the WT. Plants were grown under long day conditions (16h L: 8h D at 20℃).

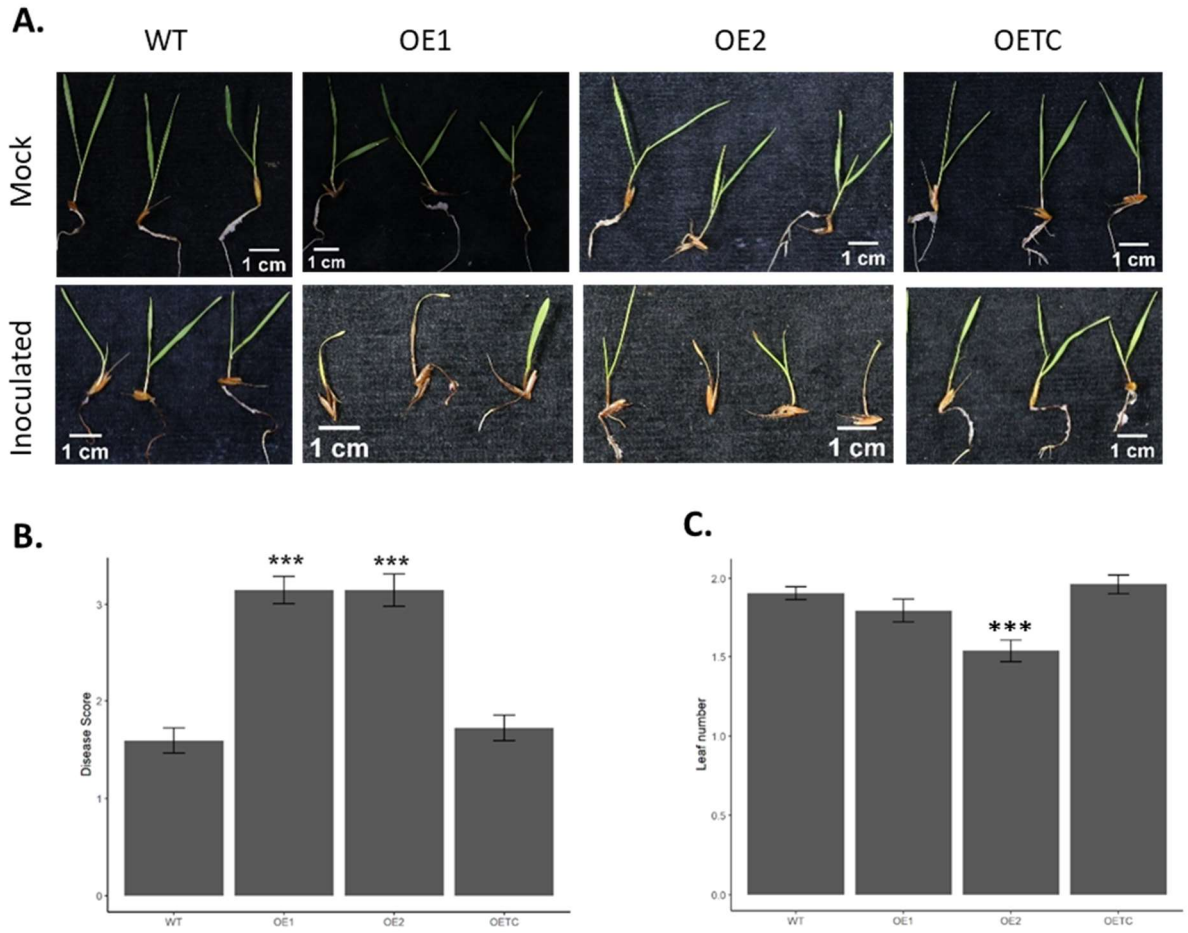

Figure 2.3: *PFT1* over expressing *Brachypodium* show enhanced disease phenotypes, under *Fp* inoculation conditions, with respect to wild type. Values were recorded from a soilless infection assay using *Brachypodium* seedlings, 9 days post inoculation (9dpi) with a 1×10^6 spores/mL *F. pseudograminearum* spore suspension. Data represents eight inoculated technical replicates of six plants per replicate. ** and *** denote statistical significance of $P < 0.01$ and $P < 0.001$ respectively, relative to inoculated WT, as per a multiple comparisons Bonferroni corrected Wilcoxon rank test. No lesions were visibly detected on the mock inoculated plants irrespective of genotype. **A.** Photographs of 9dpi mock and *Fp* inoculated plants of representative individuals. **B.** Column plot of mean disease score at 9 dpi, using a 0-5 scale of severity, ± S.E. **C.** Column plot of mean leaf number per individual plant ±S.E.

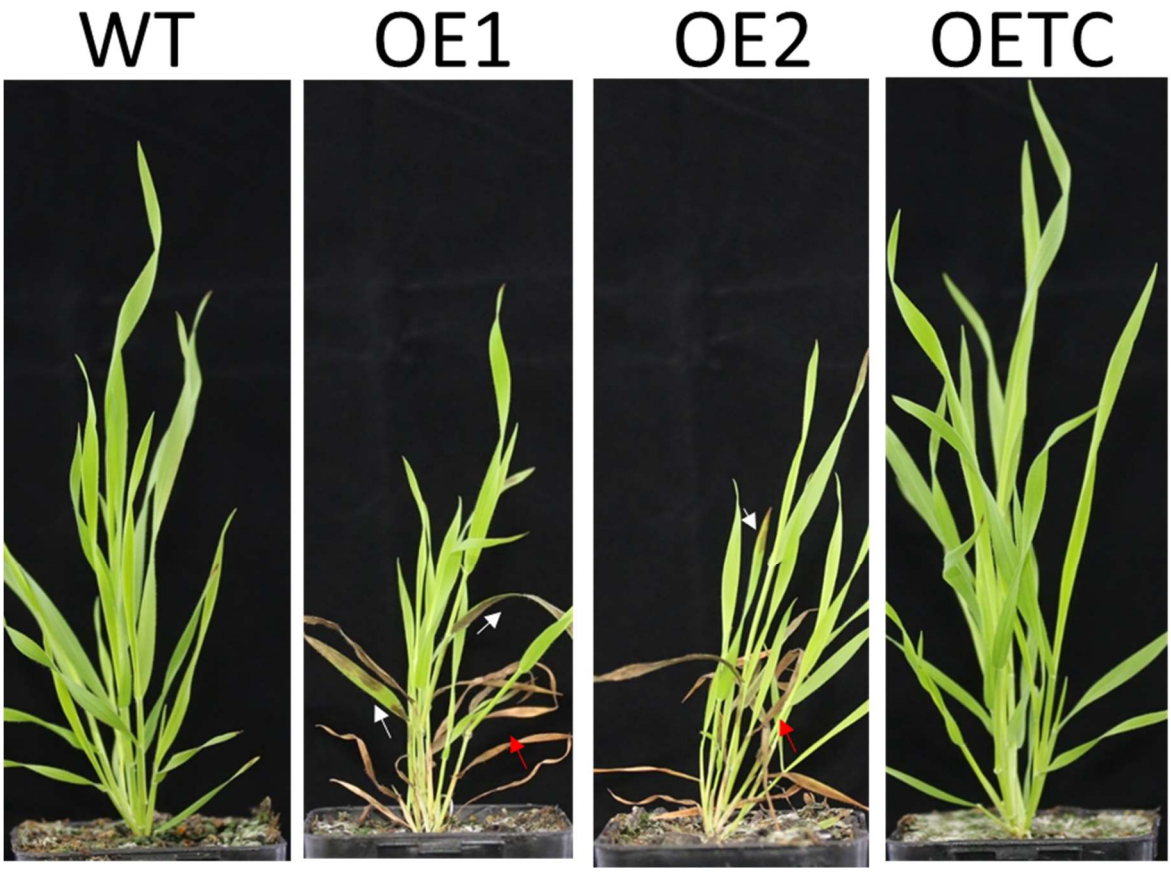

Figure 2.4: *BdPFT1* overexpressor lines display a spontaneous lesion development and stunted growth phenotype. Photographs of three-week-old representative WT, OE1, OE2, and OETC individuals, grown under long photoperiod conditions (16h L: 8h D). Note that OE1 and OE2 overall plant height is reduced in comparison to the WT and OETC genotype. White arrows indicate mature leaves displaying progressed spontaneous lesion development. Red arrows indicate completely dead leaves as a result of lesion development.

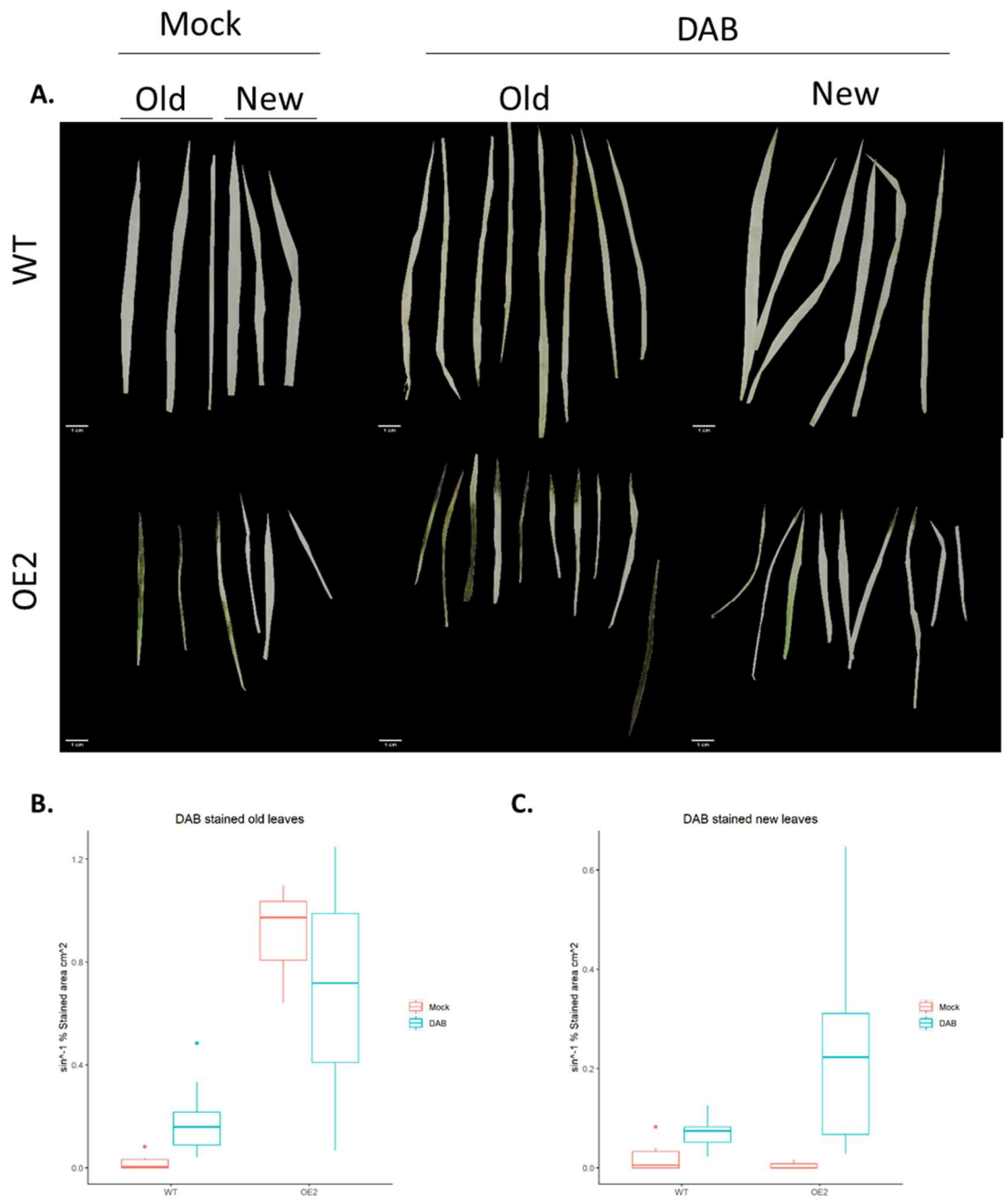

Figure 2.5: Presence of lesions in *BdPFT1*-OE 2 leaves masks the effect of 3,3'-Diamonobenzidene stain (DAB). A. Images of mock and DAB stained leaves from five-week-old *BdPFT1*-OE2 and WT plants. New refers to the most recently fully emerged leaf; while old refers to the third or fourth recently emerged leaf sampled from each plant. Note the smaller leaf size of OE2 leaves compared to the WT, due to the stunted growth phenotype of *BdPFT1*-OE plants. The DAB stain appears as a brown precipitate. **B.** Boxplot distribution of arcsin transformed percentage of coloured area (cm^2) in DAB stained old leaves. **C.** Boxplot distribution of arcsin transformed percentage of coloured area in DAB stained new leaves.

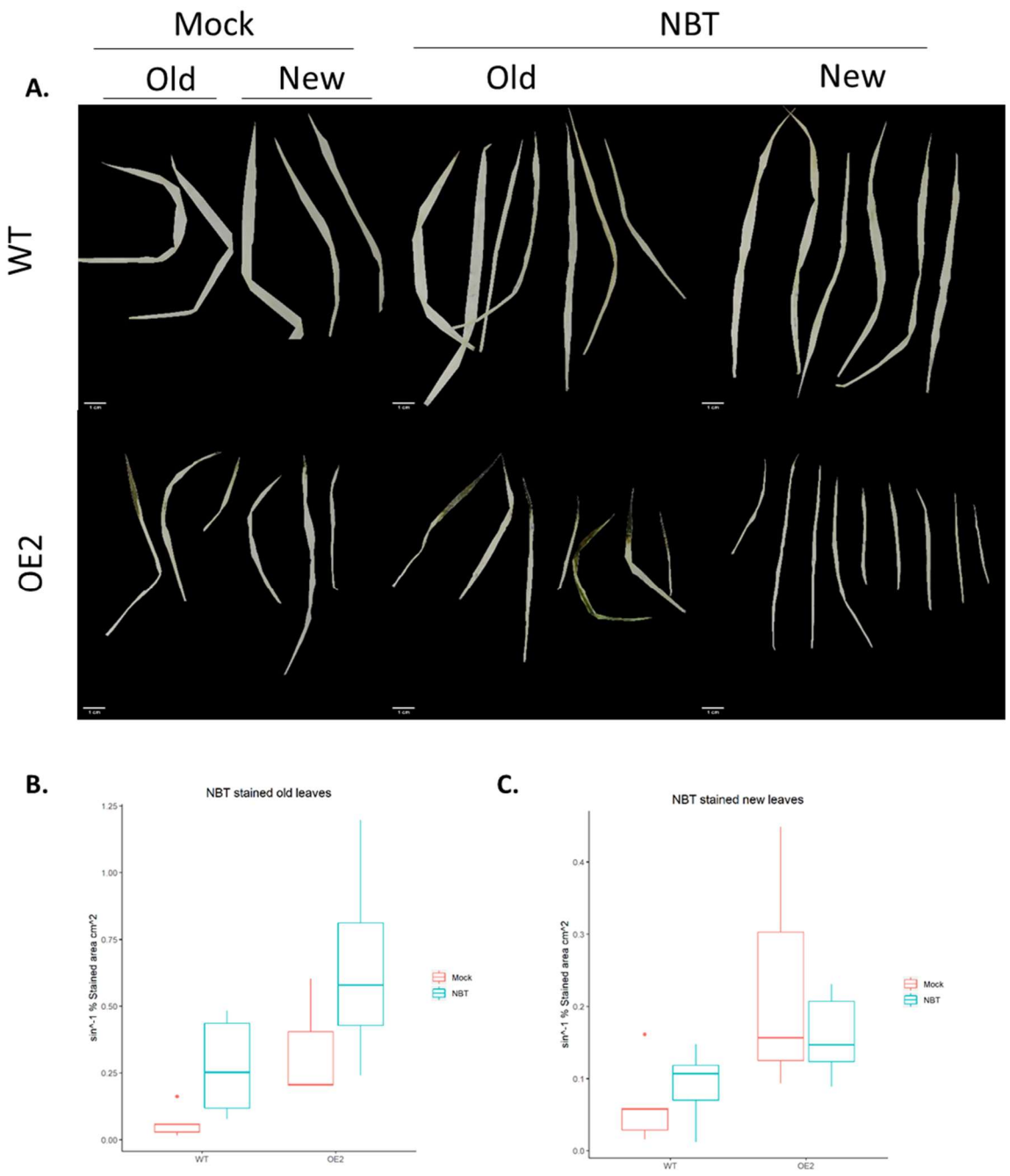

Figure 2.6: Presence of lesions in *BdPFT1*-OE 2 leaves masks the effect of nitroblue tetrazolium (NBT) stain. A. Images of mock and NBT stained leaves from five-week-old *BdPFT1*-OE2 and WT plants. New refers to the most recently fully emerged leaf; while old refers to the third or fourth recently emerged leaf sampled from each plant. The NBT stain appears as a blue precipitate. Note the smaller leaf size of OE2 leaves compared to the WT, due to the stunted growth phenotype of *BdPFT1*-OE plants. **B.** Boxplot distribution of arcsin transformed percentage of coloured area (cm^2) in NBT stained old leaves. **C.** Boxplot distribution of arcsin transformed percentage of coloured area in NBT stained new leaves.

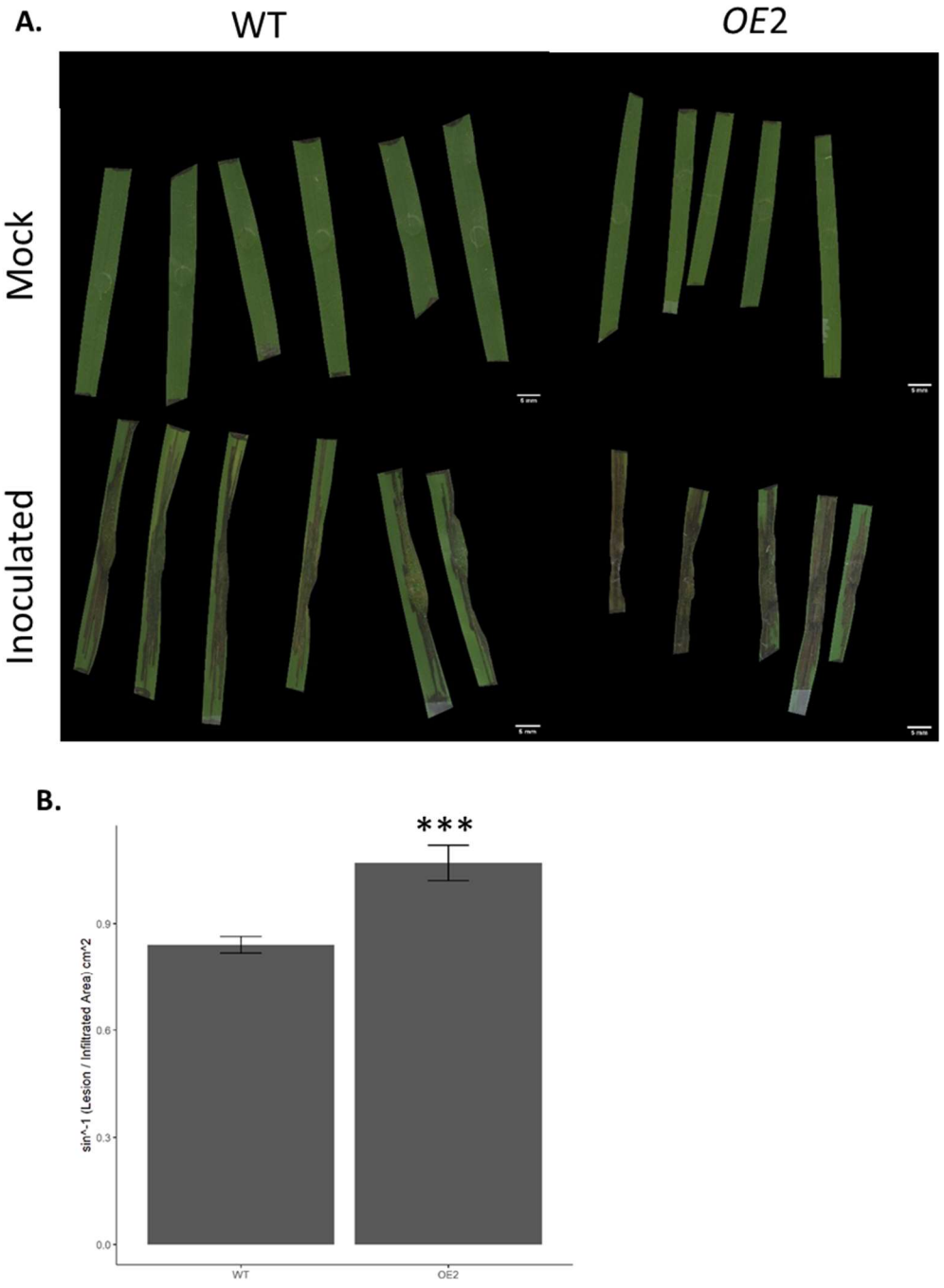

Figure 2.7: *PFT1 over*-expressing (OE) plants show enhanced lesion formation phenotypes, under *X. translucens* inoculation conditions, with respect to wild type. Values were recorded from a leaf infiltration assay at 7 days post inoculation (7 dpi) with 1mL of OD_{600} 0.05 *X. translucens* suspension in 10mM $MgCl_2$. Data represents four technical replicates with five to six plants and a single infiltration per plant per replicate. **A.** Photographs of 7 dpi mock and *X. translucens* infiltrated leaf segments. **B.** Column plot of mean sin^{-1} transformed percentage of

lesion coverage of infiltrated area ±S.E. *** denotes statistical significance of $P<0.001$ (Wilcoxon rank two-way test), compared to the WT.

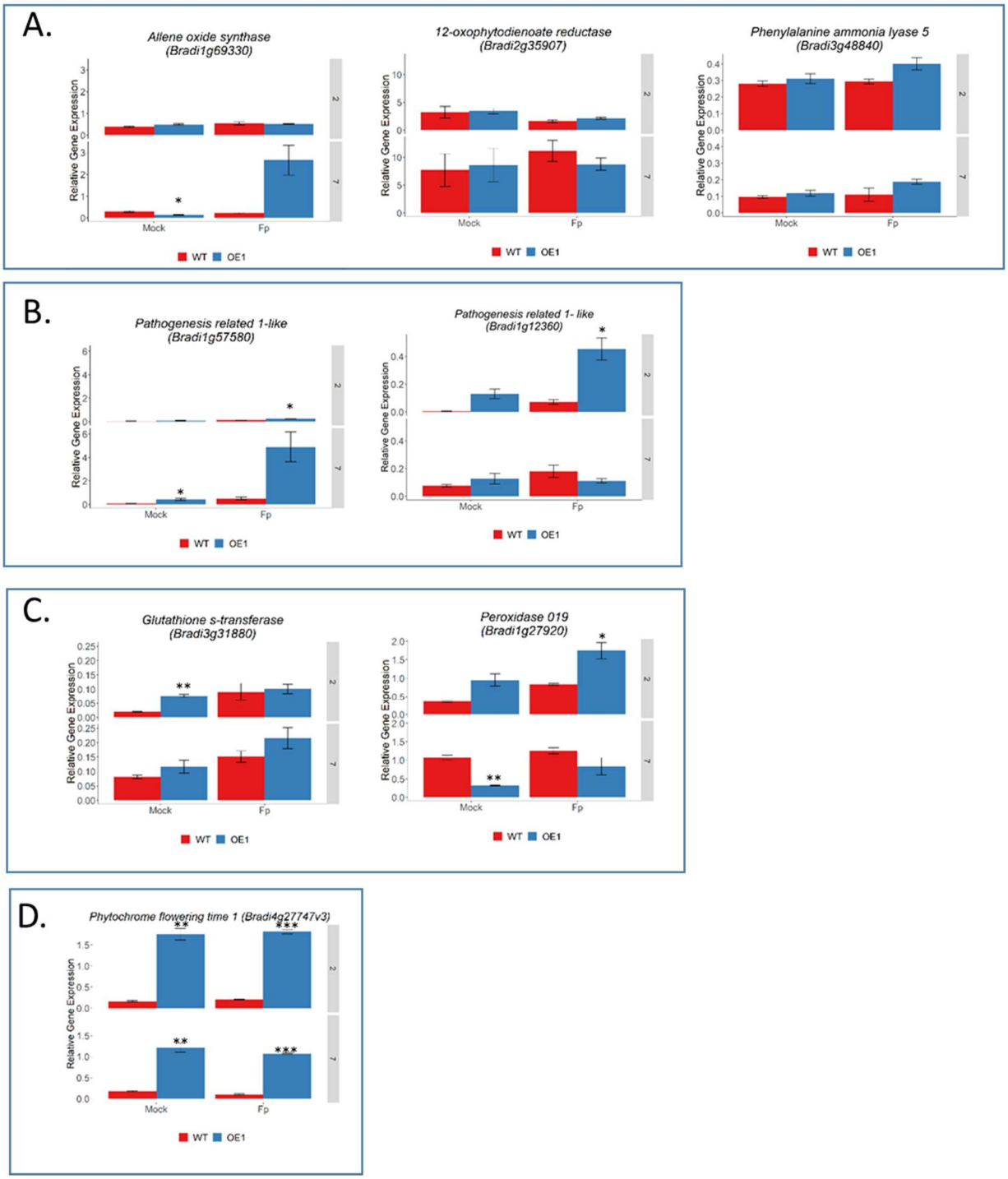

Figure 2.8: Expression of JA (A), SA (B), ROS (C) marker genes and *BdPFT1* (D) in *Brachypodium* wild type (WT) and *BdPFT1* over-expressor 1 (OE1) lines under mock and *Fp* inoculation conditions relative to the expression of reference gene *UBC18*. C_T values were recorded by quantitative real time PCR on RNA samples from a soilless infection assay using *Brachypodium* seedlings, at 2- and 7-days post inoculation (dpi) with either a mock or 1×10^6 spores/mL *F. pseudograminearum* spore suspension and ΔC_T values calculated. Data represents mean ΔC_T values from three replicates of 18 plants per replicate. *, ** and *** denote statistical significance of $P < 0.05$, $P<0.01$ and $P < 0.001$ respectively,

relative to the WT of each treatment, as per a two-sided Student's t test. Error bars represent standard error (SE) of the mean.

Tables

Table 2.1 List of marker, validation and reference genes assayed for expression levels in WT and *BdPFT1* overexpression lines under mock and *Fusarium pseudograminearum* inoculation treatments.

Gene ID	Gene description	Marker	Reference
Bradi1g69330	Allene oxide synthase	JA	Kouzai et al. (2016), Kakei et al. (2015)
Bradi2g35907	12-Oxyphtodienoate reductase	JA	Wang et al. (2017), Powell et al. (2017)
Bradi3g48840	Phenylalanine ammonia lyase 5	JA	Kouzai et al. (2016), Cass et al. (2015)
Bradi1g57580	Pathogenesis related 1-like	SA	Mandadi and Scholthof (2012), Wang et al. (2017)
Bradi1g12360	Pathogenesis related 1 -like	SA	Pasquet et al. (2014)
Bradi3g31880	Glutathione s-transferase	ROS	Gallé et al. (2019)
Bradi1g27920	Peroxidase 019	ROS	Zhu et al. (2019)
Bradi4g27747	Phytochrome flowering time 1	Validation	-
Bradi4g00660	Ubiquitin conjugating enzyme 18	Reference	Hong et al. (2008), Chambers et al. (2012)

Table 2.2: List of primers used for genotyping *BdPFT1* overexpression (OE) and hairpin T-DNA insertion lines and control gene Ubiquitin conjugating enzyme 18

Primer name	**Gene ID**	**Forward Primer**	**Reverse Primer**
F_Ubi.tm1	Transgene	5'TTTAGCCCTGCCTTCATACG3'	
BdPFT1-OE_R			5'CTGAAGCCTCCGCCACTAAA3'
BdPFT1-hairpin_R			5'TGTGTCAGATGCTGTCCCAC3'
Ubiquitin conjugating enzyme 18	*Bradi4g00660*		

Table 2.3: qRT-PCR primer sequences for JA, SA and ROS marker gene analysis of paper towel assay.				
Gene ID	**Gene description**	**Forward primer**	**Reverse primer**	**Reference**
Bradi1g69330	Allene oxide synthase	5'ACCGCCTGGACTTCTACTAC3'	5'GAGGTTCTTCTTCTCCACCT3'	Kouzai et al. (2016), Kakei et al. (2015)
Bradi2g35907	12-Oxyphtodienoate reductase	5'CGCCTTCATCTTCTGCCA3'	5'GCTGACCTTCCTATCCGTG3'	Wang et al. (2017), Powell et al. (2017)
Bradi3g48840	Phenylalanine ammonia lyase 5	5'TCTTTGAGGCAAACATTCTT3'	5'ATAGCAGCAGCCTCTATTTG3'	Kouzai et al. (2016), Cass et al. (2015)
Bradi1g57580	Pathogenesis related 1-like	5'GTGTGCTCGTGTTGTTTGTG3'	5'AATAAGGGCTCCGTCCGA3'	Mandadi and Scholthof (2012), Wang et al. (2017)
Bradi1g12360	Pathogenesis related 1 -like	5'ACTACACGCAGGTGATGTG3'	5'GTTGCAGGTGATGAAGACG3'	Pasquet et al. (2014)
Bradi3g31880	Glutathione s-transferase	5'AAGCGGAGAGCTGAAGCT3'	5'CTCCTCGACGTACTCGTACG3'	Gallé et al. (2019)
Bradi1g27920	Peroxidase 019	5'AACCACTACTTCACCAACCTGGAA3'	5'CAAAGCAGTCATGAAAAAGGAGCCT3'	Zhu et al. (2019)
Bradi4g27747v3	Phytochrome flowering time 1	5'AAGCAGTATGTTGGCAAGGC3'	5'AACTGAATCACGGCACACAG3'	
Bradi4g00660	Ubiquitin conjugating enzyme 18	5'TTTACAGCAATGGCCACATC3'	5'AGACAGCATGGACAAGATGC3'	Hong et al. (2008), Chambers et al. (2012)

Supplementary Files

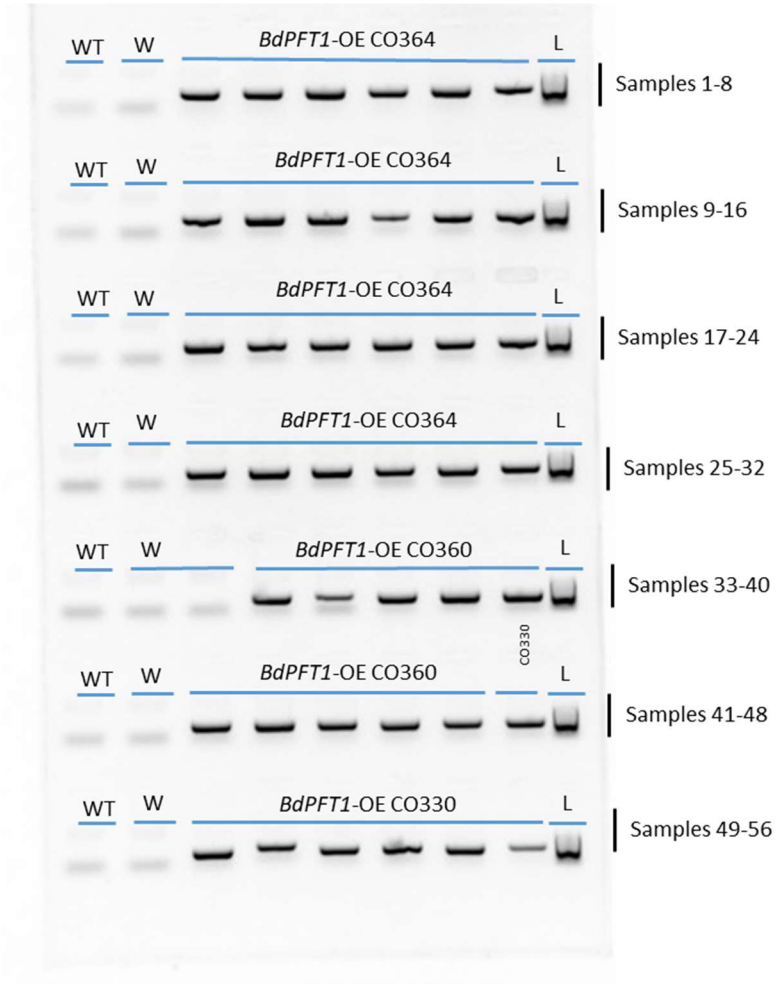

Supplementary Figure 2.1: *Brachypodium distachyon PFT1* overexpressor (*BdPFT1*-OE) lines CO364, CO360 and CO330 are homozygous lines. Image shows a genotyping PCR run on a 1% agarose gel with SYBRsafe stain (2.5µL/100ml) at 120 volts for 18 minutes. Samples were loaded from left to right lane, with each well containing a single sample. WT refers to wild type DNA used as a negative control. W refers to water control. L stands for Easyladder I. Blue lines represent PCR reactions that used *BdPFT1*-OE primers which yield a 410bp product. Note that a *BdPFT1*-OE band is present for each CO364, CO360 and CO330 sample but is absent in the wild type (WT) and water (W) samples.

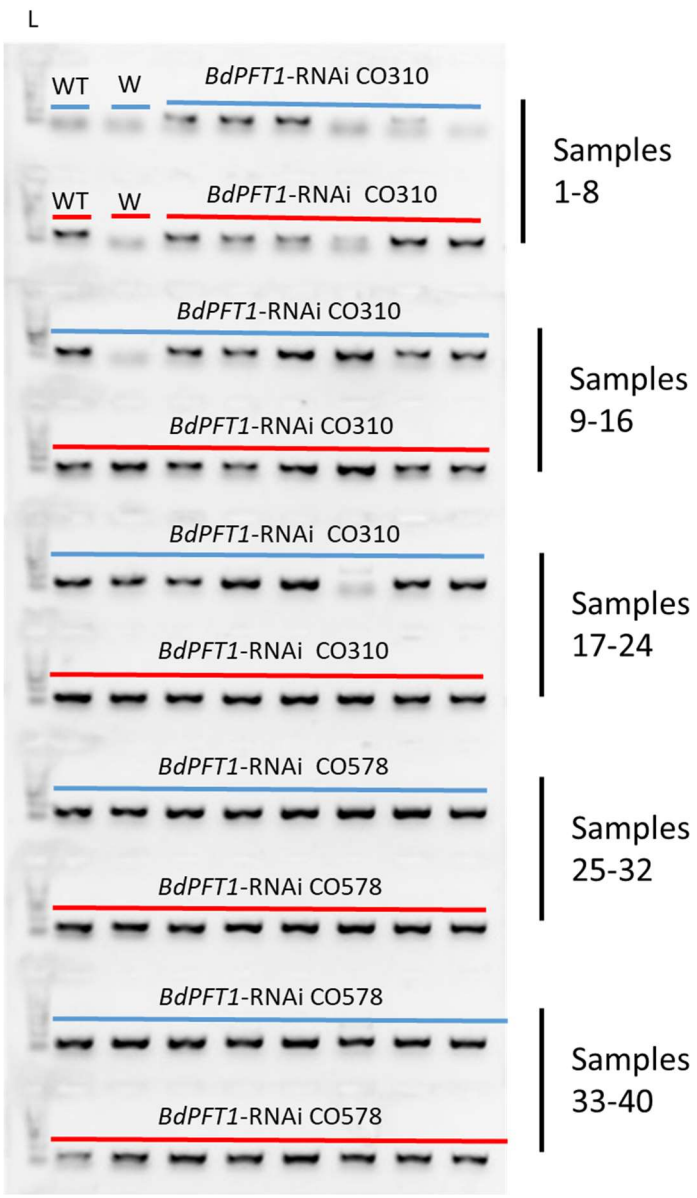

Supplementary Figure 2.2: *Brachypodium distachyon PFT1* RNAi (*BdPFT1*-RNAi) lines CO578, is a homozygous line. Image shows a genotyping PCR run on a 1% agarose gel with SYBRsafe stain (2.5µL/100ml) at 120 volts for 18 minutes. Samples were loaded from left to right lane, with each well containing a single sample. WT refers to wild type DNA used as a negative control. W refers to water control. L stands for Easyladder I. Blue and red lines represent PCR reactions that use either *BdPFT1*-RNAi or UBC18 primers which yield a 354bp and 101bp product respectively. Note that a *BdPFT1*-RNAi band is present for each CO578 sample but is absent in the wild type (WT) and water (W) samples. Further note that a UBC18 band is present in the WT and each CO578 wells, indicating that the PCR worked appropriately.

Supplementary Figure 2.3 :Disease score ranking scale for assessing Fusarium Crown Rot symptoms in *Brachypodium distachyon* based on Powell (2016). The scale is used for attributing a score from 0 to 5 in increments of 1 to each plant at an instance of time**.** The plants photographed are representative of each score. The descriptors of each score are as follows; 0 = plant with no visible disease symptoms; 1 = a plant with small necrotic lesions appearing on the stem base; 2 = a plant with progressed disease symptoms having necrotic lesions but < 25% of the plant comprised of necrotic tissue; 3 = a plant with >25% but <75% necrotic tissue; 4 = a plant comprised of >75% necrotic tissue but with some living tissue visible; 5= a dead plant, with leaf and stem tissue completely necrotised. Figure adapted from Powell (2016).

References

AKINSANMI, O. A., MITTER, V., SIMPFENDORFER, S., BACKHOUSE, D. & CHAKRABORTY, S. 2004. Identity and pathogenicity of *Fusarium* spp. isolated from wheat fields in Queensland and northern New South Wales. *Australian Journal of Agricultural Research,* 55**,** 97-107.

ALAHMAD, S., SIMPFENDORFER, S., BENTLEY, A. & HICKEY, L. 2018. Crown rot of wheat in Australia: *Fusarium pseudograminearum* taxonomy, population biology and disease management. *Australasian Plant Pathology,* 47**,** 285-299.

ALLEN, B. L. & TAATJES, D. J. 2015. The Mediator complex: a central integrator of transcription. *Nature reviews Molecular cell biology,* 16**,** 155.

AVIV, D. H., RUSTÉRUCCI, C., III, B. F. H., DIETRICH, R. A., PARKER, J. E. & DANGL, J. L. 2002. Runaway cell death, but not basal disease resistance, in *lsd1* is SA‐and *NIM1*/*NPR1*‐dependent. *The Plant Journal,* 29**,** 381-391.

BACKHOUSE, D., ABUBAKAR, A., BURGESS, L., DENNISC, J., HOLLAWAY, G., WILDERMUTH, G., WALLWORK, H. & HENRY, F. 2004. Survey of *Fusarium* species associated with crown rot of wheat and barley in eastern Australia. *Australasian Plant Pathology,* 33**,** 255-261.

BACKHOUSE, D. & BURGESS, L. 2002. Climatic analysis of the distribution of *Fusarium graminearum*, *F. pseudograminearum* and *F. culmorum* on cereals in Australia. *Australasian Plant Pathology,* 31**,** 321-327.

BÄCKSTRÖM, S., ELFVING, N., NILSSON, R., WINGSLE, G. & BJÖRKLUND, S. 2007. Purification of a plant mediator from *Arabidopsis thaliana* identifies PFT1 as the Med25 subunit. *Molecular cell,* 26**,** 717-729.

BINDSCHEDLER, L. V., DEWDNEY, J., BLEE, K. A., STONE, J. M., ASAI, T., PLOTNIKOV, J., DENOUX, C., HAYES, T., GERRISH, C. & DAVIES, D. R. 2006. Peroxidase‐dependent apoplastic oxidative burst in *Arabidopsis* required for pathogen resistance. *The Plant Journal,* 47**,** 851-863.

BOVILL, W., MA, W., RITTER, K., COLLARD, B., DAVIS, M., WILDERMUTH, G. & SUTHERLAND, M. 2006. Identification of novel QTL for resistance to crown rot in the doubled haploid wheat population 'W21MMT70'×'Mendos'. *Plant Breeding,* 125**,** 538-543.

BRAGG, J. N., WU, J., GORDON, S. P., GUTTMAN, M. E., THILMONY, R., LAZO, G. R., GU, Y. Q. & VOGEL, J. P. 2012. Generation and characterization of the Western Regional Research Center *Brachypodium* T-DNA insertional mutant collection. *PLoS One,* 7**,** e41916.

BURGESS, L., WEARING, A. & TOUSSOUN, T. 1975. Surveys of *Fusaria* associated with crown rot of wheat in eastern Australia. *Australian Journal of Agricultural Research,* 26**,** 791-799.

CASS, C. L., PERALDI, A., DOWD, P. F., MOTTIAR, Y., SANTORO, N., KARLEN, S. D., BUKHMAN, Y. V., FOSTER, C. E., THROWER, N., BRUNO, L. C., MOSKVIN, O. V., JOHNSON, E. T., WILLHOIT, M. E., PHUTANE, M., RALPH, J., MANSFIELD, S. D., NICHOLSON, P. & SEDBROOK, J. C. 2015. Effects of *PHENYLALANINE AMMONIA LYASE* (*PAL*) knockdown on cell wall composition, biomass digestibility, and biotic and abiotic stress responses in *Brachypodium*. *Journal of Experimental Botany,* 66**,** 4317-4335.

CERDÁN, P. D. & CHORY, J. 2003. Regulation of flowering time by light quality. *Nature,* 423**,** 881.

ÇEVIK, V., KIDD, B. N., ZHANG, P., HILL, C., KIDDLE, S., DENBY, K. J., HOLUB, E. B., CAHILL, D. M., MANNERS, J. M. & SCHENK, P. M. 2012. MEDIATOR25 acts as an integrative hub for the regulation of jasmonate-responsive gene expression in Arabidopsis. *Plant physiology,* 160**,** 541-555.

CHAI, T., ZHOU, J., LIU, J. & XING, D. 2015. LSD1 and HY5 antagonistically regulate red light induced-programmed cell death in *Arabidopsis*. *Frontiers in Plant Science,* 6.

CHAMBERS, J. P., BEHPOURI, A., BIRD, A. & NG, C. K. 2012. Evaluation of the use of the polyubiquitin genes, Ubi4 and Ubi10 as reference genes for expression studies in *Brachypodium distachyon*. *PloS one,* 7**,** e49372.

CHANG, C. C., ŚLESAK, I., JORDÁ, L., SOTNIKOV, A., MELZER, M., MISZALSKI, Z., MULLINEAUX, P. M., PARKER, J. E., KARPIŃSKA, B. & KARPIŃSKI, S. 2009. *Arabidopsis* chloroplastic glutathione peroxidases play a role in cross talk between photooxidative stress and immune responses. *Plant Physiology,* 150**,** 670-683.

CHEN, R., JIANG, H., LI, L., ZHAI, Q., QI, L., ZHOU, W., LIU, X., LI, H., ZHENG, W. & SUN, J. 2012. The Arabidopsis mediator subunit MED25 differentially regulates jasmonate and abscisic acid signaling through interacting with the MYC2 and ABI5 transcription factors. *The Plant Cell,* 24**,** 2898-2916.

COLL, N., EPPLE, P. & DANGL, J. 2011. Programmed cell death in the plant immune system. *Cell death and differentiation,* 18**,** 1247.

COLLARD, B., GRAMS, R., BOVILL, W., PERCY, C., JOLLEY, R., LEHMENSIEK, A., WILDERMUTH, G. & SUTHERLAND, M. 2005. Development of molecular markers for crown rot resistance in wheat: mapping of QTLs for seedling resistance in a ‘2‐49’ × ‘Janz’ population. *Plant Breeding,* 124**,** 532-537.

CONAWAY, R. C. & CONAWAY, J. W. 2011. Function and regulation of the Mediator complex. *Current opinion in genetics & development,* 21**,** 225-230.

DAUDI, A., CHENG, Z., O'BRIEN, J. A., MAMMARELLA, N., KHAN, S., AUSUBEL, F. M. & BOLWELL, G. P. 2012. The apoplastic oxidative burst peroxidase in *Arabidopsis* is a major component of pattern-triggered immunity. *The Plant Cell,* 24**,** 275-287.

DENG, W., YING, H., HELLIWELL, C. A., TAYLOR, J. M., PEACOCK, W. J. & DENNIS, E. S. 2011. FLOWERING LOCUS C (FLC) regulates development pathways throughout the life cycle of *Arabidopsis*. *Proceedings of the National Academy of Sciences,* 108**,** 6680-6685.

DIETRICH, R. A., DELANEY, T. P., UKNES, S. J., WARD, E. R., RYALS, J. A. & DANGL, J. L. 1994. *Arabidopsis* mutants simulating disease resistance response. *Cell,* 77**,** 565-577.

FITZGERALD, T. L., POWELL, J. J., SCHNEEBELI, K., HSIA, M. M., GARDINER, D. M., BRAGG, J. N., MCINTYRE, C. L., MANNERS, J. M., AYLIFFE, M. & WATT, M. 2015a. *Brachypodium* as an emerging model for cereal–pathogen interactions. *Annals of Botany,* 115**,** 717-731.

FITZGERALD, T. L., POWELL, J. J., STILLER, J., WEESE, T. L., ABE, T., ZHAO, G., JIA, J., MCINTYRE, C. L., LI, Z. & MANNERS, J. M. 2015b. An assessment of heavy ion irradiation mutagenesis for reverse genetics in wheat (*Triticum aestivum* L.). *PLoS One,* 10**,** e0117369.

FRENKEL, M., KÜLHEIM, C., JÄNKÄNPÄÄ, H. J., SKOGSTRÖM, O., DALL'OSTO, L., ÅGREN, J., BASSI, R., MORITZ, T., MOEN, J. & JANSSON, S. 2009. Improper excess light energy dissipation in *Arabidopsis* results in a metabolic reprogramming. *BMC Plant Biology,* 9**,** 12.

GALLÉ, Á., BENYÓ, D., CSISZÁR, J. & GYÖRGYEY, J. 2019. Genome-wide identification of the glutathione transferase superfamily in the model organism *Brachypodium distachyon*. *Functional Plant Biology,* 46**,** 1049-1062.

GANGAPPA, S. N. & BOTTO, J. F. 2016. The multifaceted roles of HY5 in plant growth and development. *Molecular plant,* 9**,** 1353-1365.

GARDINER, D. M., UPADHYAYA, N. M., STILLER, J., ELLIS, J. G., DODDS, P. N., KAZAN, K. & MANNERS, J. M. 2014. Genomic analysis of *Xanthomonas translucens* pathogenic on wheat and barley reveals cross-kingdom gene transfer events and diverse protein delivery systems. *PLoS One,* 9**,** e84995.

HAYWARD, A. 1993. The hosts of *Xanthomonas*. *Xanthomonas.* Springer.

HIGGINS, J. A., BAILEY, P. C. & LAURIE, D. A. 2010. Comparative genomics of flowering time pathways using *Brachypodium distachyon* as a model for the temperate grasses. *PLoS one,* 5**,** e10065.

HONG, S. H., SEO, P. J., YANG, M. S., XIANG, F. & PARK, C. M. 2008. Exploring valid reference genes for gene expression studies in *Brachypodium distachyon* by real-time PCR. *BMC Plant Biology,* 8.

IÑIGO, S., ALVAREZ, M. J., STRASSER, B., CALIFANO, A. & CERDÁN, P. D. 2012a. PFT1, the MED25 subunit of the plant Mediator complex, promotes flowering through CONSTANS dependent and independent mechanisms in *Arabidopsis*. *The Plant Journal,* 69**,** 601-612.

IÑIGO, S., GIRALDEZ, A. N., CHORY, J. & CERDÁN, P. D. 2012b. Proteasome-mediated turnover of *Arabidopsis* MED25 is coupled to the activation of *FLOWERING LOCUS T* transcription. *Plant physiology,* 160**,** 1662-1673.

INITIATIVE, T. I. B. 2010. Genome sequencing and analysis of the model grass *Brachypodium distachyon*. *Nature,* 463.

JABS, T., DIETRICH, R. A. & DANGL, J. L. 1996. Initiation of runaway cell death in an *Arabidopsis* mutant by extracellular superoxide. *Science,* 273**,** 1853-1856.

KAKEI, Y., MOCHIDA, K., SAKURAI, T., YOSHIDA, T., SHINOZAKI, K. & SHIMADA, Y. 2015. Transcriptome analysis of hormone-induced gene expression in *Brachypodium distachyon*. *Scientific reports,* 5**,** 14476.

KARIJOLICH, J. J. & HAMPSEY, M. 2012. The Mediator complex. *Current biology,* 22**,** R1030-R1031.

KAZAN, K. 2017. The multitalented MEDIATOR25. *Frontiers in plant science,* 8**,** 999.

KAZAN, K. & GARDINER, D. M. 2018. Fusarium crown rot caused by *Fusarium pseudograminearum* in cereal crops: recent progress and future prospects. *Molecular plant pathology,* 19**,** 1547-1562.

KAZAN, K., GARDINER, D. M. & MANNERS, J. M. 2012. On the trail of a cereal killer: recent advances in *Fusarium graminearum* pathogenomics and host resistance. *Mol Plant Pathol,* 13.

KAZAN, K. & LYONS, R. 2015. The link between flowering time and stress tolerance. *Journal of Experimental Botany,* 67**,** 47-60.

KHANGURA, R. K., MACNISH, G. C., MACLEOD, W. J., VANSTONE, V. A., HANBURY, C. D., LOUGHMAN, R. & SPEIJERS, J. E. 2013. Current status of cereal root diseases in Western Australia under intensive cereal production and their comparison with the historical survey conducted during 1976–1982. *Journal of Phytopathology,* 161**,** 828-840.

KIDD, B. N., EDGAR, C. I., KUMAR, K. K., AITKEN, E. A., SCHENK, P. M., MANNERS, J. M. & KAZAN, K. 2009. The mediator complex subunit PFT1 is a key regulator of jasmonate-dependent defense in *Arabidopsis*. *The Plant Cell,* 21**,** 2237-2252.

KLOSE, C., BÜCHE, C., FERNANDEZ, A. P., SCHÄFER, E., ZWICK, E. & KRETSCH, T. 2012. The mediator complex subunit PFT1 interferes with COP1 and HY5 in the regulation of *Arabidopsis* light signaling. *Plant physiology,* 160**,** 289-307.

KOPRIVOVA, A., CALDERWOOD, A., LEE, B.-R. & KOPRIVA, S. 2014. Do PFT1 and HY5 interact in regulation of sulfate assimilation by light in *Arabidopsis*? *FEBS letters,* 588**,** 1116-1121.

KORVES, T. M. & BERGELSON, J. 2003. A developmental response to pathogen infection in *Arabidopsis*. *Plant physiology,* 133**,** 339-347.

KOUZAI, Y., KIMURA, M., YAMANAKA, Y., WATANABE, M., MATSUI, H., YAMAMOTO, M., ICHINOSE, Y., TOYODA, K., ONDA, Y. & MOCHIDA, K. 2016. Expression profiling of marker genes responsive to the defence-associated phytohormones salicylic acid, jasmonic acid and ethylene in *Brachypodium distachyon*. *BMC plant biology,* 16**,** 59.

LEE, J., HE, K., STOLC, V., LEE, H., FIGUEROA, P., GAO, Y., TONGPRASIT, W., ZHAO, H., LEE, I. & DENG, X. W. 2007. Analysis of transcription factor HY5 genomic binding sites revealed its hierarchical role in light regulation of development. *The Plant Cell,* 19**,** 731-749.

LIU, C. & OGBONNAYA, F. C. 2015. Resistance to Fusarium crown rot in wheat and barley: a review. *Plant Breeding,* 134**,** 365-372.

LIU, J., CHENG, X., LIU, P., LI, D., CHEN, T., GU, X. & SUN, J. 2017. MicroRNA319-regulated TCPs interact with FBHs and PFT1 to activate *CO* transcription and control flowering time in *Arabidopsis*. *PLoS genetics,* 13**,** e1006833.

LIU, J., ZHANG, T., JIA, J. & SUN, J. 2016. The Wheat Mediator Subunit TaMED25 Interacts with the Transcription Factor TaEIL1 to Negatively Regulate Disease Resistance against Powdery Mildew. *Plant Physiology,* 170**,** 1799-1816.

LIU, Y., ZHENG, Y. L., WEI, Y., ZHOU, M. & LIU, C. 2012. Genotypic differences to crown rot caused by *Fusarium pseudograminearum* in barley (*Hordeum vulgare* L.). *Plant Breeding,* 131**,** 728-732.

LIVAK, K. J. & SCHMITTGEN, T. D. 2001. Analysis of relative gene expression data using real-time quantitative PCR and the 2− ΔΔCT method. *methods,* 25**,** 402-408.

LUNA, E., BRUCE, T. J., ROBERTS, M. R., FLORS, V. & TON, J. 2012. Next-generation systemic acquired resistance. *Plant physiology,* 158**,** 844-853.

LUNA, E. & TON, J. 2012. The epigenetic machinery controlling transgenerational systemic acquired resistance. *Plant signaling & behavior,* 7**,** 615-618.

LYONS, R., MANNERS, J. M. & KAZAN, K. 2013. Jasmonate biosynthesis and signaling in monocots: a comparative overview. *Plant Cell Reports,* 32**,** 815-827.

LYONS, R., RUSU, A., STILLER, J., POWELL, J., MANNERS, J. M. & KAZAN, K. 2015. Investigating the association between flowering time and defense in the *Arabidopsis thaliana-Fusarium oxysporum* interaction. *PLoS One,* 10**,** e0127699.

MANDADI, K. K. & SCHOLTHOF, K. B. 2012. Characterization of a viral synergism in the monocot *Brachypodium distachyon* reveals distinctly altered host molecular processes associated with disease. *Plant Physiol,* 160.

MANO, J. I., ISHIBASHI, A., MUNEUCHI, H., MORITA, C., SAKAI, H., BISWAS, M. S., KOEDUKA, T. & KITAJIMA, S. 2017. Acrolein-detoxifying isozymes of glutathione transferase in plants. *Planta,* 245**,** 255-264.

MATEO, A., MÜHLENBOCK, P., RUSTÉRUCCI, C., CHANG, C. C.-C., MISZALSKI, Z., KARPINSKA, B., PARKER, J. E., MULLINEAUX, P. M. & KARPINSKI, S. 2004. LESION SIMULATING DISEASE 1 is required for acclimation to conditions that promote excess excitation energy. *Plant Physiology,* 136**,** 2818-2830.

MCKNIGHT, T. & HART, J. 1966. Some field observations on crown rot disease of wheat caused by *Fusarium graminearum*. *Queensland Journal of Agricultural and Animal Sciences,* 23**,** 373-378.

MITTER, V., FRANCL, L., ALI, S., SIMPFENDORFER, S. & CHAKRABORTY, S. 2006. Ascosporic and conidial inoculum of *Gibberella zeae* play different roles in Fusarium head blight and crown rot of wheat in Australia and the USA. *Australasian Plant Pathology,* 35**,** 441-452.

MITTLER, R. 2002. Oxidative stress, antioxidants and stress tolerance. *Trends in plant science,* 7**,** 405-410.

MIZOBUCHI, R., SATO, H., FUKUOKA, S., TANABATA, T., TSUSHIMA, S., IMBE, T. & YANO, M. 2013. Mapping a quantitative trait locus for resistance to bacterial grain rot in rice. *Rice,* 6**,** 13.

MÜHLENBOCK, P., PLASZCZYCA, M., PLASZCZYCA, M., MELLEROWICZ, E. & KARPINSKI, S. 2007. Lysigenous aerenchyma formation in *Arabidopsis* is controlled by LESION SIMULATING DISEASE1. *The Plant Cell,* 19**,** 3819-3830.

MÜHLENBOCK, P., SZECHYŃSKA-HEBDA, M., PŁASZCZYCA, M., BAUDO, M., MATEO, A., MULLINEAUX, P. M., PARKER, J. E., KARPIŃSKA, B. & KARPIŃSKI, S. 2008. Chloroplast signaling and LESION SIMULATING DISEASE1 regulate crosstalk between light acclimation and immunity in *Arabidopsis*. *The Plant Cell,* 20**,** 2339-2356.

NOCTOR, G., REICHHELD, J.-P. & FOYER, C. H. ROS-related redox regulation and signaling in plants. Seminars in Cell & Developmental Biology, 2018. Elsevier, 3-12.

O'BRIEN, J. A., DAUDI, A., FINCH, P., BUTT, V. S., WHITELEGGE, J. P., SOUDA, P., AUSUBEL, F. M. & BOLWELL, G. P. 2012. A peroxidase-dependent apoplastic oxidative burst in cultured *Arabidopsis* cells functions in MAMP-elicited defense. *Plant Physiology,* 158**,** 2013-2027.

OKSANEN, J., KINDT, R., LEGENDRE, P., O'HARA, B., STEVENS, M. H. H., OKSANEN, M. J. & SUGGESTS, M. 2007. The vegan package. *Community ecology package,* 10**,** 631-637.

OVERMYER, K., BROSCHÉ, M. & KANGASJÄRVI, J. 2003. Reactive oxygen species and hormonal control of cell death. *Trends in plant science,* 8**,** 335-342.

PASQUET, J.-C., CHAOUCH, S., MACADRÉ, C., BALZERGUE, S., HUGUET, S., MARTIN-MAGNIETTE, M.-L., BELLVERT, F., DEGUERCY, X., THAREAU, V., HEINTZ, D., SAINDRENAN, P. & DUFRESNE, M. 2014. Differential gene expression and metabolomic analyses of *Brachypodium distachyon* infected by deoxynivalenol producing and non-producing strains of *Fusarium graminearum*. *BMC Genomics,* 15**,** 629.

PINSON, S. R., SHAHJAHAN, A. K., RUSH, M. C. & GROTH, D. E. 2010. Bacterial panicle blight resistance QTLs in rice and their association with other disease resistance loci and heading date. *Crop science,* 50**,** 1287-1297.

POWELL, J. J. 2016. *Identifying sources of resistance to Fusarium diseases using the model plant Brachypodium distachyon.* Doctor of Philosophy, University of Queensland.

POWELL, J. J., CARERE, J., SABLOK, G., FITZGERALD, T. L., STILLER, J., COLGRAVE, M. L., GARDINER, D. M., MANNERS, J. M., VOGEL, J. P., HENRY, R. J. & KAZAN, K. 2017.

Transcriptome analysis of *Brachypodium* during fungal pathogen infection reveals both shared and distinct defense responses with wheat. *Scientific Reports,* 7**,** 17212.

PURSS, G. S. 1969. Studies of varietal resistance to crown rot of wheat caused by *Fusarium graminearum* Schw. *Queensl. J. Agric. Anim. Sci.,* 23**,** 475-498.

RANA, A., KARUNAKARAN, A., FITZGERALD, T. L., SABBURG, R., AITKEN, E. A., HENRY, R. J., POWELL, J. J. & KAZAN, K. 2018. A Highly Efficient and Reproducible *Fusarium* spp. Inoculation Method for *Brachypodium distachyon*. *Brachypodium Genomics.* Springer.

RCORETEAM 2018. R: a language and environment for statistical computing computer program, version 3.5. 0. R Core Team Vienna, Austria.

RIVAL, P., PRESS, M. O., BALE, J., GRANCHAROVA, T., UNDURRAGA, S. F. & QUEITSCH, C. 2014. The conserved PFT1 tandem repeat is crucial for proper flowering in *Arabidopsis thaliana*. *Genetics,* 198**,** 747-754.

ROUET, M., MATHIEU, Y., BARBIER-BRYGOO, H. & LAURIÈRE, C. 2006. Characterization of active oxygen-producing proteins in response to hypo-osmolarity in tobacco and *Arabidopsis* cell suspensions: identification of a cell wall peroxidase. *Journal of experimental botany,* 57**,** 1323-1332.

RUSHTON, P. J., SOMSSICH, I. E., RINGLER, P. & SHEN, Q. J. 2010. WRKY transcription factors. *Trends in plant science,* 15**,** 247-258.

RUSTÉRUCCI, C., AVIV, D. H., HOLT, B. F., DANGL, J. L. & PARKER, J. E. 2001. The disease resistance signaling components *EDS1* and *PAD4* are essential regulators of the cell death pathway controlled by *LSD1* in *Arabidopsis*. *The Plant Cell,* 13**,** 2211-2224.

SCHENK, P. M., KAZAN, K., RUSU, A. G., MANNERS, J. M. & MACLEAN, D. J. 2005. The *SEN1* gene of *Arabidopsis* is regulated by signals that link plant defence responses and senescence. *Plant Physiology and Biochemistry,* 43**,** 997-1005.

SCHNEIDER, C. A., RASBAND, W. S. & ELICEIRI, K. W. 2012. NIH Image to ImageJ: 25 years of image analysis. *Nature methods,* 9**,** 671.

SORENG, R. J., PETERSON, P. M., ROMASCHENKO, K., DAVIDSE, G., ZULOAGA, F. O., JUDZIEWICZ, E. J., FILGUEIRAS, T. S., DAVIS, J. I. & MORRONE, O. 2015. A worldwide phylogenetic classification of the *Poaceae* (*Gramineae*). *Journal of Systematics and Evolution,* 53**,** 117-137.

SUNDARAVELPANDIAN, K., CHANDRIKA, N. N. P. & SCHMIDT, W. 2013a. PFT1, a transcriptional Mediator complex subunit, controls root hair differentiation through reactive oxygen species (ROS) distribution in *Arabidopsis*. *New Phytologist,* 197**,** 151-161.

SUNDARAVELPANDIAN, K., CHANDRIKA, N. N. P., TSAI, Y.-H. & SCHMIDT, W. 2013b. PFT1-controlled ROS balance is critical for multiple stages of root hair development in *Arabidopsis*. *Plant signaling & behavior,* 8**,** e24066.

THATCHER, L. F., MANNERS, J. M. & KAZAN, K. 2009. *Fusarium oxysporum* hijacks COI1‐mediated jasmonate signaling to promote disease development in *Arabidopsis*. *The Plant Journal,* 58**,** 927-939.

VAN INGHELANDT, D., MELCHINGER, A. E., MARTINANT, J.-P. & STICH, B. 2012. Genome-wide association mapping of flowering time and northern corn leaf blight (*Setosphaeria turcica*) resistance in a vast commercial maize germplasm set. *BMC Plant Biology,* 12**,** 56.

VAUCHERET, H., BÉCLIN, C., ELMAYAN, T., FEUERBACH, F., GODON, C., MOREL, J. B., MOURRAIN, P., PALAUQUI, J. C. & VERNHETTES, S. 1998. Transgene‐induced gene silencing in plants. *The Plant Journal,* 16**,** 651-659.

VOGEL, J. & HILL, T. 2008. High-efficiency agrobacterium-mediated transformation of *Brachypodium distachyon* inbred line Bd21-3. *Plant Cell Rep,* 27.

VOGEL, J. P., GARVIN, D. F., LEONG, O. M. & HAYDEN, D. M. 2006. *Agrobacterium*-mediated transformation and inbred line development in the model grass *Brachypodium distachyon*. *Plant Cell, Tissue and Organ Culture,* 84**,** 199-211.

WANG, C., YAO, J., DU, X., ZHANG, Y., SUN, Y., ROLLINS, J. A. & MOU, Z. 2015. The *Arabidopsis* mediator complex subunit16 is a key component of basal resistance against the necrotrophic fungal pathogen *Sclerotinia sclerotiorum*. *Plant physiology,* 169**,** 856-872.

WANG, G., WANG, L., CUI, Y., YU, M., DANG, C., WANG, H., JIN, X., YAN, L., WU, Q. & LI, D. 2017. RNA-seq analysis of *Brachypodium distachyon* responses to Barley stripe mosaic virus infection. *The Crop Journal,* 5**,** 1-10.

WINTER, C. M., AUSTIN, R. S., BLANVILLAIN-BAUFUME, S., REBACK, M. A., MONNIAUX, M., WU, M.-F., SANG, Y., YAMAGUCHI, A., YAMAGUCHI, N. & PARKER, J. E. 2011. LEAFY target genes reveal floral regulatory logic, cis motifs, and a link to biotic stimulus response. *Developmental cell,* 20**,** 430-443.

WOLLENBERG, A. C., STRASSER, B., CERDÁN, P. D. & AMASINO, R. M. 2008. Acceleration of flowering during shade avoidance in Arabidopsis alters the balance between *FLOWERING LOCUS C*-mediated repression and photoperiodic induction of flowering. *Plant physiology,* 148**,** 1681-1694.

YANG, Y., LI, L. & QU, L. J. 2016. Plant Mediator complex and its critical functions in transcription regulation. *Journal of integrative plant biology,* 58**,** 106-118.

YANG, Y., OU, B., ZHANG, J., SI, W., GU, H., QIN, G. & QU, L. J. 2014. The *Arabidopsis* Mediator subunit MED 16 regulates iron homeostasis by associating with EIN 3/EIL 1 through subunit MED 25. *The Plant Journal,* 77**,** 838-851.

YANO, M., KATAYOSE, Y., ASHIKARI, M., YAMANOUCHI, U., MONNA, L., FUSE, T., BABA, T., YAMAMOTO, K., UMEHARA, Y. & NAGAMURA, Y. 2000. *Hd1*, a major photoperiod sensitivity quantitative trait locus in rice, is closely related to the *Arabidopsis* flowering time gene *CONSTANS*. *The Plant Cell,* 12**,** 2473-2483.

YAO, T., PARK, B. S., MAO, H. Z., SEO, J. S., OHAMA, N., LI, Y., YU, N., MUSTAFA, N. F. B., HUANG, C. H. & CHUA, N. H. 2019. Regulation of flowering time by SPL10/MED25 module in *Arabidopsis*. *New Phytologist*.

ZHANG, F., YAO, J., KE, J., ZHANG, L., LAM, V. Q., XIN, X.-F., ZHOU, X. E., CHEN, J., BRUNZELLE, J. & GRIFFIN, P. R. 2015. Structural basis of JAZ repression of MYC transcription factors in jasmonate signalling. *Nature,* 525**,** 269.

ZHENG, W., ZHAI, Q., SUN, J., LI, C.-B., ZHANG, L., LI, H., ZHANG, X., LI, S., XU, Y. & JIANG, H. 2006. Bestatin, an inhibitor of aminopeptidases, provides a chemical genetics approach to dissect jasmonate signaling in *Arabidopsis*. *Plant physiology,* 141**,** 1400-1413.

ZHU, T., XIN, F., WEI, S., LIU, Y., HAN, Y., XIE, J., DING, Q. & MA, L. 2019. Genome-wide identification, phylogeny and expression profiling of class III peroxidases gene family in *Brachypodium distachyon*. *Gene*.

Chapter 3

The role of salicylic acid in regulating defence responses in *Brachypodium* during fungal infection

3.1 Abstract

The plant hormone salicylic acid (SA) mediates both local and systemic defence responses after pathogen attack. The role of SA in plant defence has been characterised in model plants such as *Arabidopsis thaliana* and *Nicotiana* spp. However, the role of SA in mediating defence responses against necrotrophic pathogens remains poorly understood, particularly in monocot hosts. To better understand potential roles of SA in mediating defence responses in the model cereal *Brachypodium distachyon*, we generated SA deficient plants by expressing the *nahG* transgene, which encodes a SA-degrading enzyme. RNA-seq was utilized to observe alterations to gene expression patterns within *nahG* plants under basal growth conditions and during infection. Overall, transcriptomic analysis indicated SA plays an important role in establishing basal defence levels through regulating deposition of lignin and accumulation of defence related proteins. Observing *Fusarium*-responsive genes provided insight in defence related pathways and processes which require salicylic acid signalling for their induction. *Brachypodium* provides a highly tractable system for studying the role of salicylic acid in mediating resistance to cereal-infecting pathogens as well as understanding other salicylic acid dependent physiological processes.

3.2 Introduction

As sessile organisms, plants by necessity have evolved elaborate mechanisms to perceive their biotic and abiotic environments. Plant hormones play an essential role in the regulation of a plant's response to its environment. The phytohormones salicylic acid (SA) and jasmonate (JA) were the first to be implicated in regulating defence responses against pathogens and pests, though subsequent work has shown other hormones such as; abscisic acid, auxin, gibberellins, cytokinins and strigolactones all play a role and, in many cases, interact synergistically or antagonistically with one another (Cui & Luan, 2012; Murphy, 2015).

Typically, SA is associated with response to infection by biotrophic pathogens as an important signal for triggering a hypersensitive response in which the resistant host will rapidly kill its own cells surrounding the infection site to deny the pathogen access to living tissue (Greenberg et al., 1994, Lam et al., 2001). Accordingly, SA-mediated defences may function as a susceptibility factor for interactions with necrotrophic pathogens since deployment of a hypersensitive response produces dead tissue on which the pathogen may feed (Govrin and Levine, 2000, Glazebrook, 2005). Induction of SA mediated defences may also potentially increase susceptibility to necrotrophic pathogens by negatively regulating JA-dependent defences. SA also functions in signalling responses to pathogens, by priming expression of defence genes such as *PR1* in the tissue not directly exposed to pathogen insult a phenomenon termed systemic acquired resistance (SAR) (Chen et al., 1993). In *Arabidopsis* and rice, NPR1 plays a central intermediary role in SAR (Cao et al., 1997). *NPR1* encodes a regulatory protein that localizes to the nucleus in response to pathogen challenge and interacts with TGA transcription factors to mediate expression of defence related genes (Zhou et al., 2000). Plants bearing mutant *NPR1* alleles are impaired for SAR (Zhou et al., 2000, Zhang et al., 1999, Dong, 2004) and display increased susceptibility to various pathogens (Durrant and Dong, 2004).

By contrast, JA is classically thought to be the primary signal required to mount an effective defence response against necrotrophic and hemi-biotrophic pathogens (Thaler et al., 2004). In *Arabidopsis*, JA coordinates defence responses by binding the SKP-CULLIN-FBOX complex incorporating the F-BOX receptor protein COI1 (Xie et al., 1998). COI1 marks Jasmonate Zim Domain proteins (JAZs), repressors of JA signalling, for degradation by the 28s proteosome complex. This removal of repression allows transcription factors (TF) such as MYC transcription factor MYC2 to up-regulate expression of defence related proteins like plant defensin 1.2 (PDF1.2) (Dombrecht et al., 2007). In *Arabidopsis*, JA and SA interact in a mutually antagonistic manner mediated by cross-talk between NPR1 regulation of TGA and WRKY transcription factors (Solano and Gimenez-Ibanez, 2013).

The pathogens *Fusarium graminearum* (*Fg*), predominantly causing the disease Fusarium head blight (FHB) (Aoki et al., 2012), and *Fusarium pseudograminearum* (*Fp*), predominantly causing Fusarium crown rot (FCR) (Akinsanmi et al., 2006), are both considered hemi-biotrophic or necrotrophic pathogens. Previous work has shown exogenous application of SA provides increased resistance to FHB infection in wheat (Makandar et al., 2012). The increased resistance observed has been suggested to be due to direct effects of SA on the pathogen rather than by increasing defence responses (Qi et al., 2012). Recent work has also highlighted the importance of JA and ABA signalling in mediating resistance during FHB (Qi et al., 2016). Recently, Barley plants with supressed isochorismate-based SA biosynthesis were demonstrated to have a compromised resistance towards *Fg* (*Hao et al., 2018*). JA plays a role in coordinating the host response in wheat during infection by *Fp* (Desmond et al., 2005). However, little is known regarding SA signalling during *Fp* infection or its importance in mediating effective resistance against this disease.

Brachypodium distachyon (*Brachypodium* hereafter) presents a tractable genomics model for cereals to study due to its many model characteristics such as relatively small, diploid genome (272 Mbp), amenability to transformation and short generation time (Vain et al., 2008, Initiative, 2010, Brkljacic et al., 2011). *Brachypodium* is also closely related to wheat and barley with a high degree of conservation for gene synteny and sequence similarity (Bossolini et al., 2007, Kumar et al., 2009). *Brachypodium* has been demonstrated to have similar disease characteristics as wheat, when infected by

FHB-causing *Fusarium* species (Peraldi et al., 2011). Indeed, *Brachypodium* has also been demonstrated to possess a highly similar transcriptional response towards *Fp* as wheat (Powell et al., 2017b).

Pseudomonas putida possesses a salicylate hydroxylase encoded by the gene *nahG*, which degrades SA (You et al., 1991). Plants constitutively expressing this gene have been produced in *Arabidopsis* (Van Wees and Glazebrook, 2003), rice (Yang et al., 2004), tobacco (Friedrich et al., 1995) and wheat (Makandar et al., 2012) in order to study the effect of SA on various physiological processes (Abreu and Munné-Bosch, 2009). In contrast to *Arabidopsis*, no SA deficient or over-producing lines are available in *Brachypodium*. Development of *nahG* expressing lines in *Brachypodium* will aid in studying the role of SA in various physiological responses in Pooid species and provide insight into what role SA plays in mediating response to *Fp* in wheat. Previous work has demonstrated both SA and JA are induced within *Fp* infected *Brachypodium* seedlings (Powell et al., 2017b)

In this study, we used *Agrobacterium*-mediated transformation to produce *nahG* expression lines in the *Brachypodium* community standard line, Bd21-3. *Fp* infection assays demonstrated that *nahG* plants show significantly enhanced disease phenotypes compared to WT plants. Reduction of basal and complete loss of induction of SA during *Fp* infection was observed using LC-MS. RNA-seq was then used to compare global transcriptional response of *nahG* plants with that of WT plants during infection by *Fp*. These analyses showed marked differences in the transcriptional response to infection between wild-type and *nahG* plants showing reduction in SA levels leads to impaired basal defences and muted systemic defence responses.

3.3 Results and Discussion

3.3.1 *Agrobacterium*-mediated transformation of *Brachypodium* community standard line Bd21-3 resulted in constitutive expression of *nahG*

Brachypodium distachyon inbred line Bd21-3 was selected for development of a *nahG* resource due to its adoption as the community standard line with extensive mutant resources and datasets already generated in this background (Thole et al., 2010, Bragg et al., 2012, Dalmais et al., 2013). Transformation was performed using an established method for *Agrobacterium*-mediated transformation of embryogenic callus as previously described (Vogel et al., 2006, Bragg et al., 2015). Approximately 200 pieces of embryogenic callus were infiltrated with *Agrobacterium* carrying the pVec8 vector with *nahG* coding sequence under the control of the maize ubiquitin promoter (Cornejo et al., 1993). Following incubation with *Agrobacterium*, calli were placed onto shoot regeneration media containing hygromycin to select for successful transformants. Seventy-six independent T0 plantlets were regenerated and planted into soil; 52 of these regenerants grew successfully and produced T1 seeds.

Transformants with more than one transgene insertion event have been previously shown to have a greater risk of transgene silencing (Kooter and Mol, 1993, Matzke et al., 1994). Thirty-two T1 lines were screened for expected insert segregation ratio of 3:1 using PCR amplification of insert sequence. Primers were designed to specifically amplify a 411bp product from the *nahG* insert. From these 32 lines, 11 were identified as putatively containing single insert. Progeny of these single insert lines (T2 generation) were screened for homozygous individuals (100% insert positive). In addition, transgene expression was analysed by qRT-PCR (Figure 3.1) using RNA isolated from leaf tissue harvested from mature wild-type and *nahG* plants (6 weeks post germination). A reference gene encoding a ubiquitin conjugating enzyme 18 (UBC18) was used as previously described by Hong et al. (2008) and validated by Chambers et al. (2012). Amplification of *UBC18* was detected in both wild-type and *nahG* samples. In particular, transgene expression was higher in CO354.1, CO356.1

and CO404.5 lines than the rest of the lines analysed (Figure 3.1) and these were selected for further characterisation.

3.3.2 Basal SA levels are reduced while SA induction during infection is ablated in *nahG* lines

In order to observe whether constitutive expression of *nahG* resulted in reduced SA accumulation, liquid chromatography mass spectrometry (LC-MS) was used to quantify SA levels within infected and non-infected tissue. Basal SA levels were considerably higher (~4-fold) in wild-type plants compared to *nahG* plants and induction of SA during infection was ablated in *nahG* lines while SA was found to be highly induced in wild-type plants (Figure 3.2A).

Previous work in *Arabidopsis* and rice has shown expression of pathogenesis related 1 (*PR1*) is regulated via the SA signalling pathway (Nawrath and Métraux, 1999). Consequently, *PR1* is widely used as a marker gene for SA mediated defence response in hosts under challenge by diverse pathogens (Ukness, 1993). A PR1 ortholog in *Brachypodium* (*Bradi1g57580*) has been shown to respond to infection by panicum mosaic virus and its related satellite virus (Mandadi and Scholthof, 2012), *Fp* (Powell et al., 2017b) and by exogenous application of SA (Kakei et al., 2015). Expression of *PR1* within infected wild-type and *nahG* plants was observed using qRT-PCR. Consistent with observed SA levels, *PR1* expression levels were lower in *nahG* mock samples than wild-type mock samples. *PR1* was induced during infection in both WT and *nahG* plants; however, *PR1* expression was higher in infected WT plants than *nahG* plants (Figure 3.2B).

3.3.3 Analysis of pathogen induced transcriptional change using RNA-seq shows reduced SA levels leads to alteration in host transcriptional response during infection

In order to explore how alteration to SA levels impact on host responses during infection by *Fp*, the same RNA samples used to observe reduced *PR1* expression in

nahG was sequenced on an Illumina HiSeq 2000 platform at the Australian Genome Research Facility. The sixteen samples were sequenced across two lanes on an Illumina HiSeq2000 generating 200bp paired end reads. In total, 537 million reads were generated. RNA-seq data were analysed using the Tuxedo analysis package using the *Brachypodium distachyon* v3.1 annotation and assembly. This provided sufficient coverage for Cuffdiff to estimate differential expression for an average of ~22,000 genes across all samples.

In order to identify genes whose basal and/or pathogen-induced levels might be regulated by SA, differential expression patterns across different treatments were compared. Four separate differential gene expression comparisons were made between; 1) wild-type mock inoculated and wild-type infected (WM vs. WF); 2) *nahG* mock inoculated and infected (NM vs. NF); 3) wild-type mock and *nahG* mock (WM vs. NM); 4) and wild-type infected and *nahG* infected (WF vs. NF). The overlap in differential gene expression patterns between comparisons is given in Figure 3.3. Genes which were differentially expressed in only WM (wild-type Mock) vs. WF (wild-type *Fusarium*) or NM (*nahG* Mock) vs. NF (*nahG Fusarium*) comparisons were disregarded as uninformative since induction of these genes did significantly alter expression levels between WT and *nahG* plants under mock or infected conditions. For comparison between mock and infected conditions in both *nahG* and WT, only genes differentially expressed more than four-fold ($log_2$2-fold) were used for further analysis. In comparison between mock WT and *nahG* as well as between infected WT and *nahG* samples, a two-fold cut-off was imposed. In total, 1495 genes were differentially expressed between wild-type mock and infected (1424 induced by infection >$log_2$2-fold and 71 repressed by infection > $log_2$2-fold), 887 between *nahG* mock and infected (845 induced by infection > $log_2$2-fold and 42 repressed by infection > $log_2$2-fold), 680 between wild-type mock and *nahG* mock (208 expressed more highly in *nahG* mock > $log_2$1-fold and 472 expressed more highly in WT mock > $log_2$1-fold) and 2027 between WT and *nahG* infected (496 expressed more highly in *nahG* infected > $log_2$1-fold and 1531 expressed more highly in *nahG* infected > $log_2$1) (Figure 3.3).

3.3.4 nahG plants show a muted transcriptional response to infection

As stated above, SA levels were significantly increased in infected WT plants compared to mock inoculated WT plants while no such increase was found in the case for inoculated *nahG* plants. A greater number of genes were differentially expressed between wild-type mock and *Fp* inoculated plants (1583 genes) compared with *nahG* plants in which 926 genes were differentially expressed between mock and inoculated plants. This perhaps provides cursory evidence that a stronger overall response to infection is produced in plants with greater SA levels.

The expectation was that genes induced by infection (i.e. differentially expressed between mock- and *Fusarium*-inoculated) in wild-type plants but not in *nahG* plants and have significantly higher expression in infected WT plants compared to *nahG* are dependent on SA for their induction during pathogen attack. A large number of genes were induced only by infection in WT plants (826 genes). Of these, 556 genes had significantly different expression between WT and *nahG* plants under infected conditions, suggesting that SA was required for induction of these genes during pathogen attack.

Gene ontology enrichment analysis was used to gain insight on which processes and functions were deployed differently between WT and *nahG* plants in response to infection (Figure 3.4). In total, 157 GO terms were enriched in the WM vs WF DEG comparison while 174 GO terms were enriched for genes upregulated in the NM vs NF DEG comparison (Supplementary table 3.1). Of these, 119 GO terms were commonly enriched in WT and *nahG* responses to infection, suggesting the overall molecular response between WT and *nahG* was highly similar. Some differences were also noted with WM_vs_WF having 38 uniquely enriched GO terms and NM_vs_NF having 55 uniquely enriched GO terms. A high proportion of enriched GO terms in the WT response to infection were defence related, particularly for processes associated with secondary metabolism including carotene metabolism (GO:0016119), cinnamic acid metabolism (GO: 0009803) and L-phenylalanine metabolic process (GO:0006558). Signalling related terms sequence-specific DNA binding (GO:0043565) and regulation of jasmonic acid mediated signalling pathway

(GO:2000022) were enriched, perhaps suggesting defence related signalling processes were activated to a higher degree in WT plants. Terms related to deoxynivalenol detoxification (GO:0080044) were also enriched in the WT response. WT specific GO term enrichment patterns suggest that WT plants were able to mount some additional defensive mechanisms in response to infection compared to those observed in *nahG*.

In contrast, enriched terms specific to the *nahG* response to infection were consistent with a host under strong infection pressure with enrichment of chitin metabolic process (GO:0006030), defense response to bacterium (GO:0042742) and defence response to fungus (GO:0009620) terms. Stress response related terms such as response to stress (GO: 0006950), hydrogen peroxide catabolic process (GO:0042744), peroxidase activity (GO:0004601) and antioxidant activity (GO:0016209) were also enriched. Concerted expression of genes within these GO annotations suggest that *nahG* were responding to greater accumulation of reactive oxygen species and hydrogen peroxide specifically. Response to water deprivation (GO:0009414) was also enriched, indicating *nahG* plants were responding to impaired water transport, perhaps due to increased vascular blockage or damage to vascular element caused by the pathogen.

To compare processes and functions between WT and *nahG*, genes expressed to different magnitudes between genotypes under the same treatment were assessed for GO term enrichment. During infection, 206 GO terms were enriched within the set of genes expressed more highly in *nahG* plants during infection while no significant enrichment was observed for genes expressed more highly in WT plants during infection.

In the absence of pathogen, 52 GO terms were enriched for genes expressed more highly in mock *nahG* plants while 13 GO terms were enriched for genes expressed more highly in mock WT plants. Several terms related to structural defence deposition were enriched such as lignin metabolic process (GO:0009808), xylan metabolic process (GO:0045491), hemicellulose metabolic process (GO:0010410) and plant-type cell wall organization or biogenesis (GO:0071669). Several terms associated with response to oxidative stress (GO:0006979), reactive oxygen species metabolic

process (GO:0072593), hydrogen peroxide catabolic process (GO:0042744) and cellular oxidant detoxification (GO:0098869). Considered together, the GO enrichment patterns suggest *nahG* plants have structural differences in cell walls and may either be primed to respond to ROS accumulation during infection or have higher ROS accumulation than WT plants during basal growth.

3.3.5 Comparison of *nahG* regulated genes with known SA-responsive genes and processes

A previous study observing transcriptomic response using RNA-seq in *Brachypodium* following exogenous application of phytohormones identified 78 genes responding to SA treatment (Kakei et al., 2015). Since RNA-seq analysis was performed using an earlier reference version (v1.2), a reciprocal best BLAST analysis was performed using the global coding sequence collection from each version (v1.2 and v3.1) to identify corresponding gene IDs in order to compare gene expression results between these studies. Of these, 37 genes were differentially expressed in one or more comparisons in our RNA-seq dataset. Twelve genes were differentially expressed between WT and *nahG* mock-inoculated plants; whereas, fourteen genes were differentially expressed between WT and *nahG* infected plants. For induction patterns, nine were differentially expressed by infection in wild-type plants with expression levels lower in *nahG* infected than in WT infected plants, while four genes were induced in both genotypes and did not show any differential expression between them. The high proportion of SA-responsive genes differentially expressing between WT and *nahG* lines is consistent with the expectation that this transcriptional change is due to the depletion of SA.

Several SA glycosyltransferases were differently expressed between WT and *nahG* plants. A SA binding protein was also expressed more highly in WT compared to *nahG* plants. Bradi1g42760 salicylate o-methyltransferase-like was differentially expressed 3-fold between WT and *nahG* mock-inoculated plants and 4-fold between WT and *nahG* infected plants. Salicylate o-methyltransferase enzymes produce methyl-salicylic acid (MeSA) from SA. MeSA is a volatile compound and is thought to be a primary signal in SAR (Park *et al.*, 2007). The reduced expression of genes involved

in SA metabolism is consistent with *nahG* plants having a smaller pool of available SA during infection.

Kakei et al. (2015) also observed genes responding to JA, finding 383 genes were induced after exogenous application of JA. Of the identified JA responsive genes by Kakei et al. (2015), 84 were differentially expressed between WT and *nahG* within infected samples. Seventy-six were induced by infection in wild-type plants, 40 in *nahG* plants and 36 of these were induced in both. Together, this might indicate SA may play a role in priming JA responses during infection indicating SA is required for activation of defences in response to *Fp* infection.

3.3.6 Inferred changes to SA metabolism in *nahG* plants during infection

To investigate whether *nahG* plants show altered expression of genes involved in metabolism or catabolism of SA, as well as its precursor and derivative metabolites *Bradi4g35350* encoding a putative udp-glucose:salicylic acid glucosyltransferase showed induction in WT plants but not in *nahG* leading to a 5-fold difference in expression between them under infected conditions. *Bradi5g03310* and *Bradi5g03380* encode UDP-glycosyltransferase 74f2-like enzymes and were both also expressed more highly in infected WT plants compared to *nahG* plants. A homologous enzyme in *Arabidopsis thaliana* has been shown to glycosylate salicylic acid thereby rendering it inactive (Lim et al., 2002). The greater expression of these enzymes in WT plants correlates with the greater concentration of SA detected. The differentially expressed glycosyltransferases occur in a clade of nine UDP-glycosyltransferases which have been shown to respond during infection by *Fg* as well as exogenous application of deoxynivalenol (Schweiger et al., 2013). One of the UDP-glycosyltransferases (*Bradi5g03300*) occurring in this cluster has been previously shown to detoxify the mycotoxin deoxynivalenol (Schweiger et al., 2013) which is produced by both *Fg* and *Fp* (Desjardins, 2006). *Bradi5g03300* was induced in both WT and *nahG* plants but was induced to a greater magnitude in WT plants leading to a 3.7-fold difference between WT and *nahG* infected plants.

In total, 140 genes had differing expression levels between WT and *nahG* mock-inoculated and *Fusarium* infected plants but were induced by infection in both *nahG* and WT. These genes therefore displayed a similar expression pattern to that observed for PR1 and present as a set of genes for which SA is required for full expression under basal conditions and for complete induction during pathogen attack, but which loss of SA induction did not abolish induction by pathogen. Using this set of genes as a query for GO term enrichment analysis in BLAST2GO revealed 25 terms were significantly enriched. Among enriched terms quercetin-O-glycosyltransferases and glutathione-S-transferases were over-represented. SA has a known role in regulating expression of glutathione-S-transferase during infection (Mauch and Dudler, 1993, Sappl et al., 2004).

A large number of transcription factors had altered expression patterns between WT and *nahG* plants. Among these, a large proportion were WRKY transcription factors, a class of transcription factors implicated in SAR (Pandey and Somssich, 2009). Thirty-five WRKY transcription factors were differentially expressed between one or more comparisons; of these 27 were expressed to different levels between WT and *nahG* infected plants and 15 were differentially expressed between WT and *nahG* mock-inoculated plants. Multiple WRKY72, WRKY53 and WRKY33 transcription factors were expressed more highly in WT plants under basal and infected conditions. WRKY70 in *Arabidopsis* has been implicated in facilitating crosstalk between SA and JA pathways (Knoth et al., 2007). Two genes annotated as WRKY70 were expressed to a higher level in mock-inoculated WT than *nahG* (Table 2.5).

Class III peroxidases are a large multigene family of secretory enzymes found in plants (Moural et al., 2017, Cao et al., 2016, Ren et al., 2014) and can participate in either catalytic reduction of H_2O_2 (Hiraga et al., 2001, Passardi et al., 2004b) or the production of Reactive Oxygen Species (ROS) (Liszkay et al., 2003, Passardi et al., 2004a). The roles of Class III peroxidases in higher plants are diverse including; regulating plant growth and development (Beltramo et al., 2012, Cosio et al., 2009, Mei et al., 2009); responses towards pathogen defence (Almagro et al., 2008) and abiotic stress responses (Llorente et al., 2002, Klok et al., 2002, Kidwai et al., 2019, Abercrombie et al., 2008). Interestingly, a subset of Class III peroxidases have been shown to be induced in rice, following infection with *Magnaporthe grisea*, a causal

agent of rice blast disease (Sasaki et al., 2004). Recently Zhu et al. (2019) identified 151 *Brachypodium* peroxidases (BdPrx), using bioinformatic approaches and subsequently classified them into 15 subfamily group based on gene structure and protein sequence similarity. Subfamilies 10, 12 and 14 are predicted to have roles in low oxygen responses (Klok et al., 2002), arsenic tolerance (Kidwai et al., 2019), and plant development (Sundaravelpandian et al., 2013, Hruz et al., 2008) and defence (Bindschedler et al., 2006) respectively based on homology to characterised peroxidases in rice and *Arabidopsis.* Out of the 151 BdPrxs identified, we found that 39 were differentially expressed between one or more comparisons with a fold change expression cut off $\log_2$ 2 (Supplementary table 3.2). Of the 39 differentially expressed BdPrxs genes, 16 were expressed to different levels between WT and *nahG* infected plants (8 were expressed higher in nahG and 8 were expressed higher in WT under *Fp* infection <$\log_2$1-fold). Fourteen were differentially expressed between WT and *nahG* mock-inoculated plants (7 were expressed higher in nahG and 7 were expressed higher in WT under mock conditions <$\log_2$1-fold).

3.3.7 Alteration of pathogen gene expression when infecting *nahG Brachypodium* plants

RNA sequencing of pathogen infected plant tissue can provide insight into pathogen gene expression at the same infection timepoint. The Tuxedo pipeline was utilized to assess differential expression of *Fp* genes within infected WT and *nahG* plants. A significant proportion of reads were successfully aligned to the *Fp* genome reference (Gardiner et al., 2012) across *Fusarium* infected WT and *nahG* samples, corresponding to approximately 1% and 4% of total reads respectively. The mean read alignment abundance was found to be significantly greater in *nahG* samples (Supplementary figure 3.1) (Two-way Student's t test, P<0.01) compared to WT samples. This suggests *Fp* biomass was greater in *nahG* seedlings compared to WT although independent validation of *Fp* biomass using qPCR quantification of fungal DNA is required to substantiate this claim.

Sufficient coverage allowed estimation of differential expression for 4271 pathogen genes between wild-type and *nahG* plants. 210 *Fusarium* genes were differentially

expressed between wild-type and *nahG* infected samples (Supplementary table 4.1); 138 expressed more highly in WT with a maximum log_2 fold-change of 4.5; and 70 expressed more highly in *nahG* samples with a minimum log_2 fold-change of 3.0. One of the genes with reduced expression (-log_2 FC 2.67) in *nahG* plants was a benzoate 4-monooxygenase cytochrome p450. Benzoate 4-monoxygenase cytochrome p450 enzymes catalyse the reaction from benzoate to 4-hydroxybenzoate to something else (Werck-Reichhart, 1995). The reduced expression of this gene in *nahG* samples compared to WT potentially supports the hypothesis that *Fp* exploits host SA signalling with the pathogen expressing more benzoate-4-monoxygenase p450 enzyme in order to alter the abundance of salicylic acid or an analogous compound. This altered presence of SA derivatives may allow the pathogen to exploit a host SA signalling pathway to produce disease by interfering with host phytohormone pathways.

Previous work has shown *Aspergillus nidulans* can utilise both salicylate and benzoate as carbon sources (Martins et al., 2015). *Fusarium* species are able to metabolise salicylate compounds (Dodge and Wackett, 2005). Genomic comparison across *Fusarium* species indicated salicylate catabolizing enzymes are shared across many species including *F. oxysporum* and *F. verticillioides* (Ma et al., 2010). *Fg* is known to possess orthologs of *nahG* with *FGSG_09063* and *FGSG_03657* encoding salicylate 1-monooxygenase/hydroxylases that are SA responsive (Qi et al., 2012). Furthermore, Qi et al. (2012), demonstrated that SA has a direct impact on *Fg* spore germination and mycelial growth. Similarly, we have also demonstrated that SA is inhibitory toward *Fp* mycelia growth (Supplementary figure 3.2). Using BLAST query against the *Fp* genome indicated this species also possesses a homologous salicylate hydroxylase gene, FPSE_01878; however, this gene was not significantly differentially expressed between WT and *nahG* samples ($log_2$2 FC = -0.15; adjusted p value = 1).. *Fp* may be able to exploit salicylic acid as well as precursor metabolites as nutrient resources by catabolising these compounds. An alternative hypothesis, the salicylate hydroxylase in *Fp* might function in protecting the pathogen against direct fungicidal/fungistatic effects of salicylic acid.

3.3.8 Salicylic acid deficient plants show enhanced susceptibility to Fusarium crown rot

To investigate the effect of SA deficiency on plant tolerance to *Fp* infection, a series of soilless infection assays were performed. At 12 days post inoculation (dpi), all *nahG* lines were observed to show significantly increased disease score rankings (Wilcoxon rank test, $P < 0.05$) when compared to WT. Furthermore, *nahG* lines CO354.1 and CO356.1 were observed to have a significantly reduced leaf count when compared to WT (Wilcoxon rank test, $P < 0.05$) (Figure 3.5). Additionally, when disease score and leaf count were analysed together, using a one-way permutational MANOVA, *nahG* lines CO354.1 and CO356.1 were found significantly different from WT infection control ($P < 0.05$). This experiment was repeated twice with similar results. Taken together, these results indicated that SA deficient *Brachypodium* seedlings are significantly more susceptible to *Fp* infection.

3.4 Conclusion

This study describes the development of *nahG* transformant lines in *Brachypodium distachyon* and the first use of this resource to explore the role of SA in mediating defence responses during pathogen infection. *nahG* plants show enhanced susceptibility when challenged with *Fp*; correlated with a reduction in basal defence responses and muted systemic induction of defence responses.

3.5 Materials and Methods

Powell JP performed the lab work for sections 3.5.1 to 3.5.3 and 3.5.6 to 3.5.7.

3.5.1 Design of transformation constructs

Coding sequence synthesis and cloning were performed by GenScript. The *nahG* coding sequence from *Pseudomonas putida* was synthesized and cloned into pUC57 with the addition of 5' BamHI (GGATCC) and Kozak* (ACCACC) sequence and 3' KpnI (GGTACC) sequence. Codon optimization was performed to ensure high constitutive expression in monocot species using the OptimumGene system. The coding sequence with Kozak sequence from pUC57 was subcloned into the *pWUbi.tm1* vector via *BamHI* (5') and *KpnI* (3'). The expression cassette from *pWUbi.tm1* was subcloned into pWBVec8 vector via *NotI* restriction enzyme. The *pWBVec8* transformation vector also contained a hygromycin resistance gene (*hygR*) allowing utilisation of this antibiotic as a selection agent for successfully transformed plants.

3.5.2 Agrobacterium mediated transformation of *Brachypodium* embryogenic callus

Agrobacterium mediated transformation of *Brachypodium* embryogenic callus was performed as described in (Bragg et al., 2015). Calli were derived from immature *Brachypodium distachyon* Bd21-3 embryos. Immature seeds were surface sterilized in bleach (5.25% NaOCl) with Tween20 added and placed onto Brachypodium callus inducing media (BCIM) containing 0.6 mg/L $CuSO_4$ and 2,4-D. Callus pieces were split and subcultured twice to rapidly increase to a total of ~200 calli. The pVec8 transformation construct containing the *nahG* coding sequence was transformed into *Agrobacterium tumefaciens* AGL1 hyper-virulent strain (Lazo et al., 1991) using heat shock. Calli were incubated with *Agrobacterium tumefaciens* for 5 minutes before draining, drying and placing on selection media. Selection media contained both timentin to suppress further over-growth of *Agrobacterium* and hygromycin to select for successfully transformed calli. After ~2 weeks, surviving callus pieces were

transferred onto regeneration media containing 0.2 mg/L kinetin (Sigma-Aldrich, St. Louis, MO, USA). One regenerated shootlet was recovered per calli where possible and transferred to soil.

3.5.3 PCR based insert screening

PCR based insert screening was used to screen T0 plantlets to independently confirm insert, T1 plants to infer single/low insert events based on expected segregation ratios (3:1) and T2 plants to identify homozygous T1 individuals. DNA extraction and PCR were performed using the Phire PCR direct plant kit (ThermoFisher, Waltham MA). A small amount of tissue was scraped from one leaf tip per plant using a 10µL pipette tip and submerged in extraction buffer for 5 minutes. Primer sequences F_Ubi.tm1 5'-TTTAGCCCTGCCTTCATACG-3' and nahG-R 5'-GATGGTCGCTCCCAGATAGC-3' were used to generate a 411bp product specific to the *nahG* insert. PCR reactions were set-up as per the manufactures instruction and reactions were run using a touchdown protocol with an initial set of 10 cycles with annealing temperatures decreasing 2°C/cycle followed by 95°C for 15 seconds, 60°C for 30 seconds and 72°C for 60 seconds for 40 amplification cycles.

3.5.4 Relative quantification of transgene and pathogen responsive genes using qRT-PCR

Primers were designed to span intron-exon boundaries with preference to 3' end junctions where possible. Primers for *nahG* transgene and pathogen responsive genes are given in Supplementary Table 3.3. Ubiquitin conjugating enzyme 18 (UBC18) was utilised as a reference gene as described in Hong et al. (2008) and endorsed by Chambers et al. (2012).

3.5.5 *Fusarium pseudograminearum* infection assays for disease phenotyping

To investigate the *Brachypodium* disease phenotype a series of soilless laboratory were conducted as previously described (Yang et al., 2010). Briefly, 3-5 days post germination (dpg) *Brachypodium* seedlings, with coleoptile emerging from the leaf sheath, were treated by immersion for 3 minutes in 5mL of either mock or *Fp* spore solution amended with 0.05% w/v Tween20. *Fp* spores were produced by inoculating Campbell's V8 broth with *Fp* infested agar plugs and leaving the cultures to grow and sporulate for 1 week at room temperate (~22°C). Spores were filtered through Miracloth (Calbiochem, San Diego, CA), pelleted by centrifugation and resuspended in distilled water to ~1 × 10^6 spores/mL and used immediately. *Brachypodium* seedlings (three days post-germination) were immersed in *Fp* spores (1×10^6 spores/mL) and incubated for three minutes. Eight technical replicates of six plants per replicate were included for each treatment. Seedlings were subsequently grown for a further 12 days under a neutral photoperiod and a, 22˚C day and 20˚C night temperature cycle to allow for symptom development. At 12 days post inoculation (dpi) individual seedlings were scored for their disease symptom progression, using a 0 (healthy) to 5 (dead) ranking system (Powell, 2016), and visible leaf number recorded.

Disease score and leaf number yield nominal and ordinal types of data, which results in a non-normal distribution and therefore the requirement to use non-parametric statistical tests. The data was analysed using statistical software R version 3.5.1 (RCoreTeam, 2018). The disease score and leaf number were analysed, as univariate data, using the base{stats} *pairwise.wilcox*() function to perform a Wilcoxon rank test with a Bonferroni procedure to correct for multiple comparisons (RCoreTeam, 2018). To test the relative contribution of genotype and treatment grouping factors as sources of variation for the response variables; disease score and leaf number, a permutational two way MANOVA was performed using a*donis()* function from the *vegan R* package (Oksanen et al., 2007). A Bonferroni corrected pairwise one way MANOVA was subsequently used to determine which levels of the grouping factors contributed most to the group differences (Arbizu, 2019). The *vegdist()* function from the *vegan R* package was used to compute a Gower dissimilarity matrix, from the disease score

and leaf number response variables, as input for the permutational MANOVAs (Oksanen et al., 2007).

3.5.6 *Fusarium pseudograminearum* infection assay

Inoculation of *Brachypodium* seedlings was performed using a laboratory infection assay as previously described. A soil-less infection assay was performed using *nahG* over-expresser line CO404.5 and the wild-type control (Bd21-3) to compare global transcriptional responses during infection with *Fp* isolate CS3096 (CSIRO Fusarium isolate collection). Inoculations were performed as described above in section 3.5.5 with the modified method by Yang et al. (2010). Four biological replicates with 12 plants per replicate were produced for each genotype by treatment combination. Whole shoots were harvested at 5 dpi and immediately immersed in liquid nitrogen.

Strong disease expression was noted at 14 dpi within additional infected replicates left to develop disease symptoms. Key defence response marker genes were observed using qRT-PCR applied to cDNA aliquots produced from extracted RNA samples indicating *PR1* was induced under infection in both WT and *nahG* but more highly induced in WT (Figure 3.1)... Having observed a strong molecular response at 5 dpi, RNA samples were sent for RNA sequencing at the Australian Genome Research Facility (AGRF).

3.5.7 Quantification of salicylic acid using LC-MS

SA quantification was performed as described by Powell et al. (2017a) for LC-MS quantification of metabolites and the chromatography method is reproduced below for ease of reference.. SA obtained from Sigma (Sigma, MO, USA) was used as an analytical standard. “Chromatographic separation as described by Chooi et al. (2015) with the following adjustments. Chromatographic separation was performed at room temperature using a ZORBAX Eclipse RRHD C18 column (1.8 μm particle size, 2.1 mm i.d. × 150 mm; Agilent) and an in-line filter. The mobile phase consisted of a linear gradient of 95% eluent A (0.1% (v/v) formic acid in deionized water) to 100% eluent B (0.1% (v/v) formic acid in 90% methanol) over 15 min at a flow rate of 200 μL min−1 with a sample injection volume of 5uL.” The resulting data were visualised and analysed using Microsoft Excel (MicrosoftCorporation, 2018).

3.5.8 RNA-seq analysis

RNA-seq analysis was performed as described by Powell et al. (2017b), with minor modifications as described below. Low quality sequence were removed using SolexaQA (Cox et al., 2010) with dynamic trimming to retain paired-end reads with minimum PHRED score of 30 and a minimum length of 70bp in each read. Filtered and trimmed paired-end reads were aligned to the *Brachypodium distachyon* 3.1 genome annotation (accessed on 30/05/2014 from Phytozome) using ‘Bowtie2’ in conjunction with ‘TopHat2’ to process reads spanning intron-exon boundaries. Individual transcript fragments were extracted from binary alignment maps (BAM file) were assembled into and normalised to fragments per kilobase per million (FPKM) using ‘Cufflinks’, a revised transcriptome annotation was produced by combining all ‘Cufflinks’ assemblies using ‘Cuffmerge’. Statistical analysis was performed as part of the ‘CuffDiff’ analysis to apply a false discovery rate and multiple comparison correction enabling calling of genes which are significantly differentially expressed between the various genotype/treatment combinations.

A reciprocal best BLAST approach (Moreno-Hagelsieb and Latimer 2008) was undertaken to identify corresponding genes between annotation versions v1.2 and

v3.1 using BLASTn (Altschul et al. 1990) with a minimum e-value of 1 x e^{-05} and a custom script to retrieve reciprocal matches. Primary transcript sequence multiple Fasta files for each version were downloaded from Phytozome (30/05/2014). Gene enrichment analysis was performed using the software BLAST2GO (Conesa et al., 2005) as previously described (Powell, 2016), producing the background reference genes set from the *Brachypodium distachyon* v3.1 primary transcript collection using standard BLASTx, mapping and annotation parameters within BLAST2Go and testing for enrichment within DEG comparisons using Fisher's Exact Tests with false discovery rate set to <0.05..

3.5.9 Salicylic acid (SA) growth rate inhibition assays for *Fp*

The effect of salicylic acid (SA) on *Fp* (CS3096) isolate was tested using growth on Potato Dextrose Agarose (PDA) (Difco, USA). To determine whether SA inhibited *Fp* a range of concentrations; 1.25mM, 2,5mM and 5mM, were compared to a mock solution. A 25mm plug of *Fp* infested mycelia was used to inoculate 15mL of PDA amended with 12.5mM Citrate Buffer System (CBS); buffered at 4.6pH, 2.5% DMSO (V:V), and either 0mM (Mock), 1.25mM, 2.5mM or 5mM salicylic acid. At 6 days post inoculation (dpi) the radial growth area was traced using a fine line marker pen, and the plates photographed. The plate images were analysed and radial growth area was calculated using the polygon tool in ImageJ (Schneider et al., 2012). The statistical analyses of the data was performed using R (ver.3.5.1) (RCoreTeam, 2018). The plots were generated using the R package ggplot2 (Wickham, 2011).

3.6 Figures

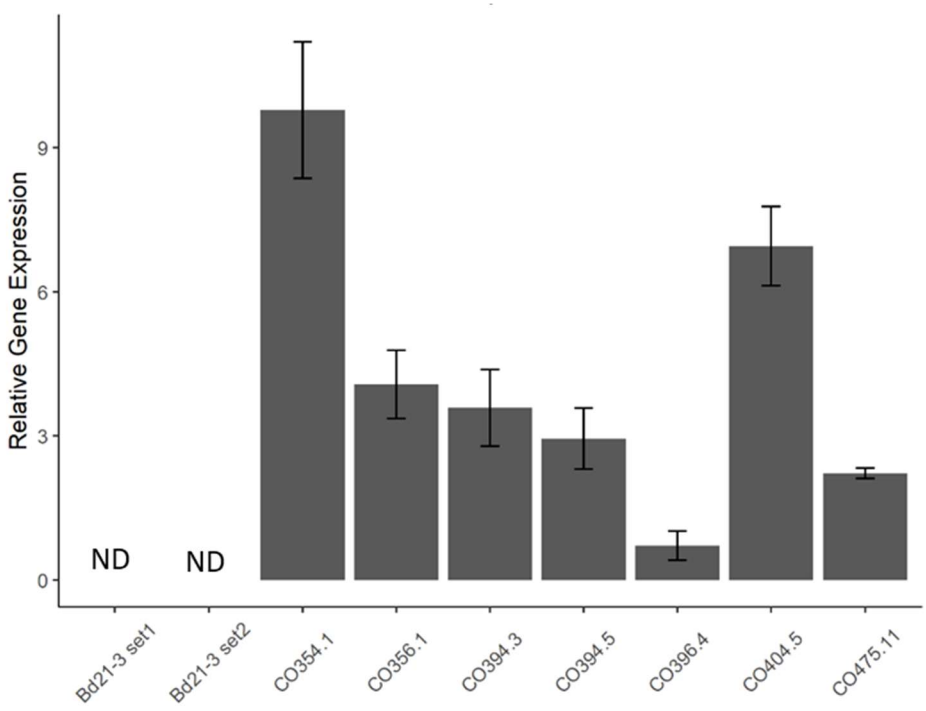

Figure 3.1: Relative expression levels of n*ah*G transgene in T2 generation transformants. Bars represent the mean expression value of the *nahG* transgene across WT controls (Bd21-3) versus independent *nahG* transformants (CO354.1 – CO475.11) which had low insert number and were homozygous for insert. Error bars represent the standard error from the mean between three biological reps. ND is not detected.

A.

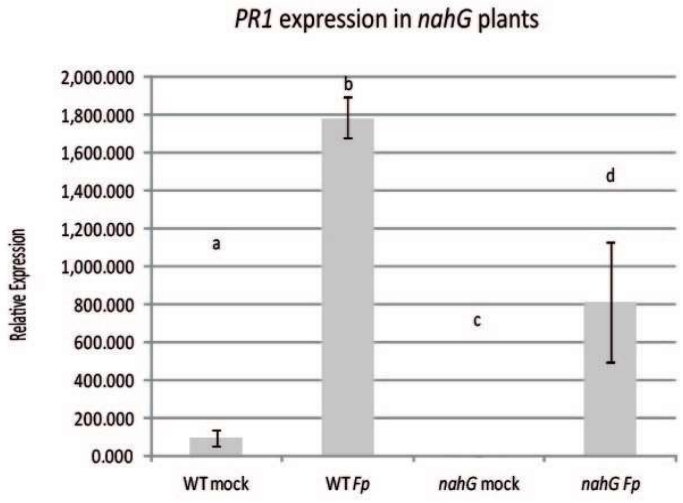

B.

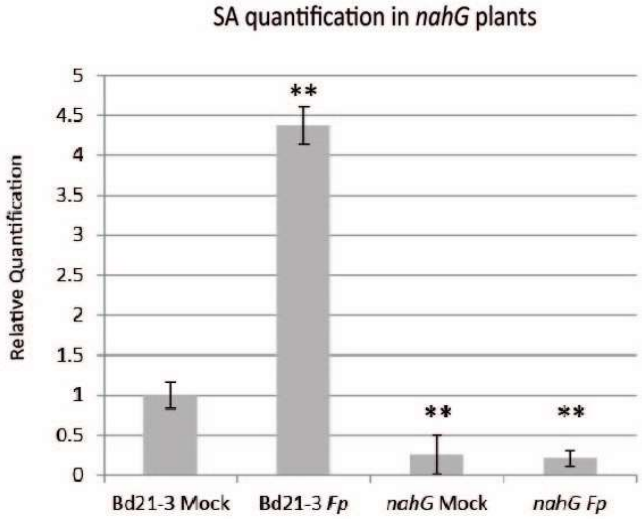

Figure 3.2: Basal SA levels are reduced while SA induction during infection is ablated in *nahG* lines. A. Quantification of *PR1* expression levels using qRT-PCR. Relative expression values display the fold-change difference between genotypes in *PR1 (Bradi1g57580)* mean expression values relative to the mean expression of *nahG* mock samples. Error bars represent the standard error from the mean between four biological reps. Letters denote statistically significant difference $P < 0.01$ between means (One-way ANOVA; Tukey HSD post-hoc test).**B.** Quantification of SA levels using LC-MS. Relative expression values display the fold-change difference between genotypes for SA detection (area under the SA signal peak normalized to sample weight) mean relative to the mean expression of WT (Bd21-3) mock samples. Error bars represent the standard error from the mean between four biological reps. ** denote statistical significance of $P < 0.01$ relative to WT mock (Pairwise Student's t test).

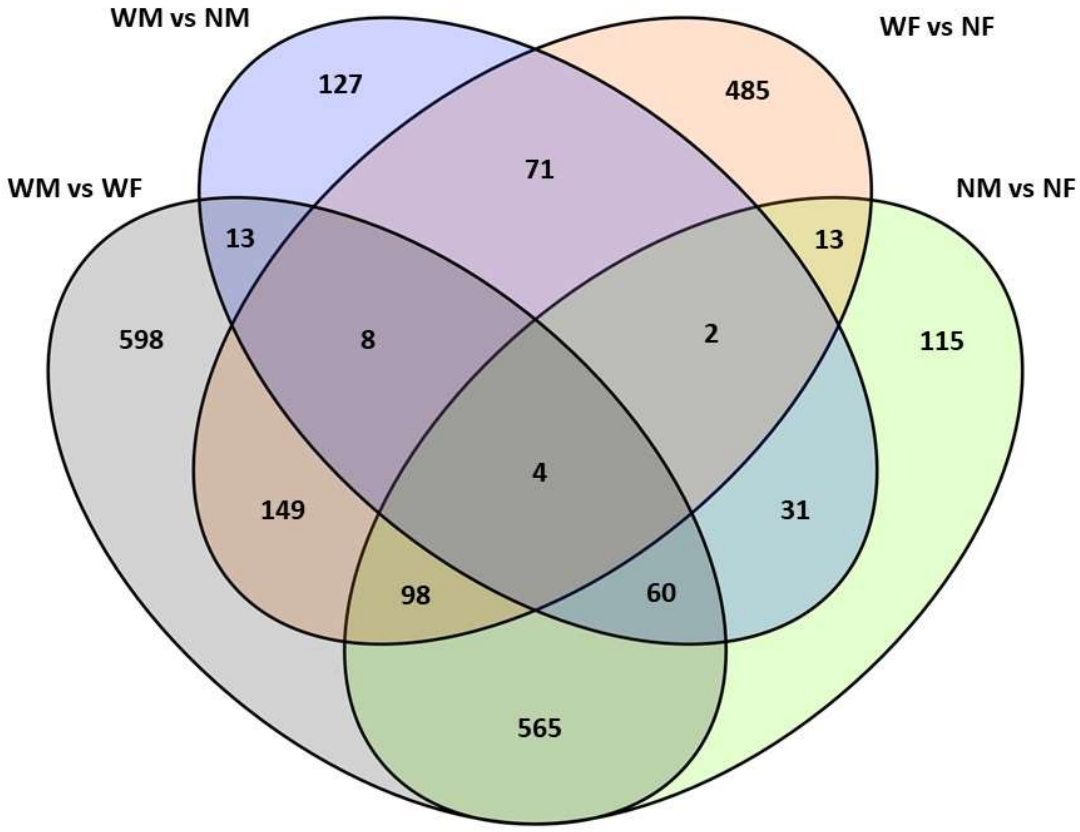

Figure 3.3: Venn diagram showing number of common and differentially expressed genes between WT (Bd21-3) and *nahG* mock (WM & NM); WT mock and WT *Fusarium pseudograminearum* (WM & WF); WT and *nahG Fusarium pseudograminearum* (WF & NF); and *nahG* mock and *nahG Fusarium pseudograminearum* (NM & NF) conditions. Genes used for this analysis had adjusted p values <0.05 and fold-change values were >$\log_2 2$ for WM vs WF and NM vs NF comparisons or were >$\log_2 1$ for WM vs NM and WF vs NF comparisons.

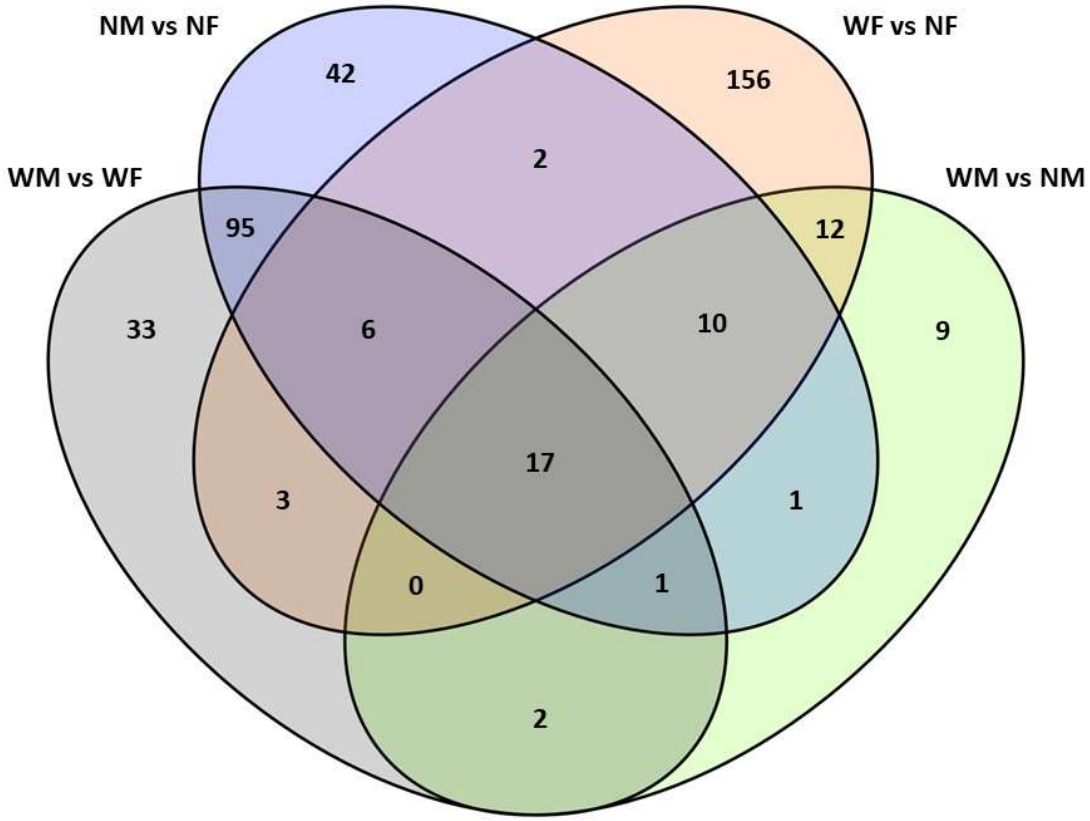

Figure 3.4: Venn diagram showing number of common and distinct enriched GO terms identified between WT (Bd21-3) and *nahG* mock (WM & NM); WT mock and WT *Fusarium pseudograminearum* (WM & WF); WT and *nahG Fusarium pseudograminearum* (WF & NF); and *nahG* mock and *nahG Fusarium pseudograminearum* (NM & NF) conditions. Genes used for this analysis had adjusted p values <0.05 and fold-change values were >$\log_2 2$ for WM vs WF and NM vs NF comparisons or were >$\log_2 1$ for WM vs NM and WF vs NF comparisons.

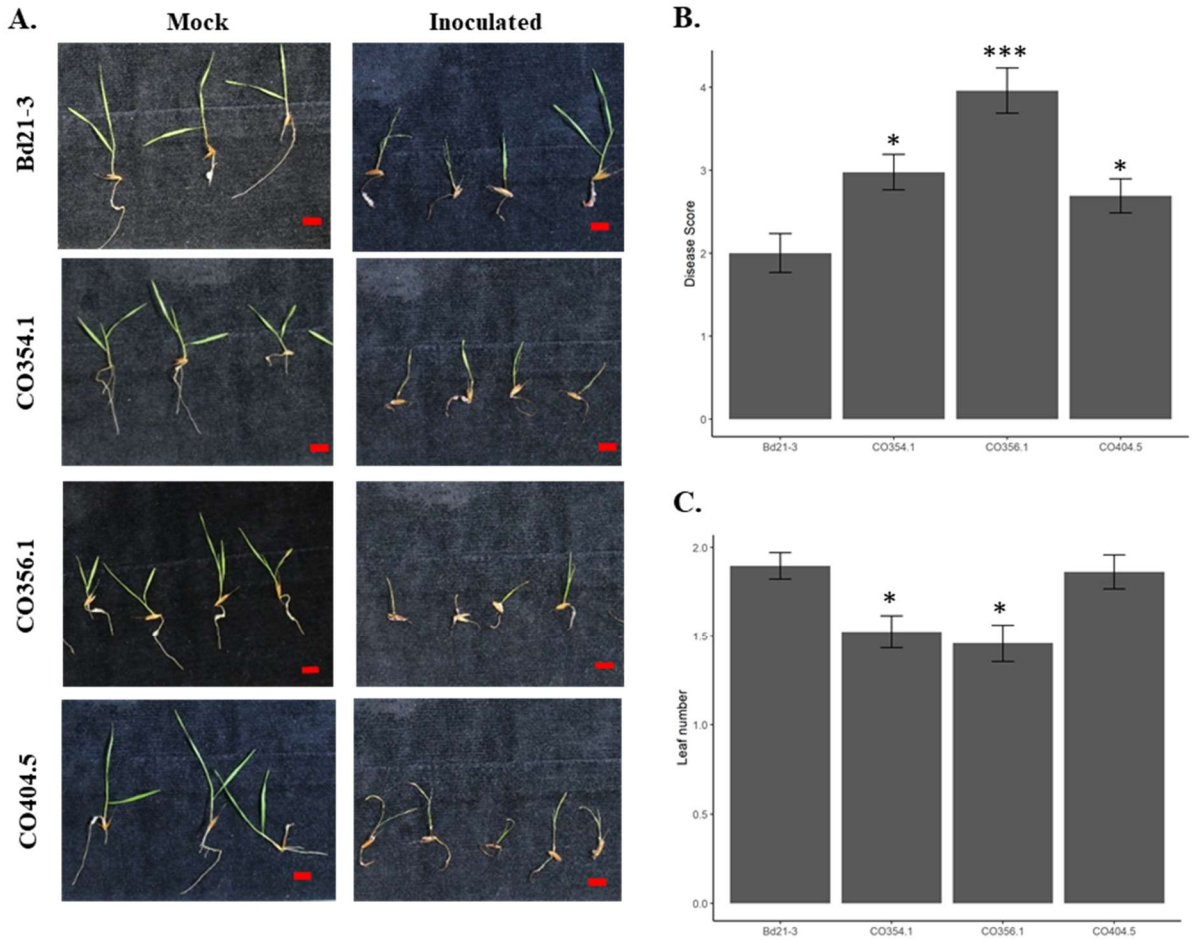

Figure 3.5: *nah*G expressing plants show enhanced disease phenotypes, under *Fp* inoculation conditions, with respect to wild type. Values were recorded from a soilless infection assay using *Brachypodium* seedlings, 12 days post inoculation (12dpi) with a 1×10^6 spores/mL *Fp* spore suspension. Data represents eight technical replicates of six plants per replicate. * and *** denote statistical significance of $P < 0.05$ and $P < 0.001$ respectively, relative to inoculated WT, as per a multiple comparisons Bonferroni corrected Wilcoxon rank test. A. Photographs of 12dpi mock and *Fp* inoculated plants of representative treated individuals. Red bar is a 1cm scale bar. B. Column chart representing the mean (n= 40) *Fp* disease score at 12 dpi, using a 0-5 scale of severity, ± S.E. C. Column chart representing the mean (n=40) leaf number per individual plant at 12dpi, ± S.E.

3.7 Supplementary Files

3.7.1 Supplementary tables

Supplementary table 3.1: Filtered list of significantly enriched Gene Ontology (GO) terms in mock and *Fusarium* inoculated wild type (WT) and *nahG Brachypodium* showing most specific GO terms (ontology branch tips). Abbreviations; biological processes (BP), cellular components (CC), molecular function (MF) WT mock (WM) *nahG* mock (NM), WT *Fusarium* (WF); *nahG Fusarium* (NF)

GO_ID	GO_Term	Category	WM_vs_WF_up	NM_vs_NF_up	WF_vs_NF_up	WM_vs_NM_up	WM_vs_NM_down
GO:0055114	oxidation-reduction process	BP	145	106		32	17
GO:0006468	protein phosphorylation	BP	84	58			
GO:0006749	glutathione metabolic process	BP	18	16			4
GO:1901617	organic hydroxy compound biosynthetic process	BP	17	11			
GO:0002229	defense response to oomycetes	BP	13	14			
GO:0007178	transmembrane receptor protein serine/threonine kinase signalling pathway	BP	12	14			
GO:0000162	tryptophan biosynthetic process	BP	9	9			
GO:0042908	xenobiotic transport	BP	9	8			
GO:0046274	lignin catabolic process	BP	8	7	7	4	
GO:0016121	carotene catabolic process	BP	6				
GO:0006558	L-phenylalanine metabolic process	BP	6				
GO:2000022	regulation of jasmonic acid mediated signalling pathway	BP	6				
GO:1901002	positive regulation of response to salt stress	BP	5				
GO:0072525	pyridine-containing compound biosynthetic process	BP	5				
GO:0009074	aromatic amino acid family catabolic process	BP	5				
GO:0009800	cinnamic acid biosynthetic process	BP	4				

GO:0042218	1-aminocyclopropane-1-carboxylate biosynthetic process	BP	3				
GO:0010731	protein glutathionylation	BP	3				
GO:0016021	integral component of membrane	CC	328	223			
GO:0048046	apoplast	CC	23	16	22	12	10
GO:0030312	external encapsulating structure	CC	22	16	16	9	
GO:0046658	anchored component of plasma membrane	CC	16			8	
GO:0005524	ATP binding	MF	129	92			
GO:0020037	heme binding	MF	51	44	16	13	10
GO:0003700	DNA-binding transcription factor activity	MF	50	34			
GO:0043565	sequence-specific DNA binding	MF	44		20		
GO:0016705	oxidoreductase activity, acting on paired donors	MF	41	33			
GO:0005506	iron ion binding	MF	40	32			
GO:0004497	monooxygenase activity	MF	38	33			7
GO:0030246	carbohydrate binding	MF	34	28			
GO:0005509	calcium ion binding	MF	27				
GO:0004364	glutathione transferase activity	MF	26	22			5
GO:0015291	secondary active transmembrane transporter activity	MF	21	16			
GO:0071949	FAD binding	MF	14	9			
GO:0045735	nutrient reservoir activity	MF	14	7			5
GO:0005507	copper ion binding	MF	13	10	7	5	
GO:0080043	quercetin 3-O-glucosyltransferase activity	MF	13				
GO:0080044	quercetin 7-O-glucosyltransferase activity	MF	13				
GO:0004675	transmembrane receptor protein serine/threonine kinase activity	MF	12	14			
GO:0030170	pyridoxal phosphate binding	MF	12	10			
GO:0016831	carboxy-lyase activity	MF	11	9			
GO:0030145	manganese ion binding	MF	11	8			4
GO:0042910	xenobiotic transmembrane transporter activity	MF	9	8			
GO:0010181	FMN binding	MF	9	7			
GO:0004568	chitinase activity	MF	8	8			

GO:0052716	hydroquinone:oxygen oxidoreductase activity	MF	8	7	7	4	
GO:0043295	glutathione binding	MF	7	6			
GO:0004834	tryptophan synthase activity	MF	4	4			
GO:0045548	phenylalanine ammonia-lyase activity	MF	4				
GO:0050734	hydroxycinnamoyltransferase activity	MF	3	3			
GO:0016847	1-aminocyclopropane-1-carboxylate synthase activity	MF	3				
GO:0045549	9-cis-epoxycarotenoid dioxygenase activity	MF	3				

Supplementary table 3.2: List of significantly differentially expressed gene DEG (log_2 fold change), encoding class III peroxidases in mock and *Fusarium* inoculated wild type (WT) and *nahG* expressing *Brachypodium*. Abbreviations; WT mock (WM) *nahG* mock (NM), WT *Fusarium* (WF); *nahG Fusarium* (NF)

			Treatment combinations resulting in DEG			
Gene name	Gene ID	Gene Description	WM vs WF	NM vs NF	WM vs NM	WF vs NF
BdPrx006	*BRADI_1g17840*	root peroxidase	2.75	3.83	-2.39	-1.30
BdPrx007	*BRADI_1g17850*	root peroxidase	2.50			-2.24
BdPrx008	*BRADI_1g17860*	class iii peroxidase	-2.71			1.39
BdPrx014	*BRADI_1g20010*	peroxidase 2-like				
BdPrx015	*BRADI_1g20020*	peroxidase 2				
BdPrx018	*BRADI_1g27910*	peroxidase n-like		5.33		
BdPrx020	*BRADI_1g32870*	peroxidase 3-like			1.38	
BdPrx023	*BRADI_1g38297*	peroxidase 52-like				
BdPrx025	*BRADI_1g38310*	peroxidase 52-like				
BdPrx026	*BRADI_1g38350*	peroxidase 4	6.98			-2.33
BdPrx027	*BRADI_1g39190*	peroxidase 4				-2.49
BdPrx028	*BRADI_1g41115*	peroxidase 52-like	-3.09	-2.04		1.68
BdPrx030	*BRADI_1g42900*	peroxidase 1			2.34	
BdPrx042	*BRADI_1g63060*	class iii peroxidase				1.09
BdPrx045	*BRADI_1g68887*	peroxidase n-like				

BdPrx046	*BRADI_1g68900*	peroxidase 15-like			1.05	
BdPrx047	*BRADI_1g68927*	peroxidase 54-like	7.02	5.04		-1.89
BdPrx051	*BRADI_2g04490*	peroxidase 25-like				
BdPrx056	*BRADI_2g09680*	peroxidase 72-like			1.10	1.20
BdPrx062	*BRADI_2g11320*	peroxidase 2		2.31		
BdPrx065	*BRADI_2g12192*	peroxidase 1-like			-1.56	
BdPrx066	*BRADI_2g12204*	peroxidase 1-like	2.18	2.33		
BdPrx070	*BRADI_2g17120*	peroxidase 12				1.20
BdPrx072	*BRADI_2g20830*	class iii peroxidase				1.52
BdPrx073	*BRADI_2g20840*	class iii peroxidase			1.07	1.33
BdPrx074	*BRADI_2g20850*	class iii peroxidase			1.47	1.61
BdPrx075	*BRADI_2g34717*	peroxidase				-1.57
BdPrx077	*BRADI_2g37010*	peroxidase 5-like	2.78	3.69		
BdPrx078	*BRADI_2g37020*	peroxidase 5-like	4.94	5.27		
BdPrx081	*BRADI_2g37060*	peroxidase 2		-4.07	2.50	
BdPrx092	*BRADI_2g40590*	peroxidase 72-like	2.19			
BdPrx119	*BRADI_4g05190*	peroxidase 15	6.07			-1.40
BdPrx120	*BRADI_4g05230*	peroxidase 15	6.07	6.55	-2.18	-1.68
BdPrx124	*BRADI_4g25660*	peroxidase 4-like		2.03	-1.22	
BdPrx125	*BRADI_4g27680*	peroxidase 12		2.81		

BdPrx142	*BRADI_5g24200*	cationic peroxidase 1-like	4.22			
BdPrx144	*BRADI_5g27130*	anionic peroxidase		3.03	-1.91	
BdPrx150	*BRADI_5g27220*	peroxidase 12-like		2.14	-1.03	
BdPrx151	*BRADI_5g27687*	peroxidase 47-like			-1.99	

Supplementary table 3.3: List of primers used for qRT-PCR to validate *nahG* transgene, pathogen responsive marker gene, *PR1*, and reference gene *UBC18*

Target Gene	**Gene**	**Forward Primer**	**Melt Temp.**	**Reverse Primer**	**Melt Temp.**	**Product Size**	**Reference**
UBC18	*Bradi4g00660*	5' TTTACAGCAATGGCCACATC 3'	59.55	5' AGACAGCATGGACAAGATGC 3'	58.83	101	Hong et al. (2008), Chambers et al. (2012)
nahG Transgene	transgene	5' AAAGGTATCGCCCAATTCAG 3'	58.42	5' GATTAGAAGGTCACAGCGG 3'	58.09	107	
PR1	*Bradi1g57590*	5' TACCACCATGACGGGAATC 3'	59.15	5' CACAAACAACACGAGCACAC 3'	58.76	106	Mandadi and Scholthof (2012)

3.7.2 Supplementary figures

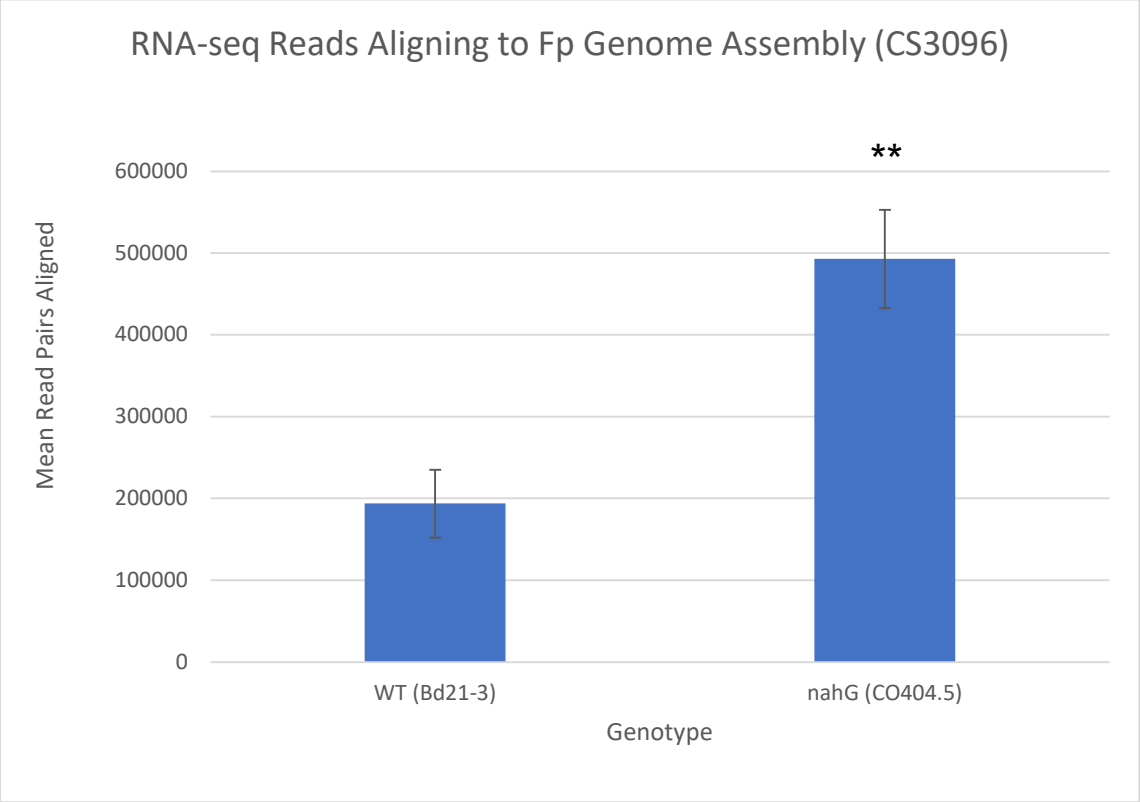

Supplementary figure 3.1: Bar plot visualizing mean ± S.E number of paired reads that aligned to the *Fp* genome from RNA samples of infected WT and *nahG Brachypodium* tissue. ** denote statistical significance of $P < 0.01$ according to a Student's T test.

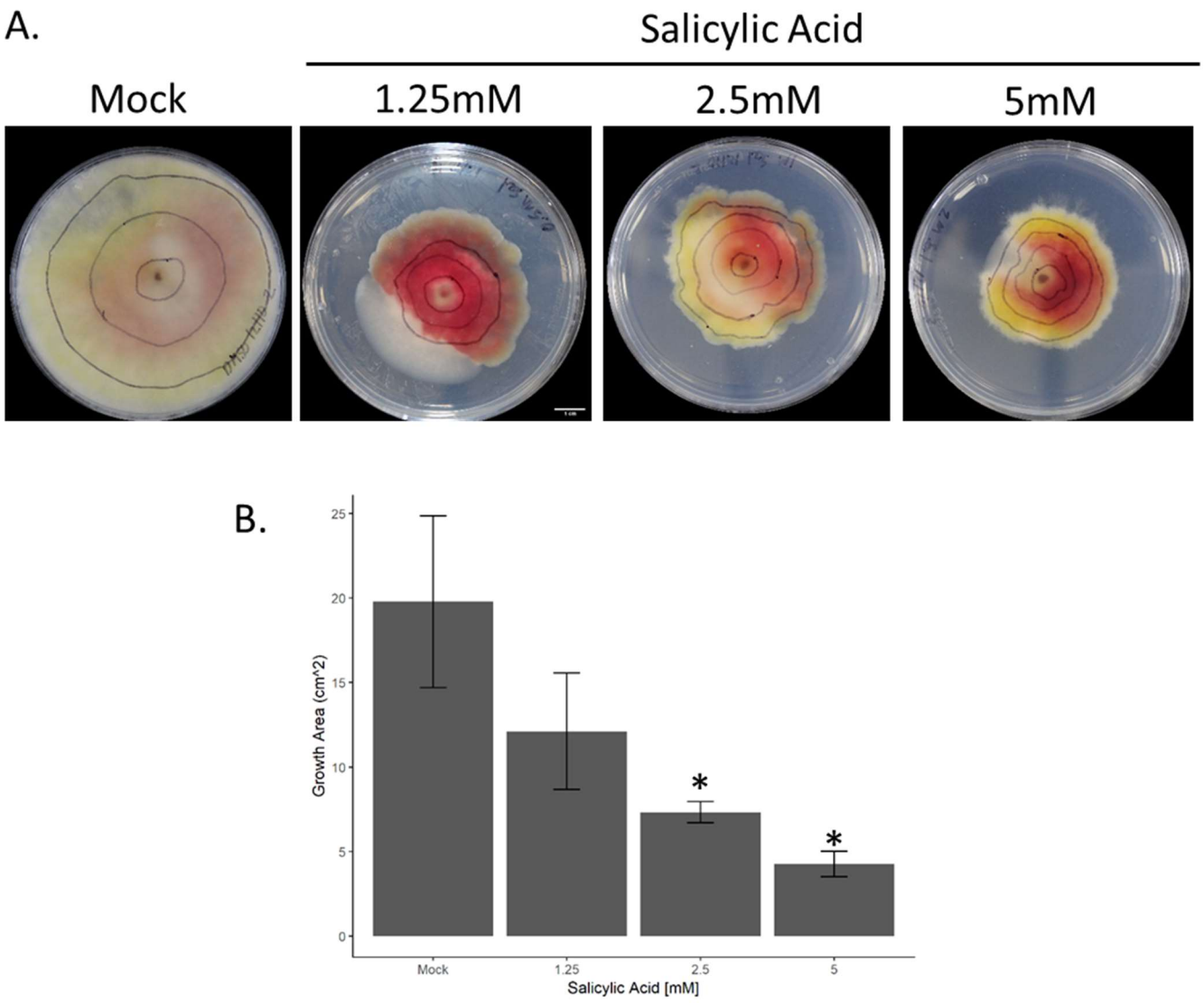

Supplementary figure 3.2: *Fusarium pseudograminearum* (*CS3096)* (*Fp)* shows inhibition of mycelial growth on Potato Dextrose Agarose (PDA) amended with salicylic acid. A 25mm plug of *Fp* infested mycelia was used to inoculate 15mL of PDA amended with 12.5mM Citrate Buffer System (CBS); buffered at 4.6pH, 2.5% DMSO (V:V), and either 0mM (Mock), 1.25mM, 2.5mM or 5mM salicylic acid. A. Pictures of representative plates at 8 days post inoculation (dpi). B. Column plot showing the mean (n=4) mycelia growth of *Fp* at 6dpi in PDA amended with mock and solutions containing different concentrations of salicylic acid. * represent statistical significance of P<0.05 relative to the Mock value, according to a *Wilcoxon rank test* with *Bonferroni's* correction for multiple comparisons.

3.8 References

ABERCROMBIE, J. M., HALFHILL, M. D., RANJAN, P., RAO, M. R., SAXTON, A. M., YUAN, J. S. & STEWART, C. N. 2008. Transcriptional responses of *Arabidopsis thaliana* plants to As (V) stress. *BMC Plant Biology,* 8**,** 87.

ABREU, M. E. & MUNNÉ-BOSCH, S. 2009. Salicylic acid deficiency in *NahG* transgenic lines and *sid2* mutants increases seed yield in the annual plant *Arabidopsis thaliana*. *Journal of experimental botany,* 60**,** 1261-1271.

AKINSANMI, O., BACKHOUSE, D., SIMPFENDORFER, S. & CHAKRABORTY, S. 2006. Genetic diversity of Australian *Fusarium graminearum* and *F. pseudograminearum*. *Plant Pathology,* 55**,** 494-504.

ALMAGRO, L., GÓMEZ ROS, L., BELCHI-NAVARRO, S., BRU, R., ROS BARCELÓ, A. & PEDRENO, M. 2008. Class III peroxidases in plant defence reactions. *Journal of experimental botany,* 60**,** 377-390.

AOKI, T., WARD, T. J., KISTLER, H. C. & O'DONNELL, K. 2012. Systematics, phylogeny and trichothecene mycotoxin potential of Fusarium head blight cereal pathogens. *JSM Mycotoxins,* 62**,** 91-102.

ARBIZU, M. 2019. Pairwise multilevel comparison using adonis. *R Package Version 0.3*.

BELTRAMO, C., MARINONI, D. T., PERRONE, I. & BOTTA, R. 2012. Isolation of a gene encoding for a class III peroxidase in female flower of *Corylus avellana* L. *Molecular biology reports,* 39**,** 4997-5008.

BINDSCHEDLER, L. V., DEWDNEY, J., BLEE, K. A., STONE, J. M., ASAI, T., PLOTNIKOV, J., DENOUX, C., HAYES, T., GERRISH, C. & DAVIES, D. R. 2006. Peroxidase‐dependent apoplastic oxidative burst in *Arabidopsis* required for pathogen resistance. *The Plant Journal,* 47**,** 851-863.

BOSSOLINI, E., WICKER, T., KNOBEL, P. A. & KELLER, B. 2007. Comparison of orthologous loci from small grass genomes *Brachypodium* and rice: implications for wheat genomics and grass genome annotation. *The Plant Journal,* 49**,** 704-717.

BRAGG, J. N., ANDERTON, A., NIEU, R. & VOGEL, J. P. 2015. *Brachypodium distachyon*. *Agrobacterium Protocols.* Springer.

BRAGG, J. N., WU, J., GORDON, S. P., GUTTMAN, M. E., THILMONY, R., LAZO, G. R., GU, Y. Q. & VOGEL, J. P. 2012. Generation and characterization of the Western Regional Research Center *Brachypodium* T-DNA insertional mutant collection. *PLoS One,* 7**,** e41916.

BRKLJACIC, J., GROTEWOLD, E., SCHOLL, R., MOCKLER, T., GARVIN, D. F., VAIN, P., BRUTNELL, T., SIBOUT, R., BEVAN, M. & BUDAK, H. 2011. *Brachypodium* as a model for the grasses: today and the future. *Plant Physiology,* 157**,** 3-13.

CAO, H., GLAZEBROOK, J., CLARKE, J. D., VOLKO, S. & DONG, X. 1997. The *Arabidopsis NPR1* gene that controls systemic acquired resistance encodes a novel protein containing ankyrin repeats. *Cell,* 88**,** 57-63.

CAO, Y., HAN, Y., MENG, D., LI, D., JIN, Q., LIN, Y. & CAI, Y. 2016. Structural, evolutionary, and functional analysis of the class III peroxidase gene family in Chinese Pear (*Pyrus bretschneideri*). *Frontiers in plant science,* 7**,** 1874.

CHAMBERS, J. P., BEHPOURI, A., BIRD, A. & NG, C. K. 2012. Evaluation of the use of the polyubiquitin genes, *Ubi4* and *Ubi10* as reference genes for expression studies in *Brachypodium distachyon*. *PloS one,* 7**,** e49372.

CHEN, Z., SILVA, H. & KLESSIG, D. F. 1993. Active oxygen species in the induction of plant systemic acquired resistance by salicylic acid. *Science,* 262**,** 1883-1886.

CHOOI, Y.-H., KRILL, C., BARROW, R. A., CHEN, S., TRENGOVE, R., OLIVER, R. P. & SOLOMON, P. S. 2015. An in planta-expressed polyketide synthase produces (R)-mellein in the wheat pathogen *Parastagonospora nodorum*. *Appl. Environ. Microbiol.,* 81**,** 177-186.

CONESA, A., GÖTZ, S., GARCÍA-GÓMEZ, J. M., TEROL, J., TALÓN, M. & ROBLES, M. 2005. Blast2GO: a universal tool for annotation, visualization and analysis in functional genomics research. *Bioinformatics,* 21**,** 3674-3676.

CORNEJO, M.-J., LUTH, D., BLANKENSHIP, K. M., ANDERSON, O. D. & BLECHL, A. E. 1993. Activity of a maize ubiquitin promoter in transgenic rice. *Plant molecular biology,* 23**,** 567-581.

COSIO, C., VUILLEMIN, L., DE MEYER, M., KEVERS, C., PENEL, C. & DUNAND, C. 2009. An anionic class III peroxidase from zucchini may regulate hypocotyl elongation through its auxin oxidase activity. *Planta,* 229**,** 823-836.

COX, M. P., PETERSON, D. A. & BIGGS, P. J. 2010. SolexaQA: At-a-glance quality assessment of Illumina second-generation sequencing data. *BMC bioinformatics,* 11**,** 1-6.

DALMAIS, M., ANTELME, S., HO-YUE-KUANG, S., WANG, Y., DARRACQ, O., D'YVOIRE, M. B., CEZARD, L., LÉGÉE, F., BLONDET, E. & ORIA, N. 2013. A TILLING platform for functional genomics in *Brachypodium distachyon*. *PLoS One,* 8**,** e65503.

DESJARDINS, A. E. 2006. *Fusarium mycotoxins: chemistry, genetics, and biology*, American Phytopathological Society (APS Press).

DESMOND, O. J., EDGAR, C. I., MANNERS, J. M., MACLEAN, D. J., SCHENK, P. M. & KAZAN, K. 2005. Methyl jasmonate induced gene expression in wheat delays symptom development by the crown rot pathogen Fusarium pseudograminearum. *Physiological and Molecular Plant Pathology,* 67**,** 171-179.

DODGE, A. G. & WACKETT, L. P. 2005. Metabolism of bismuth subsalicylate and intracellular accumulation of bismuth by *Fusarium* sp. strain BI. *Appl. Environ. Microbiol.,* 71**,** 876-882.

DOMBRECHT, B., XUE, G. P., SPRAGUE, S. J., KIRKEGAARD, J. A., ROSS, J. J., REID, J. B., FITT, G. P., SEWELAM, N., SCHENK, P. M. & MANNERS, J. M. 2007. MYC2 differentially modulates diverse jasmonate-dependent functions in *Arabidopsis*. *The Plant Cell,* 19**,** 2225-2245.

DONG, X. 2004. NPR1, all things considered. *Current opinion in plant biology,* 7**,** 547-552.

DURRANT, W. E. & DONG, X. 2004. Systemic acquired resistance. *Annu. Rev. Phytopathol.,* 42**,** 185-209.

FRIEDRICH, L., VERNOOIJ, B., GAFFNEY, T., MORSE, A. & RYALS, J. 1995. Characterization of tobacco plants expressing a bacterial salicylate hydroxylase gene. *Plant molecular biology,* 29**,** 959-968.

GARDINER, D. M., MCDONALD, M. C., COVARELLI, L., SOLOMON, P. S., RUSU, A. G., MARSHALL, M., KAZAN, K., CHAKRABORTY, S., MCDONALD, B. A. & MANNERS, J. M. 2012. Comparative pathogenomics reveals horizontally acquired novel virulence genes in fungi infecting cereal hosts. *PLoS pathogens,* 8**,** e1002952.

GLAZEBROOK, J. 2005. Contrasting mechanisms of defense against biotrophic and necrotrophic pathogens. *Annu. Rev. Phytopathol.,* 43**,** 205-227.

GOVRIN, E. M. & LEVINE, A. 2000. The hypersensitive response facilitates plant infection by the necrotrophic pathogen *Botrytis cinerea*. *Current biology,* 10**,** 751-757.

GREENBERG, J. T., GUO, A., KLESSIG, D. F. & AUSUBEL, F. M. 1994. Programmed cell death in plants: a pathogen-triggered response activated coordinately with multiple defense functions. *Cell,* 77**,** 551-563.

HAO, Q., WANG, W., HAN, X., WU, J., LYU, B., CHEN, F., CAPLAN, A., LI, C., WU, J. & WANG, W. 2018. Isochorismate‐based salicylic acid biosynthesis confers basal resistance to *Fusarium graminearum* in barley. *Molecular plant pathology,* 19**,** 1995-2010.

HIRAGA, S., SASAKI, K., ITO, H., OHASHI, Y. & MATSUI, H. 2001. A large family of class III plant peroxidases. *Plant and Cell Physiology,* 42**,** 462-468.

HONG, S. H., SEO, P. J., YANG, M. S., XIANG, F. & PARK, C. M. 2008. Exploring valid reference genes for gene expression studies in *Brachypodium distachyon* by real-time PCR. *BMC Plant Biology,* 8.

HRUZ, T., LAULE, O., SZABO, G., WESSENDORP, F., BLEULER, S., OERTLE, L., WIDMAYER, P., GRUISSEM, W. & ZIMMERMANN, P. 2008. Genevestigator v3: a reference expression database for the meta-analysis of transcriptomes. *Advances in bioinformatics,* 2008.

INITIATIVE, I. B. 2010. Genome sequencing and analysis of the model grass *Brachypodium distachyon*. *Nature,* 463**,** 763.

KAKEI, Y., MOCHIDA, K., SAKURAI, T., YOSHIDA, T., SHINOZAKI, K. & SHIMADA, Y. 2015. Transcriptome analysis of hormone-induced gene expression in *Brachypodium distachyon*. *Scientific reports,* 5**,** 14476.

KIDWAI, M., DHAR, Y. V., GAUTAM, N., TIWARI, M., AHMAD, I. Z., ASIF, M. H. & CHAKRABARTY, D. 2019. *Oryza sativa* class III peroxidase *(OsPRX38*) overexpression in *Arabidopsis thaliana* reduces arsenic accumulation due to apoplastic lignification. *Journal of hazardous materials,* 362**,** 383-393.

KLOK, E. J., WILSON, I. W., WILSON, D., CHAPMAN, S. C., EWING, R. M., SOMERVILLE, S. C., PEACOCK, W. J., DOLFERUS, R. & DENNIS, E. S. 2002. Expression profile analysis of the low-oxygen response in *Arabidopsis* root cultures. *The Plant Cell,* 14**,** 2481-2494.

KNOTH, C., RINGLER, J., DANGL, J. L. & EULGEM, T. 2007. *Arabidopsis* WRKY70 is required for full *RPP4*-mediated disease resistance and basal defense against *Hyaloperonospora parasitica*. *Molecular plant-microbe interactions,* 20**,** 120-128.

KOOTER, J. M. & MOL, J. N. 1993. Trans-inactivation of gene expression in plants. *Current Opinion in Biotechnology,* 4**,** 166-171.

KUMAR, S., MOHAN, A., BALYAN, H. S. & GUPTA, P. K. 2009. Orthology between genomes of *Brachypodium*, wheat and rice. *BMC Research Notes,* 2**,** 93.

LAM, E., KATO, N. & LAWTON, M. 2001. Programmed cell death, mitochondria and the plant hypersensitive response. *Nature,* 411**,** 848.

LAZO, G. R., STEIN, P. A. & LUDWIG, R. A. 1991. A DNA transformation–competent *Arabidopsis* genomic library in *Agrobacterium*. *Bio/technology,* 9**,** 963-967.

LIM, E.-K., DOUCET, C. J., LI, Y., ELIAS, L., WORRALL, D., SPENCER, S. P., ROSS, J. & BOWLES, D. J. 2002. The activity of *Arabidopsis* glycosyltransferases toward salicylic acid, 4-hydroxybenzoic acid, and other benzoates. *Journal of Biological Chemistry,* 277**,** 586-592.

LISZKAY, A., KENK, B. & SCHOPFER, P. 2003. Evidence for the involvement of cell wall peroxidase in the generation of hydroxyl radicals mediating extension growth. *Planta,* 217**,** 658-667.

LLORENTE, F., LÓPEZ‐COBOLLO, R. M., CATALÁ, R., MARTÍNEZ‐ZAPATER, J. M. & SALINAS, J. 2002. A novel cold‐inducible gene from *Arabidopsis*, *RCI3*, encodes a peroxidase that constitutes a component for stress tolerance. *The Plant Journal,* 32**,** 13-24.

MA, L.-J., VAN DER DOES, H. C., BORKOVICH, K. A., COLEMAN, J. J., DABOUSSI, M.-J., DI PIETRO, A., DUFRESNE, M., FREITAG, M., GRABHERR, M. & HENRISSAT, B. 2010. Comparative genomics reveals mobile pathogenicity chromosomes in *Fusarium*. *Nature,* 464**,** 367.

MAKANDAR, R., NALAM, V. J., LEE, H., TRICK, H. N., DONG, Y. & SHAH, J. 2012. Salicylic acid regulates basal resistance to Fusarium head blight in wheat. *Molecular Plant-Microbe Interactions,* 25**,** 431-439.

MANDADI, K. K. & SCHOLTHOF, K. B. 2012. Characterization of a viral synergism in the monocot *Brachypodium distachyon* reveals distinctly altered host molecular processes associated with disease. *Plant Physiol,* 160.

MARTINS, T. M., HARTMANN, D. O., PLANCHON, S., MARTINS, I., RENAUT, J. & PEREIRA, C. S. 2015. The old 3-oxoadipate pathway revisited: new insights in the catabolism of aromatics in the saprophytic fungus *Aspergillus nidulans*. *Fungal Genetics and Biology,* 74**,** 32-44.

MATZKE, A., NEUHUBER, F., PARK, Y., AMBROS, P. & MATZKE, M. 1994. Homology-dependent gene silencing in transgenic plants: epistatic silencing loci contain multiple copies of methylated transgenes. *Molecular and General Genetics MGG,* 244**,** 219-229.

MAUCH, F. & DUDLER, R. 1993. Differential induction of distinct glutathione-S-transferases of wheat by xenobiotics and by pathogen attack. *Plant Physiology,* 102**,** 1193-1201.

MEI, W., QIN, Y., SONG, W., LI, J. & ZHU, Y. 2009. Cotton *GhPOX1* encoding plant class III peroxidase may be responsible for the high level of reactive oxygen species production that is related to cotton fiber elongation. *Journal of Genetics and Genomics,* 36**,** 141-150.

MICROSOFTCORPORATION 2018. Microsoft Excel.

MOURAL, T. W., LEWIS, K. M., BARNABA, C., ZHU, F., PALMER, N. A., SARATH, G., SCULLY, E. D., JONES, J. P., SATTLER, S. E. & KANG, C. 2017. Characterization of class III peroxidases from switchgrass. *Plant physiology,* 173**,** 417-433.

NAWRATH, C. & MÉTRAUX, J.-P. 1999. Salicylic acid induction–deficient mutants of Arabidopsis express *PR-2* and *PR-5* and accumulate high levels of camalexin after pathogen inoculation. *The Plant Cell,* 11**,** 1393-1404.

OKSANEN, J., KINDT, R., LEGENDRE, P., O'HARA, B., STEVENS, M. H. H., OKSANEN, M. J. & SUGGESTS, M. 2007. The vegan package. *Community ecology package,* 10**,** 631-637.

PANDEY, S. P. & SOMSSICH, I. E. 2009. The role of WRKY transcription factors in plant immunity. *Plant physiology,* 150**,** 1648-1655.

PASSARDI, F., LONGET, D., PENEL, C. & DUNAND, C. 2004a. The class III peroxidase multigenic family in rice and its evolution in land plants. *Phytochemistry,* 65**,** 1879-1893.

PASSARDI, F., PENEL, C. & DUNAND, C. 2004b. Performing the paradoxical: how plant peroxidases modify the cell wall. *Trends in plant science,* 9**,** 534-540.

PERALDI, A., BECCARI, G., STEED, A. & NICHOLSON, P. 2011. *Brachypodium distachyon*: a new pathosystem to study Fusarium head blight and other Fusarium diseases of wheat. *BMC Plant Pathol,* 11.

POWELL, J. J. 2016. *Identifying sources of resistance to Fusarium diseases using the model plant Brachypodium distachyon.* Doctor of Philosophy, University of Queensland.

POWELL, J. J., CARERE, J., FITZGERALD, T. L., STILLER, J., COVARELLI, L., XU, Q., GUBLER, F., COLGRAVE, M. L., GARDINER, D. M., MANNERS, J. M., HENRY, R. J. & KAZAN, K. 2017a. The Fusarium crown rot pathogen *Fusarium pseudograminearum* triggers a suite of

transcriptional and metabolic changes in bread wheat (*Triticum aestivum* L.). *Ann Bot,* 119**,** 853-867.

POWELL, J. J., CARERE, J., SABLOK, G., FITZGERALD, T. L., STILLER, J., COLGRAVE, M. L., GARDINER, D. M., MANNERS, J. M., VOGEL, J. P., HENRY, R. J. & KAZAN, K. 2017b. Transcriptome analysis of *Brachypodium* during fungal pathogen infection reveals both shared and distinct defense responses with wheat. *Scientific Reports,* 7**,** 17212.

QI, P.-F., BALCERZAK, M., ROCHELEAU, H., LEUNG, W., WEI, Y.-M., ZHENG, Y.-L. & OUELLET, T. 2016. Jasmonic acid and abscisic acid play important roles in host–pathogen interaction between *Fusarium graminearum* and wheat during the early stages of Fusarium head blight. *Physiological and molecular plant pathology,* 93**,** 39-48.

QI, P.-F., JOHNSTON, A., BALCERZAK, M., ROCHELEAU, H., HARRIS, L. J., LONG, X.-Y., WEI, Y.-M., ZHENG, Y.-L. & OUELLET, T. 2012. Effect of salicylic acid on *Fusarium graminearum*, the major causal agent of fusarium head blight in wheat. *Fungal Biology,* 116**,** 413-426.

RCORETEAM 2018. R: a language and environment for statistical computing computer program, version 3.5. 0. R Core Team Vienna, Austria.

REN, L.-L., LIU, Y.-J., LIU, H.-J., QIAN, T.-T., QI, L.-W., WANG, X.-R. & ZENG, Q.-Y. 2014. Subcellular relocalization and positive selection play key roles in the retention of duplicate genes of *Populus* class III peroxidase family. *The Plant Cell,* 26**,** 2404-2419.

SAPPL, P. G., OÑATE-SÁNCHEZ, L., SINGH, K. B. & MILLAR, A. H. 2004. Proteomic analysis of glutathione S-transferases of *Arabidopsis thaliana* reveals differential salicylic acid-induced expression of the plant-specific phi and tau classes. *Plant molecular biology,* 54**,** 205-219.

SASAKI, K., IWAI, T., HIRAGA, S., KURODA, K., SEO, S., MITSUHARA, I., MIYASAKA, A., IWANO, M., ITO, H. & MATSUI, H. 2004. Ten rice peroxidases redundantly respond to multiple stresses including infection with rice blast fungus. *Plant and Cell Physiology,* 45**,** 1442-1452.

SCHNEIDER, C. A., RASBAND, W. S. & ELICEIRI, K. W. 2012. NIH Image to ImageJ: 25 years of image analysis. *Nature methods,* 9**,** 671.

SCHWEIGER, W., PASQUET, J. C., NUSSBAUMER, T., KOVALSKI, M. P., WIESENBERGER, G., MACADRÉ, C., AMETZ, T., BERTHILLER, F., LEMMENS, M., SAINDRENAN, P., MEWES, H. W., MAYER, K. F. X., DUFRESNE, M. & ADAM, G. 2013. Functional characterization of two clusters of *Brachypodium distachyon* UDP-glycosyltransferases encoding putative deoxynivalenol detoxification genes. *Mol Plant Microbe Interact,* 26.

SOLANO, R. & GIMENEZ-IBANEZ, S. 2013. Nuclear jasmonate and salicylate signaling and crosstalk in defense against pathogens. *Frontiers in Plant Science,* 4**,** 72.

SUNDARAVELPANDIAN, K., CHANDRIKA, N. N. P. & SCHMIDT, W. 2013. PFT1, a transcriptional Mediator complex subunit, controls root hair differentiation through reactive oxygen species (ROS) distribution in *Arabidopsis*. *New Phytologist,* 197**,** 151-161.

THALER, J. S., OWEN, B. & HIGGINS, V. J. 2004. The role of the jasmonate response in plant susceptibility to diverse pathogens with a range of lifestyles. *Plant Physiology,* 135**,** 530-538.

THOLE, V., WORLAND, B., WRIGHT, J., BEVAN, M. W. & VAIN, P. 2010. Distribution and characterization of more than 1000 T‐DNA tags in the genome of *Brachypodium distachyon* community standard line Bd21. *Plant biotechnology journal,* 8**,** 734-747.

UKNESS, S. 1993. Biological induction of systemic acquired resistance in *Arabidopsis*. *Mol. Plant-Microbe Interact.,* 6**,** 692-698.

VAIN, P., WORLAND, B., THOLE, V., MCKENZIE, N., ALVES, S. C., OPANOWICZ, M., FISH, L. J., BEVAN, M. W. & SNAPE, J. W. 2008. *Agrobacterium* ‐ mediated transformation of the temperate grass *Brachypodium distachyon* (genotype Bd21) for T ‐ DNA insertional mutagenesis. *Plant biotechnology journal,* 6**,** 236-245.

VAN WEES, S. C. & GLAZEBROOK, J. 2003. Loss of non ‐ host resistance of *Arabidopsis NahG* to *Pseudomonas syringae* pv. *phaseolicola* is due to degradation products of salicylic acid. *The Plant Journal,* 33**,** 733-742.

VOGEL, J. P., GARVIN, D. F., LEONG, O. M. & HAYDEN, D. M. 2006. *Agrobacterium*-mediated transformation and inbred line development in the model grass *Brachypodium distachyon*. *Plant Cell, Tissue and Organ Culture,* 84**,** 199-211.

WERCK-REICHHART, D. 1995. Cytochromes P450 in phenylpropanoid metabolism. *Drug metabolism and drug interactions,* 12**,** 221-244.

WICKHAM, H. 2011. ggplot2. *Wiley Interdisciplinary Reviews: Computational Statistics,* 3**,** 180-185.

XIE, D.-X., FEYS, B. F., JAMES, S., NIETO-ROSTRO, M. & TURNER, J. G. 1998. *COI1*: an *Arabidopsis* gene required for jasmonate-regulated defense and fertility. *Science,* 280**,** 1091-1094.

YANG, X., MA, J., LI, H., MA, H., YAO, J. & LIU, C. 2010. Different genes can be responsible for crown rot resistance at different developmental stages of wheat and barley. *European journal of plant pathology,* 128**,** 495-502.

YANG, Y., QI, M. & MEI, C. 2004. Endogenous salicylic acid protects rice plants from oxidative damage caused by aging as well as biotic and abiotic stress. *The Plant Journal,* 40**,** 909-919.

YOU, I. S., GHOSAL, D. & GUNSALUS, I. C. 1991. Nucleotide sequence analysis of the *Pseudomonas putida* PpG7 salicylate hydroxylase gene (*nahG*) and its 3'-flanking region. *Biochemistry,* 30**,** 1635-1641.

ZHANG, Y., FAN, W., KINKEMA, M., LI, X. & DONG, X. 1999. Interaction of NPR1 with basic leucine zipper protein transcription factors that bind sequences required for salicylic acid induction of the *PR-1* gene. *Proceedings of the National Academy of Sciences,* 96**,** 6523-6528.

ZHOU, J.-M., TRIFA, Y., SILVA, H., PONTIER, D., LAM, E., SHAH, J. & KLESSIG, D. F. 2000. NPR1 differentially interacts with members of the TGA/OBF family of transcription factors that bind an element of the *PR-1* gene required for induction by salicylic acid. *Molecular Plant-Microbe Interactions,* 13**,** 191-202.

ZHU, T., XIN, F., WEI, S., LIU, Y., HAN, Y., XIE, J., DING, Q. & MA, L. 2019. Genome-wide identification, phylogeny and expression profiling of class III peroxidases gene family in *Brachypodium distachyon*. *Gene*.

Chapter 4:

A putative cytochrome P450 gene attenuates virulence in *Fusarium pseudograminearum*

4.1 Abstract

Fusarium pseudograminearum (*Fp)* is the predominant causative pathogen of Fusarium Crown Rot (FCR) in wheat, costing the Australian industry over $80 million dollars annually. The phytohormone salicylic acid (SA) has been demonstrated to mediate and promote resistance towards *Fusarium* in wheat and the model grass *Brachypodium distachyon*. Potential SA-regulated genes in the pathogen have been identified based on differential gene expression in wild type versus a SA-deficient transgenic line *Brachypodium* during infection by *Fp*. Among 210 differentially expressed genes DEGs in *Fp* during infection of a SA-deficient *Brachypodium*, and the negatively regulated gene (log_2 -2.67 FC) *FPSE_08867* was selected as a candidate for further characterisation. Through phylogenetic and syntenic analysis, *FPSE_08867* and its closely linked genes, *FPSE_08866*, *FPSE_08868, FPSE_08869* and *FPSE_08870,* were found to be part of partially conserved gene cluster in *F. venenatum*, *F. sporotrichoides*, *F. coffeeatum*, *Leptosphaeria maculans* and *Lepidopterella palustris* but not in *Fusarium graminearum* (*Fg).* Thus, the gene cluster has been maintained in the *Fp* genome but not in the closely related *Fg* genome. *FPSE_08867* was initially annotated as encoding a CYTOCHROME P450 (CYP) enzyme with benzoate parahydroxylase (*bph*) activity. *Bphs* have been reported to be involved in benzoic acid (BA) metabolism and are targets of anti-fungal compounds. However, additional phylogenetic analysis showed that FPSE_08867 did not cluster with known *bph* fungal enzymes but rather it clustered with CYPs involved with biosynthesis of the mycotoxin trichothecene. Furthermore, three independent knockout lines of *FPSE_08867* (∆*fpse_08867*) did not exhibit altered sensitivity towards BA or SA. Unexpectedly, the ∆*fpse_08867* lines demonstrated similar or significantly enhanced virulence in *Brachypodium* and wheat FCR seedling assays and appeared to lack production of the mycotoxin polyketide aurofusarin. Given the genes required for aurofusarin biosynthesis are known and polyketides are reported to affect production of each other through a feedback loop, it is likely that FPSE_08867 is involved in biosynthesis of a mycotoxin polyketide rather than BA or SA metabolism. Additional research is required to dissect the role(s) of FPSE_08867 in modulating *Fp-Brachypodium*/wheat interactions.

4.2 Introduction

4.2.1 Economic impact of *Fusarium* crown rot in wheat production

The filamentous fungi genus *Fusarium* contains numerous plant pathogenic species that are economically significant, including *Fusarium pseudograminearum* (*Fp*) and *Fusarium graminearum* (*Fg*) (Dean et al., 2012). Historically, *Fp* and *Fg* were once considered as the same species and were referred to as *Fg* group 1 and group 2, respectively (Francis and Burgess, 1977). But through mating experiments (Aoki and O'Donnell, 1999) and phylogenetic analysis (Aoki and O'Donnell, 1999), *Fg* group 1 and group 2 were reclassified as separate species (Summerell, 2019). Both *Fp* and *Fg* can cause Fusarium Crown Rot (FCR) and Fusarium Head Blight (FHB) (Burgess et al., 1975, Akinsanmi et al., 2004) but in Australia, *Fp* is more frequently recovered from infected wheat crowns, whereas *Fg* is more frequently recovered from infected wheat heads (Akinsanmi et al., 2004, Backhouse et al., 2004, Backhouse and Burgess, 2002, Burgess et al., 1975, Khangura et al., 2013, McKnight and Hart, 1966). Hence, *Fp* is the predominant cause of FCR in Australia and costs the wheat industry approximately AU$ 88 million dollars annually in yield losses and grain quality reduction (Murray and Brennan, 2009). Both *Fp* and *Fg* exhibit a hemi-biotrophic lifestyle, whereby nutrition is gained biotrophically from living plant cells during initial infection and subsequently by a necrotrophic existence during later infection (Luttrell, 1974, Bacon and Yates, 2006). Currently, no highly *Fusarium* resistant varieties of wheat are available and additional molecular characterisation of the *Fusarium*-wheat interaction is required to facilitate further breeding for resistance (Liu and Ogbonnaya, 2015).

4.2.2 Role of SA in defence against *Fusarium*

During pathogen infection, the host plant's defence responses are underpinned by phytohormone signalling, leading to transcriptional reprogramming and defence gene expression (Pieterse et al., 2012, Pieterse et al., 2009). Salicylic acid (SA) is considered to be the classic defence hormone mediating responses against biotrophic and hemi-biotrophic pathogens during their initial biotrophic phase (see review by Glazebrook (2005)). SA potentiates the hypersensitive response (HR) pathway,

whereby reactive oxygen species (ROS) production leads to cell death, denying the attacking pathogen living tissue as a source of nutrition (Greenberg et al., 1994, Lam et al., 2001, Chen et al., 1993). Additionally, SA responses lead to localised fortification of plant cell walls to contain the incurring pathogens (Halim et al., 2007), production of antimicrobials, and priming of defence gene expression in uninfected leaves in a phenomenon termed systemic acquired resistance (SAR) (Delaney et al., 1994, Gaffney et al., 1993). As expected, SA accumulation-deficient wheat and *Brachypodium* have been reported to exhibit enhanced susceptibility towards FCR caused by *Fp* and FHB caused by *Fg* (Makandar et al., 2012, Chapter 3). Interestingly, SA has also been demonstrated to have an inhibitory effect on axenic *Fg* growth, in absence of the plant host, under acidic pH conditions (Qi et al., 2012). Consequently, SA is not only important for defence signalling but may have an antifungal role as well.

4.2.3 Manipulation of phytohormone signalling by *Fusarium*

SA and other phytohormones such as jasmonic acid (JA), ethylene (ET), auxin (IAA), cytokinins (CKs), brassinosteroids (BRs) and abscisic acid (ABA), have been described to interact with each other in a complex manner to fine tune defence and development (Pieterse et al., 2012, Pieterse et al., 2009). Given the underpinning importance of phytohormones in defence, it is unsurprising that *Fusarium* and other microbes have evolved and/or acquired the ability to manipulate plant phytohormones (Han and Kahmann, 2019). Adaptive metabolic processes and ecological phenotypes (Thynne et al., 2019, Gluck‐Thaler et al., 2018), such as phytohormone manipulation, are often associated with secondary metabolite production by metabolic gene clusters (MGCs) in fungal pathogens (Keller, 2015). MGCs are comprised of co-ordinately expressed neighbouring genes, with some individual gene components playing supportive functions like regulation, transport and self-protection from the encoded metabolite if required (Kjærbølling et al., 2019). Evolution of secondary metabolism can occur from gene duplication or horizontal gene transfer events of gene modules or MGCs (reviewed by Wisecaver et al. (2014)). There is extensive evidence of horizontal gene transfer events affecting virulence in multiple *Fusarium* species (Ma et al., 2013) including *F. oxysporum* (*Fo*) (Czislowski et al., 2018, Laurence et al., 2015, van Dam and Rep, 2017, Vlaardingerbroek et al., 2016), *F. verticilliodes* (Khaldi and Wolfe, 2011), *Fg* (Sieber et al., 2014) and *Fp* (Gardiner et al., 2012).

JA is a classic defence hormone reported to mediate defence against necrotrophs and operate antagonistically towards SA signalling (Glazebrook, 2005). By secreting the SECRETED-IN-XYLEM 4 (SIX4) effector (Thatcher et al., 2012) and producing bioactive JA (Cole et al., 2014), *Fo* can induce JA-signalling in *Arabidopsis.* This leads to increased senescence-associated gene expression and disease susceptibility (Thatcher et al., 2009). Relatedly, *Fg* can degrade 1-aminocyclopropane carboxylic acid (ACC), a precursor for production of ET (Svoboda et al., 2019), through an encoded ACC-Deaminase (ACD). ET synergistically interacts with JA during defence signalling against necrotrophs (Li et al., 2019, Van der Ent and Pieterse, 2018, Broekaert et al., 2006). Svoboda et al. (2019) hypothesized that degradation of ACC may interfere with the JA/ET-mediated signalling during the necrotrophic phase of *Fg*'s lifecycle; however, no differences in virulence were observed in ACD knockouts.

Interestingly, *Fp* has recently been described to induce cytokinin signalling during initial infection (Blum et al., 2019, Sørensen et al., 2018) by production of cytokinin-like molecules, referred to as *Fusarium* cytokinins (FCKs) (Sørensen et al., 2018). Plant cytokinins are responsible for growth promotion, cell differentiation and senescence delaying in plants (Ferreira and Kieber, 2005). Remarkably, the FCK biosynthetic gene cluster is present in homologous clusters in *Fo*, *F. fujikuroi and F. verticilloides* but not in the closely related fungus *Fg* (Sørensen et al., 2018). Furthermore, despite evidence that the FCK cluster is upregulated during initial infection (Blum et al., 2019), no differences in virulence were reported in *FCK1*, *FCK2*, *FCK3*, and *FCK4* knockout strains (Sørensen et al., 2018).

As mentioned previously, under acidic conditions, in axenic culture SA has an inhibitory effect on *Fg* spore germination and mycelial growth (Qi et al., 2012); however, under basic conditions *Fg* is able to metabolise SA as a carbon source. Recent investigations have characterised several SA-responsive *Fg* enzymes involved in SA metabolism, including but not limited to a salicylate hydroxylase (FgShy1) (Hao et al., 2018), a catechol 1,2-dioxygenase (FGSG_03667) and a 2,3-dihydroxybenzoic acid decarboxylase (FGSG_09061) (Rocheleau et al., 2019). The contributions of FpSHY1 to SA degradation is unclear with reports of complete abolishment (Rocheleau et al., 2019) and partial impairment (Hao et al., 2018) of SA

degradation abilities in FpSHY1 knockout mutants. Analysis of independent knockout mutants of FGSG_03367 and FGSG_09061 revealed complete and partial impairment of SA degradation, respectively (Rocheleau et al., 2019). Both FgSHY1 and FGSG_03667 were identified as the first two enzymes for oxidative SA degradation via catechol leading into the β-ketoadipate pathway, while the activity of FGSG_09061 indicates the presence of a non-oxidative pathway for the conversion of SA to catechol (Rocheleau et al., 2019). The role of SA degradation on *Fusarium* pathogenesis is unknown as independent knockout lines of *FgSHY1* (Hao et al., 2018) and *FGSG_03367* (Rocheleau et al., 2019) did not alter virulence in wheat. Hence, additional components may remain to be identified and characterized in order to understand the role of SA degradation by *Fusarium*. Given the genetic relatedness of *Fg* to *Fp*, it is likely that *Fp* is also capable of degrading SA.

4.2.4 β-ketoadipate pathway in fungi

The β-ketoadipate pathway is present among many soil dwelling bacteria and fungi, particularly those associated with plants, and represents a convergent pathway for degradation of aromatic compounds from lignin and other plant components (Harwood and Parales, 1996). Despite its toxicity towards fungi, benzoic acid (BA) is a key intermediate in metabolism of aromatic compounds and is detoxified through the β-ketoadipate pathway in fungi (Lapadatescu et al., 2000, Harwood and Parales, 1996). Interestingly, it has been reported that fungi are also capable of metabolising phenylalanine, a precursor for SA production in plants, via BA (Lapadatescu et al., 2000). Currently, the only known pathway for detoxification of BA in fungi is the β-ketoadipate pathway, involving Cytochrome P450 (CYP)-mediated para-hydroxylation of BA to form 4-hydroxybenzoic acid (4HBA), which is subsequently metabolised to 3,4 dihydroxybenzoic acid, also known as protocatechuate (pca) (see review Wright (1993)). The 3-carboxy-cis,cis-muconate lactonising enzyme (CMLE) operates in the pca arm of the β-ketoadipate. Interestingly, inactivation of CMLE causes loss of pathogenicity in *F. oxysporum f.sp lycopersici* (Michielse et al., 2012). Growth of *cmle* knockout strains is inhibited *in planta* and *in vitro* in the presence of certain phenolic compounds including 4HBA, but mycelia growth on the surface of the root is not inhibited (Michielse et al., 2012). Michielse et al. (2012) hypothesized that CMLE is

required for the breakdown of phenolic compounds, liberated during plant cell wall degradation, that would be otherwise toxic to the organism.

CYPs are a large superfamily of enzymes encoded by genes present throughout all the kingdoms of life, but they are most numerous and diverse in fungi and plants (Nelson et al., 2008, Črešnar and Petrič, 2011). CYPs belonging to the CYP53 family are responsible for the detoxification of BA to 4HBA through benzoate para-hydroxylase (bph) activity, and were first identified in *Aspergillus niger* through characterisation of CYP53A1 (Faber et al., 2001). Consequently, CYP53 family members are key enzymes in the β-ketoadipate pathway (Wright, 1993). Inhibition of CYP53A1 in the fungal pathogen *Cochliobolus lunatus* by plant defensive compounds such as eugenol, isoeugenol, thymol and vanillin, resulted in increased BA toxicity (Podobnik et al., 2008). Hence, CYP53 family members have been proposed as targets for antifungal molecules (Podobnik et al., 2008, Berne et al., 2015, Korošec et al., 2014).

Interestingly, the outcome of CYP-mediated reactions can be influenced by the redox partner co-factors, known as cytochrome P450 reductases (CPRs) (Laursen et al., 2011, Lah et al., 2011). In *F. fujikuroi,* CPR deletion results in modified CYP selectivity, reaction rate and alternate product formation by CYPs involved in gibberellin biosynthesis (Malonek et al., 2004, Troncoso et al., 2008) .

To investigate how *Fp* adapts to infecting a SA-deficient host, we used an existing RNAseq dataset of *Fp* infecting WT and *nahG* expressing *Brachypodium distachyon* (Powell et al., unpub.). A set of differentially expressed genes (DEGs) were identified and a single gene, *FPSE_08867*, that was putatively annotated as encoding a CYP was selected for further characterisation. *FPSE_08867* was significantly down regulated (-2.62 Log_2 fold change) in *Fp* during infection of SA-deficient *nahG Brachypodium* (Powell et al., unpub.). The putative annotation of *FPSE_08867* indicates that the encoded CYP may possess *bph* activity and operate in the β-ketoadipate pathway. Given the role of *bph* enzymes in metabolism of BA to 4HBA (Črešnar and Petrič, 2011), the involvement of the β-ketoadipate pathway in metabolism of SA in *Fg* (Rocheleau et al., 2019) and the corresponding reduction in *FPSE_08867* expression when infecting SA-deficient *Brachypodium* (Powell et al.,

unpub), we hypothesised that FPSE_08867 may be involved in pathogenicity. To investigate the role of FPSE_08867*,* we conducted phylogenetic analyses, created knockout Δ*fpse_08867 Fp* strains and tested their virulence and sensitivities *in vitro* towards exogenously applied SA or BA.

4.3 Results

4.3.1 *Fp* may utilize a set of genes in response to SA and related defence responses in a *Brachypodium* host

To gain an insight into how *Fp* adapts to SA and its associated defence responses in a host, a differential expression analysis was conducted on an existing RNAseq dataset of *Fp*-infected WT and *nahG* expressing *Brachypodium* (Powell et al., unpub.) A set of 210 significantly differentially expressed *Fp* genes (DEGs) were identified (Supplementary table 4.1) including *FPSE_08867*, which was significantly repressed in *Fp*-infected *nahG Brachypodium*. Earlier, *FPSE_08867* had been annotated as encoding a CYTOCHROME P450 (CYP) with benzoate 4-monoxygenase enzymatic activities through an automated annotation software pipeline using Blast2GO (Conesa et al., 2005). Given a potential role in benzoic acid metabolism, through annotation as a CYP benzoate 4-monoxygenase, the current research focussed on the characterisation of *FPSE_08867*.

4.3.2 *FPSE_08867* is a part of a partially conserved gene cluster present in a variety fungal species

The observation that *FPSE_08868* and *FPSE_08867,* which are neighbouring genes, were similarly downregulated in *Fp* when infecting *nahG Brachypodium*, suggested that *FPSE_08867* and *FPSE_08868* may be part of a metabolic gene cluster (Supplementary table 4.1). To further investigate the existence of a putative gene cluster, syntenic grouping and phylogenetic analysis was conducted. It was found that *FPSE_08867*, along with five other genes, exists as part of a putative gene cluster (Figure 4.1). The putative gene cluster is comprised of genes annotated as encoding a *Beta elim lyase* (*FPSE_08866*), a *Benzoate 4-monoxygenase* (*FPSE_08867*), a *CPSase-L-D2* (*FPSE_08868*) and two *Major Facilitator Superfamily* (MFS) *transporters* (*FPSE_08869*, *FPSE_08870*). Based on phylogenetic analysis of the individual genes comprising the putative cluster (Figures 4.2 to 4.6) and syntenic analysis (Figure 4.1), the gene cluster is partially conserved across a variety of fungal

species but is absent in closely related species *Fg*, indicating that it has not been maintained.

4.3.3 Confirmation of *FPSE_08867* knockout in recovered *Δfpse_08867* isolates

To investigate the function of *FPSE_08667,* knockout mutants were created through T-DNA insertional mutagenesis using a transformation process described by Gardiner et al. (2012). Putative transformants were screened for nourseothricin resistance, indicating either homologous recombination and insertion of the resistance gene into *FPSE_08667* or ectopic integration of the T-DNA elsewhere in the genome. Subsequently genotyping by PCR confirmed the disruption of the *FPSE_08667* by homologous recombination in three out of four independent *Fp* isolates. In the PCR assay, the intact *FPSE_08867* product appears as a 396bp product, whereas the ∆*fpse_08867* knockout allele carrying the nourseothricin resistance gene insertion fails to amplify this product. The PCR assay also detected a larger 658bp product corresponding to nourseothricin resistance gene. As expected, no nourseothricin resistance gene product was observed in the wild type (WT) *Fp* CS3096 isolate. The presence of the nourseothricin resistance gene product and absence of the *FPSE_08867* product in mutant isolates 1, 4 and 8 (M1, M4, M8) indicate they are confirmed ∆*fpse_08867* knockout isolates. The presence of both nourseothricin resistance gene and *FPSE_08867* products in mutant isolate 9 (M9) indicate that it represents an ectopic integration of the T-DNA elsewhere in the *Fp* genome (Figure 4.7).

4.3.4 *Δfpse_08867* isolates exhibit apparent lack of aurofusarin production

Surprisingly, when grown on potato dextrose agar (PDA) and compared to the WT, the three independent ∆*fpse_08867* isolates appeared to lack aurofusarin, a mycotoxin that is red/purple in colour under alkaline conditions (Figure 4.8).

4.3.5 *Δfpse_08867* isolates show increased or similar virulence compared to WT *Fp* when infecting *Brachypodium* and wheat seedlings

To investigate the effects of ∆*fpse_08867* knockout on pathogenicity when infecting *Brachypodium* and wheat seedlings, a series of soilless infection assays, using WT and ∆*fpse_08867* (M1, M4, M8) isolates were conducted. Surprisingly, at 12 days post inoculation (dpi), M1 and M4 infected WT *Brachypodium* had a higher mean disease score (*Wilcoxon rank test, P*<0.001) relative to WT *Fp* infected WT *Brachypodium* (Figure 4.9A,B). WT *Brachypodium* plants infected with either ∆*fpse_08867* M1 or M4 isolates exhibited a significant reduction in mean leaf number (*Wilcoxon rank test, P*<0.01) relative to WT *Brachypodium* infected by WT *Fp* (Figure 4.9C). The ∆*fpse_08867* M8 isolate did not differ significantly in leaf number or disease score relative to WT *Fp* infected WT *Brachypodium* (Figure 4.9A-C). Interestingly, the *nahG* 2 (N2) *Brachypodium* exhibited significantly increased mean disease score relative to WT *Fp* infected WT *Brachypodium*, when infected by either WT *Fp* or the ∆*fpse_08867* M1 isolate (*Wilcoxon rank test, P*<0.001). Additionally, the ∆*fpse_08867* M1 infected N2 *Brachypodium* exhibited significantly reduced mean leaf number (*Wilcoxon rank test, P*<0.001) when compared to WT *Fp* infected WT *Brachypodium*. Overall, the *Fp*∆*fpse08867* isolates showed significantly enhanced virulence in WT *Brachypodium* and further enhancement in the *nahG* genetic background compared to the WT *Fp* isolate.

At 14 dpi, the pathogenicity of ∆*fpse_08867* isolates M4 and M8 on wheat seedlings was significantly increased (*Tukey's HSD test*, *P*<0.001) relative to the WT *Fp,* as demonstrated by increased lesion length after controlling for differences in plant heights (*ANCOVA*, *P*<0.001) (Figure 4.10). No significant difference between lesion length of ∆*fpse_08867* M1 and WT *Fp* infected plants was observed, although the M1 isolate was trending towards an increased lesion length.

The *Brachypodium* and wheat seedling soilless infection assays were repeated twice, with both experiments yielding similar results. Possible reasons behind why different ∆*fpse_08867* isolates behaved differently on wheat and *Brachypodium* is unclear but may include variability encountered during the disease assays. Based on the behaviour of the majority of ∆*fpse_08867* lines, it was concluded that ∆*fpse_08867*

isolates possesses enhanced virulence compared to WT *Fp* when infecting *Brachypodium* and wheat infecting seedlings.

4.3.6 Δ*fpse_08867* isolates do not show altered sensitivity towards benzoic and salicylic acid in liquid culture relative to the WT *Fp* CS3096 isolate.

Previous work identified *FPSE_08867* as being significantly down-regulated in *Fp* when infecting a SA-deficient *Brachypodium* host (Powell et al., unpub.). *FPSE_08867* was previously annotated as encoding a putative benzoate 4-monoxygenase (reference). Based on this initial annotation, it was hypothesised that FPSE_08867 may play a role in interfering with the host plant's production of SA by converting toxic benzoic acid (BA) to 4-Hydroxybenzoic acid (4HBA).

To check the validity of the initial annotation of FPSE_08867, a phylogenetic analysis using a collection of characterised fungal cytochrome proteins, as reviewed by Črešnar and Petrič (2011), was conducted to determine if *FPSE_08677* and its homologs clustered with members of the CYP53 subfamily, reported to possess benzoate 4-monoxygenase abilities (Faber et al., 2001, Fraser et al., 2002, Podobnik et al., 2008, Matsuzaki and Wariishi, 2005) (Figure 4.11). Interestingly, FPSE_08677 and its homologs clustered with members of the CYP58 and CYP526 subfamilies, which are involved in mediating biosynthesis of the secondary metabolites trichothecenes (Kimura et al., 2007) and fumonisin (Butchko et al., 2006, Proctor et al., 2006); however the branch support value between the CYP53 members and the FPSE_08867 and homologs is low. Consequently, additional phylogenetic evidence is required to determine the validity of the initial automated annotation of *FPSE_08867*, as the initial annotation of this gene encoding a benzoate 4-monoxygenase may have been incorrect.

To further test the hypothetical role of *FPSE_08667* for conferring tolerance to either BA or SA, a series of inhibition assays were conducted using the WT and *fpse_08867* knockouts lines (Figure 12). Mycelial growth of the WT isolate, *Fp CS3096*, was inhibited by the presence of SA or BA in a liquid medium at concentrations greater than 0.04mM (Figure 4.12 A, D). The inhibitory concentration of BA and SA that reduced WT mycelia growth by 50% (IC50) was calculated to be 0.58 mM and 1.56

mM, respectively (Figure 4.12 B, E). The Δ*fpse_08867* isolates did not show altered sensitivity towards BA and SA in liquid culture relative to the WT isolate at the calculated IC50 concentrations (Figure 4.12 C, F). Further, the mycelia growth rate between the WT and Δ*fpse_08867* isolates were not significantly different. This experiment was repeated three times with similar results.

4.4 Discussion

Salicylic Acid (SA) is a key phytohormone that has been demonstrated to promote resistance towards *Fusarium* in *Arabidopsis thaliana* (Edgar et al., 2006), *Brachypodium distachyon* (Powell et al. unpub.) and wheat (Makandar et al., 2012). Further, it has been reported that *Fusarium* can manipulate and/or degrade plant phytohormones including SA. However, the role of SA degradation in *Fusarium graminearum* (*Fg*) during infection of wheat is unclear, with no detectable differences in virulence between WT and mutant knockouts. Consequently, it has been suggested that there are additional components remaining to be identified with roles in SA metabolism (Rocheleau et al., 2019). Due to the genetic relatedness of *Fusarium pseudograminearum* (*Fp*) and *Fg,* it is likely that *Fp* could also degrade SA. The aim of the current research was to characterise the candidate gene *FPSE_08867* in *Fp*, for a putative role in SA metabolism and pathogenicity.

FPSE_08867 is one of 210 genes (Supplementary table 4.1) that were differentially expressed by *Fp* when infecting SA-deficient *nahG Brachypodium* compared to WT. *FPSE_08867* was negatively regulated (log_2 fold change -2.67) by *Fp* when infecting SA-deficient *Brachypodium.* Earlier, *FPSE_08867* had been automatically annotated as encoding a benzoate 4-monoxygenase, otherwise known as benzoate parahydroxylase (*bph*). *bph* enzymes have roles in detoxification of aromatic compounds yielded from lignin and other plant components via the β-ketoadipate pathway (Lapadatescu et al., 2000, Harwood and Parales, 1996). *bph* enzymes convert benzoic acid, a precursor of SA, to 4-hydroxybenzoate (Faber et al., 2001). Previously, it was demonstrated that *nahG* expressing *Brachypodium* exhibited compromised basal defence, with abnormal regulation of lignin deposition, and a muted transcriptional response to *Fp* infection, resulting in an ablated accumulation of defence related protein transcripts (Powell et al., unpub.). Consequently, *nahG Brachypodium* may constitute a less stressful host environment for *Fp*, allowing differential expression of genes with roles in pathogenicity. Hence it was initially hypothesised that FPSE_08867 may play a role in stress tolerance associated with SA-mediated host defences, potentially explaining why it was negatively regulated by *Fp* when infecting *nahG Brachypodium*.

FPSE_08868, a neighbouring gene of *FPSE_08867*, exhibited a corresponding reduction in gene expression (log_2 fold change -3.04) similar to *FPSE_08867* in *Fp* infecting nahG *Brachypodium* (Supplemental table 4.1). Corresponding genetic regulation of neighbouring genes indicate that *FPSE_08867* may comprise part of a gene cluster. Upon phylogenetic and syntenic analyses it was found that *FPSE_08867* and neighbouring genes *FPSE_08866*, *FPSE_08868*, *FPSE_08869* and *FPSE_08870* were part of a gene cluster that is partially conserved in syntenic order with homologs present in members of the *Fusarium* genus and other soil dwelling plant associated fungus (Figures 4.1 to 4.7). *FPSE_08866*, *FPSE_08867, FPSE_08868* and *FPSE_08869* are putatively annotated as encoding a histidine decarboxylase, benzoate-4-monoxygenase, carbamoyl-phosphate synthase ATP binding domain and major facilitator superfamily (MFS) monocarboxylate transporter, respectively. *FPSE_08870* is a pseudogene containing an internal stop codon that has been putatively annotated as encoding a non-functional MFS monocarboxylate transporter. Interestingly, *Fusarium venenatum* (*Fv)* has a functional homolog of *FPSE_08870*. Metabolic gene clusters (MGCs) often contain genes that are co-regulated with enzymatic and support functions such as transport (Keller, 2015). The apparent corresponding regulation of *FPSE_08868* and *FPSE_08867,* and synteny associated with the cluster in related *Fusarium* species provide evidence that *FPSE_08866*, *FPSE_08868*, *FPSE_08867, FPSE_08869* and *FPSE_08870* may exist as part of a putative MGC. MGCs have been associated with phytohormone manipulation (Sørensen et al., 2018) and mycotoxin production (Malz et al., 2005) in *Fusarium*. Intriguingly, the putative MGC is entirely absent from *Fusarium graminearum* (*Fg*) despite being closely related to *Fp* and is present in unrelated fungi *Leptosphaeria maculans* and *Lepidopterella palustris.* Further, the flanking genes of the putative MGC in *Fv*, *Fs*, *Fc* and *Fp* differ. Taken together, this provides evidence that the putative MGC was acquired after speciation via horizontal gene transfer. Alternatively, the gene cluster was deleted during the evolution of *Fg*. To understand the role of the putative MGC epistatic analysis should be conducted and the resulting phenotypes of the mutants compared to the Δ*fpse_08867* isolate.

Fungal CYPs are a family of enzymes that have been assigned to subfamilies based on the chemical reactions they mediate (Črešnar and Petrič, 2011). The CYP53 subfamily members possess *bph* activity (Faber et al., 2001). Interestingly, functional phylogenetic analysis revealed that FPSE_08867 did not cluster with known CYP53 subfamily members but rather clustered with members of the CYP58 and CYP526 subfamilies (Figure 4.11). Despite low branch support value, this provides evidence against FPSE_08867 as a *bph*. Further, upon testing of BA and SA sensitivities through exogenous application, no differences in mycelia growth inhibition were observed between Δ*fpse_08867* lines and the WT (Figure 4.12). One explanation for this result is that FPSE_08867 does not contribute towards BA and SA metabolism. To test this explanation, it is necessary to conduct a SA and BA degradation assay with subsequent high-performance liquid chromatography (HPLC) analysis as described by Rocheleau et al. (2019). Briefly, in such an assay, a known quantity of mutant- and WT-mycelia is incubated separately in liquid medium containing a known concentration of chemical for a set period time. Afterwards, the media is analysed by HPLC to quantify chemical concentration change as a result of fungal metabolism.

Genetic studies of independent mutant lines (Rocheleau et al., 2019, Hao et al., 2018) have revealed the existence of enzymes positioned in both the catechol and pca arms of the β-ketoadipate pathway. Whilst disruption of *FGSG_03667* reportedly abolishes SA metabolism via the catechol arm (Rocheleau et al., 2019), disruption of *FpSHY1* (Hao et al., 2018) and *FGSC_09061* (Rocheleau et al., 2019) only impairs SA metabolism. Consequently, both Hao et al. (2018) and Rocheleau et al. (2019) conclude that additional SA metabolism components and pathways are likely to exist. Given the relatedness of *Fg* to *Fp*, it is likely that *Fp* has metabolic pathways in common (Gardiner et al., 2018). To test whether genetic/metabolic redundancy can explain the lack of chemical sensitivity phenotype in the Δ*fpse_08867* mutant strains, epistatic analysis is required. This can be achieved by identifying *Fp* homologues of genes involved in SA metabolism in related *Fusarium* species as candidates, creating respective single and multiple knockout lines in *Fp* and characterising them for their contributions towards SA metabolism.

Unexpectedly, knocking out *FPSE_08867* resulted in mutant isolates exhibiting altered pigment production when grown on potato dextrose agar (PDA). The Δ*fpse_08867* isolates appeared to lack red pigmentation when compared to the WT (Figure 4.8). The polyketide mycotoxin, aurofusarin is a pigment produced by *Fp* and related species that appears red/purple under alkaline conditions and yellow/orange under acidic conditions (Ashley et al., 1937, Medentsev and Akimenko, 1998). To determine whether aurofusarin biosynthesis is indeed disrupted, a HPLC experiment should be conducted, as described by Malz et al. (2005) to quantify aurofusarin concentrations in both WT and Δ*fpse_08867* isolates. Interestingly, disruption of aurofusarin production does not impact virulence (Malz et al., 2005); whereas *FPSE_08867* disruption resulted in increased virulence (Figures 4.9, 4.10). Mutants with decreased levels of aurofusarin are also associated with increased growth rate, conidia spore and mycotoxin zearalenone production (Malz et al., 2005). Unlike aurofusarin non-producing mutants, *fpse_08867* knockouts do not exhibit altered growth rates under basal conditions (Figure 4.12). Additional experiments are required to determine if spore structure and production have been affected by disruption of *FPSE_08867*. Notably, disruption of polyketide synthases (*pks*) involved in aurofusarin synthesis (Malz et al., 2005) results in differential expression of other *pks* involved in biosynthesis of other polyketide products such as zearalenone (Lysøe et al., 2006). Absence of both aurofusarin and zearalenone affected *pks* expression demonstrating that polyketide presence and absence can alter polyketides production in a feedback loop (Lysøe et al., 2006). Relevantly, in the maize fungal pathogen *Cochliobolus heterostrophus*, a *pks* was found to be required for trichothecene polyketide T-2 toxin production and virulence (Yang et al., 1996). Interestingly, *FPSE_12214,* described as *isoamyl alcohol* (Supplemental table 4.1) was significantly upregulated in *Fp* (1.32 $\log_2$ fold change). In *Fg*, an isoamyl alcohol oxidase is involved in biosynthesis of zearalenone (Kim et al., 2005). Consequently, this may indicate that zearaleone production is upregulated in *Fp* while the metabolic pathway involving FPSE_08867 is downregulated. Taken together, the evidence above suggests that FPSE_08867 may play a role in polyketide mycotoxin biosynthesis. To investigate *FPSE_08867* for a putative role in mycotoxin biosynthesis, the following experiments are recommended. Concentrations of zearalenone, T-2 toxin and other mycotoxins should be quantified in Δ*fpse_08867* under basal growth and infection conditions and compared to WT using HPLC as described by Malz et al. (2005). Further, qRT-PCR should be

conducted to measure *Fp PKS* (Brown and Proctor, 2016), gene expression to determine regulatory impacts of *FPSE_08867* knockout and identify associated metabolic processes with FPSE_08867. Additionally, investigations of *FPSE_08867* gene expression and *Δfpse_08867* KO mutant lines at later time points during the necrotrophic phase of infection in different bioassays could further elucidate the role of *FPSE_08867* in infection.

To conclude, the current study identified a candidate gene, *FPSE_08867*, and initially hypothesised a potential role in *Fp* stress tolerance related to SA-related host defences during infection. *FPSE_08867* was significantly downregulated in *Fp* infecting SA-deficient *Brachypodium* compared to WT. Phylogenetic and syntenic analysis revealed that *FPSE_08867* is part of a gene cluster. The gene cluster is partially conserved in select fungal and *Fusarium* species but is conspicuously absent in closely related *Fg*. *FPSE_08867* was annotated as encoding a CYP with *bph* activity; however, functional phylogenetic analysis revealed that FPSE_08867 did not cluster with other known *bph* but rather with CYPs involved in mycotoxin production. Further ∆*fpse_08867* knockout isolates did not exhibit altered sensitivities towards BA and SA. Hence, there is strong evidence against the initial hypothesis for a putative role of FPSE_08867 in BA and SA metabolism. The ∆*fpse_08867* isolates appeared to lack the red pigment aurofusarin when grown in PDA and exhibited significantly increased or similar virulence on *Brachypodium* and wheat seedlings. It has been reported that polyketide mycotoxins can impact on the expression of PKS involve in the biosynthesis of other polyketides (Lysøe et al., 2006). Given that FPSE_08867 clustered with CYPs known to be involved in mycotoxin biosynthesis, and that aurofusarin production appears to be disrupted, it is likely that FPSE_08867 may play a role in polyketide mycotoxin biosynthesis.

4.5 Materials and methods

4.5.1 Phylogenetic and syntenic analysis to identify *FPSE_08867* homologs genes and homologous gene clusters

Given that *FPSE_08868*, a neighbouring gene to *FPSE_08867*, showed similar down-regulation as *FPSE_08867* by *Fp* infecting *nahG* expressing *Brachypodium*, it was hypothesised that *FPSE_08867* and *FPSE_08868* are part of a putative gene cluster. To test this hypothesis, a phylogenetic and syntenic analysis was conducted. Protein FASTA files for *FPSE_08867* and neighbouring genes were retrieved from the NCBI Protein database. Using the NCBI Protein BLAST tool and protein FASTA files as bait, a list of homologous sequences from unique species were retrieved. The resulting list was used as input to generate a phylogram using the default "One click" settings for phylogeny.fr (Dereeper et al., 2008), as described by Gardiner et al. (2012). Briefly, using default parameters, multiple alignments were generated and subsequently curated, respectively by the MUSCLE (Edgar, 2004) and Gblocks (Talavera and Castresana, 2007) algorithms. Phylogeny was determined using PhyML (Guindon and Gascuel, 2003) with the WAG amino acid substitution matrix (Whelan and Goldman, 2001); while branch support values were calculate using the maximum likelihood-ratio test (Anisimova and Gascuel, 2006). Lastly, trees were rendered by TreeDyn and exported for publication (Chevenet et al., 2006). The flanking genes of the putative gene cluster was defined as *FPSE_04400* and *FPSE_07892* because synteny was no longer conserved across the fungal species but was re-established with *Fg*. The Genbank files was retrieved from NCBI Gene database for the regions containing the putative gene cluster were visualised and colour coded using the genoPlotR package (Guy et al., 2010) in the statistical computing language R (ver. 3.5.1) (RCoreTeam, 2018).

4.5.2 *Fusarium pseudograminearum* CS3096 transformation for Δ*fpse_08867* generation

Fusarium pseudograminearum isolate CS3096 from the CSIRO collection (Akinsanmi et al., 2004, Mitter et al., 2006) was used to generate ∆*fpse_08667*. CS3096

protoplasts were produced by germinating approximately 2-3×10^7 conidia/mL for 22h at 19˚C in TB3 media (0.3% Casamino acids, 0.3% yeast extract, 20% Sucrose w/v) shaking at 80 r.p.m. The germinated spores were collected with miracloth; washed with 1M sorbitol or KCl, before resuspension in 25mL of 1M sorbitol or KCl supplemented with 0.5mg driselase enzyme (Sigma-Aldrich, USA) and 0.2mg lysing enzyme (Sigma-Aldrich, USA). The enzyme-spore mixture was subsequently incubated at 58 r.p.m and 28˚C for a period of 45-55min to produce protoplasts. To remove undigested material the enzyme digest was filtered through 100µm nylon mesh; and the filtrate centrifuged at 1800×g and 4˚C for 10min to pellet the protoplasts. The pellet was resuspended in 10mL ice cold STC (20% sucrose, 50mM TrisHCl, pH 8, $CaCl_2$) before further centrifugation at 1800×g and 4˚C for 5min. This step was repeated twice as a method to wash the protoplasts, with the final pellet resuspended in 500µL STC. Protoplasts were concentrated to ~3-4×10^8 protoplasts / mL and checked for viability by incubating 1% protoplasts, 2% fluorescein diacetate (FDA) (v/v) in STC for 5min.

Transformation of the protoplasts was performed as described by Gardiner et al. (2012). The T-DNA (See Supplementary Figure 4.2), containing 1000bp of *FPSE_08867* sequence at the 5' end flanking an *Aspergillus nidulans* trpC promoter driving a nourseothricin acetyl transferase CDs as a selectable marker flanked at the 3' end by 992bp of *FPSE_08867* sequence to facilitate homologous recombination, was prepared and concentration checked on an electrophoresis gel by Benfield A. Briefly, 100µL of equal parts of concentrated DNA and 2M STC was mixed with 100µL of protoplasts, and then incubated on ice for 20min. Afterwards 1ml of 40% PEG solution (w/v) was added to the mixture and incubated on ice for 20min. Lastly, 5mL of TB3 was added and the mixture incubated overnight on a gentle rocker. Transformants were selected by imbedding 2mL of the "putative transformants" into 30mL of cooled TB3 agar and the mixture poured into a large petri dish. After an overnight incubation, 40ml of TB3 agar amended with the antibiotic nourseothricin at a final concentration of 50mg L^{-1} was poured over the initial TB3 agar layer. The plates were subsequently incubated in a light tight box at room temperature for a period of 1-3 weeks. During this incubation period, on a daily basis, the plates were inspected for any putative transformant colony that had grown through the selective media. These colonies were subsequently excised and subcultured onto ½ PDA (20g PDA L^{-1}) media amended with 50mg L^{-1} nourseothricin for genotyping.

4.5.3 *Δfpse_08667* genotyping assays

4.5.3.1 Extraction of *F. pseudograminearum* genomic DNA

DNA extraction solution (Sigma, St. Louis, MO) was used as per manufacturer's instruction to prepare DNA from mycelia tissue samples for PCR-based genotyping assays.

4.5.3.2 Polymerase Chain Reaction (PCR)

Each reaction contained 1µL of 10× PCR buffer (Thermo Fisher, Waltham, MA), 2.5mM $MgCl_2$ (Thermo Fisher, Waltham, MA) and 0.2µM dNTPs (Bioline, London, UK) , 0.12µM of each oligonucleotide primer, 1.5ng of DNA, and 1 unit of non-proofreading Taq DNA polymerase in a final reaction volume of 10µL. A heated lid ABI 2720 Thermal Cycler (Applied Biosystems; Thermo Fisher Scientific, MA, USA) was used.

4.5.3.3 PCR based assay for detection of T-DNA insert and endogenous *FPSE_08667*

To confirm ∆*fpse_08667* knockouts, the putative transformants were screened by PCR amplification for the presence of the transgene insert and absence of the endogenous gene. The primers used included two reverse primers one specific to the *FPSE_08867* and the other to the antibiotic resistance marker gene (Table 4.1). Both reverse primers pair with a common forward primer specific to *FPSE_08867*. If the T-DNA insert integrated at the correct location than the forward and reverse primers, specific to *FPSE_08867,* would fail to amplify a product. Whereas the *FPSE_08867* specific forward primer would amplify a product with the antibiotic resistance marker gene primer. If the T-DNA insert is integrated ectopically then both PCR products would be amplified. Thermal cycle conditions comprised of a 3min denaturation step at 94˚C; followed by 35 cycles of 94˚C for 30sec, 55˚C for 30sec, 72˚C for 90sec; and a final elongation step at 72˚C for 5min. The PCR products were run on a 1% Agarose:TAE gel at 100V for 30min and subsequently visualised under ultraviolet light using a transilluminator

4.5.4 Soilless laboratory-based paper towel infection assay for wheat

Sterile seedlings, 4 days post germination, of the *Fusarium* susceptible wheat variety "Mace" were used in the soilless laboratory-based infection assay. Seedlings were immersed in either inoculum (1×10^6 spores / mL) or sterile water, as a mock control, for a period of 5 min. Afterwards the treated seedlings were rolled in a single layer of paper towel, 10 seedlings per towel. The paper towels containing the seedlings were incubated on the benchtop under fluorescent lights (7.7µmol, m^2/s) set to a neutral day length (12h L: 12h D). At 14 days post inoculation the paper towels were unrolled and the length of the lesion and total plant height recorded. Statistical analysis was conducted using R (ver. 3.5.1) (RCoreTeam, 2018). To analyse the effect of the fungus isolate on lesion length after controlling for plant height an analysis of covariance (ANCOVA) was conducted. ANCOVAs, otherwise known as a generalised mixed model, use a covariant to reduce the unexplained variation associated with the response variable. Plant height has been demonstrated to affect resistance towards *Fusarium* infection. Hence, plant height was treated as a covariant to lesion length and fungus isolate. Initially the analysis involved checking the ANCOVA assumptions and transforming the data as required. The final linear model was visualised using a scatter plot and analysed with a summary table. Furthermore, a post-hoc Tukey HSD test was performed to identify which fungal isolates differed significantly from the WT isolate with respect to lesion length. The lesion length data grouped by fungal isolate was visualised using a column plot. All graphics were generated using the ggplot2 R package (Wickham, 2011).

4.5.5 Fusarium Head Blight infection assay

Sterilised seeds of the *Fusarium* susceptible wheat variety 'Kennedy' were sown, 4 pet 10cm pot, in UQ23 potting mix (University of Queensland, Australia). The plants were grown under a mix of HID and incandescent lamps (500µmol/m^2/s) set to long day conditions (15h L: 9h D) with a diurnal temperature of 24˚C and 15˚C, and relative humidity of 68% and 80%. At flowering, mid-anthesis, a single central floret per plant was either inoculated with 10µL of spore suspension (1×10^6 spores/ mL) or sterile water as a mock. The inoculated spikers were then covered with a moist plastic bag for a period of 3 days and then subsequently with a paper bag. At 14 days post inoculation (dpi), the bagged spikes were harvested and the number of infected florets

and rachi and total number of florets and rachi were recorded for each spike. The statistical analysis of the data was conducted using R (ver. 3.5.1). Because the data represents a proportion of infected to uninfected seed and rachis; and the total sample size is small (<1000), fisher's exact test of independence was applied using the *base{stats} fisher.test()* function.

4.5.6 Functional phylogenetic analysis of *FPSE_08867* and homologous genes with characterised fungal cytochrome P450s

FPSE_08867 is predicted to encode a cytochrome P450 (CYPs) enzyme with benzoate parahydroxylase (*bph*) activity. To gather evidence for *FPSE_08867* predicted *bph* activity, a phylogenetic analysis was conducted with *FPSE_08867* homologs and characterised fungal CYPs. Protein sequences for characterised CYPs as listed in Črešnar and Petrič (2011), *FPSE_08867* and homologs were retrieved from the NCBI protein database. The sequences were used as input to generate a phylogram using the default "One click" settings for phylogeny.fr (Dereeper et al., 2008), as described by Gardiner et al. (2012).

4.5.7 Growth rate inhibition assays for Δ*fpse_08867*

The effect of benzoic and salicylic acid (BA and SA, respectively) on Δ*fpse_08867* isolates and the WT (CS3096) isolate was tested using growth in liquid media. To determine the BA and SA inhibition concentrations that reduced growth by 50% (IC_{50}) a range of concentrations; 0.04mM, 0.09mM, 0.39mM, 0.78mM, 1.56mM, 3.13mM and 6.25mM, were compared to a mock solution.

4.5.7.1 Culture and preparation of Fusarium pseudograminerum mycelia

Plugs of *Fp* mycelia infested potato dextrose agar (PDA) (6g L^{-1}, BD Difco) were placed in 90mL petri dishes; containing 25ml $\frac{1}{2}$ PDB and incubated on the bench at room temperature (22˚C) to generate mycelia. After 7 days the agar plug was excised; the mycelia mat drained on sterile mira-cloth; and resuspended in 50mL of half strength PDB. Afterwards the mycelia mat was homogenized using a polytron stick

mixer at speed setting eight for one minute. The shredded mycelia OD_{600} was checked and diluted to an OD of ~0.3 using half strength PDB.

4.5.7.2 Chemical stock solution preparation

Chemical stock solutions were prepared by dissolving BA or SA in DMSO to a concentration of 5M. Subsequently a seven step, one-in-two serial dilution using DMSO was performed to make the remaining stock solutions. For each chemical stock solution, a master mix media was prepared using half strength Potato Dextrose Broth ($\frac{1}{2}$ PDB) (6g L^{-1}, BD Difco), amended with 25mM of Citrate Buffer System (CBS) buffered at a pH of 4.6 and 0.125% (v:v) of DMSO; with dissolved BA or SA varying concentrations; or without dissolved chemicals as a mock.

4.5.7.3 Assay preparation and conduction

The assay was performed in a 96-well plate (Thermo Fisher, Waltham, MA). 20µL of the adjusted shredded mycelia was loaded into a well with a single master-mix and diluted with $\frac{1}{2}$ PDB to a final volume of 200 µL and a final concentration of 12.5mM CBS and 0.06% DMSO. Eight wells were uses as technical replicates per treatment condition. Absorbance at 595nm was used as a measurement of mycelia growth. An initial absorbance reading was performed immediately after inoculation and a final plate reading at 2 days post inoculation. The webtool IC_{50} calculator from AAT Bioquest® < https://www.aatbio.com/tools/ic50-calculator > was used to fit a four-parameter logistic regression model to calculate the IC_{50} for WT of 0.58mM and 1.58mM for BA and SA respectively. The IC_{50} concentrations for WT *Fp*'s response to BA and SA were used to test if the *Fp*Δ*fpse08867* isolates had an altered sensitivity relative to the WT. The statistical analyses of the data was performed using R (ver.3.5.1) (RCoreTeam, 2018). The plots were generated using the R package ggplot2 (Wickham, 2011).

4.6 Figures

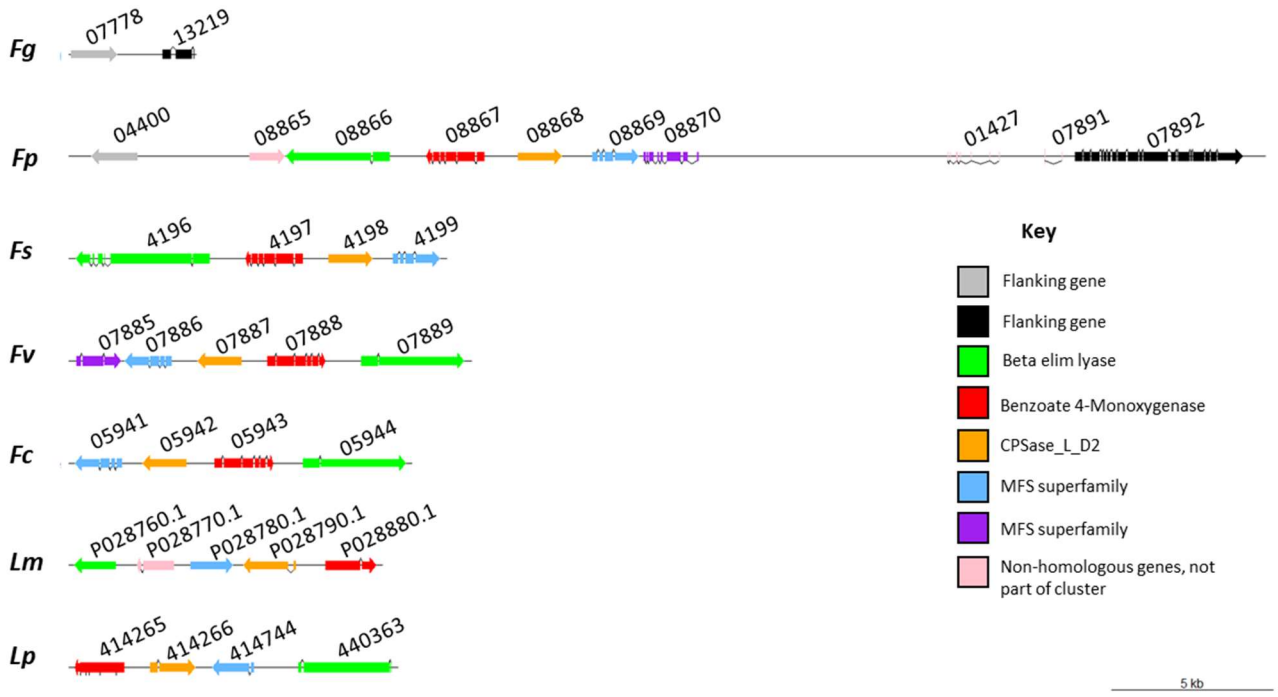

Figure 4.1: Genetic synteny map of the putative *FPSE_08667* gene cluster in *Fusarium pseudograminearum* (*Fp*) showing absence in closely related *F. graminearum* (*Fg*) and varying levels of conservation in other *Fusarium* species; *F. sporotrichoides* (*Fs*), *F. venenatum (Fv), F. coffeatum (Fc),* and in the hemi-biotrophic pathogen *Leptosphaeria maculans* (*Lm*) and the aquatic saprophytic fungus *Lepidopterella palustris* (*Lp*). Colours denote homologous genes based on phylogenetic analyses of protein sequences. Rectangles and angled lines represent exons and introns, respectively. Number labels refer to locus tags.

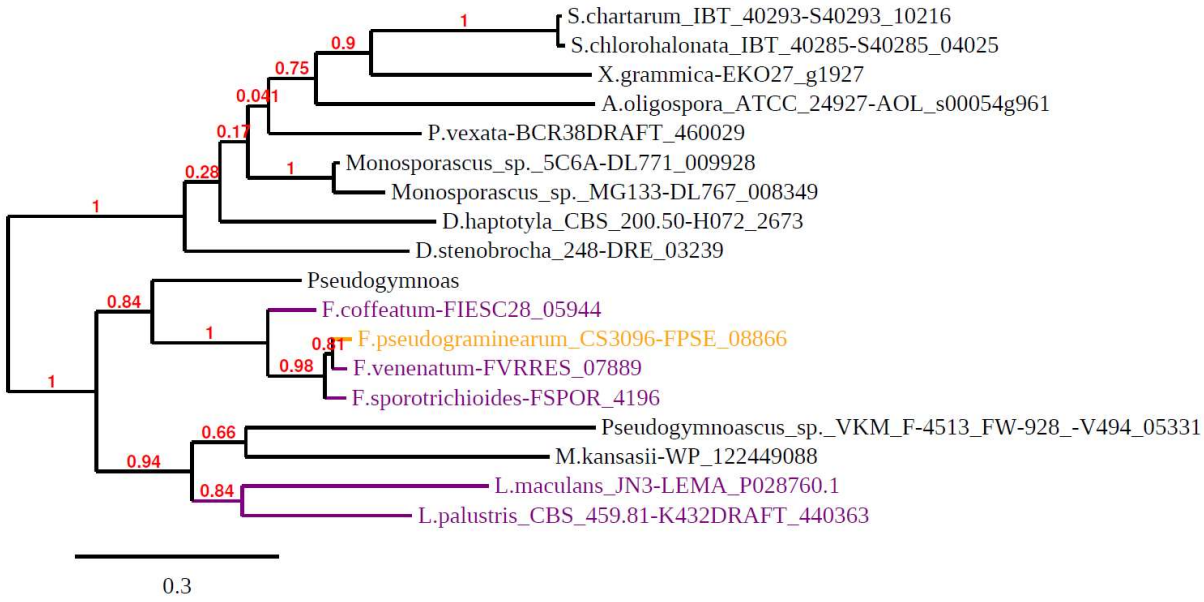

Figure 4.2: *Fusarium pseudograminearum* (*Fp*) protein FPSE_08866 has similar proteins present throughout a variety of fungal species but is absent in *Fusarium graminearum*. Phylogenetic analysis of returned protein sequences from unique species by a BLAST search with the *Fp* FPSE_08866 protein sequence as bait. Leaf names state; abbreviated species name_strain-locus_tag. Red numbers display branch support values. Orange label is FPSE_08866, part of the gene cluster in *Fp*. Purple labels show FPSE_08866 homologs that are members of the conserved gene cluster apparent in other fungi.

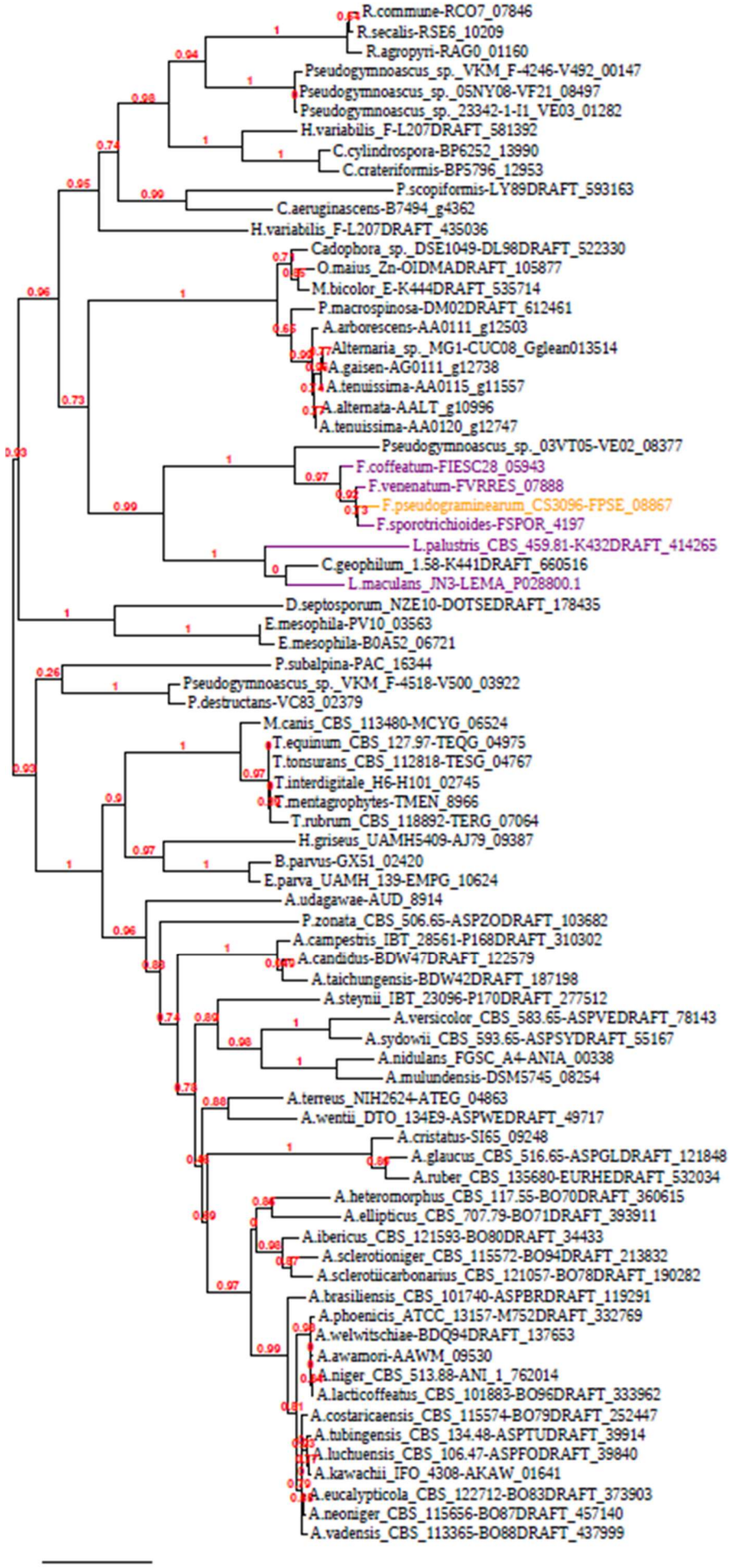
R.commune-RCO7_07846
R.secalis-RSE6_10209
R.agropyri-RAG0_01160
Pseudogymnoascus_sp._VKM_F-4246-V492_00147
Pseudogymnoascus_sp._05NY08-VF21_08497
Pseudogymnoascus_sp._23342-1-I1_VE03_01282
H.variabilis_F-L207DRAFT_581392
C.cylindrospora-BP6252_13990
C.crateriformis-BP5796_12953
P.scopiformis-LY89DRAFT_593163
C.aeruginascens-B7494_g4362
H.variabilis_F-L207DRAFT_435036
Cadophora_sp._DSE1049-DL98DRAFT_522330
O.maius_Zn-OIDMADRAFT_105877
M.bicolor_E-K444DRAFT_535714
P.macrospinosa-DM02DRAFT_612461
A.arborescens-AA0111_g12503
Alternaria_sp._MG1-CUC08_Gglean013514
A.gaisen-AG0111_g12738
A.tenuissima-AA0115_g11557
A.alternata-AALT_g10996
A.tenuissima-AA0120_g12747
Pseudogymnoascus_sp._03VT05-VE02_08377
F.coffeatum-FIESC28_05943
F.venenatum-FVRRES_07888
F.pseudograminearum_CS3096-FPSE_08867
F.sporotrichioides-FSPOR_4197
L.palustris_CBS_459.81-K432DRAFT_414265
C.geophilum_1.58-K441DRAFT_660516
L.maculans_JN3-LEMA_P028800.1
D.septosporum_NZE10-DOTSEDRAFT_178435
E.mesophila-PV10_03563
E.mesophila-B0A52_06721
P.subalpina-PAC_16344
Pseudogymnoascus_sp._VKM_F-4518-V500_03922
P.destructans-VC83_02379
M.canis_CBS_113480-MCYG_06524
T.equinum_CBS_127.97-TEQG_04975
T.tonsurans_CBS_112818-TESG_04767
T.interdigitale_H6-H101_02745
T.mentagrophytes-TMEN_8966
T.rubrum_CBS_118892-TERG_07064
H.griseus_UAMH5409-AJ79_09387
B.parvus-GX51_02420
E.parva_UAMH_139-EMPG_10624
A.udagawae-AUD_8914
P.zonata_CBS_506.65-ASPZODRAFT_103682
A.campestris_IBT_28561-P168DRAFT_310302
A.candidus-BDW47DRAFT_122579
A.taichungensis-BDW42DRAFT_187198
A.steynii_IBT_23096-P170DRAFT_277512
A.versicolor_CBS_583.65-ASPVEDRAFT_78143
A.sydowii_CBS_593.65-ASPSYDRAFT_55167
A.nidulans_FGSC_A4-ANIA_00338
A.mulundensis-DSM5745_08254
A.terreus_NIH2624-ATEG_04863
A.wentii_DTO_134E9-ASPWEDRAFT_49717
A.cristatus-SI65_09248
A.glaucus_CBS_516.65-ASPGLDRAFT_121848
A.ruber_CBS_135680-EURHEDRAFT_532034
A.heteromorphus_CBS_117.55-BO70DRAFT_360615
A.ellipticus_CBS_707.79-BO71DRAFT_393911
A.ibericus_CBS_121593-BO80DRAFT_34433
A.sclerotioniger_CBS_115572-BO94DRAFT_213832
A.sclerotiicarbonarius_CBS_121057-BO78DRAFT_190282
A.brasiliensis_CBS_101740-ASPBRDRAFT_119291
A.phoenicis_ATCC_13157-M752DRAFT_332769
A.welwitschiae-BDQ94DRAFT_137653
A.awamori-AAWM_09530
A.niger_CBS_513.88-ANI_1_762014
A.lacticoffeatus_CBS_101883-BO96DRAFT_333962
A.costaricaensis_CBS_115574-BO79DRAFT_252447
A.tubingensis_CBS_134.48-ASPTUDRAFT_39914
A.luchuensis_CBS_106.47-ASPFODRAFT_39840
A.kawachii_IFO_4308-AKAW_01641
A.eucalypticola_CBS_122712-BO83DRAFT_373903
A.neoniger_CBS_115656-BO87DRAFT_457140
A.vadensis_CBS_113365-BO88DRAFT_437999
0.2

Figure 4.3: *Fusarium pseudograminearum* (*Fp*) protein FPSE_08867 has similar proteins present throughout a variety of fungal species but is absent in *Fusarium graminearum*. Phylogenetic analysis of returned protein sequences from unique species by a BLAST search with the *Fp* FPSE_08867 protein sequence as bait. Leaf names state; abbreviated species name_strain-locus_tag. Red numbers display branch support values. Orange label is FPSE_08867, part of the gene cluster in *Fp.* Purple labels show FPSE_08867 homologs that are members of the conserved gene cluster apparent in other fungi.

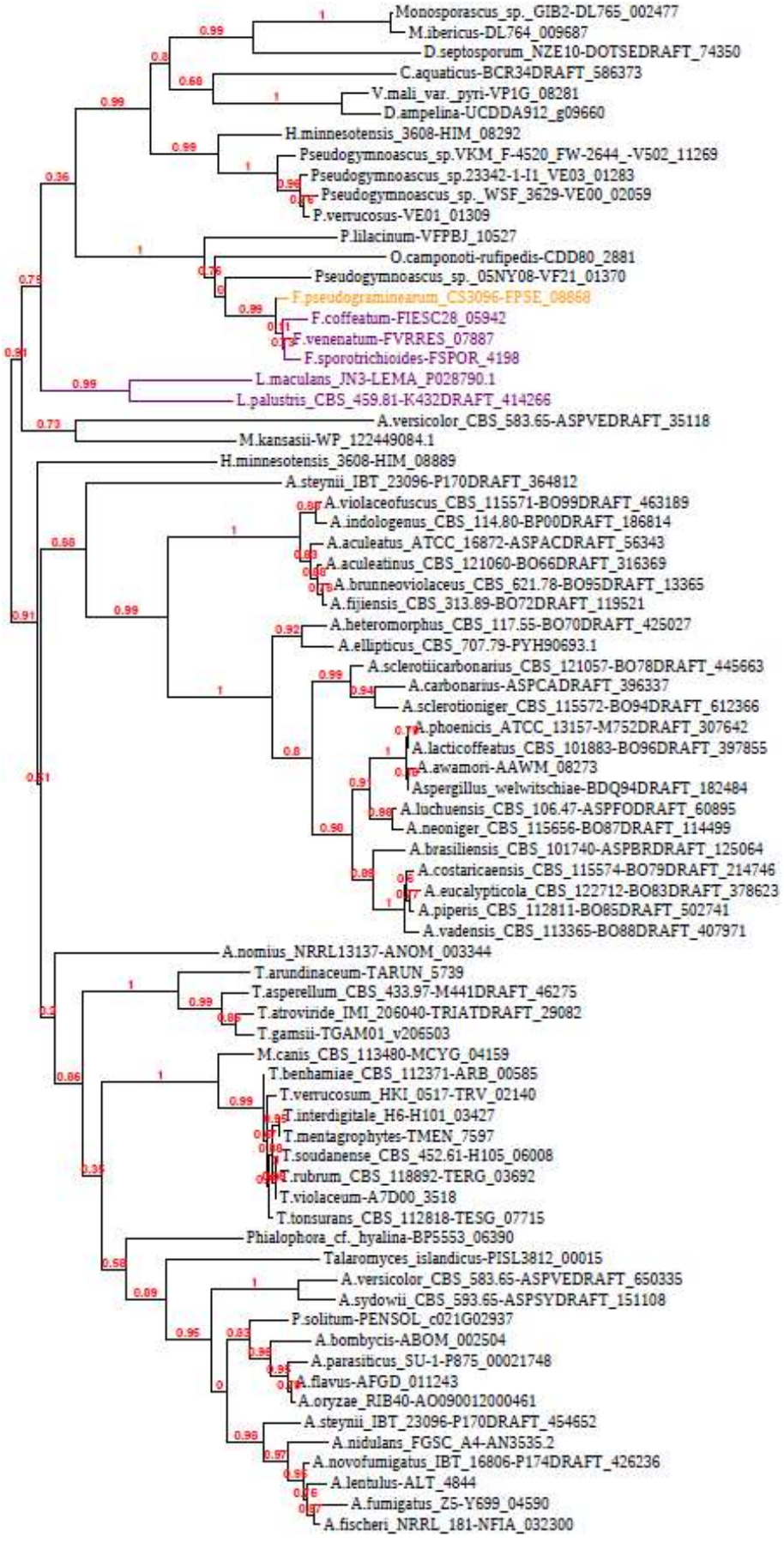
Monosporascus_sp._GIB2-DL765_002477
M.ibericus-DL764_009687
D.septosporum_NZE10-DOTSEDRAFT_74350
C.aquaticus-BCR34DRAFT_586373
V.mali_var._pyri-VP1G_08281
D.ampelina-UCDDA912_g09660
H.minnesotensis_3608-HIM_08292
Pseudogymnoascus_sp.VKM_F-4520_FW-2644_-V502_11269
Pseudogymnoascus_sp.23342-1-I1_VE03_01283
Pseudogymnoascus_sp._WSF_3629-VE00_02059
P.verrucosus-VE01_01309
P.lilacinum-VFPBJ_10527
O.camponoti-rufipedis-CDD80_2881
Pseudogymnoascus_sp._05NY08-VF21_01370
F.pseudograminearum_CS3096-FPSE_08868
F.coffeatum-FIESC28_05942
F.venenatum-FVRRES_07887
F.sporotrichioides-FSPOR_4198
L.maculans_JN3-LEMA_P028790.1
L.palustris_CBS_459.81-K432DRAFT_414266
A.versicolor_CBS_583.65-ASPVEDRAFT_35118
M.kansasii-WP_122449084.1
H.minnesotensis_3608-HIM_08889
A.steynii_IBT_23096-P170DRAFT_364812
A.violaceofuscus_CBS_115571-BO99DRAFT_463189
A.indologenus_CBS_114.80-BP00DRAFT_186814
A.aculeatus_ATCC_16872-ASPACDRAFT_56343
A.aculeatinus_CBS_121060-BO66DRAFT_316369
A.brunneoviolaceus_CBS_621.78-BO95DRAFT_13365
A.fijiensis_CBS_313.89-BO72DRAFT_119521
A.heteromorphus_CBS_117.55-BO70DRAFT_425027
A.ellipticus_CBS_707.79-PYH90693.1
A.sclerotiicarbonarius_CBS_121057-BO78DRAFT_445663
A.carbonarius-ASPCADRAFT_396337
A.sclerotioniger_CBS_115572-BO94DRAFT_612366
A.phoenicis_ATCC_13157-M752DRAFT_307642
A.lacticoffeatus_CBS_101883-BO96DRAFT_397855
A.awamori-AAWM_08273
Aspergillus_welwitschiae-BDQ94DRAFT_182484
A.luchuensis_CBS_106.47-ASPFODRAFT_60895
A.neoniger_CBS_115656-BO87DRAFT_114499
A.brasiliensis_CBS_101740-ASPBRDRAFT_125064
A.costaricaensis_CBS_115574-BO79DRAFT_214746
A.eucalypticola_CBS_122712-BO83DRAFT_378623
A.piperis_CBS_112811-BO85DRAFT_502741
A.vadensis_CBS_113365-BO88DRAFT_407971
A.nomius_NRRL13137-ANOM_003344
T.arundinaceum-TARUN_5739
T.asperellum_CBS_433.97-M441DRAFT_46275
T.atroviride_IMI_206040-TRIATDRAFT_29082
T.gamsii-TGAM01_v206503
M.canis_CBS_113480-MCYG_04159
T.benhamiae_CBS_112371-ARB_00585
T.verrucosum_HKI_0517-TRV_02140
T.interdigitale_H6-H101_03427
T.mentagrophytes-TMEN_7597
T.soudanense_CBS_452.61-H105_06008
T.rubrum_CBS_118892-TERG_03692
T.violaceum-A7D00_3518
T.tonsurans_CBS_112818-TESG_07715
Phialophora_cf._hyalina-BP5553_06390
Talaromyces_islandicus-PISL3812_00015
A.versicolor_CBS_583.65-ASPVEDRAFT_650335
A.sydowii_CBS_593.65-ASPSYDRAFT_151108
P.solitum-PENSOL_c021G02937
A.bombycis-ABOM_002504
A.parasiticus_SU-1-P875_00021748
A.flavus-AFGD_011243
A.oryzae_RIB40-AO090012000461
A.steynii_IBT_23096-P170DRAFT_454652
A.nidulans_FGSC_A4-AN3535.2
A.novofumigatus_IBT_16806-P174DRAFT_426236
A.lentulus-ALT_4844
A.fumigatus_Z5-Y699_04590
A.fischeri_NRRL_181-NFIA_032300
0.4

Figure 4.4: *Fusarium pseudograminearum* (*Fp*) protein FPSE_08868 has similar proteins present throughout a variety of fungal species but is absent in *Fusarium graminearum*. Phylogenetic analysis of returned protein sequences from unique species by a BLAST search with the *Fp* FPSE_08868 protein sequence as bait. Leaf names state; abbreviated species name_strain-locus_tag. Red numbers display branch support values. Orange label is FPSE_08868, part of the gene cluster in *Fp.* Purple labels show FPSE_08867 homologs that are members of the conserved gene cluster apparent in other fungi.

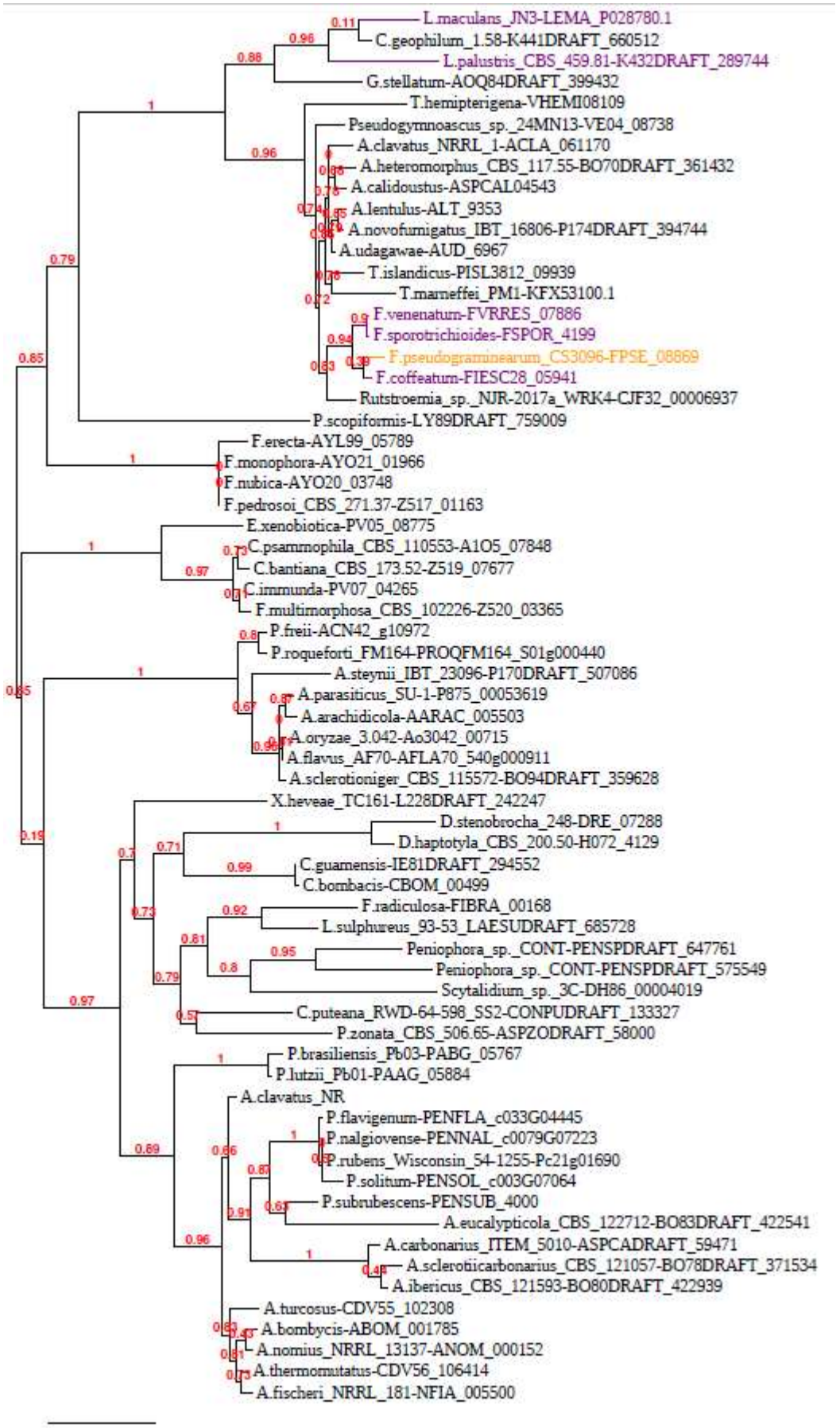
L.maculans_JN3-LEMA_P028780.1
C.geophilum_1.58-K441DRAFT_660512
L.palustris_CBS_459.81-K432DRAFT_289744
G.stellatum-AOQ84DRAFT_399432
T.hemipterigena-VHEMI08109
Pseudogymnoascus_sp._24MN13-VE04_08738
A.clavatus_NRRL_1-ACLA_061170
A.heteromorphus_CBS_117.55-BO70DRAFT_361432
A.calidoustus-ASPCAL04543
A.lentulus-ALT_9353
A.novofumigatus_IBT_16806-P174DRAFT_394744
A.udagawae-AUD_6967
T.islandicus-PISL3812_09939
T.marneffei_PM1-KFX53100.1
F.venenatum-FVRRES_07886
F.sporotrichioides-FSPOR_4199
F.pseudograminearum_CS3096-FPSE_08869
F.coffeatum-FIESC28_05941
Rutstroemia_sp._NJR-2017a_WRK4-CJF32_00006937
P.scopiformis-LY89DRAFT_759009
F.erecta-AYL99_05789
F.monophora-AYO21_01966
F.nubica-AYO20_03748
F.pedrosoi_CBS_271.37-Z517_01163
E.xenobiotica-PV05_08775
C.psammophila_CBS_110553-A1O5_07848
C.bantiana_CBS_173.52-Z519_07677
C.immunda-PV07_04265
F.multimorphosa_CBS_102226-Z520_03365
P.freii-ACN42_g10972
P.roqueforti_FM164-PROQFM164_S01g000440
A.steynii_IBT_23096-P170DRAFT_507086
A.parasiticus_SU-1-P875_00053619
A.arachidicola-AARAC_005503
A.oryzae_3.042-Ao3042_00715
A.flavus_AF70-AFLA70_540g000911
A.sclerotioniger_CBS_115572-BO94DRAFT_359628
X.heveae_TC161-L228DRAFT_242247
D.stenobrocha_248-DRE_07288
D.haptotyla_CBS_200.50-H072_4129
C.guamensis-IE81DRAFT_294552
C.bombacis-CBOM_00499
F.radiculosa-FIBRA_00168
L.sulphureus_93-53_LAESUDRAFT_685728
Peniophora_sp._CONT-PENSPDRAFT_647761
Peniophora_sp._CONT-PENSPDRAFT_575549
Scytalidium_sp._3C-DH86_00004019
C.puteana_RWD-64-598_SS2-CONPUDRAFT_133327
P.zonata_CBS_506.65-ASPZODRAFT_58000
P.brasiliensis_Pb03-PABG_05767
P.lutzii_Pb01-PAAG_05884
A.clavatus_NR
P.flavigenum-PENFLA_c033G04445
P.nalgiovense-PENNAL_c0079G07223
P.rubens_Wisconsin_54-1255-Pc21g01690
P.solitum-PENSOL_c003G07064
P.subrubescens-PENSUB_4000
A.eucalypticola_CBS_122712-BO83DRAFT_422541
A.carbonarius_ITEM_5010-ASPCADRAFT_59471
A.sclerotiicarbonarius_CBS_121057-BO78DRAFT_371534
A.ibericus_CBS_121593-BO80DRAFT_422939
A.turcosus-CDV55_102308
A.bombycis-ABOM_001785
A.nomius_NRRL_13137-ANOM_000152
A.thermomutatus-CDV56_106414
A.fischeri_NRRL_181-NFIA_005500
0.3

Figure 4.5: *Fusarium pseudograminearum* (*Fp*) protein FPSE_08869 has similar proteins present throughout a variety of fungal species but is absent in *Fusarium graminearum*. Phylogenetic analysis of returned protein sequences from unique species by a BLAST search with the *Fp* FPSE_08869 protein sequence as bait. Leaf names state; abbreviated species name_strain-locus_tag. Red numbers display branch support values. Orange label is FPSE_08869, part of the gene cluster in *Fp.* Purple labels show FPSE_08869 homologs that are members of the conserved gene cluster apparent in other fungi.

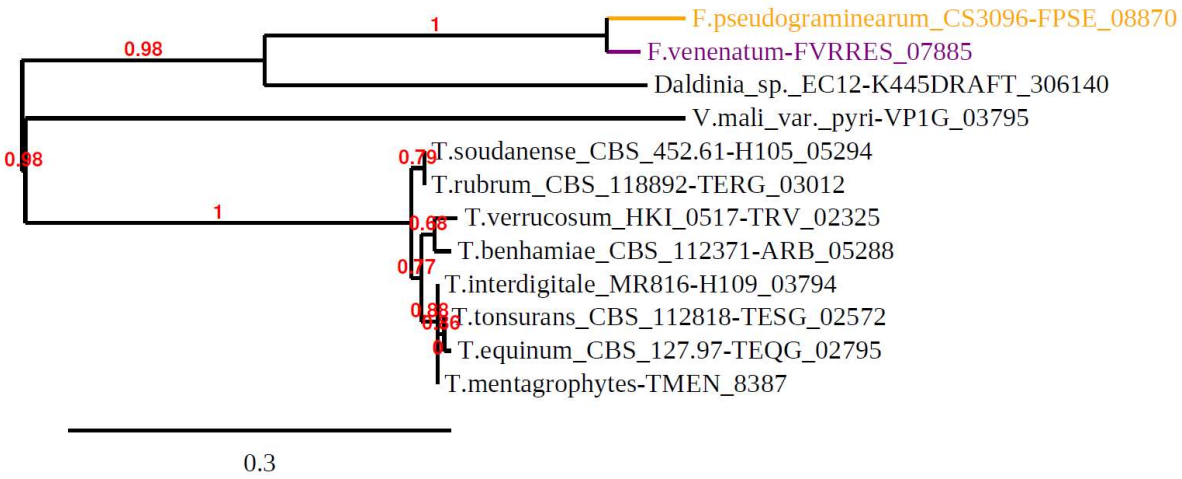

Figure 4.6: *Fusarium pseudograminearum* (*Fp*) protein FPSE_08870 has similar proteins present throughout a variety of fungal species but is absent in *Fusarium graminearum*. Phylogenetic analysis of returned protein sequences from unique species by a BLAST search with the *Fp* FPSE_08870 protein sequence as bait. Leaf names state; abbreviated species name_strain-locus_tag. Red numbers display branch support values. Orange label is FPSE_08870, part of the gene cluster in *Fp*. Purple labels show FPSE_08870 homologs that are members of the conserved gene cluster apparent in other fungi.

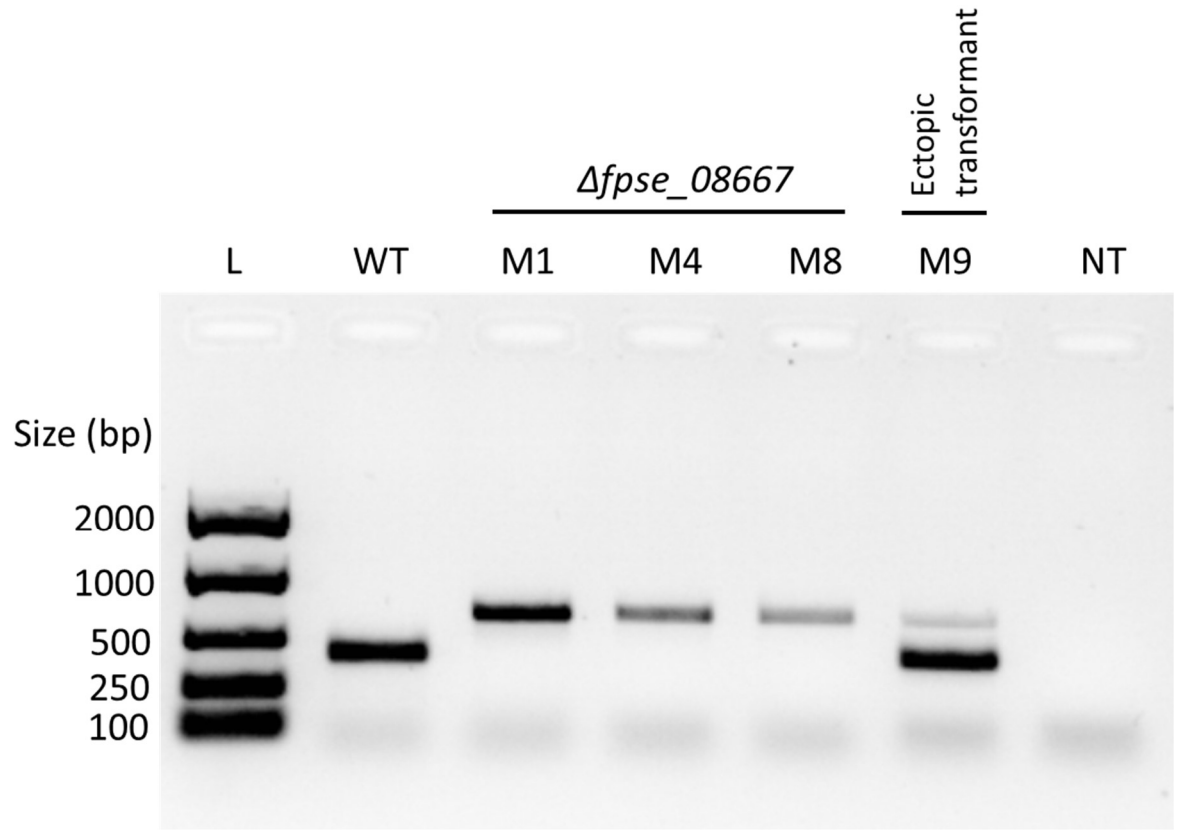

Figure 4.7: Diagnostic PCR assay for the detection the absence of the endogenous wild-type *FPSE_08867* gene and the presence of nourseothricin resistance gene insert in independent Δ*fpse_08667* isolates. Three isolates; M1, M4 and M8, were confirmed as Δ*fpse_08667* knockouts carrying nourseothricin resistance gene inserted in *FPSE_08867*. The PCR assay detected a larger product corresponding to nourseothricin resistance gene, and a smaller product amplified from the endogenous wild-type *FPSE_08867* allele but not from the three independent Δ*fpse_08667* knockout alleles. The M9 isolate was identified as containing a wild-type *FPSE_08867* allele and an ectopic integration of the T-DNA elsewhere in the *Fp* genome. L stands for Easyladder I. NT refers to a no DNA template control.

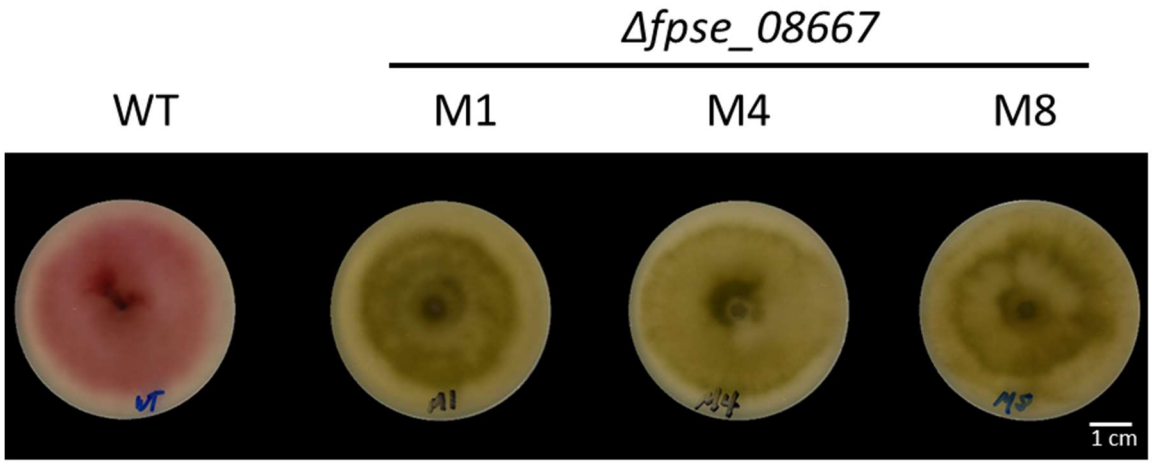

Figure 4.8: Δ*fpse_08667 isolates* apparent lack of mycotoxin aurofusarin production when grown on potato dextrose agar (PDA) media under alkaline conditions. Aurofusarin is a mycotoxin pigment produced by *Fp* that appears red/purple under alkaline conditions (Ashley et al., 1937, Medentsev and Akimenko, 1998). Photograph of wild type (WT) and three Δ*fpse_08667* knockouts isolates (M1, M4 M8). Note apparent lack of aurofusarin, visible as red pigment, in the Δ*fpse_08867* knockout lines. White bar represents 1cm scale.

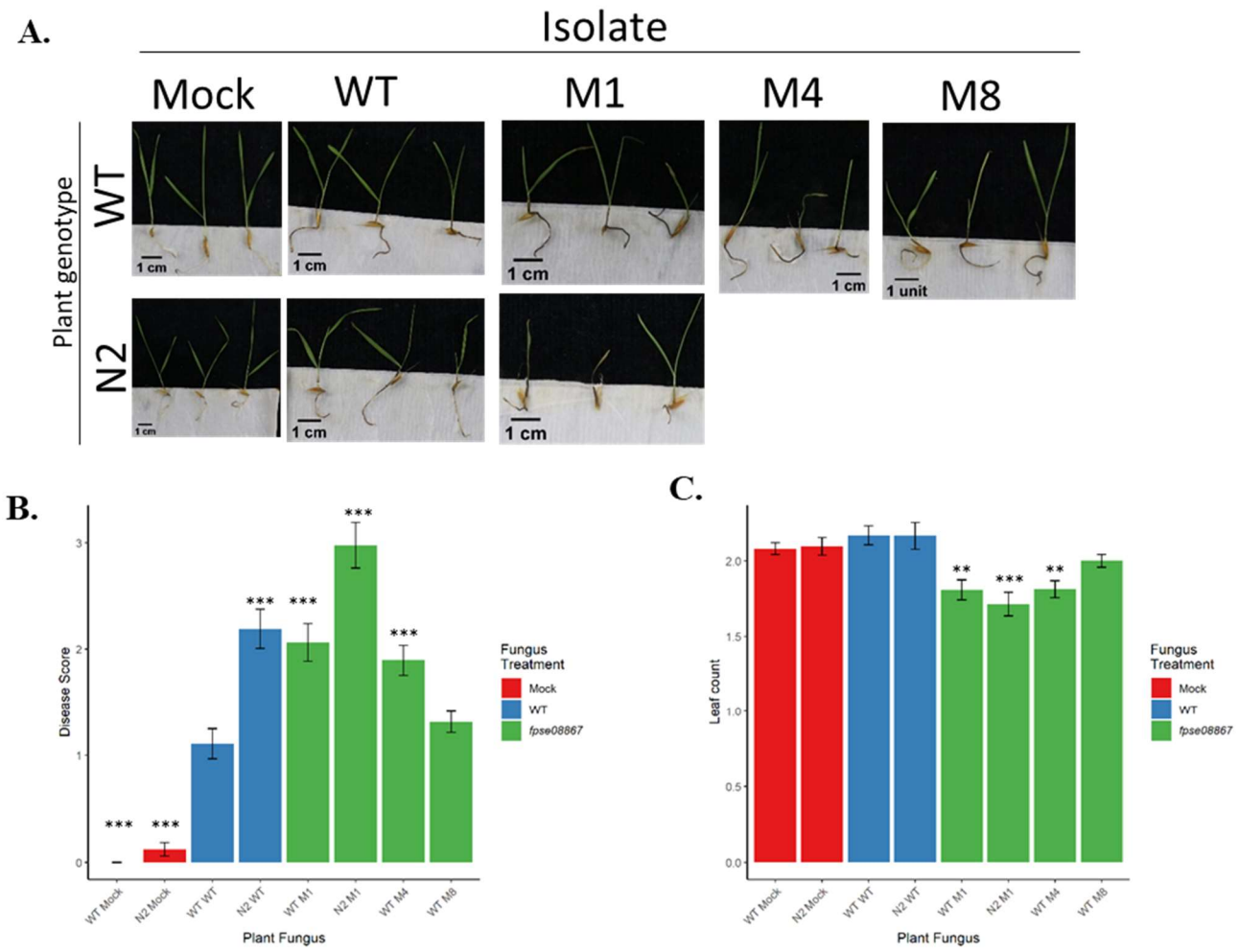

Figure 4.9: Δ*fpse_08667* (M1, M4 and M8) isolates cause enhanced *Fusarium* crown rot (FCR) disease severity phenotypes, when infecting wild type (WT) and *nahG Brachypodium* seedlings (N2), relative to the wild type (WT) isolate. Values were recorded from a soilless infection assay using *Brachypodium* seedlings, 12 days post inoculation (dpi) with a 1×10^6 spores/mL spore suspension or water as a mock control. Data represents mean ± SE of eight technical replicates with six plants per replicate. ** and *** denote statistical significance of $P < 0.01$ and $P < 0.001$ respectively, relative to WT *B. distachyon* inoculated with the WT *Fp* isolate, as per a pairwise Wilcoxon rank test corrected for multiple comparisons with Bonferroni's procedure. **A.** Photographs of 12dpi mock, *Fp* and Δ*fpse_08667* inoculated plants of representative treated individuals. Red bar is a 1cm scale bar. **B.** Column plot of FCR disease symptoms at 12 dpi, using a 0-5 scale of severity. **C.** Column plot of leaf number per individual plant at 12dpi.

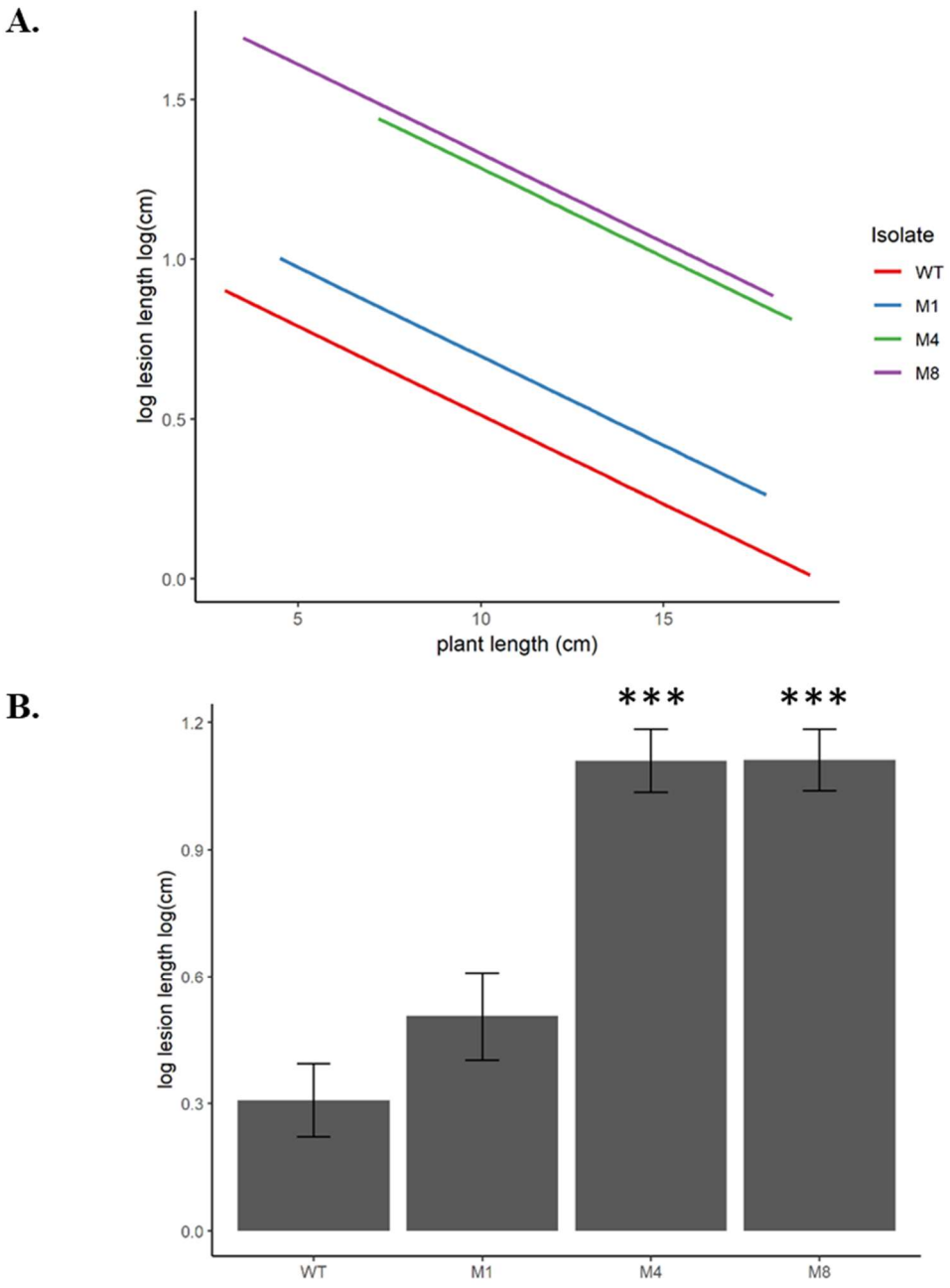

Figure 4.10: ∆*fpse_08667* isolates cause enhanced *Fusarium* crown rot disease severity phenotypes, when infecting *Triticum aestivum* var. "Mace" seedlings, with respect to wild type isolate. Values represent plant length (cm) and log_{10} transformed lesion length of five technical replicates each containing ten plants at 14 days post inoculation. **A.** Multiple linear regression showing the effect of isolate on log_{10} lesion length adjusted for plant length. **B.** Column plot of mean log_{10} lesion length ± SE for each fungal isolate. *** denote statistical significance of $p < 0.001$ relative to the WT, as per *Tukey's HSD* test.

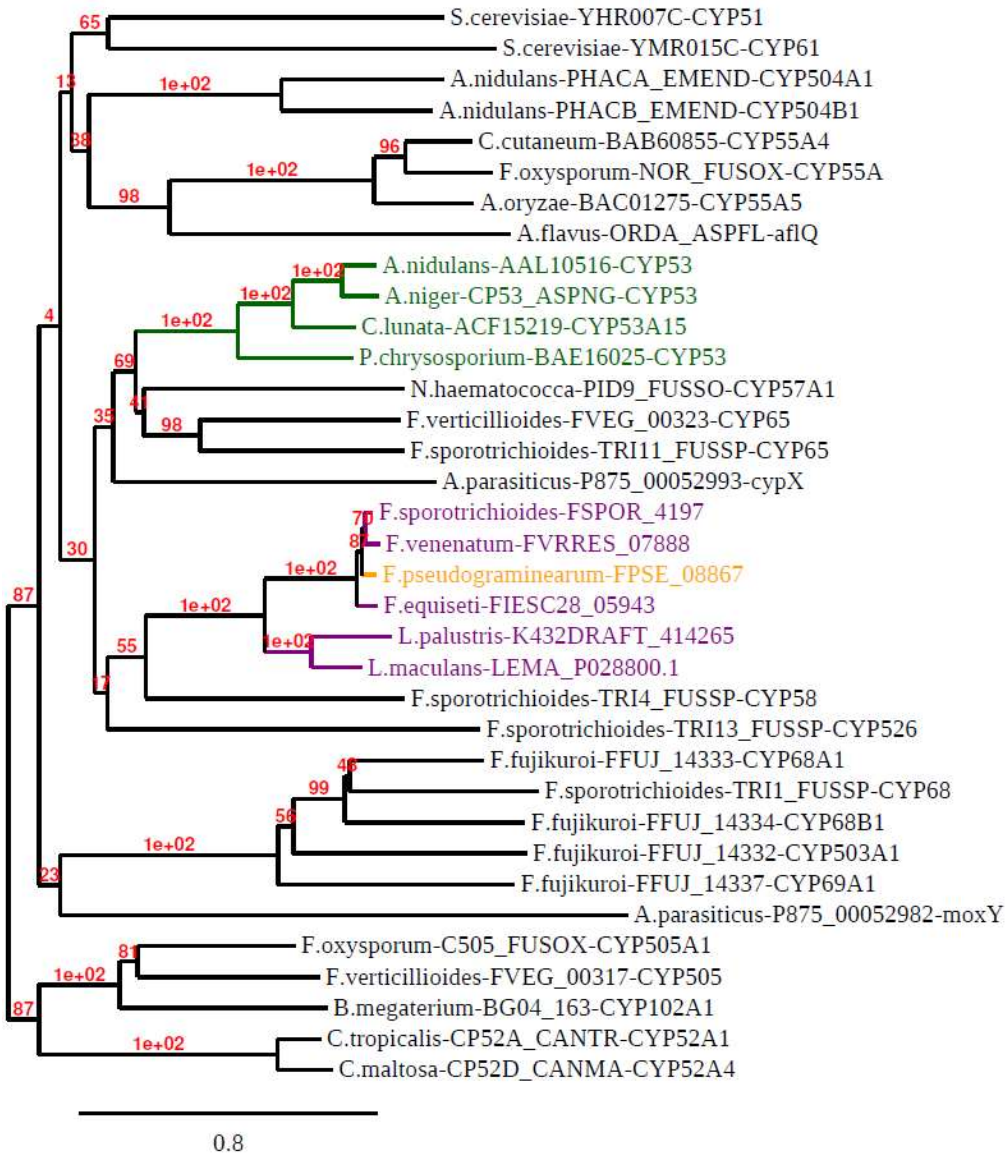

Figure 4.11: FPSE_08867 and homologs cluster with CYTOCHROME P450s (CYPs) involved in mycotoxin synthesis. Phylogenetic analysis of *Fusarium pseudograminearum* (*Fp*) protein *FPSE_08867* sequence (orange label) and its homologs from other fungal species (purple labels) do not cluster with CYTOCHROME P450s that possess known benzoate-4-monoxygenase enzymatic activity (green label). Red numbers display branch support values. Leaf names state; abbreviated species name-Locus tag-Cytochrome P450 subfamily membership.

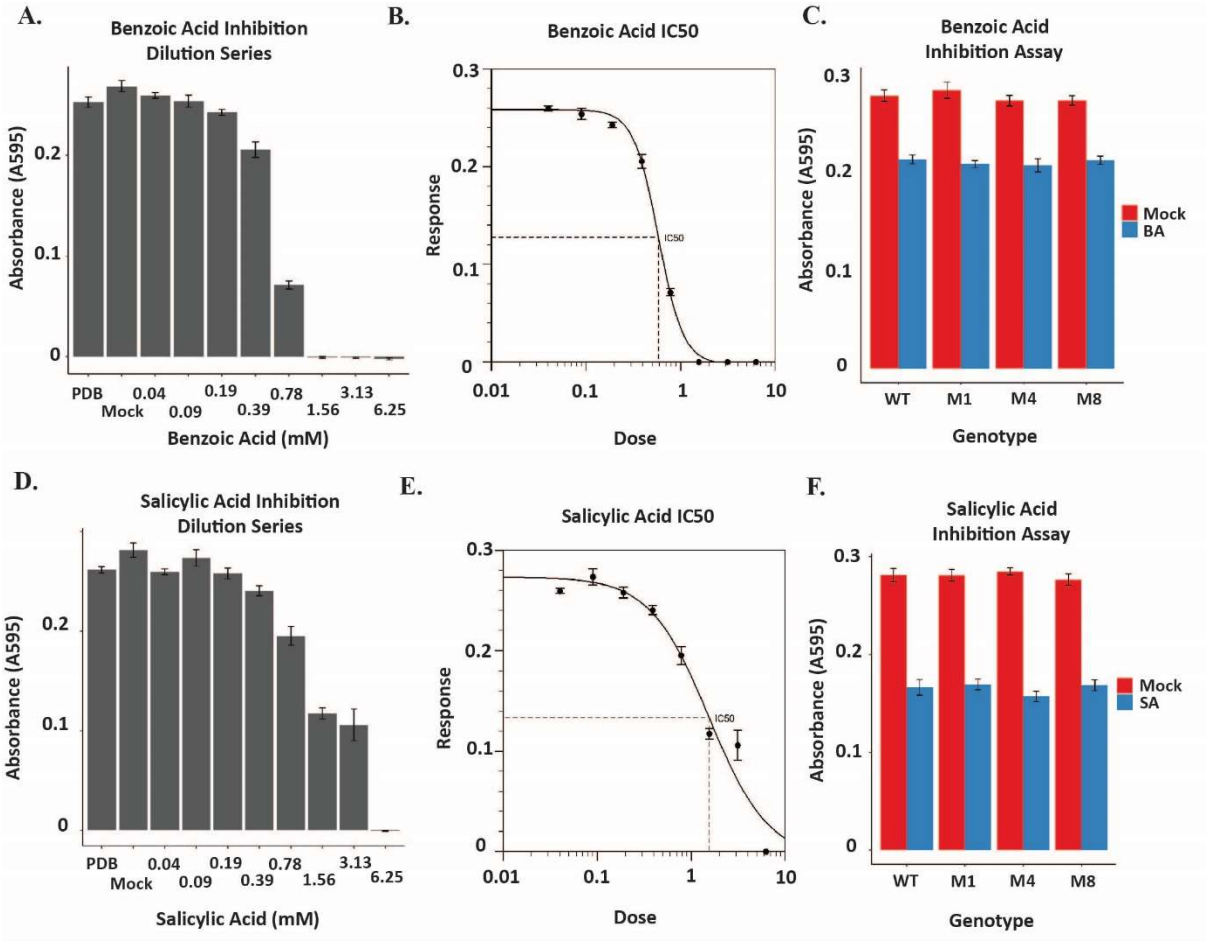

Figure 4.12: Δ*fpse08667* isolates do not show altered mycelial growth in Potato Dextrose Broth (PDB) amended with 12.5mM Citrate Buffer System (CBS), buffered at 4.6 pH, 0.06% DMSO (V:V) and supplemented with 0.58mM benzoic acid or 1.56mM salicylic acid. Absorbance values at 595nm were recorded using a EnVision Multilabel plate reader (PerkinElmer, Waltham, MA); as a proxy for mycelia growth, initially at 0 days post inoculation (dpi) and finally at 2dpi. Values represent the mean difference between the final and initial reads for eight technical replicates ± standard error. **A.** Column plot showing the mean mycelia growth of the WT isolate after two days in PDB, mock and solutions containing different concentrations of benzoic acid. **B.** A four parameter logistic regression model fitted to the WT mycelia growth data in mock and benzoic acid solution to calculate an IC50. The benzoic acid WT IC_{50} was calculated to be 0.58mM. **C.** Column plot showing the mean mycelia growth of the WT and *Fp*Δ*fpse08667* (M1, M4, M8) isolates in mock or 0.58mM benzoic acid solution. **D.** Column plot showing the mean mycelia growth of the WT isolate after two days in PDB, mock and solutions containing different concentrations of salicylic acid. **E.** A four parameter logistic regression model fitted to the WT mycelia

growth data in mock and salicylic acid solution to calculate an IC50. The salicylic acid WT IC_{50} was calculated to be 1.56mM. **F.** Column plot showing the mean mycelia growth of the WT and Δ*fpse08667* (M1, M4, M8) isolates in mock or 1.56mM salicylic acid solution.

4.7 Tables

Table 4.1: List of primers used for genotyping ∆fpse_088671 lines

Primer name	**Primer sequences**
Nst-screenR	5'CGTGTCGTCAAGAGTGGTCA3'
FPSE_08867_screen F	5'GACAAAGAGGAACGTGAGTGC3'
FPSE_08867_screen R	5'AACGACTTCCACCCACAAAG3'

4.8 Supplementary Files

Supplementary table 4.1: List of significantly differentially expressed genes by *Fusarium pseudograminearum* infecting *nahG* expressing *Brachypodium distachyon* versus wild type *Brachypodium.* Genes mentioned in text are highlighted yellow.

Fp locus tag	Gene description	log_2 FC	P.adj
gene_FPSE_08868	solid-state culture specific protein	-3.041	0.00314044
gene_FPSE_02227	integral membrane protein	-2.67917	0.00871633
gene_FPSE_08867	benzoate 4-monooxygenase cytochrome p450	-2.67287	0.00736379
gene_FPSE_04556	ww domain-containing oxidoreductase	-2.5706	0.00314044
gene_FPSE_12003	glucuronyl hydrolase	-2.38896	0.0246404
gene_FPSE_09604	hypothetical protein FPSE_09604	-2.25319	0.00314044
gene_FPSE_05343	integral membrane protein	-2.11085	0.0276824
gene_FPSE_07528	glutamate decarboxylase	-2.09795	0.00314044
gene_FPSE_02129	hypothetical protein FPSE_02129	-2.0946	0.0284733
gene_FPSE_04081	hypothetical protein FPSE_04081	-2.08697	0.0237278
gene_FPSE_10547	hypothetical protein FPSE_10547	-2.08671	0.00314044
gene_FPSE_10548	hypothetical protein FPSE_10548	-2.07118	0.00314044
gene_FPSE_10934	tripeptidyl aminopeptidase	-2.03284	0.0171464
gene_FPSE_08424	csr1-phosphatidylinositol transfer protein	-1.98596	0.00314044
gene_FPSE_00695	6-hydroxy-d-nicotine oxidase	-1.8956	0.00314044
gene_FPSE_12215	antifungal protein	-1.84494	0.010169
gene_FPSE_01889	major facilitator superfamily transporter	-1.82105	0.00736379
gene_FPSE_02157	dihydrodipicolinate synthetase family protein	-1.8035	0.00314044
gene_FPSE_07530	2og-fe oxygenase family protein	-1.79487	0.0142367
gene_FPSE_00764	cutinase precursor	-1.74399	0.00314044
gene_FPSE_07753	unnamed protein product	-1.71001	0.00314044

gene_FPSE_08426	hypothetical protein FPSE_08426	-1.69075	0.00314044
gene_FPSE_00266	nonribosomal peptide synthetase	-1.67808	0.00314044
gene_FPSE_06703	hypothetical protein FPSE_06703	-1.66851	0.010169
gene_FPSE_11612	carnitine o-acetyltransferase	-1.66156	0.00314044
gene_FPSE_04678	pot family proton-dependent oligopeptide transporter	-1.63184	0.0142367
gene_FPSE_07628	glycerol kinase	-1.60621	0.00533875
gene_FPSE_07350	hydrophobin 3 precursor	-1.59725	0.00314044
gene_FPSE_08422	cytochrome p450 3a13	-1.59595	0.00314044
gene_FPSE_08959	serine mitochondrial	-1.58646	0.00314044
gene_FPSE_01888	dihydrodipicolinate synthase	-1.55539	0.0142367
gene_FPSE_08386	l-pipecolate oxidase	-1.54972	0.00314044
gene_FPSE_01422	isocitrate lyase	-1.54043	0.00314044
gene_FPSE_08425	hypothetical protein FPSE_08425	-1.49311	0.00314044
gene_FPSE_07032	siderophore iron transporter mirb	-1.46677	0.010169
gene_FPSE_05371	beta-galactosidase	-1.46277	0.0171464
gene_FPSE_03275	alkylglycerol monooxygenase	-1.45424	0.00533875
gene_FPSE_05702	six-bladed beta-propeller	-1.45217	0.00314044
gene_FPSE_01887	oxidoreductase	-1.44977	0.0171464
gene_FPSE_05341	sugar transporter	-1.43742	0.00871633
gene_FPSE_10294	sugar transport protein	-1.42835	0.00533875
gene_FPSE_10710	hypothetical protein FPSE_10710	-1.42482	0.0433443
gene_FPSE_03469	neutral amino acid permease	-1.398	0.0327605
gene_FPSE_07533	hypothetical protein FPSE_07533	-1.37516	0.00314044
gene_FPSE_01699	benzoylformate decarboxylase	-1.37027	0.0175521
gene_FPSE_09097	4-aminobutyrate aminotransferase	-1.36895	0.0118639
gene_FPSE_03781	carbohydrate esterase family 5 protein	-1.36447	0.0202007
gene_FPSE_11094	3-beta-hydroxysteroid dehydrogenase protein	-1.35656	0.00314044
gene_FPSE_11095	udpglucose 4-epimerase	-1.35124	0.00314044

gene_FPSE_08419	short-chain dehydrogenase reductase family 16c member 6	-1.31226	0.00533875
gene_FPSE_11725	malate glyoxysomal	-1.27486	0.00314044
gene_FPSE_06216	threonine aldolase	-1.25804	0.00533875
gene_FPSE_10435	cell division cycle atpase	-1.24753	0.00314044
gene_FPSE_08388	dimethylglycine mitochondrial precursor	-1.21723	0.0175521
gene_FPSE_05476	xylosidase glycosyl hydrolase	-1.17432	0.0433443
gene_FPSE_08081	hypothetical protein FPSE_08081	-1.15034	0.0171464
gene_FPSE_10976	arginase	-1.15017	0.0416149
gene_FPSE_08385	cytochrome p450 oxidoreductase	-1.13966	0.00736379
gene_FPSE_08417	fad-containing monooxygenase	-1.11256	0.010169
gene_FPSE_10119	alpha-n-arabinofuranosidase a	-1.09384	0.0118639
gene_FPSE_05150	alpha-galactosidase b	-1.08472	0.0237278
gene_FPSE_04601	hypothetical protein FPSE_04601	-1.02903	0.0369384
gene_FPSE_07681	acetyl-coenzyme a synthetase	-1.02237	0.0156256
gene_FPSE_05978	phenol hydroxylase	-0.988909	0.0384164
gene_FPSE_06928	xylanase 1	-0.979623	0.0327605
gene_FPSE_07883	phosphoenolpyruvate carboxykinase	-0.972515	0.0378879
gene_FPSE_09346	minor extracellular protease vpr	-0.970648	0.0246404
gene_FPSE_02076	uracil catabolism protein 4	-0.923084	0.0485801
gene_FPSE_05704	membrane primary amine oxidase	-0.921586	0.0456126
gene_FPSE_03345	tyrosinase precursor	-0.852122	0.0437517
gene_FPSE_02115	plant pr-1 class of pathogen related protein	0	0.00314044
gene_FPSE_10520	hypothetical protein FPSE_10520	0	0.0299719
gene_FPSE_11777	transmembrane protein	0.891333	0.0407286
gene_FPSE_02955	necrosis inducing protein	0.896653	0.0437517
gene_FPSE_10952	hypothetical protein FPSE_10952	0.907346	0.0294111
gene_FPSE_01384	hypothetical protein FPSE_01384	0.916316	0.0299719
gene_FPSE_01368	endo-polygalacturonase 6	0.919958	0.0472274

gene_FPSE_02628	class iii chitinase 1	0.921368	0.0337819
gene_FPSE_10385	general amino acid permease agp2	0.966972	0.0320942
gene_FPSE_05664	hect-type ubiquitin ligase-interacting protein cred	0.973259	0.0424921
gene_FPSE_11019	nonribosomal peptide synthetase	0.977689	0.021355
gene_FPSE_07401	hypothetical protein FPSE_07401	0.987643	0.0166836
gene_FPSE_11714	zsp1 zinc sensitive phenotype 1	0.992947	0.0327605
gene_FPSE_05160	5 -nucleotidase	0.997204	0.0299719
gene_FPSE_00934	ring-like domain-containing protein	1.00599	0.0344053
gene_FPSE_06017	polyketide synthase	1.0112	0.0171464
gene_FPSE_02275	extracellular serine-rich protein	1.01291	0.0226278
gene_FPSE_02473	choline dehydrogenase	1.01382	0.0156256
gene_FPSE_11682	sphingolipid long chain base-responsive protein lsp1	1.02904	0.0142367
gene_FPSE_00550	tgf beta induced protein ig-h3 precursor	1.03309	0.0433443
gene_FPSE_06880	ankyrin repeat domain-containing protein 50	1.03317	0.0266938
gene_FPSE_06614	nhl repeat-containing protein	1.03471	0.0256801
gene_FPSE_03418	ahmp1 protein	1.03649	0.0175521
gene_FPSE_07124	family protein	1.03799	0.0142367
gene_FPSE_06018	o-methyltransferase	1.04398	0.010169
gene_FPSE_02493	hc-toxin synthetase	1.0647	0.0171464
gene_FPSE_06247	protein rsn1	1.07404	0.00871633
gene_FPSE_10645	hypothetical protein FPSE_10645	1.08244	0.0485801
gene_FPSE_03048	acid phosphatase	1.09085	0.0171464
gene_FPSE_08336	interferon-regulated resistance gtp-binding protein	1.09942	0.0133469
gene_FPSE_04697	pho12-secreted acid phosphatase	1.09982	0.010169
gene_FPSE_02286	ist2 protein	1.12033	0.0166836
gene_FPSE_02223	carboxypeptidase 2	1.13515	0.0437517
gene_FPSE_05809	mfs sit siderophore-iron:h+ symporter	1.14097	0.00871633

gene_FPSE_05289	hypothetical protein FPSE_05289	1.14293	0.0202007
gene_FPSE_06052	chitinase	1.14689	0.0166836
gene_FPSE_09451	hypothetical protein FPSE_09451	1.15052	0.00736379
gene_FPSE_02800	secreted protein	1.16018	0.00314044
gene_FPSE_04191	alkaline phosphatase	1.16423	0.00314044
gene_FPSE_08108	amino-acid permease inda1	1.17126	0.0344053
gene_FPSE_02490	plp-dependent transferase	1.17427	0.00314044
gene_FPSE_00791	ankyrin repeat protein nuc-2	1.17624	0.0142367
gene_FPSE_02092	hypothetical protein FPSE_02092	1.17839	0.0175521
gene_FPSE_01992	hypothetical protein FPSE_01992	1.18157	0.0491265
gene_FPSE_10804	phosphomutase pmu1	1.18239	0.0166836
gene_FPSE_08743	potassium sodium efflux p-type fungal-type	1.19155	0.0166836
gene_FPSE_06871	primary-amine oxidase	1.20133	0.0344053
gene_FPSE_06006	hypothetical protein FPSE_06006	1.23693	0.0133469
gene_FPSE_05267	zinc-binding oxidoreductase	1.24782	0.00314044
gene_FPSE_05619	hypothetical protein FPSE_05619	1.2558	0.0433443
gene_FPSE_10841	geranylgeranyl pyrophosphate synthetase	1.25673	0.00314044
gene_FPSE_08553	hypothetical protein FPSE_08553	1.2599	0.0284733
gene_FPSE_02494	short-chain dehydrogenase	1.2822	0.00736379
gene_FPSE_05291	endonuclease exonuclease phosphatase family	1.2888	0.00314044
gene_FPSE_02448	hypothetical protein FG05_11033	1.30319	0.0384164
gene_FPSE_02491	glycoside hydrolase beta alpha-barrel	1.3067	0.00871633
gene_FPSE_09948	subtilisin	1.30743	0.00314044
gene_FPSE_04403	sphingolipid long chain base-responsive protein lsp1	1.31401	0.00871633
gene_FPSE_12214	isoamyl alcohol	1.31982	0.00533875
gene_FPSE_02056	family inorganic phosphate transporter	1.32892	0.00314044
gene_FPSE_10940	phosphatidic acid phosphatase beta	1.33809	0.0133469

gene_FPSE_00736	membrane primary amine oxidase	1.34199	0.00314044
gene_FPSE_03171	pot family proton-dependent oligopeptide transporter	1.34762	0.00871633
gene_FPSE_00815	hypothetical protein FPSE_00815	1.38035	0.00314044
gene_FPSE_07797	hypothetical protein FPSE_07797	1.39689	0.0400406
gene_FPSE_12103	mfs dha1 multidrug resistance protein	1.39903	0.00871633
gene_FPSE_00941	cell wall protein sed1	1.40402	0.0246404
gene_FPSE_03017	hypothetical protein FPSE_03017	1.44109	0.00314044
gene_FPSE_01554	stress protein ddr48	1.44129	0.00314044
gene_FPSE_12274	transcription factor ask10p	1.44575	0.00314044
gene_FPSE_00079	mfs nnp nitrate nitrite transporter	1.46011	0.0400406
gene_FPSE_11465	hypothetical protein FPSE_11465	1.47294	0.00314044
gene_FPSE_10978	hypothetical protein FPSE_10978	1.5484	0.00533875
gene_FPSE_09453	glycerophosphoryl diester phosphodiesterase	1.55479	0.00314044
gene_FPSE_04900	tartrate transporter	1.5635	0.00533875
gene_FPSE_02829	guanyl-specific ribonuclease f1	1.56406	0.00314044
gene_FPSE_09389	hypothetical protein FPSE_09389	1.56642	0.00314044
gene_FPSE_02144	mate efflux family protein subfamily	1.56842	0.00533875
gene_FPSE_10605	the plant pr-1 class pathogen related protein	1.58484	0.0359785
gene_FPSE_10168	anion transport protein	1.58522	0.00736379
gene_FPSE_05377	fad-binding protein	1.58668	0.0384164
gene_FPSE_02644	ph-response regulator	1.59995	0.0133469
gene_FPSE_00757	transcription factor	1.60083	0.0175521
gene_FPSE_03044	phospholipase a2	1.60439	0.0284733
gene_FPSE_07647	ph domain-containing protein	1.60545	0.0171464
gene_FPSE_02492	cytochrome p450 family protein	1.6274	0.0118639
gene_FPSE_04731	hypothetical protein FPSE_04731	1.63432	0.0393382
gene_FPSE_01758	hypothetical protein FPSE_01758	1.63435	0.00533875
gene_FPSE_06543	gtpase (g3e family)	1.64373	0.0350082

gene_FPSE_07438	related to coq2-para-hydroxybenzoate--polyprenyltransferase	1.66397	0.010169
gene_FPSE_04904	exopolyphosphatase	1.67149	0.0485801
gene_FPSE_00507	mismatched base pair and cruciform dna recognition protein	1.67471	0.00314044
gene_FPSE_03965	hypothetical protein FPSE_03965	1.73651	0.0142367
gene_FPSE_04809	zinc finger protein rsv2	1.73872	0.00314044
gene_FPSE_03766	udp-glucuronic acid decarboxylase 1	1.80601	0.0175521
gene_FPSE_01808	mitochondrial integral membrane protein	1.80865	0.0433443
gene_FPSE_06319	hypothetical protein FPSE_06319	1.83152	0.0472274
gene_FPSE_01261	s-adenosylmethionine:diacylglycerol 3-amino-3-carboxypropyl transferase	1.86457	0.00871633
gene_FPSE_10695	hypothetical protein FPSE_10695	1.87579	0.0407286
gene_FPSE_11463	hypothetical protein FPSE_11463	1.89027	0.00314044
gene_FPSE_09169	nitrate reductase	1.8928	0.00314044
gene_FPSE_10664	hypothetical protein FPSE_10664	1.91481	0.0299719
gene_FPSE_03786	protein kinase c epsilon type	1.94491	0.00533875
gene_FPSE_00212	n4-(beta-n-acetylglucosaminyl)-l-asparaginase	1.96763	0.00314044
gene_FPSE_06429	thaumatin family protein	1.96847	0.0142367
gene_FPSE_01641	alkaline phosphatase	2.00155	0.00314044
gene_FPSE_08809	phospholipase c	2.00475	0.00533875
gene_FPSE_05945	hypothetical protein FPSE_05945	2.01241	0.00314044
gene_FPSE_11406	hypothetical protein FPSE_11406	2.05805	0.0491265
gene_FPSE_01025	sterol regulatory element-binding protein 2	2.05849	0.0350082
gene_FPSE_02113	urea active transporter	2.0726	0.00314044
gene_FPSE_03961	hypothetical protein FPSE_03961	2.09718	0.0256801

gene_FPSE_06825	mitochondrial phosphate carrier protein	2.10115	0.00314044
gene_FPSE_08014	hypothetical protein FPSE_08014	2.15774	0.0171464
gene_FPSE_09926	translation machinery-associated protein 64	2.16589	0.0175521
gene_FPSE_09019	nitrite reductase	2.20803	0.00314044
gene_FPSE_03230	mfs transporter protein	2.30752	0.0175521
gene_FPSE_09496	neurofilament medium polypeptide	2.38723	0.00314044
gene_FPSE_08396	hypothetical protein FPSE_08396	2.41289	0.00314044
gene_FPSE_06282	ethanolamine utilization protein	2.46384	0.0175521
gene_FPSE_10923	---NA---	2.51391	0.00736379
gene_FPSE_01980	phosphate-repressible phosphate permease	2.5173	0.00314044
gene_FPSE_02180	dtdp-glucose -dehydratase	2.5929	0.0433443
gene_FPSE_04719	hypothetical protein FPSE_04719	2.60134	0.0294111
gene_FPSE_01756	aspartic proteinase precursor	2.62189	0.00314044
gene_FPSE_00452	hypothetical protein FPSE_00452	2.62421	0.00871633
gene_FPSE_06591	neurofilament medium polypeptide	2.68614	0.00314044
gene_FPSE_10134	hypothetical protein FPSE_10134	2.80963	0.00314044
gene_FPSE_01570	hypothetical protein FPSE_01570	2.88456	0.00314044
gene_FPSE_10726	glycosyl transferase gt-a type structural fold protein	2.96559	0.00871633
gene_FPSE_08755	glycosyl transferase	3.05029	0.0266938
gene_FPSE_10240	hypothetical protein FPSE_10240	3.39419	0.00314044
gene_FPSE_10187	transforming growth factor-beta-induced protein ig-h3	3.64036	0.0350082
gene_FPSE_11500	hypothetical protein FPSE_11500	3.65612	0.021355
gene_FPSE_06883	alpha-glucosidase 2	3.68475	0.00314044
gene_FPSE_06882	laccase precursor	3.69171	0.0156256
gene_FPSE_06580	bys1 protein	3.80291	0.00314044
gene_FPSE_00196	fungistatic metabolite	3.96993	0.0276824
gene_FPSE_10365	hypothetical protein FPSE_10365	4.2658	0.00314044
gene_FPSE_04396	hypothetical protein FPSE_04396	4.46748	0.00314044

>16AAVFQC_1863363

5’CACTATAGGGCGAATTGAAGGAAGGCCGTCAAGGCCGCATATTGATGTGATG

AAGTTGACCTTTTCTTATAGCCGTCAAATTTCGGCATCAAGTTGCGTAAAGATCT

TCATATACTTGTCTGAGCGTATTTATTGGTAACACGGGTTGCATGTATGTTATGG

AAGGAGATCCGGACTCTCAACTGTGGAGTTATAGACTTTGGTACAGATACATCC

CTCAAATTTTACTCTCTTGTGTTTTGCTGGCGTGTCCATCTTGCTCAGACTGTCC

CACGGTCCTTCCTTAACTTTCGTATAGGTTCATGACGAAAAACATCATGACTCC

GATGCTTGCATGAGACTATTGCCCTTATCCTGACATAAGGTTTACACGGGGATT

TGTACGATGACTCTTTTGCCGTCATCCTTTTCAGTCTGTTTTCGGACTGTCTCAC

ATGTAGAGTAGAGTAAAACAAGGAGGAGAGAACTAGATCTGTCGGTAGTTCCCA

ATATCACATCATTGTCCCTTTCATTTCAACCTTCACGATGATATTTTAGCTTACAG

AAACGGCTTATTATATCCGACGTTACATTGTGAGGTTACAGCCGATGAGGGCGG

AAATATCGTGCAGCCATCGGAGTCATGATGTTCTTTTCTCTTGTGAACTTTGACC

AAACTCTAAACGTACGAGGTTATAGCCTCCGCCCCCTGCGTAACATGGGGAGG

CTCTGCGGCAAGAGAGTGGCTCTAGTGGTAACAAGGGTCGTGAAACAGCTCTC

TCAAGCCGGATGTCTTGGCAAAAAACTCCAGAAGTTGCGGAATTCAGTAATTAA

TCCTTCTACAGGGGTATTGAAGTCATGACAAAGAGGAACGTGAGTGCTATACGT

ATGCTTACCAGTGAAGAATATGAAAGTTCTGCATCTATCGTATGGTACAGTCTAC

AAAATCCGTTTTGCTTAGTTCATAAGAATCTCAGAGTACACTTCAGAAGTCTGCC

TTACGTCCCTTGGAAACATAGTCAACTTGCACGATTCACCAACCAAGCTTCACA

TTATTCACCGATGTCCACGAGGTCTCTAGCCATAACGTTGGACCGTTCGTACGC

TGCAGGTCGACTCGACAGAAGATGACATTGAAGGAGCACTTTTTGGGCTTGGC

TGGAGCTAGTGGAGGTCAACAATGAATGCCTATTTTGGTTTAGTCGTCCAGGCG

GTGAGCACAAAATTTGTGTCGTTTGACAAGATGGTTCATTTAGGCAACTGGTCA

GATCAGCCCCACTTGTAGCAGTAGCGGCGGCGCTCGAAGTGTGACTCTTATTA

GCAGACAGGAACGAGGACATTATTATCATCTGCTGCTTGGTGCACGATAACTTG

GTGCGTTTGTCAAGCAAGGTAAGTGAACGACCCGGTCATACCTTCTTAAGTTCG

CCCTTCCTCCCTTTATTTCAGATTCAATCTGACTTACCTATTCTACCCAAGCATC

GATAAGCTGATCCATATGACCACTCTTGACGACACGGCTTACCGGTACCGCAC

CAGTGTCCCGGGGGACGCCGAGGCCATCGAGGCACTGGATGGGTCCTTCACC

ACCGACACCGTCTTCCGCGTCACCGCCACCGGGGACGGCTTCACCCTGCGGG

AGGTGCCGGTGGACCCGCCCCTGACCAAGGTGTTCCCCGACGACGAATCGGA

CGACGAATCGGACGACGGGGAGGACGGCGACCCGGACTCCCGGACGTTCGTC

GCGTACGGGGACGACGGCGACCTGGCGGGCTTCGTGGTCGTCTCGTACTCCG

GCTGGAACCGCCGGCTGACCGTCGAGGACATCGAGGTCGCCCCGGAGCACCG
GGGGCACGGGGTCGGGCGCGCGTTGATGGGGCTCGCGACGGAGTTCGCCCG
CGAGCGGGGCGCCGGGCACCTCTGGCTGGAGGTCACCAACGTCAACGCACCG
GCGATCCACGCGTACCGGCGGATGGGGTTCACCCTCTGCGGCCTGGACACCG
CCCTGTACGACGGCACCGCCTCGGACGGCGAGCAGGCGCTCTACATGAGCAT
GCCCTGCCCCTGATCTACAGGCTCATTCTTGGTGATTGATTACGCAATGCCACT
AGTTAGAAATAGTTAAGGACGTTTCATTAGAGTGCAACAATGCGTATCTTCCAAG
AGAAAGATAAAGGCTGTAGGAATGGTCAGAGTAGGATTACTTCTAGCCTTGGTT
TTGCTACGGGGAAAGAATCATGAGACCTATTCATGGTGTATACAGAGCTCAATC
CCTGTCACAATGGATCTTCAAATTGAGAAATTGATTACATTGTATTTGGCCCAAG
CGACGAGACTGAAATCTTTTGTAAGCATCGGAGTTATGATGTTTTCCGTTGTGA
ATCTCCACGAAAGTTGAAGGACCGAGACCTTCACTGTATGATTTGATATCTAGG
GTTAATACTGCTGGGCCACGGATGCTGCATAAACCTGCCACTATGAGTATGGTG
CAATAGATTCCTTCGTTGAACTACACCTAATGCTACTCATCATCGTACCGTGAGA
CTTTGGTGTAAGTTCACAAACCAAACTCATCATGACTCACTACTCATCATTAGTT
TCAAGATTTGCTTACAGGCTAAGACAGGTTCTTTGACCGCCCTTTCCACAATAC
AATTTTAATCATTTAAATTTATGACCTATAACTATTCAACTGAGCGTCCTCATGTC
ATAAGGCCTTACATGCATATCCCGCGGGAACTCTCAGACTGTTCTTCATTCATAT
CCTCAGAATTCGGTCCACGCATATAGGCGACTTACGTAAGTATGATATAGTATG
TCTCAAAAGAACGGCACTTCAAACCAAAGTATCAGTACATAGTAACGACCAAGT
CAGGGGTCGGCAGTTATACCCGGCTGTGGGTCATCGTCTGTGCAGAAGGTCAC
AGGGGCGACGTTTCATGATTAACGCACATGAACATGCGGGAACTAATCGAGTTA
TACGAAAACGGTATAAACGGCTCTTTGATAATTCCACGTCATCACAACCACGGC
AGTCTTACTAGATCTGGATTTGAGTTTCTGGGCCTCATGGGCCTTCCTTTCACT
GCCCGCTTTCCAG 3’

Supplementary figure 4.2: **FASTA file sequence for the T-DNA used to transform *Fp* protoplasts**. The *FPSE_08867* gene sequence has been highlighted yellow, the *Aspergillus nidulans* trpC promoter has been highlighted in pink and the antibiotic resistance marker nourseothricin acetyl transferase CDs has been highlighted in green.

4.9 References

AKINSANMI, O. A., MITTER, V., SIMPFENDORFER, S., BACKHOUSE, D. & CHAKRABORTY, S. 2004. Identity and pathogenicity of *Fusarium* spp. isolated from wheat fields in Queensland and northern New South Wales. *Australian Journal of Agricultural Research,* 55**,** 97-107.

ANISIMOVA, M. & GASCUEL, O. 2006. Approximate likelihood-ratio test for branches: a fast, accurate, and powerful alternative. *Systematic biology,* 55**,** 539-552.

AOKI, T. & O'DONNELL, K. 1999. Morphological and molecular characterization of *Fusarium pseudograminearum* sp. *nov*., formerly recognized as the Group 1 population of *F. graminearum*. *Mycologia,* 91**,** 597-609.

AOKI, T. & O'DONNELL, K. 1999. Morphological characterization of *Gibberella coronicola* sp. *nov*., obtained through mating experiments of *Fusarium pseudograminearum*. *Mycoscience,* 40**,** 443-453.

ASHLEY, J. N., HOBBS, B. C. & RAISTRICK, H. 1937. Studies in the biochemistry of micro-organisms: The crystalline colouring matters of *Fusarium culmorum* (WG Smith) Sacc. and related forms. *Biochemical Journal,* 31**,** 385.

BACKHOUSE, D., ABUBAKAR, A., BURGESS, L., DENNISC, J., HOLLAWAY, G., WILDERMUTH, G., WALLWORK, H. & HENRY, F. 2004. Survey of *Fusarium* species associated with crown rot of wheat and barley in eastern Australia. *Australasian Plant Pathology,* 33**,** 255-261.

BACKHOUSE, D. & BURGESS, L. 2002. Climatic analysis of the distribution of *Fusarium graminearum*, *F. pseudograminearum* and *F. culmorum* on cereals in Australia. *Australasian Plant Pathology,* 31**,** 321-327.

BACON, C. W. & YATES, I. E. 2006. Endophytic root colonization by *Fusarium s*pecies: histology, plant interactions, and toxicity. *In:* SCHULZ, B. J. E., BOYLE, C. J. C. & SIEBER, T. N. (eds.) *Microbial Root Endophytes.* Berlin, Heidelberg: Springer Berlin Heidelberg.

BERNE, S., KOVAČIČ, L., SOVA, M., KRAŠEVEC, N., GOBEC, S., KRIŽAJ, I. & KOMEL, R. 2015. Benzoic acid derivatives with improved antifungal activity: Design, synthesis, structure–activity relationship (SAR) and CYP53 docking studies. *Bioorganic & medicinal chemistry,* 23**,** 4264-4276.

BLUM, A., BENFIELD, A. H., SØRENSEN, J. L., NIELSEN, M. R., BACHLEITNER, S., STUDT, L., BECCARI, G., COVARELLI, L., BATLEY, J. & GARDINER, D. M. 2019. Regulation of a novel *Fusarium* cytokinin in *Fusarium pseudograminearum*. *Fungal biology,* 123**,** 255-266.

BROEKAERT, W. F., DELAURÉ, S. L., DE BOLLE, M. F. & CAMMUE, B. P. 2006. The role of ethylene in host-pathogen interactions. *Annu. Rev. Phytopathol.,* 44**,** 393-416.

BROWN, D. W. & PROCTOR, R. H. 2016. Insights into natural products biosynthesis from analysis of 490 polyketide synthases from *Fusarium*. *Fungal Genetics and Biology,* 89**,** 37-51.

BURGESS, L., WEARING, A. & TOUSSOUN, T. 1975. Surveys of *Fusaria* associated with crown rot of wheat in eastern Australia. *Australian Journal of Agricultural Research,* 26**,** 791-799.

BUTCHKO, R. A., PLATTNER, R. D. & PROCTOR, R. H. 2006. Deletion analysis of *FUM* genes involved in tricarballylic ester formation during fumonisin biosynthesis. *Journal of agricultural and food chemistry,* 54**,** 9398-9404.

CHEN, Z., SILVA, H. & KLESSIG, D. F. 1993. Active oxygen species in the induction of plant systemic acquired resistance by salicylic acid. *Science,* 262**,** 1883-1886.

CHEVENET, F., BRUN, C., BAÑULS, A.-L., JACQ, B. & CHRISTEN, R. 2006. TreeDyn: towards dynamic graphics and annotations for analyses of trees. *BMC bioinformatics,* 7**,** 439.

COLE, S. J., YOON, A. J., FAULL, K. F. & DIENER, A. C. 2014. Host perception of jasmonates promotes infection by *Fusarium oxysporum* formae speciales that produce isoleucine‐and leucine‐conjugated jasmonates. *Molecular plant pathology,* 15**,** 589-600.

CONESA, A., GÖTZ, S., GARCÍA-GÓMEZ, J. M., TEROL, J., TALÓN, M. & ROBLES, M. 2005. Blast2GO: a universal tool for annotation, visualization and analysis in functional genomics research. *Bioinformatics,* 21**,** 3674-3676.

ČREŠNAR, B. & PETRIČ, Š. 2011. Cytochrome P450 enzymes in the fungal kingdom. *Biochimica et Biophysica Acta (BBA)-Proteins and Proteomics,* 1814**,** 29-35.

CZISLOWSKI, E., FRASER‐SMITH, S., ZANDER, M., O'NEILL, W. T., MELDRUM, R. A., TRAN‐NGUYEN, L. T., BATLEY, J. & AITKEN, E. A. 2018. Investigation of the diversity of effector genes in the banana pathogen, *Fusarium oxysporum* f. sp. *cubense*, reveals evidence of horizontal gene transfer. *Molecular plant pathology,* 19**,** 1155-1171.

DEAN, R., VAN KAN, J. A., PRETORIUS, Z. A., HAMMOND‐KOSACK, K. E., DI PIETRO, A., SPANU, P. D., RUDD, J. J., DICKMAN, M., KAHMANN, R. & ELLIS, J. 2012. The Top 10 fungal pathogens in molecular plant pathology. *Molecular plant pathology,* 13**,** 414-430.

DELANEY, T. P., UKNES, S., VERNOOIJ, B., FRIEDRICH, L., WEYMANN, K., NEGROTTO, D., GAFFNEY, T., GUT-RELLA, M., KESSMANN, H. & WARD, E. 1994. A central role of salicylic acid in plant disease resistance. *Science,* 266**,** 1247-1250.

DEREEPER, A., GUIGNON, V., BLANC, G., AUDIC, S., BUFFET, S., CHEVENET, F., DUFAYARD, J.-F., GUINDON, S., LEFORT, V. & LESCOT, M. 2008. Phylogeny. fr: robust phylogenetic analysis for the non-specialist. *Nucleic acids research,* 36**,** W465-W469.

EDGAR, C., MCGRATH, K., DOMBRECHT, B., MANNERS, J., MACLEAN, D., SCHENK, P. & KAZAN, K. 2006. Salicylic acid mediates resistance to the vascular wilt pathogen *Fusarium oxysporum* in the model host *Arabidopsis thaliana*. *Australasian Plant Pathology,* 35**,** 581-591.

EDGAR, R. C. 2004. MUSCLE: a multiple sequence alignment method with reduced time and space complexity. *BMC bioinformatics,* 5**,** 113.

FABER, B. W., VAN GORCOM, R. F. & DUINE, J. A. 2001. Purification and characterization of benzoate-para-hydroxylase, a cytochrome P450 (CYP53A1), from *Aspergillus niger*. *Archives of biochemistry and biophysics,* 394**,** 245-254.

FERREIRA, F. J. & KIEBER, J. J. 2005. Cytokinin signaling. *Current opinion in plant biology,* 8**,** 518-525.

FRASER, J. A., DAVIS, M. A. & HYNES, M. J. 2002. The genes *gmdA*, encoding an amidase, and *bzuA*, encoding a cytochrome P450, are required for benzamide utilization in *Aspergillus nidulans*. *Fungal Genetics and Biology,* 35**,** 135-146.

GAFFNEY, T., FRIEDRICH, L., VERNOOIJ, B., NEGROTTO, D., NYE, G., UKNES, S., WARD, E., KESSMANN, H. & RYALS, J. 1993. Requirement of salicylic acid for the induction of systemic acquired resistance. *Science,* 261**,** 754-756.

GARDINER, D. M., BENFIELD, A. H., STILLER, J., STEPHEN, S., AITKEN, K., LIU, C. & KAZAN, K. 2018. A high‐resolution genetic map of the cereal crown rot pathogen *Fusarium pseudograminearum* provides a near‐complete genome assembly. *Molecular plant pathology,* 19**,** 217-226.

GARDINER, D. M., MCDONALD, M. C., COVARELLI, L., SOLOMON, P. S., RUSU, A. G., MARSHALL, M., KAZAN, K., CHAKRABORTY, S., MCDONALD, B. A. & MANNERS, J. M.

2012. Comparative pathogenomics reveals horizontally acquired novel virulence genes in fungi infecting cereal hosts. *PLoS pathogens,* 8**,** e1002952.

GLAZEBROOK, J. 2005. Contrasting mechanisms of defense against biotrophic and necrotrophic pathogens. *Annu. Rev. Phytopathol.,* 43**,** 205-227.

GLUCK‐THALER, E., VIJAYAKUMAR, V. & SLOT, J. C. 2018. Fungal adaptation to plant defences through convergent assembly of metabolic modules. *Molecular ecology,* 27**,** 5120-5136.

GREENBERG, J. T., GUO, A., KLESSIG, D. F. & AUSUBEL, F. M. 1994. Programmed cell death in plants: a pathogen-triggered response activated coordinately with multiple defense functions. *Cell,* 77**,** 551-563.

GUINDON, S. & GASCUEL, O. 2003. A simple, fast, and accurate algorithm to estimate large phylogenies by maximum likelihood. *Systematic biology,* 52**,** 696-704.

GUY, L., ROAT KULTIMA, J. & ANDERSSON, S. G. 2010. genoPlotR: comparative gene and genome visualization in R. *Bioinformatics,* 26**,** 2334-2335.

HALIM, V. A., ESCHEN-LIPPOLD, L., ALTMANN, S., BIRSCHWILKS, M., SCHEEL, D. & ROSAHL, S. 2007. Salicylic acid is important for basal defense of *Solanum tuberosum* against *Phytophthora infestans*. *Molecular Plant-Microbe Interactions,* 20**,** 1346-1352.

HAN, X. & KAHMANN, R. 2019. Manipulation of phytohormone pathways by effectors of filamentous plant pathogens. *Frontiers in plant science,* 10.

HAO, G., NAUMANN, T. A., VAUGHAN, M. M., MCCORMICK, S., USGAARD, T., KELLY, A. & WARD, T. J. 2018. Characterization of a *Fusarium graminearum* salicylate hydroxylase. *Frontiers in microbiology,* 9**,** 3219.

HARWOOD, C. S. & PARALES, R. E. 1996. The β-ketoadipate pathway and the biology of self-identity. *Annual review of microbiology,* 50**,** 553-590.

KELLER, N. P. 2015. Translating biosynthetic gene clusters into fungal armor and weaponry. *Nature chemical biology,* 11**,** 671.

KHALDI, N. & WOLFE, K. H. 2011. Evolutionary origins of the fumonisin secondary metabolite gene cluster in *Fusarium verticillioides* and *Aspergillus niger*. *International journal of evolutionary biology,* 2011.

KHANGURA, R. K., MACNISH, G. C., MACLEOD, W. J., VANSTONE, V. A., HANBURY, C. D., LOUGHMAN, R. & SPEIJERS, J. E. 2013. Current status of cereal root diseases in Western Australia under intensive cereal production and their comparison with the historical survey conducted during 1976–1982. *Journal of Phytopathology,* 161**,** 828-840.

KIM, Y. T., LEE, Y. R., JIN, J., HAN, K. H., KIM, H., KIM, J. C., LEE, T., YUN, S. H. & LEE, Y. W. 2005. Two different polyketide synthase genes are required for synthesis of zearalenone in *Gibberella zeae*. *Molecular microbiology,* 58**,** 1102-1113.

KIMURA, M., TOKAI, T., TAKAHASHI-ANDO, N., OHSATO, S. & FUJIMURA, M. 2007. Molecular and genetic studies of *Fusarium* trichothecene biosynthesis: pathways, genes, and evolution. *Bioscience, biotechnology, and biochemistry***,** 0707310525-0707310525.

KJÆRBØLLING, I., VESTH, T. & ANDERSEN, M. R. 2019. Resistance Gene-Directed Genome Mining of 50 *Aspergillus* species. *MSystems,* 4**,** e00085-19.

KOROŠEC, B., SOVA, M., TURK, S., KRAŠEVEC, N., NOVAK, M., LAH, L., STOJAN, J., PODOBNIK, B., BERNE, S. & ZUPANEC, N. 2014. Antifungal activity of cinnamic acid derivatives involves inhibition of benzoate 4‐hydroxylase (CYP 53). *Journal of applied microbiology,* 116**,** 955-966.

LAH, L., PODOBNIK, B., NOVAK, M., KOROŠEC, B., BERNE, S., VOGELSANG, M., KRAŠEVEC, N., ZUPANEC, N., STOJAN, J. & BOHLMANN, J. 2011. The versatility of the fungal cytochrome P450 monooxygenase system is instrumental in xenobiotic detoxification. *Molecular microbiology,* 81**,** 1374-1389.

LAM, E., KATO, N. & LAWTON, M. 2001. Programmed cell death, mitochondria and the plant hypersensitive response. *Nature,* 411**,** 848.

LAPADATESCU, C., GINIÈS, C., LE QUÉRÉ, J.-L. & BONNARME, P. 2000. Novel Scheme for Biosynthesis of Aryl Metabolites from l-Phenylalanine in the Fungus *Bjerkandera adusta*. *Appl. Environ. Microbiol.,* 66**,** 1517-1522.

LAURENCE, M., SUMMERELL, B. & LIEW, E. 2015. *Fusarium oxysporum* f. sp. *canariensis*: evidence for horizontal gene transfer of putative pathogenicity genes. *Plant pathology,* 64**,** 1068-1075.

LAURSEN, T., JENSEN, K. & MØLLER, B. L. 2011. Conformational changes of the NADPH-dependent cytochrome P450 reductase in the course of electron transfer to cytochromes P450. *Biochimica et Biophysica Acta (BBA)-Proteins and Proteomics,* 1814**,** 132-138.

LI, N., HAN, X., FENG, D., YUAN, D. & HUANG, L.-J. 2019. Signaling crosstalk between salicylic acid and ethylene/jasmonate in plant defense: do we understand what they are whispering? *International journal of molecular sciences,* 20**,** 671.

LIU, C. & OGBONNAYA, F. C. 2015. Resistance to Fusarium crown rot in wheat and barley: a review. *Plant Breeding,* 134**,** 365-372.

LUTTRELL, E. 1974. Parasitism of fungi on vascular plants. *Mycologia,* 66**,** 1-15.

LYSØE, E., KLEMSDAL, S. S., BONE, K. R., FRANDSEN, R. J., JOHANSEN, T., THRANE, U. & GIESE, H. 2006. The *PKS4* gene of *Fusarium graminearum* is essential for zearalenone production. *Appl. Environ. Microbiol.,* 72**,** 3924-3932.

MA, L.-J., GEISER, D. M., PROCTOR, R. H., ROONEY, A. P., O'DONNELL, K., TRAIL, F., GARDINER, D. M., MANNERS, J. M. & KAZAN, K. 2013. *Fusarium* pathogenomics. *Annual review of microbiology,* 67**,** 399-416.

MAKANDAR, R., NALAM, V. J., LEE, H., TRICK, H. N., DONG, Y. & SHAH, J. 2012. Salicylic acid regulates basal resistance to Fusarium head blight in wheat. *Molecular Plant-Microbe Interactions,* 25**,** 431-439.

MALONEK, S., ROJAS, M. C., HEDDEN, P., GASKIN, P., HOPKINS, P. & TUDZYNSKI, B. 2004. The NADPH-cytochrome P450 reductase gene from *Gibberella fujikuroi* is essential for gibberellin biosynthesis. *Journal of Biological Chemistry,* 279**,** 25075-25084.

MALZ, S., GRELL, M. N., THRANE, C., MAIER, F. J., ROSAGER, P., FELK, A., ALBERTSEN, K. S., SALOMON, S., BOHN, L. & SCHÄFER, W. 2005. Identification of a gene cluster responsible for the biosynthesis of aurofusarin in the *Fusarium graminearum* species complex. *Fungal Genetics and Biology,* 42**,** 420-433.

MATSUZAKI, F. & WARIISHI, H. 2005. Molecular characterization of cytochrome P450 catalyzing hydroxylation of benzoates from the white-rot fungus *Phanerochaete chrysosporium*. *Biochemical and biophysical research communications,* 334**,** 1184-1190.

MCKNIGHT, T. & HART, J. 1966. Some field observations on crown rot disease of wheat caused by *Fusarium graminearum*. *Queensland Journal of Agricultural and Animal Sciences,* 23**,** 373-378.

MEDENTSEV, A. & AKIMENKO, V. 1998. Naphthoquinone metabolites of the fungi. Elsevier.

MICHIELSE, C. B., REIJNEN, L., OLIVAIN, C., ALABOUVETTE, C. & REP, M. 2012. Degradation of aromatic compounds through the β - ketoadipate pathway is required for pathogenicity of the tomato wilt pathogen *Fusarium oxysporum* f. sp. *lycopersici*. *Molecular plant pathology,* 13**,** 1089-1100.

MITTER, V., FRANCL, L., ALI, S., SIMPFENDORFER, S. & CHAKRABORTY, S. 2006. Ascosporic and conidial inoculum of *Gibberella zeae* play different roles in Fusarium head blight and crown rot of wheat in Australia and the USA. *Australasian Plant Pathology,* 35**,** 441-452.

MURRAY, G. M. & BRENNAN, J. P. 2009. Estimating disease losses to the Australian wheat industry. *Australasian Plant Pathology,* 38**,** 558-570.

NELSON, D. R., MING, R., ALAM, M. & SCHULER, M. A. 2008. Comparison of cytochrome P450 genes from six plant genomes. *Tropical Plant Biology,* 1**,** 216-235.

PIETERSE, C. M., LEON-REYES, A., VAN DER ENT, S. & VAN WEES, S. C. 2009. Networking by small-molecule hormones in plant immunity. *Nature chemical biology,* 5**,** 308.

PIETERSE, C. M., VAN DER DOES, D., ZAMIOUDIS, C., LEON-REYES, A. & VAN WEES, S. C. 2012. Hormonal modulation of plant immunity. *Annual review of cell and developmental biology,* 28**,** 489-521.

PODOBNIK, B., STOJAN, J., LAH, L., KRASEVEC, N., SELISKAR, M., RIZNER, T. L., ROZMAN, D. & KOMEL, R. 2008. CYP53A15 of *Cochliobolus lunatus*, a target for natural antifungal compounds. *Journal of medicinal chemistry,* 51**,** 3480-3486.

PROCTOR, R. H., PLATTNER, R. D., DESJARDINS, A. E., BUSMAN, M. & BUTCHKO, R. A. 2006. Fumonisin production in the maize pathogen *Fusarium verticillioides*: genetic basis of naturally occurring chemical variation. *Journal of agricultural and food chemistry,* 54**,** 2424-2430.

QI, P.-F., JOHNSTON, A., BALCERZAK, M., ROCHELEAU, H., HARRIS, L. J., LONG, X.-Y., WEI, Y.-M., ZHENG, Y.-L. & OUELLET, T. 2012. Effect of salicylic acid on *Fusarium graminearum*, the major causal agent of fusarium head blight in wheat. *Fungal Biology,* 116**,** 413-426.

RCORETEAM 2018. R: a language and environment for statistical computing computer program, version 3.5. 0. R Core Team Vienna, Austria.

ROCHELEAU, H., AL-HARTHI, R. & OUELLET, T. 2019. Degradation of salicylic acid by *Fusarium graminearum*. *Fungal biology,* 123**,** 77-86.

SIEBER, C. M., LEE, W., WONG, P., MÜNSTERKÖTTER, M., MEWES, H.-W., SCHMEITZL, C., VARGA, E., BERTHILLER, F., ADAM, G. & GÜLDENER, U. 2014. The *Fusarium graminearum* genome reveals more secondary metabolite gene clusters and hints of horizontal gene transfer. *PLoS One,* 9**,** e110311.

SØRENSEN, J. L., BENFIELD, A. H., WOLLENBERG, R. D., WESTPHAL, K., WIMMER, R., NIELSEN, M. R., NIELSEN, K. F., CARERE, J., COVARELLI, L., BECCARI, G., POWELL, J., YAMASHINO, T., KOGLER, H., SONDERGAARD, T. E. & GARDINER, D. M. 2018. The cereal pathogen *Fusarium pseudograminearum* produces a new class of active cytokinins during infection. *Molecular Plant Pathology,* 19**,** 1140-1154.

SUMMERELL, B. A. 2019. Resolving *Fusarium*: Current Status of the Genus. *Annual review of phytopathology,* 57**,** 323-339.

SVOBODA, T., PARICH, A., GÜLDENER, U., SCHÖFBECK, D., TWARUSCHEK, K., VÁCLAVÍKOVÁ, M., HELLINGER, R., WIESENBERGER, G., SCHUHMACHER, R. & ADAM, G. 2019. Biochemical Characterization of the *Fusarium graminearum* Candidate ACC-

Deaminases and Virulence Testing of Knockout Mutant Strains. *Frontiers in Plant Science,* 10.

TALAVERA, G. & CASTRESANA, J. 2007. Improvement of phylogenies after removing divergent and ambiguously aligned blocks from protein sequence alignments. *Systematic biology,* 56**,** 564-577.

THATCHER, L. F., GARDINER, D. M., KAZAN, K. & MANNERS, J. M. 2012. A highly conserved effector in *Fusarium oxysporum* is required for full virulence on *Arabidopsis*. *Molecular plant-microbe interactions,* 25**,** 180-190.

THATCHER, L. F., MANNERS, J. M. & KAZAN, K. 2009. *Fusarium oxysporum* hijacks COI1‐mediated jasmonate signaling to promote disease development in *Arabidopsis*. *The Plant Journal,* 58**,** 927-939.

THYNNE, E., MEAD, O. L., CHOOI, Y.-H., MCDONALD, M. C. & SOLOMON, P. S. 2019. Acquisition and loss of secondary metabolites shaped the evolutionary path of three emerging phytopathogens of wheat. *Genome biology and evolution,* 11**,** 890-905.

TRONCOSO, C., CÁRCAMO, J., HEDDEN, P., TUDZYNSKI, B. & ROJAS, M. C. 2008. Influence of electron transport proteins on the reactions catalyzed by *Fusarium fujikuroi* gibberellin monooxygenases. *Phytochemistry,* 69**,** 672-683.

VAN DAM, P. & REP, M. 2017. The distribution of Miniature Impala elements and *SIX* genes in the *Fusarium* genus is suggestive of horizontal gene transfer. *Journal of molecular evolution,* 85**,** 14-25.

VAN DER ENT, S. & PIETERSE, C. M. 2018. Ethylene: multi‐tasker in plant‐attacker interactions. *Annual Plant Reviews online***,** 343-377.

VLAARDINGERBROEK, I., BEERENS, B., ROSE, L., FOKKENS, L., CORNELISSEN, B. J. & REP, M. 2016. Exchange of core chromosomes and horizontal transfer of lineage‐specific chromosomes in *Fusarium oxysporum*. *Environmental microbiology,* 18**,** 3702-3713.

WHELAN, S. & GOLDMAN, N. 2001. A general empirical model of protein evolution derived from multiple protein families using a maximum-likelihood approach. *Molecular biology and evolution,* 18**,** 691-699.

WICKHAM, H. 2011. ggplot2. *Wiley Interdisciplinary Reviews: Computational Statistics,* 3**,** 180-185.

WISECAVER, J. H., SLOT, J. C. & ROKAS, A. 2014. The evolution of fungal metabolic pathways. *PLoS Genetics,* 10**,** e1004816.

WRIGHT, J. 1993. Fungal degradation of benzoic acid and related compounds. *World journal of microbiology and biotechnology,* 9**,** 9-16.

YANG, G., ROSE, M. S., TURGEON, B. G. & YODER, O. 1996. A polyketide synthase is required for fungal virulence and production of the polyketide T-toxin. *The Plant Cell,* 8**,** 2139-2150.

Chapter 5

General discussion

5.1 Project Overview

Fusarium Crown Rot (FCR) is a significant global crop disease of wheat and barley, and in Australia it is predominantly caused by *Fusarium pseudograminearum* (*Fp*) *Fp* can live saprophytically on wheat stubble and can produce pseudo-chlamydospores that can endure in the soil for up to three years. Consequently, present FCR control measures involve practices to limit inoculum load; however, implementation thereof can be constrained by social and economic factors. Resistance to FCR is variable with differing levels reported amongst elite wheat cultivars, indicating the possibility of breeding a highly resistant high yielding cultivar (Liu and Ogbonnaya, 2015). Resistance to FCR is a quantitative trait; however, currently no underlying genes have been identified and cloned. Hence, it has been reported by Liu and Ogbonnaya (2015) that additional studies centred on characterising candidate genes involved in inducible defence signalling pathways and the pathways themselves should be conducted to gain a deeper understanding of the genetic basis of resistance. Genetic studies in wheat have been reportedly hampered due to the inherent complexities of wheat's hexaploid genome, as described by Fitzgerald et al. (2015). Hence, studies using a suitable model organism appear as a tractable approach to further knowledge of the genetic basis of FCR resistance.

This PhD project aimed to characterise the host-*Fp* interaction during FCR pathogenesis by utilising *Brachypodium distachyon* as a model organism for wheat. Three unique investigative perspectives were adopted to dissect the host-*Fp* interaction. Firstly, the role of a *Brachypodium* candidate gene with reported involvement in conferring susceptibility to *Fusarium oxysporum* (*Fo*) in *Arabidopsis* (Kidd et al., 2009), *PHYTOCHROME AND FLOWERING TIME 1* (*AtPFT1),* was investigated (Chapter 2). Secondly, the impact of phytohormone salicylic acid (SA) on basal and inducible defence pathways at a genomic and organismal level during basal growth and infection by *Fp* was also investigated (Chapter 3). Lastly, to gain an understanding of how *Fp* adapts to endogenous SA and/or SA-dependent host defences during host infection, a fungal candidate gene *FPSE_08867* that was repressed during infection of SA-deficient but not wild-type *Brachypodium* was characterised (Chapter 4). Each of the investigations will be discussed further below with respect to major findings and avenues for further research.

5.2 *Brachypodium* as a tool to identify sources of FCR resistance

Prior to planning of this PhD project, wheat's very large hexaploid genome had been reported to hamper genetic studies and only *Arabidopsis thaliana* had been extensively used to characterise the interaction between *Fusarium* and the host plant. Whilst the knowledge gained from these studies has guided investigations in wheat, *Arabidopsis* is no longer considered a suitable model organism for wheat due to inherent differences between dicots and monocots and the availability of another more suitable model. In 2015, during the initial planning of the PhD project, *Brachypodium distachyon* had been developed as a model to investigate cereal-*Fusarium pseudograminearum* interactions (Powell et al., 2017). Unlike *Arabidopsis*, *Brachypodium* shares a closer evolutionary history to wheat as reflected by the high amounts of genetic synteny and similar global transcriptomic changes under *Fp* infection. Hence, genes and processes affecting FCR resistance in *Brachypodium* are likely to play a similar role in wheat. Further, *Brachypodium* possesses a small sequenced diploid genome and is amenable to genetic manipulation. During a previous project, genetic resources such as *BdPFT1* over expressor (*BdPFT1*-OE) and three independent *nahG* expressing *Brachypodium* lines were developed. This is because *PFT1* had been extensively characterised in *Arabidopsis* for roles in defence against *Fusarium* but attempts to generate knockout mutants in wheat to characterise *TaPFT1* were unsuccessful. *nahG* is a bacterial enzyme that degrades SA. *nahG* expressing plants are SA-deficient. By creating SA-deficient *Brachypodium* lines, SA regulated defensive processes can be characterised and candidate genes identified for further investigation. Given *Brachypodium's* position as a model for cereal crops like wheat and the availability of genetic resources, it was selected for use in the PhD project.

5.3 BdPFT1 over-expression promotes susceptibility to *Fusarium pseudograminearum* in *Brachypodium* and results in spontaneous necrotic lesion development

During the PhD project, I continued to characterize the *BdPFT1*-OE lines by identifying two stable independent homozygous lines with single insert number and demonstrating that expression was significantly elevated. The *BdPFT1*-OE lines were subsequently characterised for altered basal growth and disease phenotypes. It was found that BdPFT1 plays a similar role to AtPFT1 promoting transition to flowering. However, the mode of action for BdPFT1 in flowering may be different to AtPFT1 and requires further research, because the mode of action for some components of the photoperiod induction of flowering pathway in monocots and dicots have reportedly diverged (Yano et al., 2000). I demonstrated that *BdPFT1* overexpression confers susceptibility to *Fusarium pseudograminearum* infection. It is unclear whether *BdPFT1*-mediated susceptibility is JA-dependent as in *Arabidopsis*, because qRT-PCR analysis of SA and JA marker gene expression under basal growth and *Fp* infection conditions were not conclusive but inferred that JA biosynthesis and signalling were elevated in *BdPFT1* over-expressor lines both during basal growth conditions and infection. Some inference toward increased expression of reactive oxygen species (ROS) formation was also observed as increased expression of ROS-related peroxidase genes. If this inference holds true, it would suggest *BdPFT1* can be exploited by *Fp* as a susceptibility factor by overstimulation of JA-regulated defences leading to host-induced necrosis/senescence similar to findings for *AtPFT1* in the *Arabidopsis-F. oxysporum* pathosystem. Therefore, further work would benefit from a global transcriptomic analysis (such as RNA-seq) of *BdPFT1*-OE lines under infection to determine if a consistent pattern of enhanced JA-mediated defence signalling and ROS production occurs when *BdPFT1* is modulated and to identify regulatory genes which function downstream of BdPFT1 to modulate defence/ROS responses.

Assuming conserved function between *PFT1* in wheat and *Brachypodium*, over-expression of *TaPFT1* would increase susceptibility to FCR in wheat. Conversely, it

seems possible that rendering TaPFT1 non-functional or reducing the expression of its encoding gene might produce increased resistance levels in wheat. Previous attempts to knockout all three homoeologous copies of *TaPFT1* in hexaploid wheat, employed screening of fast neutron mutagenesis lines for individual homoeolog knockouts before crossing these lines to stack homoeolog knockouts. This approach was ultimately unsuccessful since hexa-knockouts were lethal or produced male infertile lines (Fitzgerald et al., 2015). However, whether the lethality/infertility was due to loss of all functional *TaPFT1* or due to loss of other genes within the large deletions created by fast neutron bombardment surrounding the TaPFT1 homoeologs could not be distinguished. Development of *BdPFT1* RNAi lines provided an opportunity to assess whether PFT1 knock-down increases resistance to *Fp* without the confounding effect of multiple homoeolog copies and large chromosomal deletions. However, since only a single RNAi line was identified, the effect of PFT1 silencing on altered resistance to *Fp* could not be reliably assessed. The difficulty in identifying *BdPFT1* RNAi lines with ablated *BdPFT1* expression from a relatively large collection of independent T_0 transformants perhaps suggests that plants with strong knockdowns were often either lethal or infertile. Recent work has produced wheat lines with all three homoeologous using a Virus Induced Gene Silencing (VIGS) approach and demonstrated that knock-down of all three homoeologous copies of *TaPFT1* resulted in reduced susceptibility to powdery mildew caused by *Blumeria graminis* f. sp. *tritici* (Liu et al., 2016). Assaying these genetic materials could allow us to test whether TaPFT1 results in reduced susceptibility to *Fp* in wheat. Furthermore, targeting genes which function downstream of *PFT1* could potentially uncouple the effect of altering resistance to *Fp* from pleiotropic effects on flowering time.

Interestingly, a potential role for *BdPFT1* in inducing cell death was uncovered. *BdPFT1* overexpression was found to be associated with a spontaneous lesion development phenotype. When grown under basal growth conditions, at approximately 3 weeks post emergence, lesions would begin to develop on photosynthetic tissue and proceed until the organ was completely covered or dead. This phenotype is not apparent in *Arabidopsis AtPFT1* overexpression lines. We hypothesised that the lesion phenotype maybe due to mis-regulation of ROS production during photosynthesis. Initial evidence of differential regulation of ROS marker genes in *BdPFT1*-OE plants has been gathered to support this hypothesis.

However, histochemical staining for differential ROS accumulation was inconclusive due to the masking of ROS staining by unclearable pigments within and surrounding the lesions. This work has highlighted that although there are similarities in roles of PFT1 between monocots and dicots, the mode of action may be different due to divergence of genetic regulatory pathways. Further genetic resources have been developed for use in other experiment and additional avenues of research have been suggested in Chapter 2 to further elucidate the role of BdPFT1 in relation to flowering time, defence and regulation of cell death.

5.4 SA plays an important role in mediating resistance against *Fp* in *Brachypodium*

Classical molecular plant pathology dogma postulates that JA plays a primary role in regulating defence responses against necrotrophic pathogens while SA provides effective defence responses against biotrophic pathogens. Previous work in the *Brachypodium-Fp* pathosystem found that both JA- and SA-dependent defence responses were induced during infection by *Fp* and levels of both signalling compounds increased significantly during infection (Powell et al., 2017). To determine whether SA contributes resistance or susceptibility to *Fp*, *Brachypodium* transformants expressing a bacterial enzyme (salicylate hydroxylase) which degrades SA were developed. This PhD project characterised three independent *nahG* expressing, SA-deficient, *Brachypodium* lines for differences in genetic regulation compared to WT during basal growth and infection with *Fp*. I was able to demonstrate that SA is an important resistance factor against *Fp* as *nahG* lines showed enhanced susceptibility compared to WT control lines. Further analysis of a previously generated RNA-seq dataset provided some insight into the role of SA increasing resistance against *Fp*. It was determined via transcriptomic alterations that SA is vital to establishing basal defences by regulating lignin deposition and accumulation of defence related proteins. I also demonstrated that both SA and a major degradation product of SA, benzoic acid (BA), were able to inhibit growth of *Fp* in axenic culture at biologically relevant concentrations. These findings provide evidence to guide some strategies for increasing FCR resistance levels in wheat germplasm. Firstly, assuming SA

accumulation levels in wheat is under genetic control and genetic diversity for this trait exists, germplasm could be screened for lines with higher basal SA levels. Such lines could be used to introgress alleles that are associated with higher SA levels into elite Australian wheat cultivars. As a complementary approach, SA production and associated signalling responses could be manipulated in the host through chemical compounds such as benzothiadiazole (BTH), which function as analogs of SA and induce SA-mediated defence mechanisms, or inoculation with beneficial microbes that trigger systemic defence responses. The *nahG Brachypodium* lines are invaluable genetic resources because they enable identification of *Fp*-responsive SA-regulated genes as candidates for additional research.

5.5 *Fp* differentially regulates genes to adapt to SA-related host defence

Following on from the *nahG* investigation, I identified a set of differentially expressed genes in *Fp* infecting *nahG* compared to the WT control. Two neighbouring genes, *FPSE_08867* and *FPSE_08868*, were found to be expressed more highly when infecting WT compared to *nahG* plants, and as both encoded enzymes we hypothesised these might be functioning as part of a metabolite cluster. The gene *FPSE_08867* had been earlier annotated as encoding a benzoate 4-monoxygenase and we hypothesised a role for it in the manipulation of an SA-related pathway either by metabolising benzoic acid (BA) or potentially degrading SA. FPSE_08867 was therefore selected as a candidate gene for further characterisation. Using transgenic techniques, I knocked out the candidate gene and created three independent Δ*fpse_08867* knock out isolates to enable further characterisation. In order to assess whether this enzyme was acting on SA or BA, I conducted chemical sensitivity assays. Surprisingly, the Δ*fpse_08867* knockout lines did not exhibit altered sensitivities towards exogenously applied SA or BA, indicating that FPSE_08867 may not participate in the metabolism of SA and BA. The Δ*fpse_08867* lines also exhibited an apparent loss of a polyketide pigment, aurofusarin, production when grown in culture. Given that aurofusarin biosynthesis genes have been previously characterised, this indicated that FPSE_08867 may be involved in biosynthesis of a related polyketide

that has altered the biosynthesis of aurofusarin through feedback mechanisms. Pathology assays revealed that loss of *FPSE_08867* enhanced the virulence of these mutant lines when infecting either *Brachypodium* or wheat. Given that FPSE_08867 negatively influences virulence, it is surprising that it has been maintained by *Fp*. However, it is possible that FPSE_08867 may positively influence fitness by other means such as exclusion of other competing micro-organisms. Further research is required to dissect the role(s) of FPSE_08867 in modulating the *Fp*-*Brachypodium*/wheat interaction, but one possibility is that it produces a molecular signature that can be perceived by an unknown resistance mechanism in both wheat and *Brachypodium*. Overall, this research has uncovered a set of candidate genes with potential roles in facilitating adaption of *Fp* to endogenous SA and/or SA-related processes *in planta*. Through the characterisation of one of these genes, *FPSE_08867*, we have demonstrated it to be a novel gene that attenuates virulence in the pathogen.

5.6 Conclusions

In summary, this PhD project has examined how candidate genes *BdPFT1* and *FPSE_*08867, and the plant phytohormone SA regulate *Brachypodium*:*Fp* interactions. *BdPFT1* overexpression was found to promote susceptibility to FCR, as well as the spontaneous formation of lesions. SA was demonstrated to confer resistance towards FCR, and SA-dependent Fusarium responsive pathways were identified. Lastly, *FPSE_08867* and its associated cluster was found to be maintained in *Fp* but lost in *Fg*, in spite of reducing virulence, highlighting *FPSE_08867* as a novel target for manipulation to control *Fp* virulence. Hence, this PhD project has yielded knowledge and genetic resources that can be used in future investigations designed to limit the impact of FCR on wheat and barley in Australia.

5.7 References

FITZGERALD, T. L., POWELL, J. J., STILLER, J., WEESE, T. L., ABE, T., ZHAO, G., JIA, J., MCINTYRE, C. L., LI, Z. & MANNERS, J. M. 2015. An assessment of heavy ion irradiation mutagenesis for reverse genetics in wheat (*Triticum aestivum* L.). *PLoS One,* 10**,** e0117369.

KIDD, B. N., EDGAR, C. I., KUMAR, K. K., AITKEN, E. A., SCHENK, P. M., MANNERS, J. M. & KAZAN, K. 2009. The mediator complex subunit PFT1 is a key regulator of jasmonate-dependent defense in *Arabidopsis*. *The Plant Cell,* 21**,** 2237-2252.

LIU, C. & OGBONNAYA, F. C. 2015. Resistance to Fusarium crown rot in wheat and barley: a review. *Plant Breeding,* 134**,** 365-372.

LIU, J., ZHANG, T., JIA, J. & SUN, J. 2016. The Wheat Mediator Subunit TaMED25 Interacts with the Transcription Factor TaEIL1 to Negatively Regulate Disease Resistance against Powdery Mildew. *Plant Physiology,* 170**,** 1799-1816.

POWELL, J. J., CARERE, J., SABLOK, G., FITZGERALD, T. L., STILLER, J., COLGRAVE, M. L., GARDINER, D. M., MANNERS, J. M., VOGEL, J. P., HENRY, R. J. & KAZAN, K. 2017. Transcriptome analysis of *Brachypodium* during fungal pathogen infection reveals both shared and distinct defense responses with wheat. *Scientific Reports,* 7**,** 17212.

YANO, M., KATAYOSE, Y., ASHIKARI, M., YAMANOUCHI, U., MONNA, L., FUSE, T., BABA, T., YAMAMOTO, K., UMEHARA, Y. & NAGAMURA, Y. 2000. *Hd1*, a major photoperiod sensitivity quantitative trait locus in rice, is closely related to the *Arabidopsis* flowering time gene *CONSTANS*. *The Plant Cell,* 12**,** 2473-2483.